

Aspects of Tailings Filtration in Recessed Plate Filter Presses

Zur Erlangung des akademischen Grades eines
DOKTORS DER INGENIEURWISSENSCHAFTEN

von der KIT-Fakultät für Chemieingenieurwesen und Verfahrenstechnik des
Karlsruher Instituts für Technologie (KIT)
genehmigte

DISSERTATION

von

Bernd Fränkle, M.Sc.

aus Pforzheim

Tag der mündlichen Prüfung: 13.05.2024

Erstgutachter: Prof. Dr.-Ing. Hermann Nirschl

Zweitgutachter: Prof. Dr.-Ing. Christoph Klahn

Acknowledgements

Foremost, my heartfelt gratitude goes to Prof. Dr.-Ing. habil. Nirschl for extending the invitation to join his research group. The confidence bestowed upon me, coupled with insightful professional discussions, not only fostered a delightful working environment but consistently propelled our collaborative efforts forward. Similarly, I express my appreciation to Prof. Dr.-Ing. Christoph Klahn for assuming the co-referendum responsibilities.

Special thanks are extended to Dr.-Ing. Patrick Morsch, who guided me through my bachelor and master theses at MVM, inspired me to accept the position, and facilitated a smooth project handover, including a collaborative business trip to Salt Lake City.

Gratitude is also owed to Thien Sok, James Chaponnel, Burçin Temel McKenna, Michael Madsen and other FLSmidth staff for their unwavering support throughout the project. The provision of equipment and samples by FLSmidth was instrumental, without which this doctoral thesis would not have been feasible.

I am grateful to Dr.-Ing. Marco Gleiß and Dr.-Ing. Harald Anlauf for their enlightening and inspiring discussions, as well as their support throughout this project. Additionally, I extend my appreciation to Kirsten, Tolga, and Volker for fostering a pleasant office atmosphere where open communication was encouraged, creating an environment conducive to engaging technical discussions and enjoyable conversations.

A special acknowledgment is reserved for Volker, whose dedication included numerous training sessions with me. Over the course of my time at MVM, I deepened existing friendships from my studies and formed new connections, with business trips standing out as memorable experiences we shared.

Integral to the institute were its permanent employees, particularly Richard, Amutha, Alexandr, Olaf, Adam, Hans, Thomas, Andreas, Klaus, Astrid, Regina, Kerstin, Andreas, Stefan, Mr. Schweigler, Kerstin, Verena, and the entire administration team. Furthermore, I would like to thank the team at the Institute of Applied Geosciences, especially Dr. Elisabeth Eiche, for their support.

Gratitude is also extended to all the students I had the privilege of supervising, including Felix Müller, Maik Langsenkamp, Christoph Kessler, Ali Al Ali, Rame Alzamel, Tom Shange, Philip Junginger, Leon Künkler, Noah Memis, Patrick Held,

Julius Zolg, and Maximilian Stockert. It brings me immense joy that many of them have maintained close contact, either as supporting scientific staff or in other capacities.

I reserve special thanks for Julius Zolg, Noah Memis, Selin Saltuklar, Nina Schladebach, Leon Künkler, Alexander Kessler, Simon Hesse, Jérôme Kühn, Adrian Arnold, and Hannah Burg for their dedicated support in the lab, some spanning several years.

Last but not least, I express profound gratitude to my parents, Roland and Renate, who have made many things possible for me. Additionally, I extend my thanks to my wife, Anja, for her unwavering and unconditional support.

Abstract

The aim of this work is to investigate various problems in tailings filtration. The aspects are the detachment of the filter cake, abrasive wear of the filter medium by cake detachment and the blocking of the filter medium due to permanently adhering fine particles. However, the filtration is characterized by a complex interplay of the different elements. Therefore, this thesis creates an additional scientific benefit by connecting the findings of the individual aspects.

In the first part of this dissertation, filtration tests using iron ore and copper mine tailings have shown that the parameters of the filtration process, primarily the filtration pressure, the differential pressure for post-desaturation by means of compressed air, the so-called air blow, and the duration of the air blow can be used to control the properties of the filter cake. Subsequent to filtration in a laboratory filter press, filter cake to filter cloth adhesion and filter cake cohesion tests were carried out using special test rigs for a tensile testing machine. Residual water content and desaturation were determined by subsequent thermal drying and weighing. In advance, various filter media were selected in collaboration with the project partner, exhibiting suitable particle retention with acceptable pressure loss and turbidity impact. They show no significant differences on the laboratory scale with respect to residual water content, desaturation, adhesion between filter cake and filter medium, and cohesion of the filter cake. However, the variations of the process parameters filtration pressure, pressure of the air blow and duration of the air blow have a significant effect on the target properties. While residual water content and saturation decrease with an increase of the three process parameters, adhesion and cohesion increase. Being able to adjust residual water content, desaturation, adhesion and cohesion is of utmost importance with regard to the subsequent process steps, process stability and economic efficiency. For this reason, a simplified mathematical model was developed which describes the desaturation behavior. It allows prediction of the relevant variables with sufficient accuracy as a function of the duration of the air blow.

The abrasive wear of the filter medium occurring at protruding points of the filtration chamber by the detachment of the cake is another aspect of the investigations in this thesis. The focus is on the various filter media, all of which are suitable for filtration of tailings due to their particle retention but differ in their type and material. Polypropylene and polyamide were used to investigate two standard filter media materials used in

tailings filtration. An abrasion apparatus was developed which, compared to available devices, can reproduce the application-specific load. It is evident that the woven fabric exhibits higher resistance to abrasion compared to the nonwoven fabric of the same material. Additionally, the polyamide fabric studied outperforms in terms of the number of abrasions until rupture compared to the fabric made of polypropylene. Furthermore, the study of different simplified edge shapes showed that its geometry influences abrasion behavior. This recommends geometric optimization of the filter plate edge underneath the filter medium in future.

With successful operation of the filter presses in terms of cake release and resistance of the filter medium to abrasive wear, increasingly fine particles are deposited in the pores of the filter medium over time. This effect is referred to as blinding. It results in an increase in pressure loss and the requirement of replacement or cleaning. An evaluation of different cleanings is the third part of this thesis. For three industrially used filter cloths affected by blinding, investigations were carried out into regeneration with water jets, various chemicals, and ultrasonic baths. Water jet cleaning is the industry standard. Permeability tests were used for the quantitative characterization. It was found that the investigated multifilament filter cloths can be successfully cleaned with water jets, while hydrochloric acid cleaning performs well for the monofilament. For water jet cleaning, a certain threshold value of jet flux and spraying time is necessary. Likewise, chemical cleaning shows a dependence on application time and concentration. Bases and ultrasound did not show significant improvements for any of the specimens. When the corresponding cleanings were applied at a moderate level, no significant damage due to regeneration was observed in the laboratory tests, but this risk is present if the procedure is too intensive. If cleaning with the water jet method is possible, it is competitive to a replacement of the filter medium in a simplified cost estimation. In addition, the cleaning of blinded filter media results in a significant reduction in the amount of plastic waste caused by replacement.

It is of enormous importance to consider tailings filtration as a process that represents a complex interaction of many different elements, including the problems that have been investigated in this work. This is since improving one of the issues usually has an impact on the others and increases their importance. Successful cleaning of the filter medium would, for example, require that abrasive wear becomes the determining factor in the timing of medium replacement. Consequently, an even more careful selection of the filter medium in terms of abrasion resistance is necessary. At the same

time, successful cleaning of the filter medium shows to have a positive effect on the continuity of filter cake detachment. Since the shear plane is in the layer affected by blinding, the accumulation of fines there with consequent stronger adhesion or cohesion is limited by regeneration. This holistic approach is pursued in this thesis, and the individual publications. Thus, their consolidation generates a benefit for further scientific work in this field, as well as for suppliers and operators of recessed plate filter presses in tailings filtration.

Zusammenfassung

Ziel dieser Arbeit ist es, verschiedene Probleme der Filtration von Tailings zu untersuchen. Die betrachteten Aspekte sind das Ablösen des Filterkuchens, der abrasive Verschleiß des Filtermediums durch die Kuchenablösung und die Verblockung desselben durch die permanente Einlagerung von feinen Partikeln. Hervorzuheben ist, dass die Filtration durch ein komplexes Zusammenspiel der unterschiedlichen Elemente charakterisiert ist. Deshalb generiert diese Dissertation einen zusätzlichen wissenschaftlichen Mehrwert, indem sie die Erkenntnisse der einzelnen Aspekte verknüpft.

Im ersten Teil dieser Arbeit zeigen Filtrationsversuche, dass für die untersuchten Tailings aus einer Eisenerz- und einer Kupfermine die Parameter des Filtrationsprozesses, vorrangig der Filtrationsdruck, der Differenzdruck zur Nachentfeuchtung mittels Druckluft, dem sogenannte Air Blow, und der Dauer des Air Blows gezielt die Eigenschaften des Filterkuchens gesteuert werden können. Für die Filtrationskammer der verwendeten Laborfilterpresse entwickelte Aufbauten an einer Zugmaschine ermöglichen an die Filtrationen anschließende Adhäsions- bzw. Kohäsionsversuche zur Charakterisierung dieser beiden Eigenschaften. Die Bestimmung der Restfeuchte und der Untersättigung erfolgte mittels darauffolgender thermischer Trocknung und Wägung. Die verschiedenen Filtermedien, die im Vorfeld in Zusammenarbeit mit dem Projektpartner ausgewählt worden sind und einen geeigneten Partikelrückhalt bei vertretbarem Druckverlust und Trübstoß aufweisen, zeigen im Labormaßstab keine signifikanten Unterschiede auf die Restfeuchte, die Untersättigung, die Adhäsion zwischen Filterkuchen und Filtermedium sowie die Kohäsion des Filterkuchens. Die Variationen der Prozessparameter Filtrationsdruck, Druck des Air Blows und Dauer desselben resultieren jedoch in signifikanten Unterschieden der Zieleigenschaften. Während die Restfeuchte und die Sättigung mit Zunahme der drei Prozessparameter sinken, erhöhen sich Adhäsion und Kohäsion. Restfeuchte, Untersättigung, Adhäsion und Kohäsion einstellen zu können, ist von größter Wichtigkeit bezüglich der nachfolgenden Prozessschritte sowie der Prozessstabilität und seiner Wirtschaftlichkeit. Aus diesem Grund wurde für die Untersättigung ein vereinfachtes mathematisches Modell entwickelt, welches in ausreichender Genauigkeit die Vorhersage der relevanten Größen in Abhängigkeit der Zeit des Air Blows ermöglicht.

Der auftretende abrasive Verschleiß des Filtermedium an hervorstehenden Stellen der Filtrationskammer durch Abgleiten des Kuchens ist ein weiterer Aspekt der Untersuchungen dieser Arbeit. Hierbei liegt der Fokus auf den verschiedenen Filtermedien, die alle aufgrund ihres Partikelrückhalts für die Filtration der Tailings geeignet sind, sich jedoch in ihrem Typus und Material unterscheiden. Mit Polypropylen und Polyamid erfolgten die Untersuchung zweier standardmäßig in der Tailings-Filtration eingesetzter Filtermedien. Es wurde eine Abrasionsapparatur entwickelt, die im Vergleich zu verfügbaren Geräten in der Lage ist, die für die Applikation spezifische Belastung nachzubilden. Aus den Ergebnissen ist ersichtlich, dass das Gewebe einen höheren Widerstand gegen Abrasion gegenüber dem Nadelfilz aus dem gleichen Material aufweist. Zusätzlich übertrifft das untersuchte Polyamidgewebe das Gewebe aus Polypropylen hinsichtlich der Anzahl an Belastungen bis zum Riss um ein Vielfaches. Die Evaluation unterschiedlicher vereinfachter Kantenformen zeigt, dass die Geometrie sich auf das Abrasionsverhalten auswirkt. Dies zeigt auf, dass zukünftig eine Optimierung der Geometrie der unter dem Filtermedium liegenden Filterplatten sinnvoll ist.

Bei einem erfolgreichen Betrieb der Filterpressen bezüglich der Kuchenablösung und des Widerstands des Filtermediums gegen abrasiven Verschleiß lagern sich mit der Zeit zunehmend feine Partikel in den Poren des Filtermediums ab. Dieser Effekt wird als Blinding bezeichnet. Der steigende Druckverlust, der daraus resultiert, erfordert einen Austausch oder eine Reinigung. Untersuchungen der Reinigung stellen den dritten Teil dieser Arbeit dar. Für drei industriell eingesetzte und vom Blinding betroffene Filtergewebe erfolgten Evaluationen zur Regeneration mit Wasserdüsen, verschiedenen Chemikalien und Ultraschallbädern. Die Düsenreinigung stellt dabei den industriellen Standard dar. Die quantitative Beschreibung erfolgte mittels Durchströmungsversuchen. Es zeigte sich, dass die untersuchten multifilen Filtergewebe mit Wasserdüsen erfolgreich zu reinigen sind, während das monofile Gewebe mittels Salzsäure am besten regenerierbar ist. Für die Wasserdüsenreinigung ist ein gewisser Schwellwert an Strahlstärke bzw. Flussdichte und Sprühzeit notwendig. Ebenso zeigt die chemische Reinigung eine Abhängigkeit von der Anwendungszeit und der Konzentration. Basen und Ultraschall zeigten bei keiner der Proben signifikante Verbesserungen. Bei Anwendung der entsprechenden Reinigungen in einem moderaten Maß konnte in den Laborversuchen keine signifikante Beschädigung durch die Regenerierung beobachtet werden, jedoch ist

diese Gefahr bei zu intensivem Vorgehen präsent. Falls eine Düsenreinigung möglich ist, ist diese in vereinfachter Abschätzung kostentechnisch kompetitiv zu einem Austausch des Filtermediums. Zusätzlich erfolgt durch die Reinigung von durch Blinding betroffenen Filtermedien eine signifikante Reduktion der Menge an Kunststoffmüll, die bei einem Austausch der Medien verursacht wird.

Von enormer Wichtigkeit ist es, die Tailings-Filtration als ganzheitlichen Prozess zu sehen, der ein komplexes Zusammenspiel aus vielen verschiedenen Elementen darstellt. Dazu zählen die untersuchten Probleme. Dies liegt darin begründet, dass die Verbesserung einer der Punkte Auswirkungen auf die anderen hat bzw. Ihre Wichtigkeit erhöht. Beispielsweise würde eine erfolgreiche Reinigung der Filtermedien bedingen, dass der abrasive Verschleiß den entscheidenden Faktor für den Zeitpunkt des Austausches darstellt. Daraus folgend ist eine noch sorgfältigere Auswahl des Filtermediums in Bezug auf den Abrasionswiderstand abzuleiten. Gleichzeitig zeigt eine erfolgreiche Reinigung des Filtermediums einen positiven Effekt auf die Kontinuität der Filterkuchenablösung. Da die Scherebene in der vom Blinding betroffenen Schicht liegt, ist die dortige Akkumulation von Feinstkorn mit daraus folgender stärkerer Adhäsion bzw. Kohäsion begrenzt. Dieser ganzheitliche Ansatz wird in dieser Arbeit verfolgt und generiert mit den einzelnen Publikationen und ihrer Zusammenführung einen Mehrwert für Zulieferer, Betreiber und weitere wissenschaftliche Arbeiten im Bereich von Kammerfilterpressen in der Tailings-Filtration.

Table of Contents

Acknowledgements	I
Abstract	III
Zusammenfassung	VII
1 Introduction.....	1
1.1 Motivation	1
1.2 Objectives.....	5
1.2.1 Cake Detachment	5
1.2.2 Filter Media Abrasion	5
1.2.3 Filter Media Blinding	6
1.3 State of the Art.....	7
1.3.1 Cake Detachment	8
1.3.2 Filter Media Abrasion	8
1.3.3 Filter Media Blinding	9
2 Background and Fundamentals.....	11
2.1 Filtration in Recessed Plate Filter Presses	11
2.2 Flow of a Fluid through Porous Structures in Filtration	14
2.3 Filter Media for Mining Filter Presses	16
2.3.1 Filter Media Characteristics.....	16
2.3.2 Filter Media Contamination	22
2.4 Properties of Tailings and Slurries.....	25
2.4.1 Mineral Composition	25
2.4.2 Particle Size Distribution	26
2.4.3 Rheological Behavior	27
2.5 Properties of Particulate Networks	29
3 Methods.....	35
3.1.1 Cake Detachment	35
3.1.2 Filter Media Abrasion	40
	XI

3.1.3	Filter Media Blinding	41
4	Filter Cake Detachment and Desaturation.....	43
4.1	Iron Ore Tailings Dewatering: Measurement of Adhesion and Cohesion for Filter Press Operation	43
4.1.1	Introduction	43
4.1.2	Theory.....	44
4.1.3	Materials and Methods.....	50
4.1.4	Results.....	54
4.1.5	Discussion.....	60
4.1.6	Conclusion	61
4.2	Copper Tailings Filtration: Influence of Filter Cake Desaturation.....	62
4.2.1	Introduction	62
4.2.2	Materials and Methods.....	66
4.2.3	Results and Discussion.....	72
4.2.4	Conclusions	79
5	Filter Media Abrasion.....	83
5.1	Tailings Filtration Using Recessed Plate Filter Presses: Improving Filter Media Selection by Replicating the Abrasive Wear of Filter Media Caused by Falling Filter Cake after Cake Detachment.....	83
5.1.1	Introduction	83
5.1.2	Material and Methods	87
5.1.3	Results.....	91
5.1.4	Discussion.....	96
5.1.5	Conclusions	96
6	Filter Media Blinding	99
6.1	Tailings Filtration: Water Jet Spray Cleaning of a Blinded Iron Ore Filter Cloth	99
6.1.1	Introduction	99
6.1.2	Materials and Methods.....	102

6.1.3	Results and Discussion.....	109
6.1.4	Conclusions	116
6.2	Regeneration Assessments of Filter Fabrics of Filter Presses in the Mining Sector.....	117
6.2.1	Introduction	117
6.2.2	Theory.....	118
6.2.3	Experimental Studies	122
6.2.4	Results & Discussion	128
6.2.5	Conclusions and Outlook	137
7	Conclusion.....	139
8	Outlook.....	145
	Symbols.....	149
	Latin Symbols	149
	Greek symbols	152
	Abbreviations.....	155
	List of Figures	157
	List of Tables	163
	Appendix.....	165
	A Additional Information to Chapter 4.2	165
	B Additional Information to Chapter 6.1	169
	B1 Silver Mine Filter Cloth Water Jet Cleaning.....	169
	B2 Gold Mine Filter Cloth Water Jet Cleaning	171
	C Additional Information to Chapter 6.2	173
	D Copyright Information of Industrial Filter Media Abrasion Image	174
	List of Publications, Presentations and Posters.....	175
	Journal Publications	175
	Conference Publications	175
	Presentations	176

Posters.....	177
References	179

1 Introduction

Continuous population growth, industrialization and electricity-based mobility lead to an increasing demand for commodities such as copper as well as higher mining rates [1]. Appropriate disposal of the huge amount of mine ore processing residue, so-called tailings, and water recovery are key safety issues and sustainability concerns. As a result, an optimization of tailings filtration in recessed plate filter presses is crucial.

1.1 Motivation

The necessity to optimize tailings filtration is particularly evident when considering the example of copper. In 2017, the global demand of approximately 24.4 million tons of copper was met mostly by a mine output of 20.4 million tons [2]. Figure 1-1 shows the production flowsheet of copper concentrate in a simplified way. It is based on the processing of porphyry deposits. They contain a low-grade ore, with a copper content of normally less than two mass percent [3], but also with around 60% the majority of the world's copper [4]. According to Mudd the daily production in a big mine can be assumed to be 270,000 tons per day [5, 6], of which two thirds are waste rock and deposited without further processing. The remaining 90,000 tons per day containing copper minerals and gangue are going through several comminution steps for processing. For ore dressing a high volume of water is needed during grinding and, especially, during flotation [7]. In total, process water of 114,000 tons per day is assumed [5, 6].

80% of sulfidic copper ores are concentrated using flotation, normally froth flotation [4]. By using reactants to adjust properties of the solids surface and the fluid, i.e., collectors, frothers, depressants and modifiers, the copper minerals are transported by air bubbles to the top of the flotation vessels. This froth contains the copper concentrate and between 25 to 40 w% process water [8, 9]. Most of the water within the concentrate froth is recycled by a filtration step. Approx. 10 w% concentrate water content, achieved by drying after filtration, is required for transport [10], e.g., for dust control [11]. Due to the low ore grade both solids and water mass of the concentrate are not significant in regard to total mass flow. The vast majority of milled rock which has now become tailings as well as most of the process water must be disposed. Comparing different commodities copper production generates nearly half of all tailings worldwide which was 9 billion tons in 2016 due to the combination of high demand, high production rate and low ore grade [12]. Gold and iron are subsequent in the volume of

tailings. Although significantly more iron is produced, an approximate ore grade of 30 % results in less tailings in absolute terms [13].

The classic approach of tailings management is pumping the suspension with a water content of typically slightly above 40 w% into a pond [8]. These are usually secured by dams consisting of waste rock characterized by coarse particle size. In contrast, the solids in the slurry typically have a particle size distribution with a high percentage of fines, which settle down slowly [14]. This directly results in various disadvantages. First, the large volume of solids and water leads to a significant area footprint [15]. Furthermore, due to evaporation, entrainment, and seepage issues only a small amount of water can be recirculated [8, 16]. In semi-arid regions the resulting recovery rate is around 40% [8].

Besides water recovery, embankment stability is a serious safety concern as dam breaks are regularly reported [5, 17, 18, 19]. Recent examples are:

- Ajka, Hungary 2010 (bauxite, 10 casualties, approx. 1 million m³) [19, 20],
- Mount Polley, Canada 2014 (copper and gold, approx. 25 million m³) [19, 21, 22],
- Brumadinho, Brazil 2019 (iron ore, 270 casualties, approx. 25 million m³) [19, 23].

This frequency is partly attributable to the fact that tailings are artificial granular materials not behaving exactly like ideal soil on which classical embankment stability approaches are based [24]. Often, apart from direct hazard by the impact of mud dam breaks these failures cause environmental contamination, e.g., heavy metals pollution [25, 26]. Also, seepage might be a source of problems in terms of mineral weathering resulting in acid mine drainage [27, 28].

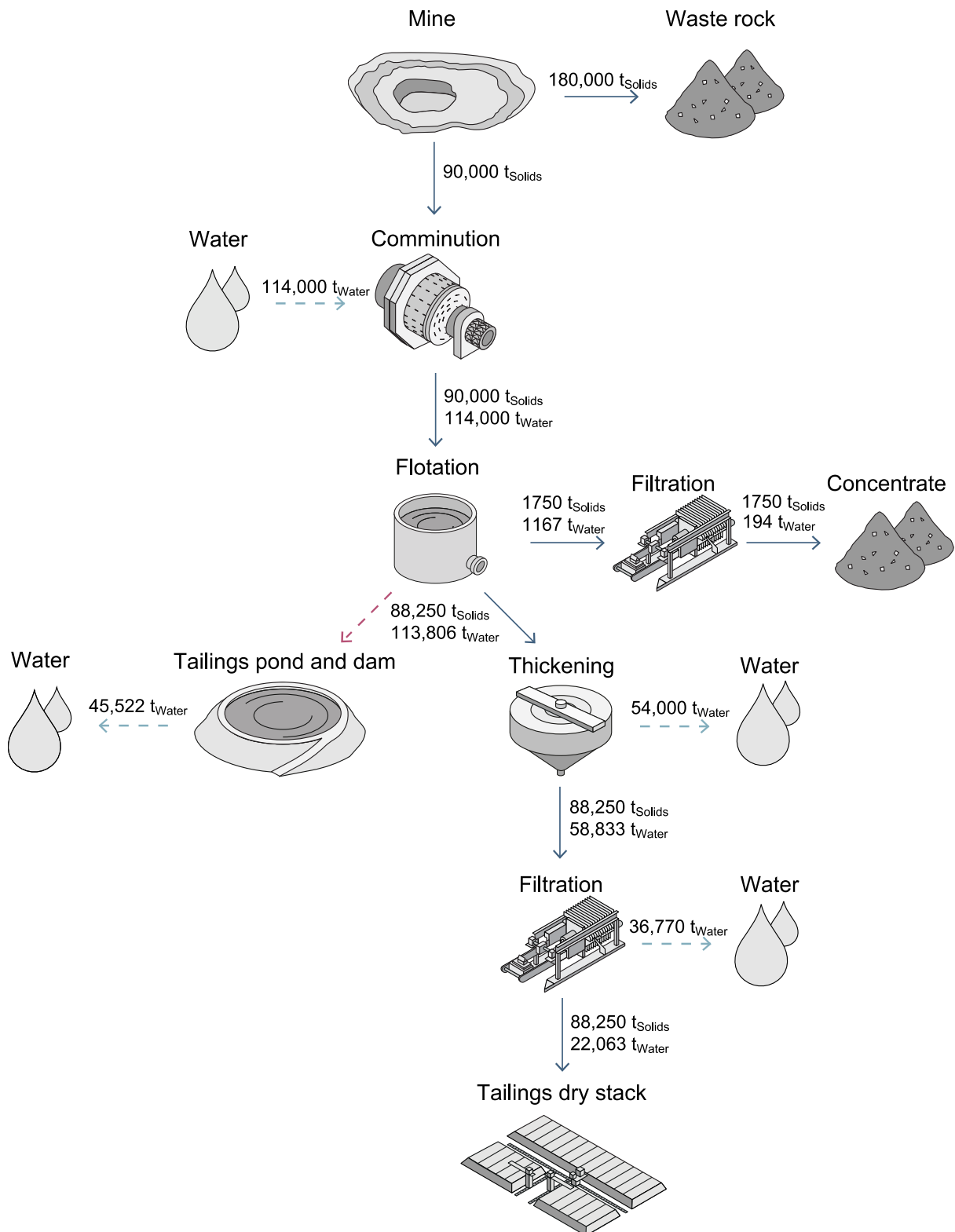


Figure 1-1: Simplified illustration of copper ore processing in a big scale mine including exemplary water and mass flows. Icons are extracted from [29, 30, 31]. Data and split ratios are based on [5, 6, 8, 9, 10, 32].

In the last decades tailings storage facilities (TSF) regulations became more stringent due to increasing global attention towards embankment failures. After the brumadinho dam disaster 2019 the global tailings review, an initiative to develop a new standard

on tailings management best practice was co-convened by the International Council on Mining and Metals, the United Nations Environment Programme, and the Principles for Responsible Investment [33]. The resulting standard was introduced in 2020 [34] and other initiatives followed [35]. They encourage mine owners to use other tailings management approaches with improved social acceptance, reduced water disposal and safer storage.

Further dewater processing is more challenging but generates benefits concerning disposal safety and reduction of water costs, the latter especially in arid regions [36]. Common possibilities are thickened or paste tailings [37]. This approach enables the controlled and enhanced sedimentation of the solids by using thickeners and slurry treatment, e.g., with flocculants. While these techniques can handle high mass flows, alternate approaches are restricted by comparably small scales [38]. After thickening, solid contents of 60 w% solids are common and limited by allowed yield stress for pumping. At this point the area footprint is reduced, the storage safety enhanced, and the water recovery rate already improved but in general the dewatering is not yet sufficient. As an additional operation, a filtration step can be used to further reduce the water content of the slurry [39, 40]. This is usually realized by pressure filtration in recessed plate filter presses. The main advantages of this technique are the high throughput and the possibility to apply sufficiently high pressure for dewatering of tailings characterized by fines and clay minerals [41]. Even in moderate tonnage applications several fast-filtering filter presses are needed each of them working in batch operation. Eventually, the required water content of approximately 20 w% can be reached [32]. This water content is optimized for tailings transportation on conveyor belts and dry stacking. Additionally, it results in a small footprint paired with a high geotechnical stability and a big water recovery rate. Especially the undersaturation of filter cakes by pressurized air desaturation inhibits liquefaction of the stack [37].

1.2 Objectives

Even if a selected filter medium fulfills the separation task in terms of particle retention, operation of tailings filtration plants is a challenging task. To ensure the best performance a holistic understanding of the filtration process in recessed plate filter presses is required. Figure 1-2 shows a sliding filter cake (brown) in front of the adjacent filter plate (white). The plate is covered with a filter medium (beige), which is discolored in the filtration area by adhering particles (lighter brown). In addition, the main and most frequently occurring difficulties are depicted. Achieving the required target water content as well as predicting cycle time including filtration and technical time correctly is very important. The latter is strongly affected by cake detachment behavior. In addition, the handling of cloth lifetime related issues like abrasive wear or blinding by adhering particles is crucial [42, 43]. The objectives of the investigations in this dissertation are to improve the understanding of these problems and to provide guidelines and recommendations.

1.2.1 Cake Detachment

For maximized throughput, target water content and cake saturation level must be reached as fast as possible, e.g., by pressurized air cake post-treatment. Moreover, it is beneficial to reduce technical downtime by a good and complete cake detachment which depends on cake to cloth adhesion and cake stability. These aspects are investigated in two publications: A first paper using iron ore tailings determines the basic relationships [44]. In a subsequent second publication this is supplemented by experiments with copper tailings and a detailed examination and mathematical description of desaturation kinetics [45]. The presented results provide guidance for process parameter optimization to improve cake detachment.

1.2.2 Filter Media Abrasion

The detaching cakes result in abrasive wear of the filter medium mainly at protruding points of the plate. In detail, these are the stay bosses and the sealing edge. Especially the geometries and the material of the overlying filter medium is of importance. The development of an apparatus which replicates the specific direction-dependent load case and investigations on various filter media were published and are part of this work [46]. Recommendations are provided to increase the number of filtration cycles until abrasive wear hampers further usage of the filter cloth.

1.2.3 Filter Media Blinding

During the high number of filtration cycles fine particles adhere permanently to the fibers and blind the pores of the filter medium. This leads to an increase in flow resistance which at a certain point culminates in the necessity to replace the filter media due to unacceptable prolongation of filtration time. Improvement of this intra-fabric contamination can be achieved by adequate cleaning procedures. Investigations were carried out for various industrially used and blinded filter fabrics, resulting in two publications, one on high pressure water jet and the other on chemical cleaning methods [47, 48]. The presented results provide guidance for cleaning procedure selection.

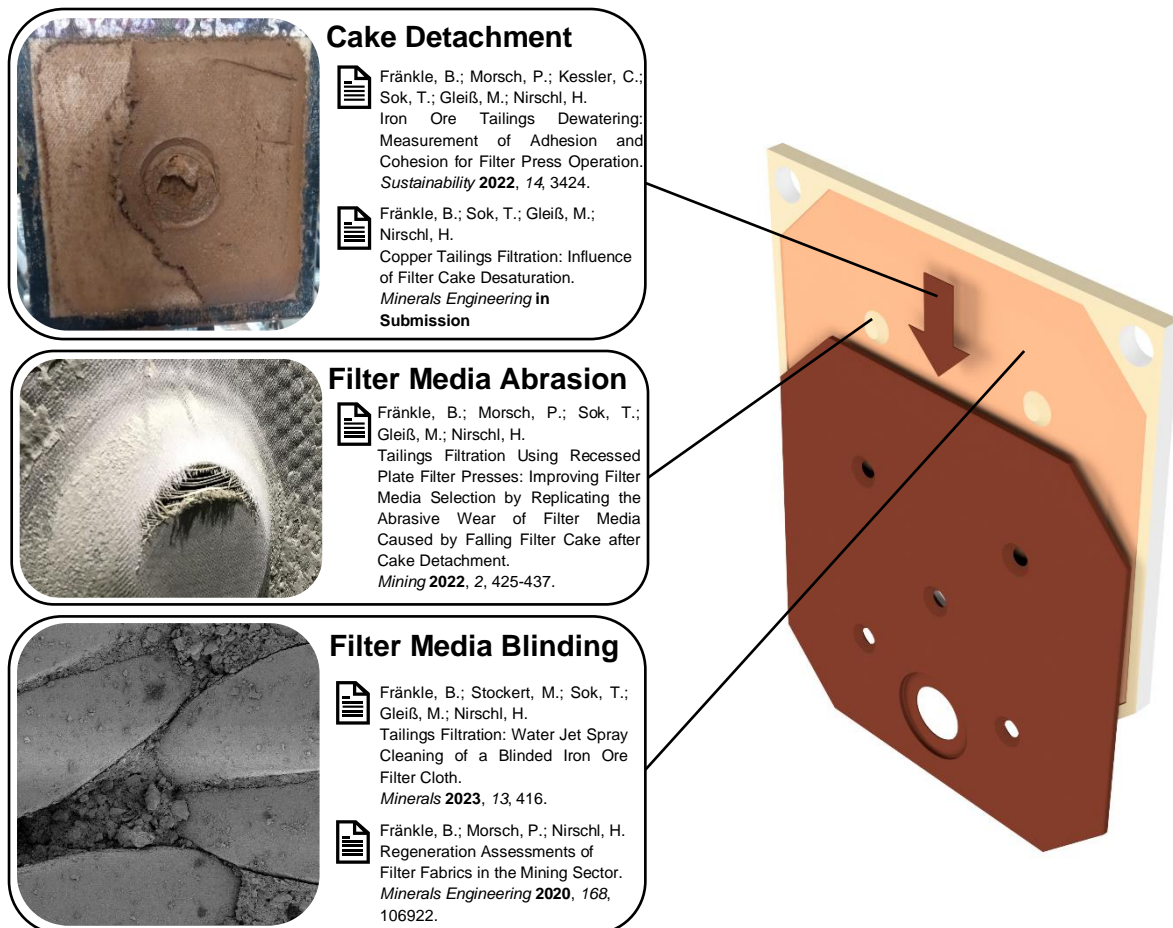


Figure 1-2: Overview of the investigated problems of tailings filtration in recessed plate filter presses. The illustration shows a sliding filter cake (brown) in front of the filter plate (white). The plate equipped with a filter medium (beige), is discolored by adhering particles in the filtration area (lighter brown). Filter cloth abrasion image: ©FLSmidth.

1.3 State of the Art

Due to the immense importance of raw materials, mining and ore processing for society, tailings and related topics are a frequent subject of research. However, the research directions are wide-ranging. Tailings management is one key aspect. One approach is to reduce residue production by optimized mining or better flotation methods [49]. Concerning surface storage and tailings dams, geotechnical properties have been widely studied [36, 50]. This includes strength of tailings [24] or blends of tailings and waste rock [51].

Furthermore, monitoring methods of the embankments are continuously improving [52]. Additionally, the geochemical behavior, heavy metal containment and the associated impact on the environment, wildlife and society are subject of publications [21, 53]. These aspects are often investigated as a consequence of dam failures. Another research aspect is the reuse of existing and growing tailings deposits to reduce their volume while creating a benefit [54]. One example in the context of underground mining is the usage of a mixture of tailings and cement for mine backfill. Furthermore, older tailings can contain valuable substances, the extraction of which has become either interesting or economical. The latter through improved or new processes, such as bioleaching [55]. As a result, tailings become secondary sources of raw materials, the advantage of which is that an energy-intensive comminution process has already taken place. The remediation and the use of the tailings, for example as construction material or raw material for other products [26], are additional aspects. Furthermore, there are approaches to store CO₂ in tailings as carbonates by artificial weathering [56].

While thickening and related aspects, such as flocculation, have been specifically studied for a longer time [36, 57], filtration of tailings became a focus of research especially in the last decades. The reasons for the increasing interest in filtration are the tightening of regulations and an increasing need for water recovery. Therefore, an increase in the number of case studies is reported which is dominated by studies allowing for higher mass flows [50, 58]. Also, problems with longer operation of the plants are increasingly present whereby the filtration of the tailings or the overall process is often considered from an economic perspective [59]. Despite these scientific advancements, a transfer gap between the existing knowledge on filtration technology and the particular translation to tailings applications remains. In particular, this includes

a lack of specific investigations on tailings related process parameter optimization and filter media behavior, which represents the primary motivation behind the present work. The subsequent sections elude in more detail the remaining knowledge gaps for the three considered process elements, namely cake detachment, filter media abrasion and blinding, individually and highlight the contribution of the present dissertation.

1.3.1 Cake Detachment

The detachment of the filter cake is crucial in any application of filtration. Therefore, different authors dealt with the adhesion of the filter cake to the filter medium in solid-liquid filtration for various particle systems apart from tailings. Examples are Ginisty [60], Morris [61], Morsch [62, 63, 64, 65, 66], Möller [67], Müller [68], Ward [69], and Weigert [70, 71, 72, 73, 74, 75]. The same applies for studies on the stability of particulate networks [76, 77, 78, 79, 80]. Additionally, these investigations focus on the impact of surface cleaning on cake detachment. In more detail, Morsch considered the detachment behavior of filter cakes on a candle filter in relation to various model systems, the curvature of the filter fabric, and the surrounding medium. An important aspect in his investigations on surface cleaning was the application of backwashing of candle filters which is not transferable to filter presses where the shear adhesion is to be overcome by gravitation. In contrast to the work conducted by Morsch, this thesis covers the relevant aspects for filter presses. In more detail, this thesis goes beyond the investigation of surface cleaning by evaluating the influence of multiple process parameters specific to filter presses, i.e., gas differential pressure desaturation.

1.3.2 Filter Media Abrasion

Abrasive wear of the filter medium is one of the major problems in tailings filtration. Besides blasting at areas of high flow velocities [42, 81], friction of the falling cake on protruding parts of the filter press causes damage [82]. Since the suppliers and literature only make a rough categorization of the wear resistances, further characterization is required to identify potential optimization opportunities. In particular, the combination of the fabric's direction-dependent properties due to weaving with repetitive stress in one direction are not adequately covered by standardized test methodologies available and used in other publications [83, 84, 85]. Thus, the apparatus invented for replicating a direction-specific load on the filter media, as presented in this dissertation, opens up new ways for process optimization. This innovative approach is specifically designed for tailings filtration in recessed plate filter

presses and, in particular, allows for advanced filter cloth selection and plate design optimization.

1.3.3 Filter Media Blinding

The increasing blinding of filter media with fines is a well-known problem in filtration technology [86, 87]. However, there is hardly any published knowledge regarding mining applications [88]. Experience lies mainly with operators and suppliers. In general, cleaning is carried out by means of water jet nozzles [43, 89, 90]. These are more familiar from surface cleaning in other industries [91]. For example, Morsch investigated the surface cleaning for beer mash filter press media [66, 92, 93]. However, the focus was primarily on the detection of contamination by means of image evaluation and the dirt was only applied artificially. Furthermore, only surface cleaning by low pressure water jets was analyzed. This was also subject of investigations performed by other authors in the food sector [91, 94]. Previous work on intra-fabric regeneration used flow from different directions and pulsation [95]. Lam evaluated high pressure water jet cleaning for membrane fouling by algae showing promising results for intra-fabric cleaning [96]. In conclusion, previous research in the field of water jet cleaning has primarily focused on investigating surface effects. Additionally, there is a lack of data on tailings filtration and industrially blinded mining filter cloths. Therefore, this dissertation aims to fill this knowledge gap by evaluating the impact of water jet cleaning on intra-fabric blinding in fabrics previously used in tailings filtration. The findings of this thesis are of significant importance to the mining industry, as they provide new insights and advancements. Additionally, this study offers fabric type- and material-dependent recommendations and analyzes the potential damage caused by the cleaning process on the filter cloths.

2 Background and Fundamentals

The dewatering of suspensions by recessed plate filter presses is an established process that is utilized in many applications [97]. To optimize the design and operation of such equipment, it is crucial to understand the handled materials (e.g., tailings), the process requirements such as total volume flow rates, and the underlying process fundamentals. The latter include the flow of fluids through porous structures and the properties of solid-liquid mixtures, which range from suspensions to particulate semi-solid structures, as the solids volume content increases.

2.1 Filtration in Recessed Plate Filter Presses

Figure 2-1 shows the principal steps during operation of a recessed plate filter press which is a pressure filter using cake filtration. Normally, a filter press in tailings filtration consists of a stack with more than 100 plates of relatively large dimensions, e.g., 2.5 m × 2.5 m [36, 98, 99]. The illustrations show a cross-sectional view of two adjoined plates in the middle of the stack, orientated longitudinal to the feed direction of the press. In general, a plate consists of protruding stay bosses for mechanical stability of the stack and protruding edges which generate a chamber for cake build up. Furthermore, each plate has a drainage structure usually consisting of small pips and inside pipes for filtrate transport to the corner ports. For simplicity, the filtrate pipes and corner ports are projected to the cross-sectional plane depicted in the illustration. In addition, each plate has a feed hole for slurry distribution within the stack which is normally located below or above the center in tailings application.

Each side of each plate is equipped with a filter medium. In general, plastic cloths or needle felts are used for mining applications [100]. Critical spots concerning sealing function and abrasive wear are the sealing edge, the stay bosses, the filtrate holes, and the filtrate pipe regions. At the beginning of the process all chambers are empty, and a pump fills the press with the thickener underflow (Figure 2-1a). By using a low inlet position a relatively even rise of the slurry level can be assumed.

Once the press is filled, further feeding increases pressure. The occurring differential pressure between the chamber and the filtrate drainage structure results in a flow of the liquid through the filter medium.

Usually in cake filtration, the pores of the cloth or needle felt are bigger than the suspended particles in the slurry and some of them pass the medium in the beginning

of filtration. However, if the solid concentration in the slurry is sufficiently high multiple particles reaching the same pore at the same time interfere and block each other. This is called particle bridging and is the essential pre-condition for cake filtration [87]. Later arriving particles are not able to pass the smaller pore structure between the already immobilized particles. Consequently, the filter cake builds up on both sides of the chamber at both filter media (Figure 2-1b).

While the filtration proceeds both cakes grow until they touch in the middle and fill the entire chamber with a particulate network. Cake porosity and conformity depend on the particle system properties, especially compressibility. A compressible cake has a denser particulate network the closer to the filter medium. In general, particles below 10 μm form compressible cakes [101]. Tailings having a high fraction of fines, but also bigger particles, can be assumed as slightly compressible [44]. By continued feeding, further compression occurs for compressible cakes. An equilibrium between water drainage caused by increase of pore water pressure and consolidation caused by the residual effective stress can be assumed based on Terzaghi's principle [102].

Often, the resulting water content of the cakes (i.e., when the voids are fully saturated), is not sufficiently low for transportation and stacking. For example, the concerning cake properties for detachment, e.g., shear and tensile strength of the cake are too low and shear and tensile adhesion of the cake to the filter medium are too high. In this case, further dewatering can be achieved with a gas differential pressure cake post-treatment. To be more precise, this application reduces the saturation of the water-filled voids within the particulate network. The saturation S is defined based on the volume of water-filled voids $V_{v,\text{water-filled}}$ and the total voids volume $V_{v,\text{total}}$ according to Equation 2-1. For this reason, the related process is more accurately described as desaturation.

$$S = \frac{V_{v,\text{water-filled}}}{V_{v,\text{total}}} \quad \text{Equation 2-1}$$

Figure 2-1c) illustrates the gas differential pressure dewatering, also referred to as air blow. For this application, two different types of plates are mounted alternately in the stack. One type of plate allows pressurized air to be introduced over the filtrate holes and the drainage structure, while the connection to the filtrate pipes is closed. This allows the air to dewater certain pores based on the capillary inlet pressure distribution of the filter medium and the pore structure of the cake. The air passes through one

cloth, the cake, and the adverted cloth. The adjacent plate, which is still connected to the filtrate pipe, is used to remove any remaining filtrate via its drainage structure.

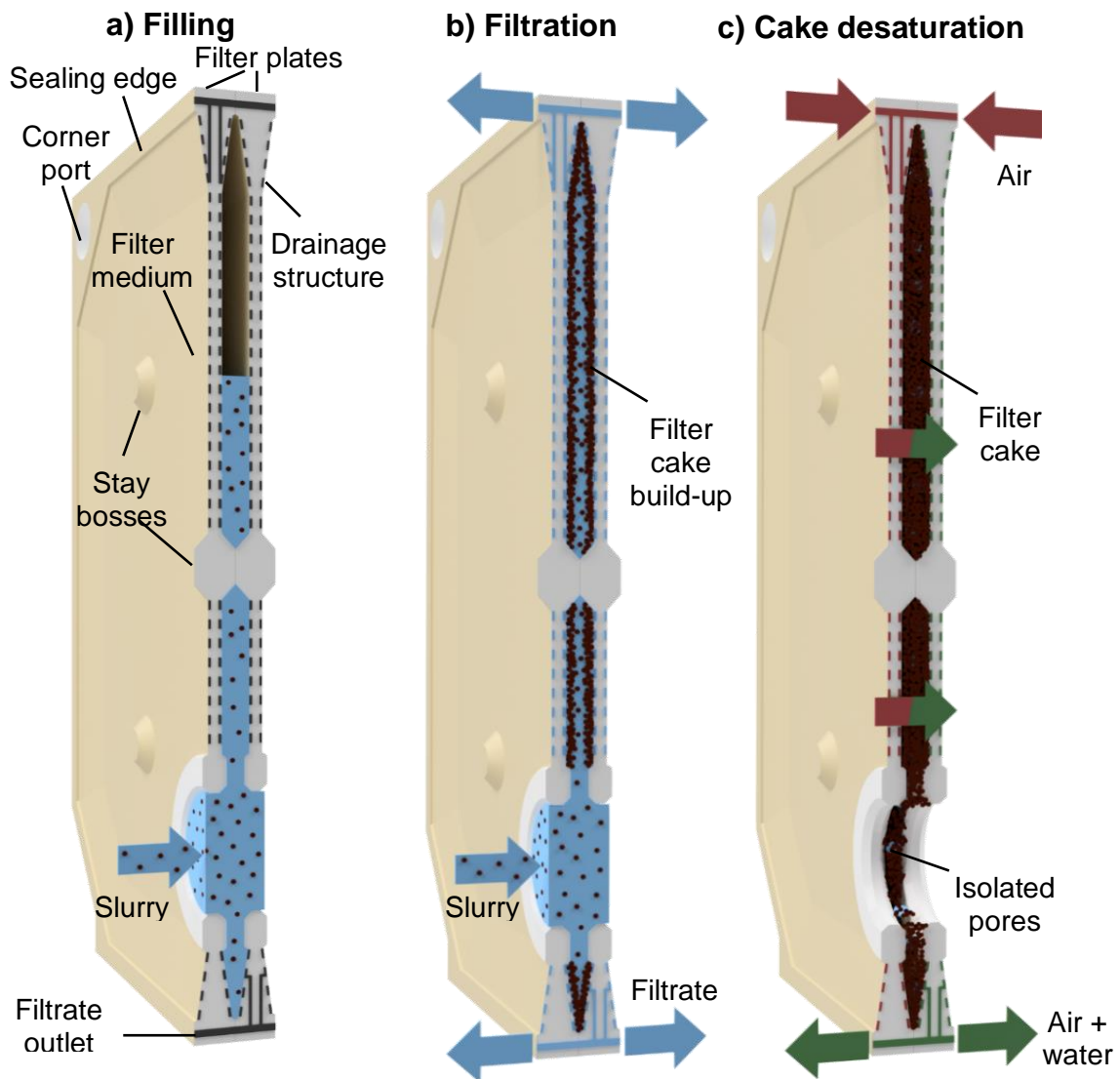


Figure 2-1: Simplified illustration of filtration steps in a recessed plate filter press using a cross-sectional view of two plates and one chamber in the middle of the plate stack: (a) During filling slurry level rises; (b) Differential pressure between cake and filtrate drainage system generates a liquid flow through the filter medium and a cake build-up by retained particles; (c) For further water content reduction pressurized air is introduced into the filtrate pipes of every second plate. By overcoming capillary inlet pressure desaturation of the cake is carried out.

When the biggest pore is emptied a gas-breakthrough occurs leading to a decrease in desaturation performance and an increase in air consumption. Furthermore, operation time and air pressure are crucial parameters of the post-treatment. In addition, besides too high capillary inlet pressures, isolated pores significantly limit the achievable water content [87]. After completion of the post-treatment, the plate stack opens, and the filter cake is supposed to detach and fall.

2.2 Flow of a Fluid through Porous Structures in Filtration

The flow through porous structures is of enormous importance in many applications. Explicitly, it plays a decisive role in filtration, which aims to fulfill a separation task with the lowest possible energy consumption [103]. Therefore, knowledge about the flow resistances of the filter medium and the filter cake is crucial. Both individually and their combination, which determines the resulting total resistance during filtration, can be regarded as porous structures.

A porous structure is a combination of void volume V_v and an interconnected solid phase V_s . This connection can either be solid itself or build up by contacts between individual solid elements. Particulate structures are an example of the latter. A characteristic value for such structures is the ratio of the void volume to the volume of the solid phase or the total volume. In filtration technology, the porosity ε is used for this purpose. It is defined as follows:

$$\varepsilon = \frac{V_v}{V_s + V_v} \quad \text{Equation 2-2}$$

For laminar flows, the velocity of the flow of porous structures is described by the so-called Darcy's law according to Equation 2-3 [104, 105]. The velocity v_{total} describes the volume flow \dot{V}_{total} in relation to the area A_{total} . Experimentally, \dot{V}_{total} is usually determined by the mass flow \dot{m} and the density of the liquid ρ_l . Decisive for the flow is the pressure difference Δp , the dynamic viscosity of the liquid η_l , the length L of the structure in the direction of flow and a structure-specific parameter P , the permeability.

$$v_{\text{total}} = \frac{\dot{V}_{\text{total}}}{A_{\text{total}}} = \frac{\dot{m}}{\rho_l \cdot A_{\text{total}}} = \frac{P \cdot \Delta p}{\eta_l \cdot L} \quad \text{Equation 2-3}$$

The resulting velocity v_{total} refers to the position outside the structure rather than the velocity inside the voids v_v . It is higher due to the reduction in the flow area resulting from the porosity ε , as stated in Equation 2-4.

$$v_{\text{total}} = \varepsilon \cdot v_v \quad \text{Equation 2-4}$$

Processes in filtration technology are usually described with the reciprocal value of the permeability P , the so-called flow resistance R [105, 106].

$$R = \frac{1}{P} \quad \text{Equation 2-5}$$

In wet cake filtration, several combined resistances must be considered, as is stated in Equation 2-6. The total time-dependent resistance $R(t)$, is a combination of the filter medium resistance R_{fm} , which is constant over time, and the resistance of the growing cake $R_c(t)$, which changes over time according to cake height.

$$R(t) = R_{fm} + R_c(t) \quad \text{Equation 2-6}$$

One crucial aspect to consider is that the filter medium resistance describes the interaction of the filter medium with the particle system. Thus, it is characterized by the combination of filter medium and the first particle-bridging cake layer. By contrast the permeability of the filter medium as specified by the manufacturers is independent of the separation application. Therefore, the filter cake resistance is described by the sum of the flow resistance of the unused filter medium $R_{fm,unused}$ and a so-called reference resistance R_{in} , as can be seen in Equation 2-7 [66, 106].

$$R_{fm} = R_{fm,unused} + R_{in} \quad \text{Equation 2-7}$$

The filter cake resistance is usually defined by the product of a height-specific filter cake resistance α_h and the time-dependent cake height $H_c(t)$ (see Equation 2-8). α_h is a quantity describing the particulate network, which is constant for incompressible networks. $H_c(t)$ increases during filtration, and, thus, it is time dependent.

$$R_c(t) = \alpha_h \cdot H_c(t) \quad \text{Equation 2-8}$$

The filter media resistance and filter cake resistance parameters can be obtained from filtration tests in accordance with VDI guideline 2762 and a linearized fit [87, 105, 107]. Among other things, this allows to compare different filter media for the same application. For the explicit equations and their derivation, please refer to the work by Morsch [66].

The cake resistance in compressible particle systems varies depending on the filtration pressure. A rough guideline is that compressible behavior occurs in systems that have a significant proportion of particles smaller than 10 μm [101]. However, it must be noted that not only the overall resistance of the particulate network changes, but that the resistance is different significantly in different heights of the filter cake. Layers on the filter medium become more compressed, their porosity decreases and their resistance increases [87].

2.3 Filter Media for Mining Filter Presses

Choosing the right filter medium for a particular application can be difficult. This is true also in mining, where the specific needs of the process and the filtration equipment used must be taken into account. For instance, the requirements for removing water from the concentrate will be different from those for processing tailings. As a result, there are many factors to consider beyond just the main characteristics of the filter medium and the separation task. These factors also include considerations of cleaning and wear properties.

2.3.1 Filter Media Characteristics

The main function of the filter medium is to retain particles while minimizing the energy required to overcome the resulting flow resistance [101]. As an essential component of solid-liquid separation, the filter medium represents the interface between the filtration apparatus and the suspension, and its correct selection is of enormous importance for efficient operation in terms of energy and process considerations [87]. Especially the increased availability of synthetic filaments and fabrics in the second half of the 20th century, catalyzed research in solid liquid separation and related fields focusing on the filtration properties of filter media and their appropriate selection for a specific process [86].

Due to the relevance and complexity of the task that is fulfilled by the filter medium, a variety of properties must be considered and evaluated during its selection. Purchas and Sutherland specify several priority properties divided into the following three main categories [86, 108]. Several of the most important examples are given for each category.

- Machine-oriented properties
 - Rigidity
 - Strength
 - Resistance to abrasion
 - Available sizes
- Application-oriented properties
 - Chemical stability
 - Thermal stability

-
- Cost
 - Wettability
 - Filtration-oriented properties
 - Size of smallest particle retained
 - Retention efficiency for a specific size
 - Resistance to fluid flow
 - Tendency to blind

The selection of a medium in cake filtration is primarily based on filtrations in standardized laboratory apparatuses, e.g. a pressure housing according to VDI guideline 2762 [109] or similar devices [110]. Mainly particle retention and flow resistances are determined. Concerning the resistances three aspects can be distinguished: permeability of the filter medium (measured using non-particle-loaded liquid), filter medium resistance (also called β -value, includes permeability and interference with the first particle layer) and height- or mass-specific filter cake resistance (also called α -value). These measures represent the primary characteristics of a filter medium and a filtration task. The pore size should be as small as necessary to ensure the clarity of the filtrate and the permeability of the filter medium should be as large as possible to keep the flow resistance low. For a specific application, various filter media pre-selected based on experience are compared. However, each medium is only subjected to a small number of filtration cycles during lab testing, which does not necessarily correspond to the industrial service life. With the aid of material parameters, e.g. chemical and mechanical stability, as well as application-related empirical values or case studies, the findings obtained are transferred to the filtration cycle numbers relevant in industry [87, 97, 105, 111, 112], some of which are in the four-digit range [43]. The adaptation to an optimized medium is only made iteratively during the operation of a plant.

The relevance of cake filtration in a variety of applications results in a large market across a wide range of industries. One example is the enormous demand of filter cloths in the mining industry. In larger mines (97,000 t ore per day of the Minera Esperanza Antofagasta in Chile [113]) parallel operation of several filter presses is mandatory [36]. A press in tailings filtration has usually plate dimensions of at least 2 m × 2 m and a plate pack of sometimes more than 100 plates [114, 115]. Since an enormous flow of

waste rock must be handled, the presses are highly optimized regarding their cycle time, which means that a four-digit number of filtration cycles is already achieved within one to two months. Each inner plate of the package is equipped with a filter medium on both sides, which, with an area per plate of 8 m², results in an approximate total area of 800 m² per press. This enormous area results in high five-digit US\$ sums per change and a six-digit US\$ sum for the replacement of the wear material filter medium for each individual press per year [100].

In more detail, the operation of these tailings filtration plants is a challenging task in regard to filter media concerns especially because of the complexity of cloth lifetime related issues. These include abrasive wear, blinding by adhering particles [46, 47, 48, 42, 43] and necessity for good cake detachment characteristics for maintaining high throughputs [86]. Additionally, these aspects are subject to a complex interplay. Thus, improvement of one cause of damage may allow one of the other lifetime limiting factors to become determinant. It can be stated that elongation of service life of the filter medium through better knowledge of the long-term behavior and the associated improved selection have a direct effect on the operating costs and the amount of plastic waste.

In the mining sector, woven filter media and needle felts, typically composed of polypropylene or polyamide, are predominantly used [86, 100, 116, 117]. However, there are also some applications of ceramics, for example in the iron ore sector [88]. Figure 2-2 shows examples of a needle felt and a woven filter medium suitable for tailings filtration. The needle felt is characterized by proportionally smaller and unoriented fibers. This reduces their mechanical and chemical resilience even for identical materials. To produce felts, several layers of fibers are formed into a bulky web, which is then compressed. Subsequent needling is applied to entangle the fibers and further reduce the thickness.

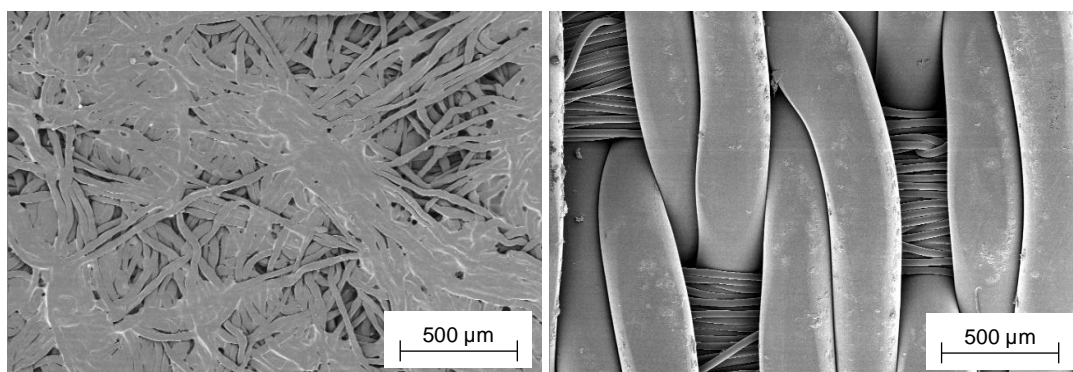


Figure 2-2: SEM-image of a needle felt (left) and woven (right) tailings filtration filter medium.

In contrast, the woven consists of different fiber types and relatively large yarn diameters. One aspect of distinguishing woven filter media is the fiber type. There are three categories:

- Monofile
- Multifile
- Staple

Monofilament fibers consist of single, continuous filaments, multifilament fibers, on the other hand, are composed of several smaller filaments. Staple yarns are made from spun or twisted short filaments.

In addition to the yarn type, cloths differ in the way they are bonded. The binding system is created during the weaving process. A so-called weft fiber is shot vertically through several warp threads lying next to each other. Depending on whether the warp threads are in front of or behind the weft thread, and how their orientation changes before the next weft thread is inserted, a specific binding system result. Figure 2-3 shows the three main weave types plain, twill and satin [118]. Together with the type of yarns used, the binding system is decisive for the size and distribution of the pores. The weave types (and their derivatives) are characterized by their smallest repeating unit [119]. Plain weave is the simplest arrangement. The weft fiber is woven above and below the warp yarns alternatingly (Figure 2-3a). It is also possible to have multiple yarns grouped, for example, a double warp yarn instead of weaving one singly. The plain weave is relatively rigid [86]. Furthermore, it consists of relatively large threads and, thus, also pores, which is why other weave types must be used for smaller sizes [120]. In twill weave, the weft yarn skips at least two warp fibers (Figure 2-3b). Compared to the plain fabric a twill structure is more flexible which is beneficial for fitting them into a certain geometry, e.g., a filtration apparatus. This is even more pronounced with the satin weave. As can be seen in Figure 2-3c, in this bonding system type a weft yarn skips at least two warp fibers. However, it is a prerequisite that the wraps are not directly adjacent. It has the highest flexibility and the smoothest surface.

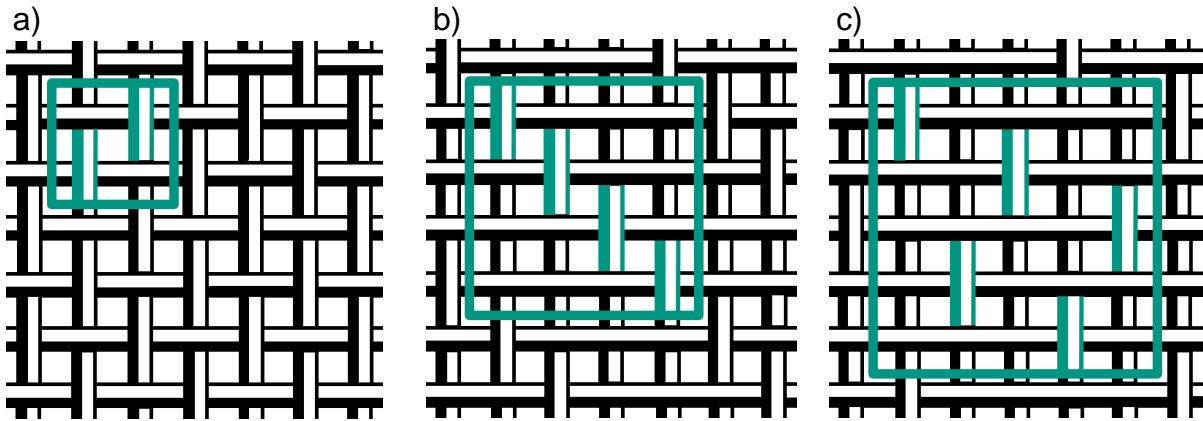


Figure 2-3: Schematic representation of main weave structures a) and their characteristic repeating unit (green): a) plain weave, b) twill weave and c) satin weave.

Table 2-1 lists the fiber and fabric types according to their suitability related to specific aspects of filtration technology [86, 121]. For an explicit separation task, various advantages and disadvantages of a bonding structure type must be considered and, usually, a compromise is chosen. For example, the long float of the fibers of a satin weave on one side produces a very smooth surface, which is a benefit for cake release, but at the same time this reduces the resistance to abrasion [86].

Table 2-1: Ranking of the different types of fibers and fabrics according to their performance in various aspects of filtration technology [86] based on [121].

		Particle retention	Permeability	Cake dewatering	Cake discharge	Fabric life	Resistance to blinding
Fiber Type	1	Staple	Monofil	Monofil	Monofil	Staple	Monofil
	2	Multifil	Multifil	Multifil	Multifil	Multifil	Multifil
	3	Monofil	Staple	Staple	Staple	Monofil	Staple
Weave type	1	Plain	Satin	Satin	Satin	Twill	Satin
	2	Twill	Twill	Twill	Twill	Plain	Twill
	3	Satin	Plain	Plain	Plain	Satin	Plain

The chemical, thermal and mechanical properties are usually related to the material data of the starting materials of the fibers. Exemplary data for the discussed materials polypropylene and polyamides from Purchas and Bremus can be found in Table 2-2 and Table 2-3 [108, 122]. These data are consistent with those from fabric manufacturers and permit a rough classification [116, 123]. Ductile-elastic behavior can be considered as beneficial for wear resistance [124]. It must be noted, however, that the complexity of plastics technology and the resulting variants (crystallization

state, copolymerization, etc.) make it necessary to consider each material and application individually.

Table 2-2: Chemical properties of polypropylene and polyamide graded as poor, fair, good, or excellent [86, 122].

	Polypropylene	Polyamide
Mineral acids	Excellent	Poor
Organic acids	Excellent	Fair
Alkalis	Excellent	Excellent
Oxidizing agents	Fair	Fair
Organic solvents	Fair	Good

Table 2-3: Selected mechanical and thermal properties of polypropylene and polyamide graded as poor, fair, good, or excellent [86, 122, 125].

	Polypropylene	Polyamide (Nylon)
Resistance to wear	Good	Excellent
Elongation at break / %	15-35	30-70
Safe continuous temperature / °C	120	105-120

Post-processing is a crucial step in the production of woven and nonwoven filter media. In addition to quality control regarding possible defects, this also includes possible cleaning or decolorization as well as a targeted adjustment of the properties. The latter can be divided into the three aspects of stabilization, adjustment of the surface properties and modification of the permeability [126]. Stabilization primarily means releasing stresses that have arisen during production, through thermal treatment or targeted pre-loading in a controlled environment. A further approach for stabilization can be the production of composite meshes, in the case of metal fabrics, for example, by sintering a filter mesh with one or more support meshes. In some cases, direct combination during weaving is possible. Examples of surface modification are coating or singeing. The latter means the removal of protruding fiber parts (from staple fibers or nonwoven) by means of a flame or hot surfaces. The permeability is usually adjusted via the so-called calendering. In this process, heated rollers apply pressure to the filter medium as it passes through. Both singeing and calendering smoothen the surface of the filter medium, which has a positive effect on cake discharge behavior [65, 71, 86].

In a holistic view, which includes the economic operation of a filtration plant, costs play an important role. Especially for mining applications, this must be considered, due to the significant wear which result in a need for filter medium replacement and operating expense. For this reason, Table 2-4 relates the costs of the filter media relevant for mining based on literature data [86]. For example, while polypropylene is outperformed by polyamide regarding abrasion properties it benefits from lower costs. Thus, it becomes clear once again that a complex case-by-case consideration is necessary regarding cost effectiveness, operational reliability, waste quantity and downtimes.

Table 2-4: Relative cost of polypropylene and polyamide filter media [86].

	Polypropylene	Polyamide
Needle felt	1.0 ± 0.1	1.1 – 1.7
Woven (multifilament)	0.9 – 1.3	1.1 – 1.7
Woven (staple)	1.1 – 1.7	1.3 – 1.9

Due to the aspects mentioned and, in addition, the possibility to vary the diameters of the filaments, it becomes obvious that there are a multitude of possibilities to produce a filter medium. This is reflected in the large number of media available and, also, the number of manufacturers. However, this allows to select a medium optimally adapted for a specific separation task.

2.3.2 Filter Media Contamination

With regard to the contamination of filter media, a fundamental distinction must be made between two things, namely contamination of the surface by adhering cakes or cake fragments and contamination within the fabric, i.e., in the pores, as illustrated in Figure 2-4. Surface contamination occurs if a filter cake is not discharged at all, or fragments adhere to the filter medium. This leads to a reduced process chamber for the next filtration cycle and a decrease in throughput. Furthermore, cross-contamination occurs, and remaining cake alters subsequent filter cake build-up. There is a variety of ways to reduce the amount of adhering cake, such as tilting, vibration, use of scrapers and jet cleaning. More detailed information is provided by Morsch and Weigert [66, 75]. Morsch investigated cleaning of artificially placed cake fragments on filter press fabrics using water jets in addition to detecting contaminated areas using image analysis [92, 93]. He also evaluated cake detachment and fabric deformation on filter candles using backwash for different surrounding fluids [62, 63, 64, 65].

Weigert investigated the adhesion of filter cakes to filter cloths for classical model systems ($\text{Al}(\text{OH})_3$, CaCO_3 , glass spheres and kaolin) under variation of various parameters, for example filter cloth, saturation, surface tension of the pore fluid, and particle size [75]. He concluded that a constant shear stress range results after a few filtration cycles for a specific filter medium [71]. Weigert's observation that particles adhering in the fabric affect cake detachment represents the interface between surface and intra-fabric contamination.

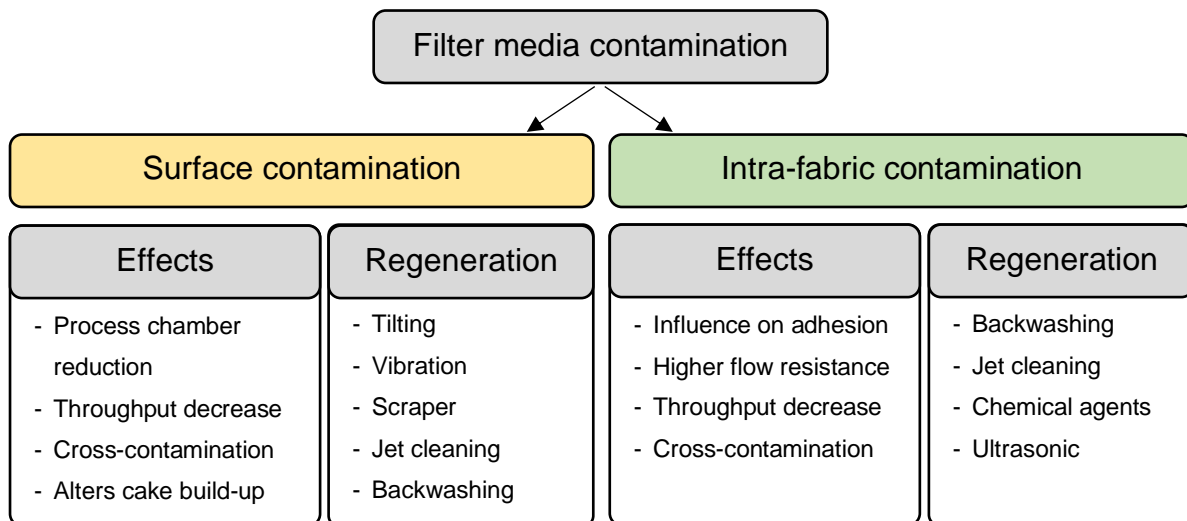


Figure 2-4: General distinctions among contamination mechanisms, their corresponding effects, and regeneration opportunities for filter fabrics.

Schematically, Figure 2-5 depicts the results of blinding, which is a permanent and increasing adherence of fines. The effective pore size is reduced, which results in an increase in flow resistance. This results in several negative effects concerning the filtration apparatus performance: if a defined filtrate volume is specified (for filter presses this corresponds to a specified residual water content of the filter cake), the filtration time will be extended; if the cycle time is fixed, the filtrate volume will be reduced, and the filter cake will have a higher water content. In any case, a performance reduction occurs. Furthermore, the possible cross-contamination caused by blinding is another reason why cleaning is necessary. This is particularly relevant in the field of food processing technology. Cleaning is usually carried out by backwashing, water jet cleaning with nozzles, chemical reagents, or ultrasound [91, 127].

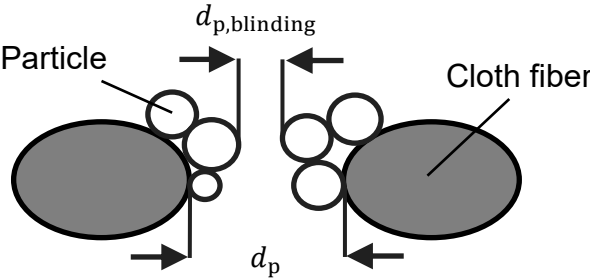


Figure 2-5: Schematic cross-sectional view of a filter medium affected by blinding [48].

2.4 Properties of Tailings and Slurries

The process stream of tailings after separation of the valuable minerals is a suspension consisting of the mineral particles and process water. As mentioned before the solid concentration is slightly above 44 w%. In general, solid liquid mixtures have several aspects of important properties, especially when having higher solid concentration. The following subsections introduce to the most important of them with special regard to tailings.

2.4.1 Mineral Composition

Tailings are a mixture of several minerals and differ between mine sites due to the individual ore composition. In general, there is a hazard if the residues contain heavy metals or even radioactive components. However, tailings can be relatively harmless in terms of geochemical reactions as well [128].

An enormous problem emerges from the fact, that run-of-mine minerals get in contact with oxygen and humidity. For example, weathering of pyrite generates acid mine drainage (AMD). This causes an enormous decrease in pH value and affects aquatic wildlife significantly [28, 129]. In contrast, a high alkalinity is possible as well. For example, alumina production is based on the Bayer processes. It uses bauxite, containing at least 45% aluminum oxide [130] which is dissolved by use of sodium hydroxide. Processing residues, which are also called red mud due to the color given by iron oxides, have pH values about 12 [131].

Furthermore, clay minerals hold a prominent position in minerals processing. In general, tailings often contain quartz; however, silicon is present also in other silicate minerals [14] like plagioclases, tectosilicates, inosilicates, and phyllosilicates. Phyllosilicates are also called sheet silicates since they consist of parallel sheets of tetrahedra. Swelling clay minerals, for example montmorillonite, are a certain group of phyllosilicates. These minerals hamper dewatering [132, 133].

2.4.2 Particle Size Distribution

The particle size distribution (PSD) of tailings is dependent on the ore processing applied and varies, for example, for different commodities. However, tailings have usually a broad distribution in the range of micrometers and a high number of fines [14]. A common definition of fines in mining is a particle size $<63 \mu\text{m}$ based on geotechnical considerations, which includes silt and clay sized particles [14, 134]. It should be noted that in filtration technology, particles $<10 \mu\text{m}$ are usually referred to as fines, since their filter cakes exhibit increasingly compressible properties [101]. The presence of small particles results in a variety of effects to be considered during thickening, filtration, transportation, disposal and storage [36], since small particles highly affect settling velocity, filter cake compressibility, filter cake permeability, rheology, and yield stress [87]. However, the site-specific tailings distribution and the possibility of mixing the ore processing residues with waste rock particles, mainly of bigger size, results in a high number of different particle systems for different mines and a high number of case studies [36].

Today, tailings handling is already a big challenge in the mining industry due to the high volume of production and the mentioned aspects of their PSD. However, these problems are predicted to become even more difficult as ore grades are decreasing. The necessity for mining of finer ore bodies and enhanced comminution for separation of the valuable minerals will result in an even smaller PSD of the tailings. The smaller particles are the bigger is the influence of non-gravity forces on their behavior and the properties of their macroscopic matter [135], e.g., of the tailings slurry.

The wide PSD is of great importance for filtration in recessed plate filter presses, as particles of different sizes sediment at different rates. The slurry tends to segregate especially in geometries with a high expansion in the vertical direction, such as filtration chambers. This results from the quadratic dependence of the Stokes' settling velocity on the diameter (see Equation 2-9).

$$v_s = \frac{(\rho_s - \rho_l) \cdot g \cdot x^2}{18 \cdot \eta_l} \quad \text{Equation 2-9}$$

The effect is particularly pronounced for low concentrations. Therefore, it can be limited by thickening the filter press feed. If the number of particles in the slurry increases sufficiently, the particles interaction hinders segregation. The corresponding solid volume concentration is called segregation threshold [36]. Another possibility is

intervention in the PSD by coagulation and flocculation. During coagulation particle-particle interaction is adjusted by means of altering pH and ionic concentration of the slurry, e.g., by use of highly charged cations like Al^{3+} or Fe^{3+} . Therefore, particles form agglomerates, which increase settling velocity. Flocculation poses another possibility to increase sedimentation velocity of small particles. Flocculants are long-chained water-soluble polymers of high molecular weight, e.g., polyacrylamide, which generate bridges between particles.

In mining application, especially concerning the issue of segregation in pipes and filtration, an evaluation of the adequate solid concentration for every process step is crucial. During piping higher energy requirements might be chosen to reach turbulence to avoid settling and segregation [136]. Also, during filtration a homogenous suspension is necessary to prevent inhomogeneous cake build-up causing problems concerning filtration time, water content and post-treatment.

2.4.3 Rheological Behavior

The continuous phase of the tailings slurry is water and, thus, a Newtonian fluid. Therefore, the dynamic viscosity η links shear stress τ and shear rate $\dot{\gamma}$ according to Equation 2-10:

$$\tau = \eta \cdot \dot{\gamma} \qquad \text{Equation 2-10}$$

However, this behavior changes significantly during the ore dressing process due to the solid content of the slurry. In general, the particle concentration is very relevant for tailings management since it increases significantly by thickening and filtration. An increase in solid particle concentration affects the rheological behavior due to an increase in viscosity. Furthermore, particle interactions play an important role, especially for a finer PSD.

At a certain solid volume concentration, a point is reached where the disperse particles are in contact with each other. This point is called the gel point and states the transition towards a semi-solid network. Properties of an individual particle system such as PSD and particle interactions affect the gel point which can vary in a wide range between different slurries. Since the resulting particulate network now transfers stresses, a significant alternation in rheological behavior occurs. Figure 2-6 shows Newtonian and three standard non-Newtonian fluids in a shear stress over shear rate diagram. A Newtonian behavior results in a straight line starting at 0 and is described by Equation 2-10. That means it flows as soon as a shear stress is applied, and the viscosity is

constant. In contrast, a Bingham fluid is deformed at a certain load below the so-called yield stress but does not flow. It starts to flow with constant viscosity when the yield shear stress is exceeded. If a fluid becomes less viscous at higher shear rates, it is known as shear-thinning or pseudoelastic. If the fluid also has a minimum shear stress required to flow, it is called yield-pseudoelastic. A behavior showing a decreasing viscosity by higher shear rates is called shear thickening or dilatant. In combination with a yield shear stress, it is referred to as yield-dilatant. In general, tailings are yield-pseudoelastic due to alignment of flocs or particles [36].

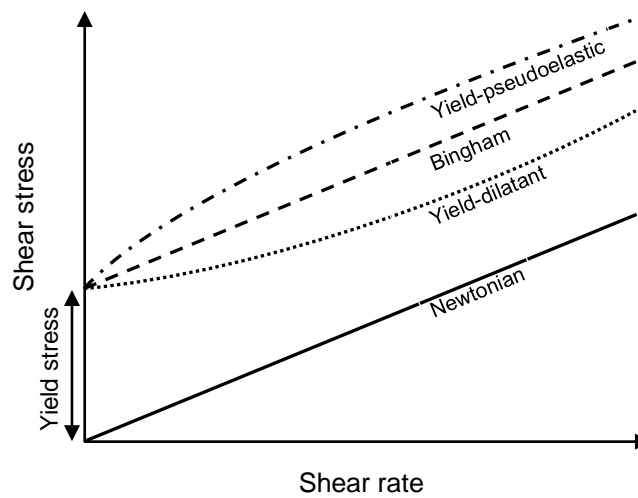


Figure 2-6: Schematic representation of different rheological behaviors, adapted from [36].

A common approach to describe the different rheological behaviors, based on the experimentally determined constants yield shear stress τ_{ys} , K and n , is the Herschel-Bulkley approach (Equation 2-11) [36].

$$\tau = \tau_{ys} + K\dot{\gamma}^n \quad \text{Equation 2-11}$$

2.5 Properties of Particulate Networks

Increase in particle concentration changes the rheological behavior of a solid-liquid mixture. Furthermore, the state of the two-phase system alters at certain concentrations, which are specific for every particulate system. There are several definitions of state transitions and regimes that originate from rheology or other fields like soil mechanics [137].

As mentioned in Chapter 2.4 a suspension reaches the so-called gel point at a concentration where inter-particulate contacts occur [80]. Then, the mixture can withstand a yield shear stress and can be referred to as particulate network. Further increase in solid fraction of the mixture increases yield shear stress. Figure 2-7 shows schematically the increase for some tailings from various mines based on experimentally determined data from Sofra [36, 138]. As the diagram illustrates, tailings suspensions differ in onset concentration and shape of the yield stress increase. Even tailings of the same commodity vary in their behavior between mines.

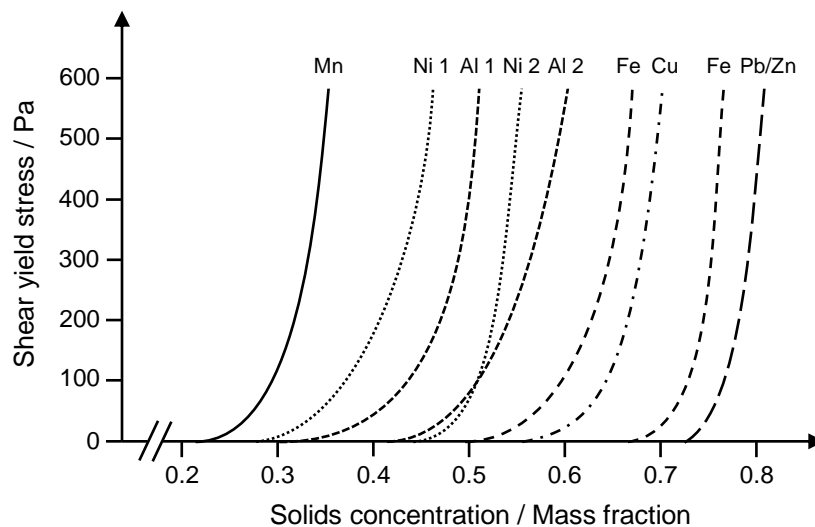


Figure 2-7: Shear yield stress data of different tailings from various commodities [36, 138].

If the concentration increases further, the solid particles in the suspension start to build a self-supporting structure. The mixture is now called a paste. A common test to determine the transition point between suspension and paste is a sedimentation experiment using 30 cm of slurry in a graduated cylinder [36]. Lack of sedimentation at a certain solids concentration, i.e., lack of clear water above the sediment, defines the initial settled density and paste state.

If the mixture reaches a concentration at which it ceases to flow, it exhibits plastic behavior. In geotechnical terms, this critical point is known as the liquid limit and

represents the first Atterberg limit [139]. This concept was established in the early 20th century and corresponds to a yield shear stress of approximately 2 kPa [139, 140]. For instance, adequately consolidated and fully saturated filter cakes can have plastic properties. The second Atterberg limit delineates the concentration at which the particulate network's behavior shifts from plastic to semi-solid. Generally, undersaturated filter cakes can be characterized as semi-solid in appearance. Furthermore, the third Atterberg limit marks the transition from a semi-solid to a solid state, denoted by the end of shrinkage during further drying [139]. In a process engineering point of view this also represents the point of a starting desaturation. It is of outstanding importance for particulate networks of small particles since shrinkage cracks might occur during further reduction of the water content. The effect of shrinkage cracks is very problematic for further processing, like enhanced desaturation or filter cake washing [87].

The stresses in semi-solid and solid materials can be categorized in shear and tensile stresses based on their direction of action. In engineering most applications allow a two-dimensional investigation. In this case the corresponding Cauchy stress tensor can be derived according to Equation 2-12. τ_{yx} and τ_{xy} are identical.

$$\sigma = \begin{pmatrix} \sigma_{xx} & \tau_{yx} \\ \tau_{xy} & \sigma_{yy} \end{pmatrix}; \tau_{yx} = \tau_{xy} \quad \text{Equation 2-12}$$

Figure 2-8 shows the stress state in a volume element. When considering particulate networks, it is assumed that there is a homogeneous composition and a very small particle size [80]. The values of the stresses depend on the coordinate system.

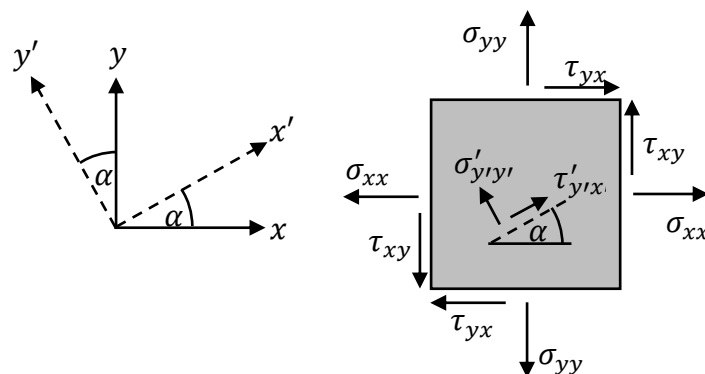


Figure 2-8: Schematic representation of the two-dimensional stress state.

The so-called Mohr's circle is used for visualization of the stress states. For this purpose, the normal and shear forces are inserted as schematically shown in Figure 2-9. This enables to display to all stress states based on the equilibrium of forces

independent of the coordinate system. For example, a clockwise rotation of the coordinate system in Figure 2-8 by the angle α , results in a rotation of 2α counterclockwise in the Mohr's circle (see Figure 2-9). The maximum shear stress τ_{\max} is therefore at an angle of 45° to the principal stresses. In a coordinate system with $\tau'_{x'y'} = 0$, $\sigma'_{x'x'}$ becomes the so-called principal stress σ_1 .

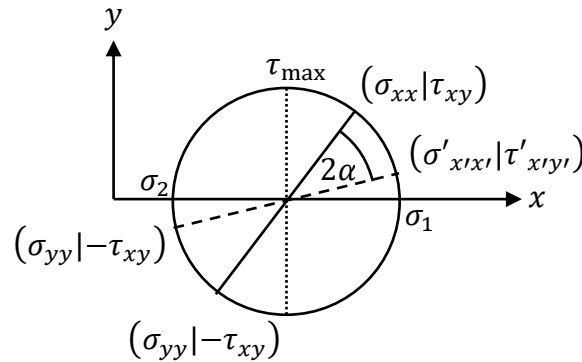


Figure 2-9: Schematic representation of Mohr's circle.

In addition, Mohr's circles are used to determine the flow behavior of granular materials such as bulk solids or filter cakes, as the relationship between compressive stress, shear stress and failure can be represented [75, 80, 140, 141]. According to Hill's method and the Mohr-Coulomb failure criterion, the shear and tensile strength can be determined in a simplified manner, as shown in Figure 2-10 [142]. For this purpose, the normal stresses and the experimentally determined correlating maximum shear stress ($\sigma_n | \tau_{\max}$) from multiple shear tests are inserted. A linear fit, which represents the Mohr-Coulomb failure criterion, is applied for the maximum tensile stress, according to Equation 2-13. The intersection with the vertical axis τ_s describes the shear strength of the particulate network [75]. Additionally, the intersection with the horizontal axis represents the tensile strength σ_t [143]. The third characteristic value of a particulate network is the angle φ , which is referred to as the angle of internal friction [142].

$$\tau = \sigma \cdot \tan \varphi + \tau_s \quad \text{Equation 2-13}$$

Hill's method using the Mohr-Coulomb failure criterion is based on two significant simplifications [142]. First, the failure criterion is modelled by a straight line while the yield locus is more accurately described by a bent curve. In addition, the intersection with the horizontal axis is assumed to be at a 90° angle [140]. The second simplification is the usage of the maxima of the Mohr's circles for modeling of the failure criterion. In fact, a failure occurs already once the failure criterion tangentially touches a stress

circle. As a result, the Mohr-Coulomb failure criterion overestimates both the real tensile strength τ'_s and, particularly, the real shear strength σ'_t .

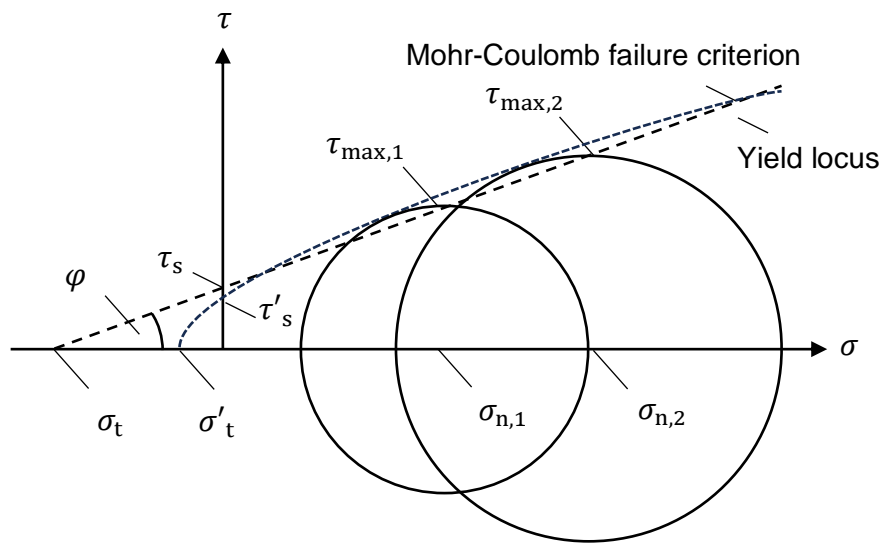


Figure 2-10: Schematic representation of the Mohr-Coulomb failure criterion with Mohr's circles using shear tests and Hill's method, along with a schematic representation of the yield locus.

The yield locus depends on the properties of the particulate network. Of decisive importance is the compaction state, which is increased, for example, by a higher filtration pressure. Furthermore, the formation of liquid bridges alters the properties of the network significantly.

Schubert investigated the dependence of the saturation S on the tensile strength σ_t of particulate networks in detail [79]. In Figure 2-11 his measurement of the tensile strength and the capillary pressure curve is schematically depicted in blue and orange, respectively. He experimentally determined these data for limestone particles with a diameter of $x = 71 \mu\text{m}$ and a porosity of $\varepsilon = 0.415$. Initially, the tensile strength increases with increasing saturation. Starting at $S = 0$ and continuing for lower saturations, liquid bridges form at the particle-particle contact points. The tensile strength σ_t is described by Equation 2-14 and depends on the porosity ε of the network, the average adhesion force F_a , and the particle diameter x [79, 135].

$$\sigma_t = \frac{1 - \varepsilon}{\varepsilon} \cdot \frac{F_a}{x^2} \quad \text{Equation 2-14}$$

In this case, the adhesion force represents the sum of the line force F_l and the capillary force F_c [87]. Assuming two spheres, this results in Equation 2-15 with the length of the three-phase boundary L , the surface tension of the liquid γ , the wetting angle θ , the inner radius of the liquid bridge R_1 , and the capillary pressure p_c .

$$F_a = F_l + F_c = L \cdot \gamma \cdot \cos \theta + \pi \cdot R_1^2 \cdot p_c \quad \text{Equation 2-15}$$

The capillary pressure is described by Equation 2-16. R_2 is the radius of curvature of the liquid bridge.

$$p_c = \gamma \cdot \left(\frac{1}{R_1} + \frac{1}{R_2} \right) \quad \text{Equation 2-16}$$

The volume of the liquid bridges increases for higher saturation until the individual liquid bridges connect, as shown by the illustration on the left and in the middle. As a result, the transmissible tensile stress increases until it reaches a peak at a saturation of approximately $S = 0.9$. This range is referred to as transition region. The peak results by capillary forces and is linked to the capillary inlet pressure p_{ce} . Tensile stress between the peak and $S = 1$ is described by Equation 2-17 [79].

$$\sigma_t = S \cdot p_{ce} \quad \text{Equation 2-17}$$

Measurements in the literature suggest a slight shift of the peak towards lower saturations when considering the shear strength instead of the tensile strength [75, 76, 77, 78].

Besides the transmissible tensile strength, the capillary pressure curve is shown in orange. This measure is characteristic for every porous structure and shows the achievable value at equilibrium for mechanical desaturation at a certain applied air pressure [87]. Using a simplified approach of cylindrical pores, the relationship can be described by the Young-Laplace equation (Equation 2-18). This equation describes the pore diameter d_p in terms of the surface tension of the liquid γ , the wetting angle θ and the applied overpressure Δp .

$$d_p = \frac{4 \cdot \gamma \cdot \cos \theta}{\Delta p} \quad \text{Equation 2-18}$$

The sharp increase between $S = 1$ and $S = 0.9$ is directly attributable to the capillary inlet pressure of the particulate network. This is because there is theoretically a largest pore in the structure that corresponds to the lowest capillary inlet pressure. During the almost linear behavior of the capillary pressure curve in the transition region, further pores are emptied with increasing pressure. However, mechanical desaturation is

limited by water on the surface or in internal pores. This results in a steep increase of the capillary pressure curve at low saturations [144].

If the saturation exceeds a value of $S = 1$, the state changes per definition from a particulate network to a suspension (right-hand illustration in Figure 2-11).

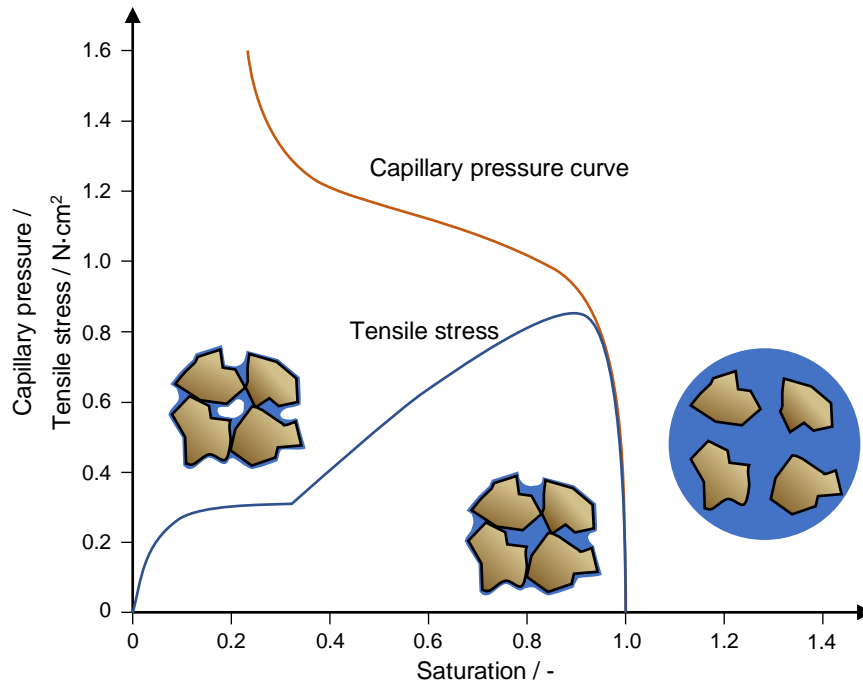


Figure 2-11: Schubert's capillary pressure and tensile stress data of limestone filter cakes ($\varepsilon = 0.415$; diameter $x = 71 \mu\text{m}$), adapted from [79].

The saturation at a certain gas differential pressure is declining with increasing application time. The kinetics can be described using the approach suggested by Nicolaou, given in Equation 2-19 [144, 145]. The time-dependent saturation $S(t)$ reaches a value at equilibrium of the saturation S_∞ for long air blow times. The kinetics depend on the corresponding desaturation pressure Δp , the capillary entry pressure p_{ce} , the height-specific cake resistance α_h , the cake porosity ε , the dynamic viscosity of the liquid η_l , and the cake thickness H_c . a and b are two fit parameters.

$$\frac{S(t) - S_\infty}{1 - S_\infty} = \left(1 + a \cdot \frac{\Delta p - p_{ce}}{\alpha_h \cdot \varepsilon \cdot \eta_l \cdot H_c^2 \cdot t} \right)^{-b} \quad \text{Equation 2-19}$$

The characteristic constants are experimentally determined in the standardized pressure housing according to VDI guideline 2762 [109].

3 Methods

Suitable methods were developed in this work for investigating the three aspects cake detachment, filter media abrasion and filter media blinding. For detachment and desaturation, filtrations of tailings suspensions were carried out in a laboratory plate and frame press with subsequent measurement of characteristic parameters directly on the filter cake using a special set-up. A newly developed apparatus enables the characterization of the abrasion resistance of unused filter media by visual observation in terms of number of abrasions until rupture. The evaluation of the blinding and its regeneration of industrially used and blinded filter cloths includes cleaning tests and subsequent investigations of the flow behavior.

3.1.1 Cake Detachment¹

The filtration setup consists of a stirred tank in which suspensions of tailings particles from an iron ore or copper mine, provided by FLSmidth, can be mixed with tap water. The concentration of the solids is set to 30 v%, as this is comparable to the underflow of the upstream thickeners in the industry. Compressed air conveys the suspension into the filter press via a riser pipe. The applied overpressure relative to the atmosphere represents the filtration pressure. Control and measurement data acquisition are carried out via a process control system (Lab-View, National Instruments, Austin, USA). The laboratory filter press is designed as a plate and frame filter press. Figure 3-1 shows the apparatus and the individual components in the opened position. The tailings slurry enters the cylindrical filtration chamber via a feed pipe. The chamber has a diameter of 100 mm and a height of 40 mm. The filter cake forms in this cylinder and the height corresponds to the cake thickness. Other chambers and, therefore, cake heights can also be installed. The filtration chamber is fixed by two end plates with the aid of a spindle. A circular filter medium is inserted into the recess of the end plates on each side, retaining the particles in the chamber during filtration. The edge of each filter medium is sealed by liquid rubber. Each end plate has a drainage structure that is connected to both filtrate outlets, one at the top and one at the bottom of each end plate.

¹ The content of this chapter was published in *Sustainability* 2022, 14, 3424, is in submission in *Minerals Engineering* and was adapted for the thesis.

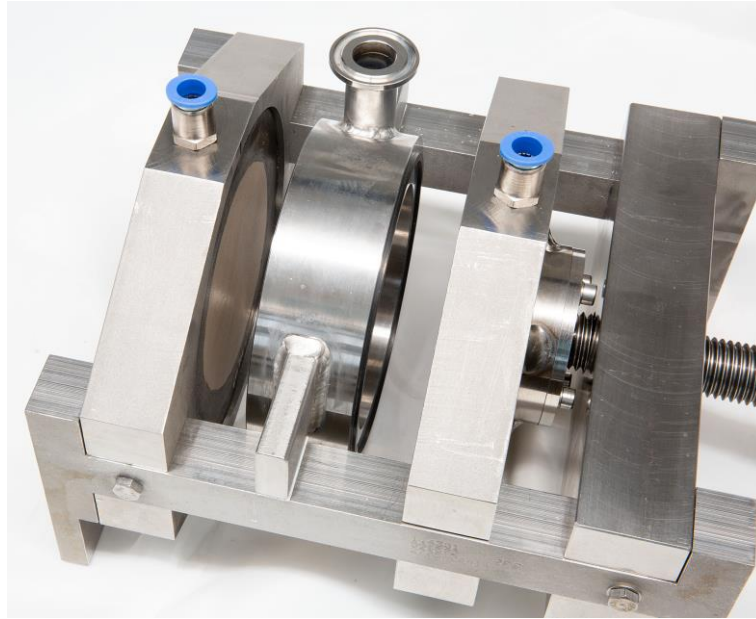


Figure 3-1: Laboratory filter press in open condition including filter cloths inserted into the end plate.

Figure 3-2a shows a cross-sectional view of the closed filter press during the filtration process [44, 45]. The filtrate flows into a container which is positioned on a scale. After filtration, care is taken to ensure that no water remains in the drainage structure to prevent the cake from humidifying. Furthermore, the inlet and all four filtrate outlets in the periphery are connected or equipped with valves to enable post-treatment of the cake in the form of desaturation by differential gas pressure. In the mining industry gas differential pressure desaturation is referred to as air blow. For this purpose, the inlet, the lower outlet of one end plate and the upper filtrate outlet of the other opposite plate are closed. The open upper filtrate outlet is now switched and no longer leads into the weighing container but allows for the application of compressed air. The pressure is also regulated via the process control system. Then, the air flows through the facing drainage structure, the first filter medium, the filter cake, the second filter medium and the adjacent drainage structure. A certain proportion of the pore water is discharged and gravimetrically recorded in accordance with the ratio of the pressure of the air and the distribution of the capillary inlet pressure across the pores of the filter cake. This results in filter cake desaturation.

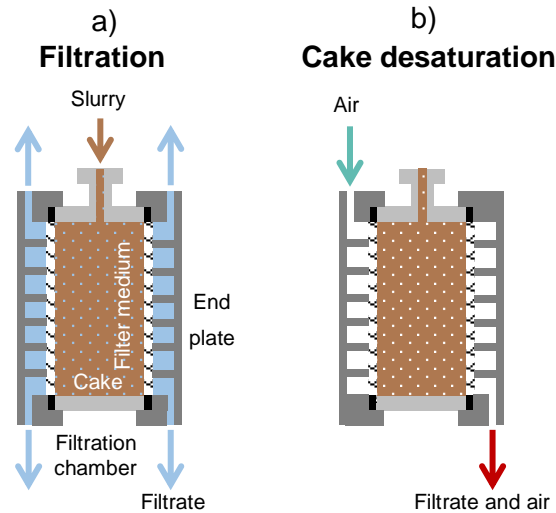


Figure 3-2: Schematic cross-sectional view of the lab filter press filtration (a) and desaturation procedure (b) [44, 45].

To enable the direct measurement of the parameters relevant for cake detachment, namely shear adhesion of filter cake to filter fabric and filter cake cohesion after filtration, special test rigs were designed for a tensile testing machine. This process was optimized to be performed using the filtration chamber. After filtration, the cake adheres to the inside of the chamber as well as the two filter media on the outside.

First, the chamber is positioned horizontally on a support plate in front of the tensile testing machine with the aid of a spacer. Figure 3-3a shows this in cross-sectional view. The filter fabric is fixed in a crescent-shaped clamp and then sheared off at a constant velocity of 0.01 m min^{-1} by an integrated pulley. This is an analogous process to cake detachment, in which the filter cake is sheared off the cloth by its own weight. The use of such a procedure to determine cake to cloth shear adhesion, by measuring cake to cloth shear stress τ_{cc} for detachment, has already been established by Ginisty [60]. From the force peak occurring at the moment of detachment the cake thickness required for detachment can be calculated by taking into account the adhesive area. The basis for this is the balance between the gravitational force F_g of the cake and the adhesion force F_a [75]. F_g is determined by the width W_c , the height H_c , the thickness T_c , the porosity ε , the void saturation of the cake S , the density of the solid ρ_s , the density of the fluid ρ_l , and the gravitational constant g . However, this calculation does not consider protruding at the sealing edges or secondary effects, such as deformation of the cake when the plate stack is opened.

$$T_c \cdot W_c \cdot H_c \cdot ((1 - \varepsilon) \cdot \rho_s + \varepsilon \cdot S \cdot \rho_l) \cdot g = F_g > F_a \quad \text{Equation 3-1}$$

After the adhesion test, the cake cohesion is determined by measuring the peak cake shear stress τ_c . An additional disc spacer is used to push half of the cake out of the filtration chamber. Figure 3-3b shows this in the lateral cross-sectional view. A lid is then placed over the upper half of the cake and a direct shear test is carried out with the aid of the tensile testing machine, analogous to a Jenike shear tester [146]. The velocity is also set to 0.01 m min^{-1} . According to Hill's procedure, the force peak related to the shear area is taken as a point of the yield locus at the associated normal stress [142]. For yield loci determination, the filtration is considered as preconsolidation.

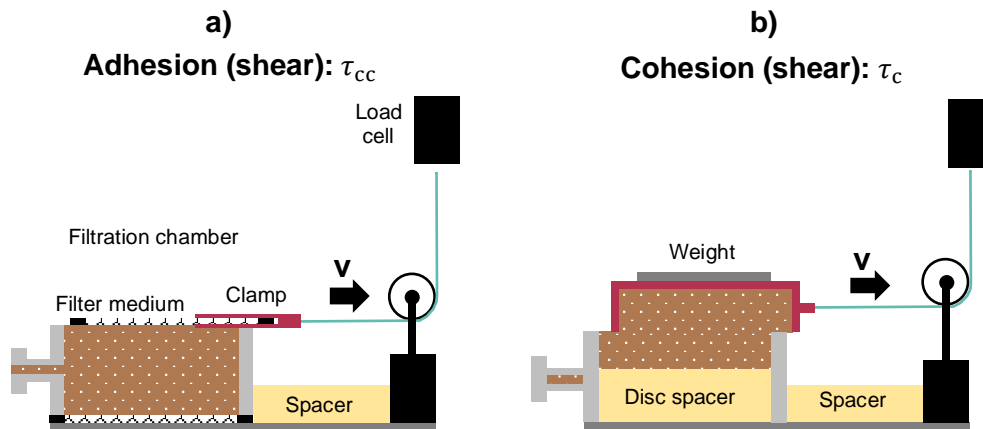


Figure 3-3: Schematic cross-sectional view of the shear adhesion test (a) and the shear cohesion test (b) [44, 45].

To determine the water content the cake is weighed after the tests, then dried 24 h in a drying oven at 100°C and weighed again afterwards. The determination of the desaturation is based on a comparison of the water content to fully saturated cakes obtained with the same parameter combinations.

The extended studies on cake detachment and desaturation in Chapter 4.2 also include a mathematical description of the water content, saturation, adhesion and cohesion for variation of the air blow time. This is based on exponential behavior according to Equation 3-2 as first assumption. $x(t)_{i,j}$ describes the time-dependent quantity. Furthermore, $x_{i,j,\infty}$ is the value at equilibrium, $x_{i,j,0}$ is the initial value and $a_{i,j,h}$ is the kinetics parameter. In this nomenclature i and j indicate the filtration pressure and the air blow pressure, respectively. h is the cake height, which represents cake thickness for filtration in recessed plate filter presses.

$$x(t)_{i,j} = x_{i,j,\infty} - (x_{i,j,\infty} - x_{i,j,0}) \cdot e^{-a_{i,j,h}t} \quad \text{Equation 3-2}$$

The second assumption is that the initial value of the quantity is invariable and can, thus, be experimentally determined by:

$$x_{i,j,0} = \hat{x}_{i,j,0} \quad \text{Equation 3-3}$$

There are two fit parameters $a_{i,j,h}$ and $x_{i,j,\infty}$. $a_{i,j,h}$ characterizes the exponential behavior caused by desaturation. It is assumed that $a_{i,j,h}$ is specific for every combination of filtration pressure, air blow pressure and cake thickness (Equation 3-4).

$$a_{1,1,1} \neq a_{2,1,1} \neq a_{2,2,1} \quad \text{Equation 3-4}$$

The second fit parameter $x_{i,j,\infty}$ determines the limit of the constrained behavior. Furthermore, it is assumed that for a certain cake thickness this value only depends on the air blow pressure and not on the filtration pressure (Equation 3-5).

$$x_{1,j,\infty} = x_{2,j,\infty} \quad \text{Equation 3-5}$$

A further assumption is that 180 s is close to the value at equilibrium for a cake thickness of 40 mm. For two different filtration pressures the ratio of the measured points is therefore taken as ratio of the values at equilibrium, as can be seen in Equation 3-6.

$$\frac{x_{i,2,\infty}}{x_{i,1,\infty}} = \frac{x_{i,2,180}}{x_{i,1,180}} = \frac{x_{1250,550,180}}{0.5 \cdot (x_{250,250,180} + x_{1250,250,180})} = \text{const.} \quad \text{Equation 3-6}$$

For the mathematical approach all fit parameters are determined by minimizing the sum of square residuals (Equation 3-7).

$$\min_{a_{i,j,h}; x_{i,j,\infty}} S = \sum_{k=1}^n (x_{1,1,k} - \hat{x}_{1,1,k})^2 + \sum_{k=1}^n (x_{2,1,k} - \hat{x}_{2,1,k})^2 + \sum_{k=1}^n (x_{2,2,k} - \hat{x}_{2,2,k})^2 \quad \text{Equation 3-7}$$

3.1.2 Filter Media Abrasion²

To investigate the resistance of filter media to abrasive stress, an apparatus based on a circulating chain system (Mink Kett-System[®] KBL 120, August Mink GmbH & Co., KG, Göppingen, Germany) driven by an electric motor was modified [46]. It replicates the load that occurs during tailings filtration due to the falling cake which is not the case for available abrasion testing machines. For this purpose, alternating stainless steel brush elements having 120 mm width, 76 mm length and 25 mm brush height and spacer elements are mounted on the chain. The height of the apparatus and the brushes is adjusted using screw feet. Under the apparatus is a frame on which either a square, circular, or hexagonal edge geometry is mounted. The filter media specimen having 60 mm width is stretched over the edge geometry, as can be seen in Figure 3-4a. Using a spindle with a limited torque for clamping, it is ensured that the sample is only loaded elastically. The overlap between the brushes and the sample is set using the height adjustment. Figure 3-4b shows a sample at the end of a test. The test is terminated when a rupture of half the sample width (30 mm) is visually detected. The device registers the rotations made up to that point. Multiplied by the number of brushes, which is 14, this gives the number of abrasions until rupture. The appearance of the damage is comparable to that found in industrial applications (Figure 3-4c).

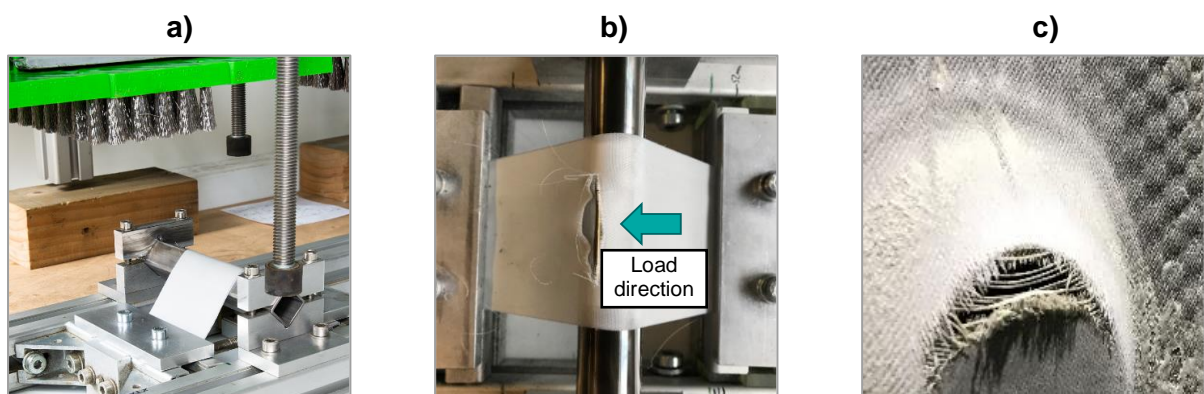


Figure 3-4: a) Specimen positioning below the brush apparatus. b) Specimen with the load defined as the threshold value of a rupture of half the sample width. c) Industrial filter cloth abrasion appearance (©FLSmidth).

In addition to the use of different edge geometries and filter media, it is possible to vary the clamping torque, brush overlap and velocity. The latter is limited by visual monitoring.

² The content of this chapter was published in *Mining* 2022, 2, 425-437 and was adapted for the thesis.
40

3.1.3 Filter Media Blinding³

In the third part of this work, the regeneration of industrially blinded cloths is investigated. In more detail the pores of these cloths are characterized by permanently adhering particles which results in increased flow resistance. For this purpose, FLSmidth provided three different filter fabrics from a silver, a gold, and an iron ore mine in used and unused condition. These fabrics have 2 m × 2 m in size (see Figure 3-5) and were sent to Germany in dry condition. Samples in the size of filter media specimens according to VDI 2762 [109] were cut out and then subjected to water jet, ultrasonic or chemical cleaning.

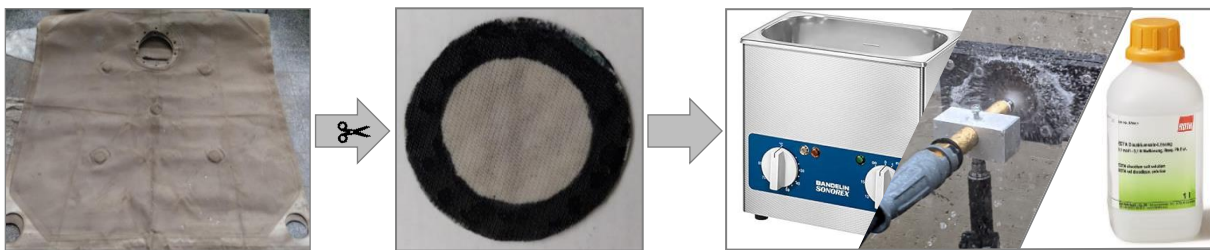


Figure 3-5: Schematic representation of the cleaning test workflow based on the industrially blinded 2 × 2 m filter cloths. Specimens the size of pressure filter according to VDI 2762 were cut out and then subjected to a cleaning method.

The water jet cleaning setup consisted of an axial piston positive displacement pump having three pistons of a high-pressure cleaner (Kärcher HD 6/15 C Plus, Alfons Kärcher, Winnenden, Germany) in combination with a 60° full cone nozzle (4906041YCE000, Lechler, Metzingen, Germany). The full cone nozzle provides a more uniform liquid distribution and a more defined impinging area in comparison to a flat nozzle [147]. Furthermore, a 90° impinging angle was applied. This ensures a uniform flux distribution at the impinging area. For the study, the flux was varied by adjusting the distance of the nozzle to the sample and the spraying time. In addition, front-wash and back-wash tests were carried out for each fabric. Here, front-wash describes a water jet cleaning from the same orientation as the filtration direction. For cleaning, the samples and an underlying stainless-steel mesh were clamped to a holder to ensure mechanical stability. The design allowed drainage of the spray water from the front to the side as well as downwards behind the sample to avoid any influence on the cleaning performance due to accumulation. The potential to damage the specimens by cleaning was examined using SEM imaging.

³ The content of this chapter was published in *Minerals* 2023, 13, 416 and in *Minerals Engineering* 2021, 168, 106922 and was adapted for the thesis.

For the second regeneration study several acids and bases were used: hydrochloric acid, acetic acid, sulfamic acid, formic acid, sodium hydroxide and potassium hydroxide. For comparison of the different cleaning agents, each sample was subjected to a 1-molar bath of 100 ml for 30 min. The area-related concentration amounted to 20.83 mol m⁻². The concentration and exposure time were reduced in further tests to investigate the kinetics of chemical cleaning. Besides chemical cleaning, ultrasound baths of 47 kHz/35 W (Branson 1210E-MT, Branson Ultrasonics Corp.), of 130 kHz/100 W (Transonic TI-H-5, Elma Schmidbauer GmbH), and a combination of 47 kHz/35 W ultrasound and 0.1-molar hydrochloric acid was applied. In addition, to check whether the chemical cleaning or the ultrasound treatment damaged the cloth, a tensile test is carried out until rupture.

The evaluation of the cleaning performance was based on the flow resistance of the fabric since it correlates with the amount of blinding. For this purpose, the clear water was pressed through the cloth specimen by applying a slight overpressure in a pressure housing according to VDI 2762 standard. The permeate mass flow \dot{m} was recorded gravimetrically and the resistance $R_{\text{fm,clear water}}$ was calculated using an adapted version of the Darcy equation (Equation 3-8).

$$R_{\text{fm,clear water}} = \frac{A}{\dot{m}} \cdot \rho_l \cdot \frac{\Delta p}{\eta_l} \quad \text{Equation 3-8}$$

In addition, the pore diameter d_p , to be more precise the pore diameter distribution, was measured using porometry for chemical cleaning. For this purpose, all pores are first filled with a completely wetting fluid. In the case of low-energy surfaces, such as plastic fabrics, this is ensured by using a linear, non-reactive polydimethylsiloxane with low surface tension of 20 mN m⁻¹. The air pressure required to empty the pores is related to their size via the Young-Laplace equation (Equation 3-9).

$$d_p = \frac{4 \cdot \gamma \cdot \cos \theta}{\Delta p} \quad \text{Equation 3-9}$$

The pore size distribution can be determined by measuring the air flow rate [148].

4 Filter Cake Detachment and Desaturation

This chapter presents the research progress in the field of cake detachment generated by this dissertation. It is divided into two parts, each based on a separate publication. The first part investigates and quantifies the influence of different filter media and process parameters on cake water content, cake saturation, cake to filter medium adhesion and cake cohesion. These results are reported for iron ore mine tailings. The second part focuses on a detailed investigation of the post-treatment of copper tailings filter cakes using gas differential pressure desaturation. The primary objective is to investigate its influence on the quantities defining detachment behavior. The secondary is the development of a mathematical description.

4.1 Iron Ore Tailings Dewatering: Measurement of Adhesion and Cohesion for Filter Press Operation⁴

Bernd Fränkle^a, Patrick Morsch^a, Christoph Kessler^a, Thien Sok^b, Marco Gleiß^a, Hermann Nirschl^a

^a Institute of Mechanical Process Engineering and Mechanics, Karlsruhe Institute of Technology, Karlsruhe, Germany

^b FLSmidth Inc., Salt Lake City Operations, Midvale, USA

4.1.1 Introduction

Due to the steadily growing demand for raw materials, the amount of mined material is also increasing [149]. Therefore, metal ores are extracted in large open pit mines around the world. Since only a small fraction of the mined rock consists of valuable product [3], an increasing amount of waste rock has to be handled, which is present as tailings at the end of the process. However, tailings management has been a major challenge for the industry for some time now [36]. Storage in tailings ponds has been increasingly replaced by dry storage (dry stacked tailings) due to process water loss and the risk of dam breaks. Increasing mechanical dewatering using thickeners and subsequent filtration can reduce the water content of the tailings, thus recovering a

⁴ The content of this chapter was published in *Sustainability* 2022, 14, 3424 and was adapted for the thesis.

large part of the process water and enabling dry stacking [150]. Improved process water management and safer storage reduce costs and are an important aspect in terms of sustainable mining. For this reason, the number of filtered tailings solutions is steadily increasing [39] and larger and larger plants are being operated [58].

Due to the process-related characteristics of the tailings, their filtration is non-trivial and an existing challenge in solid-liquid separation. During the processing of valuable material, rock has to be crushed to a particle size below 100 μm . However, the particle size distribution is broad, and there is a significant clay content in the lower micrometer range [14]. These particles form a compressible filter cake [101] and influence the filtration process drastically. Therefore, high pressure difference in the form of mechanical pressure is crucial for dewatering. From an engineering point of view, chamber filter presses are suitable for this purpose [32]. These are operated in batch mode, i.e., they must be regenerated after each filtration. This happens by opening the individual press chambers, followed by detachment of the cakes from the filter medium caused by their weight and falling down on a conveyor belt placed below the filter press. Economical handling of the large process streams is given by a parallel connection of large presses (e.g., chamber dimensions of 5 m \times 3 m and 160 plates) [151]. However, it is obvious that trouble-free operation is necessary in order not to represent the bottleneck of the entire process chain. Common problems concerning filter presses are the correct selection of the filter medium, mechanical wear or blinding of the filter cloth [48] and detachment problems of the cakes. In the latter case, completely adherent cakes or partial drop-off can occur due to partial reaching of the yield limit and breaking. Remaining cake parts reduce the available process space and thus reduce throughput or lead to leaks and damages if they are attached in the sealing area. This paper therefore presents practical test procedures for determining the adhesion of the cake to the fabric and characterizing the strength of the particulate network (cohesion), as well as investigates relevant parameters (filtration pressure, cake post-treatment, fabric).

4.1.2 Theory

Analogous to the time sequences of the tailings filtration process in chamber filter presses, this section provides a brief insight into the relevant fundamentals and interrelationships of cake filtration. Furthermore, the properties of the network of solid particles after filtration are discussed. Eventually, the prerequisites for cake detachment are outlined.

4.1.2.1 *Filtration*

Recessed plate filter presses operate on the principle of cake filtration. At the beginning of filtration, particle breakthrough occurs because the pores of the filter medium are usually selected to be larger than the particle diameter in order to reduce hydraulic resistance. If the particle concentration is sufficient, bridging over the pores occurs after a short time and afterwards the approaching particles are progressively deposited on the network of solid particles. Thus, the cake grows. Since the pressure drop within the cake is reciprocal to the pressure of the consolidated network of solid particles, mechanical support is provided behind the filter cloth by means of backing cloths or drainage structures.

The filter cake is a network of solid particles whose structure and properties are strongly dependent on the particle size distribution of the slurry. Clay-sized particles, for example, cause compressible behavior [101]. Normally, tailings have a relevant content of clay and corresponding filter cakes are therefore compressible [14, 39, 57, 110] [39, 152]. In order to ensure achieving crucial residual water contents, compaction of the network of solid particles by sufficient filtration pressure is necessary. For this reason, filter presses are used in a lot of applications [32, 39, 151, 153, 154]. Furthermore, mechanical desaturation by applying gas differential pressure can be implemented in filter presses with little constructive effort to reduce cake water content by decreasing pore saturation even more. The adjusted differential pressure dewateres filter cake pores with a corresponding and lower capillary entry pressure [144, 155].

The strength of a wet network of solid particles depends strongly on its saturation S (proportion of voids filled with liquid to entire void volume). In the saturation range between $S = 0.3$ to 0.9 , liquid bridges are present, and capillaries are increasingly filled, i.e., capillary forces act; therefore, the largest tensile forces can be transmitted [75, 156, 157]. A maximum is to be expected for $S = 0.8$ to 0.9 [78, 158].

4.1.2.2 *Approach to Describe Cake Detachment*

For the description of the detachment behavior of filter cakes, four stresses are relevant [75], which are shown in Figure 4-1. A distinction must be made between adhesion as the stress between two different systems (e.g., filter medium and cake) and the cohesion of the cake itself. In each case, a further subdivision can be made into shear stress τ and tensile stress σ . The volume on which the force acts is depicted in blue,

whereas the surface associated with the stress is shown in orange. The sketched stresses and their abbreviations in this paper are as follows:

- a) Shear adhesion (adhesion (shear)): τ_{cc}
- b) Tensile adhesion (adhesion (tensile)): σ_{cc}
- c) Shear cohesion (cohesion (shear)): τ_c
- d) Tensile cohesion (cohesion (tensile)): σ_c

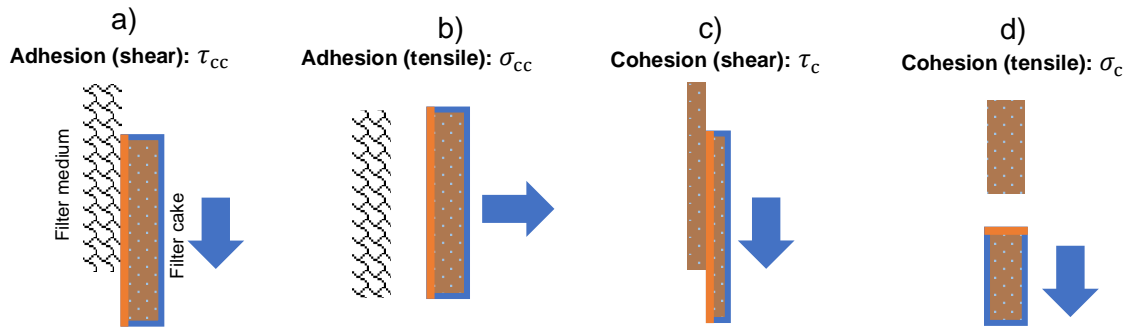


Figure 4-1: Schematic representation of important stresses for the description of cake detachment. (a) Shear adhesion: τ_{cc} (b) Tensile adhesion σ_{cc} (c) Shear cohesion: τ_c (d) Tensile cohesion σ_c . Blue: volume on which the force acts. Orange: stress area.

Shear adhesion causes the sticking of filter cakes to filter media and must be overcome for cake detachment [75]. Corresponding to the apparatus used this can, e.g., be proceeded by compressed air blowing (vacuum disc filters), back washing (candle filters), filter media movement (tower filter presses) or gravity (chamber filter presses).

The driving force for cake detachment in tailings filtration in chamber filter presses is the weight force acting on the cake. The condition of complete detachment requires the following relationship in Equation 4-1, which assumes sufficiently high cohesion of the cake and an infinitely extended plate, i.e., neglecting support at the sealing edge and other chamber structures as well as detachment of the cake with subsequent wedging between two adjacent plates. Besides cake dimensions (thickness T_c , width W_c and height H_c), its porosity ε and saturation S , as well as the density of the solid ρ_s and the liquid ρ_l , are decisive for the weight force.

$$T_c \cdot W_c \cdot H_c \cdot ((1 - \varepsilon) \cdot \rho_s + \varepsilon \cdot S \cdot \rho_l) \cdot g = F_g > F_a \quad \text{Equation 4-1}$$

A common problem is an incomplete cake detachment (complete sticking or partial detachment). There are several cake detachment scenarios where the loading parameters mentioned in Figure 4-1 are crucial. Figure 4-2 shows these scenarios. It can be divided between the requested detachment (a) and the problematic cases (b–d). In detail, these can be described as follows:

- a) The weight of the cake is sufficient. The cake falls off in one piece. Assumption: cohesion sufficient, no breaking.
- b) The weight force is too low; the cake adheres. Assumption: cohesion sufficient, no breaking.
- c) The tensile stresses transmitted during plate moving rupture the cake. If there are several fractures, partial falling may occur. Assumption: insufficient shear strength of the cake and low weight force.
- d) A higher adhesion (tensile) than cohesion (tensile) splits the cake. If there are several fractures, partial falling may occur. Assumption: low weight force and local saturation/compaction differences.

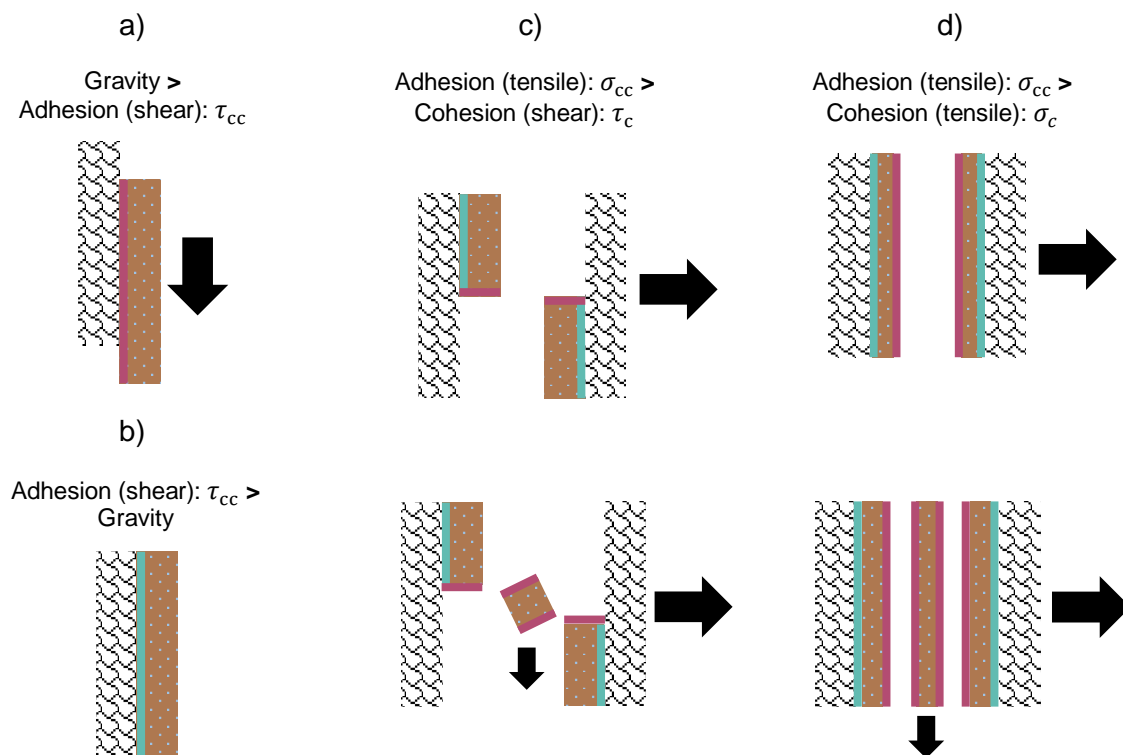


Figure 4-2: Schematic representation of different detachment behaviors regarding underlying mechanisms. (a) The weight of the cake is sufficient. The cake falls off in one piece. (b) The weight force is too low; the cake adheres. (c) The tensile stresses transmitted during plate moving rupture the cake. If there are several fractures, partial falling may occur. (d) A higher adhesion (tensile) than cohesion (tensile) splits the cake. If there are several fractures, partial falling may occur. Green: stress area without detachment. Red: stress area with detachment.

It can be taken advantage of the interdependency of the four stresses mentioned. A relationship between cohesion (tensile) and adhesion (tensile) (σ_c/σ_{cc}) can be derived from the theory of contact points. Using a bulk solids mechanics approach, the ratio between cohesion (shear) and cohesion (tensile) (τ_c/σ_c) can be determined. Therefore, measurements of shear adhesion and shear cohesion allow the determination of all relevant stresses.

4.1.2.3 Theory of Contact Points

Using close-packed structure theory, it is obvious that the number of contacts to a wall is smaller than the number of contacts within a network of solid particles. Based on theoretical approaches combined with measurements of real polydisperse systems, the ratio of tensile strength in an undersaturated wet network of solid particles to tensile strength of the same network to a wall can be approximated with 1.15 according to Douglas [159]. Translated into the application and the nomenclature of this investigation, it is referred to as the ratio between the transmissible tensile cohesion inside the cake and tensile adhesion between cake and cloth (σ_c/σ_{cc}) in the following Equation (2):

$$\frac{\sigma_c}{\sigma_{cc}} \approx \frac{3.6}{\pi} \approx 1.15 \quad \text{Equation 4-2}$$

However, it should be noted that a network of solid particles deviates from an ideal packing structure if it is compressible (e.g., tailings). Here, the state of compression (e.g., corresponding to filtration pressure) plays an important role. For compressible structures, a higher filtration pressure leads to an increase in the number of contact points, and it becomes closer to the approximation of ideal packings.

4.1.2.4 Bulk Solid Mechanics

In contrast to rheology describing stress states of flowing systems, bulk solid mechanics characterizes the flow behavior of dry or undersaturated wet networks of solid particles [141]. After consolidation, they deform or rearrange at certain yield stresses due to internal friction caused by particle contacts. The flow properties, especially of initial flow, are depending on several parameters, for example, solid volume fraction, applied normal stress and stress at preshearing [140].

Relationships and derivable quantities can be depicted in a plot out of experimental shear measurement data, which are referred to as the yield locus and schematically illustrated in Figure 4-3. Consolidated bulk material starts to deform or rearrange under stresses above the yield locus. Such networks (e.g., filter cakes) have a positive shear stress at $\sigma = 0$, which is referred to as cohesion (shear) in this paper. The tensile strength of cohesive networks at $\tau = 0$ occurs for negative normal tensions, which is referred to cohesion (tensile) in this paper. The yield locus for tensile fracture ends vertical to the abscissa [160].

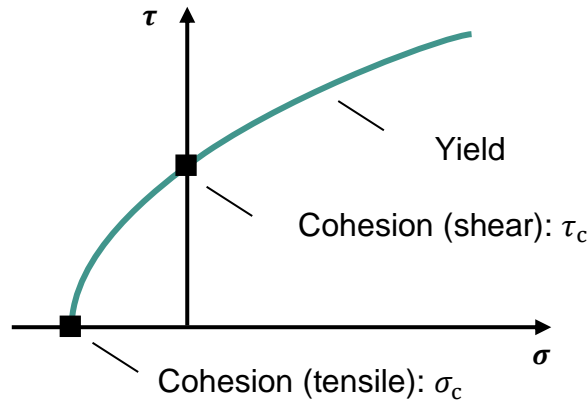


Figure 4-3: Schematic representation of yield locus, τ_c and σ_c .

The ratio of τ_c/σ_c describes the brittleness of the network of solid particles in simplified terms. As can be seen in the literature, a prediction of τ_c/σ_c is not possible. However, it can be stated that τ_c/σ_c is in general between one and five, but even ratios below 1 and up to 25 are reported [75]. Regarding undersaturated limestone particle networks, Rumpf mentioned $\tau_c/\sigma_c > 2$ leads to a brittle breaking behavior [135]. Stitch-proof-to-brittle properties are stated to be crucial for cake detachment [75], as well as the fact that cake texture changes in a small range of residual water content, as reported by Tittel [161]. Generally, τ_c/σ_c increases due to the progressive decreasing of saturation of the network of solid particles [135]. However, slurries at concentrations of the gel point or higher are also able to transfer forces, e.g., wet filter cakes after filtration [137]. Since they theoretically have a saturation of one, this work extends the method of the yield locus for this specific case. This assumption is justified since in the literature brittle behavior is also mentioned for full-saturated networks of solid particles [75].

4.1.2.5 Shear Breaking

It is important to note that the acting forces are always proportional to the area where they are acting. This is to be exemplified in Table 4-1 by scenario c using realistic chamber dimensions (2 m × 2 m × 0.05 m) and a cohesion/adhesion ratio (σ_c/σ_{cc}) of 1.15 (see Section 4.1.2.3). If the shear strength of the filter cake is too low, the cake becomes ruptured by shearing due to the adhesion of the cake parts sticking to the cloths. The area ratio of the attaching cake part in relation to the shear area is important and is therefore defining a critical ratio of τ_c/σ_c needed for the avoidance of rupture by shearing. If τ_c/σ_c is sufficient (over 17.4), no rupture of the cake is possible.

If incomplete detachment occurs, in addition to manual cleaning, there are some ways developed over time to remove the cake or remnants of it. Weigert lists some patents

for this, using the following ideas: stretching medium, plate tilting, vibration, shaking, scrapers and nozzles [75]. However, it would be optimal if an autonomous detachment of the complete cake could be achieved by systematic process parameter control. Therefore, it is obvious that not only filtration tests with regard to separation efficiency and hydraulic properties of the filter media are necessary for the design of filter presses. In addition, knowledge of the stresses and the parameters influencing them is of enormous importance.

Therefore, besides presentation of a suitable, application-related measurement method for relevant variables, this paper aims to show the impact of various process parameters (e.g., filtration pressure and desaturation).

Table 4-1: Exemplary calculation of critical τ_c/σ_c ratio whose undercutting causes shear breaking.

Assumptions: Cake 2 m × 2 m × 0.05 m, $\sigma_c/\sigma_{cc} = 1.15$	
Area ratio one cake part is adhering to	0.5
Area adhesion (tensile) acts	1 m × 2 m
Area cohesion (shear) acts	0.05 m × 2 m
Ratio $\text{area}_{\text{adhesion (tensile)}}/\text{area}_{\text{cohesion (shear)}}$	20
Resulting critical ratio of τ_c/σ_c	17.4

4.1.3 Materials and Methods

Test equipment and procedures used are described in this section. Furthermore, investigated process parameters are discussed.

4.1.3.1 Properties of the Tailings

The study considered iron ore tailings having a size distribution and a mass concentration typical for tailings. Detailed properties are listed in Table 4-2. As referred to in Section 4.1.2, a high fraction of fine particles can be stated. The elemental composition measured by angle dispersive XRF can be found in a previous publication [162].

Table 4-2: Properties of the iron ore tailings.

Iron Ore Tailings		
Solid density		3050 kg m ⁻³ *
Slurry concentration		30 v%
Particle size distribution	X _{10,3}	7.2 μm *
	X _{50,3}	38.2 μm *
	X _{90,3}	120.8 μm *

* [162]

4.1.3.2 Procedure

It would be ideal if a characterization of the stresses could be realized with the least possible effort while at the same time providing sufficient information. In the following, a possibility is therefore presented. The idea is to combine filtration tests and shear tests using one apparatus (a cylindric one-chamber frame filter press) and, in addition, commercial standard equipment with minimal adjustments (a tensile testing machine).

The tests in this paper used a laboratory frame filter press provided by FLSmidth, also used in previous investigations [162]. It consists of a cylindrical frame element (inner diameter 10 cm, height 4 cm) with a suspension inlet at the top and pressed by a spindle between two end plates. These end plates have drainage channels and four filtrate outlets, one at the top and at the bottom (Figure 4-4a). The four filtrate outlets are equipped with valves. Closing the lower filtrate outlet on one side and the upper filtrate outlet on the other side and introducing compressed air at the open upper filtrate outlet thus enables gas differential pressure desaturation of the filter cake (Figure 4-4b). Filling of the chamber is carried out using a stirred pressure vessel with a riser pipe overlaid with compressed air.

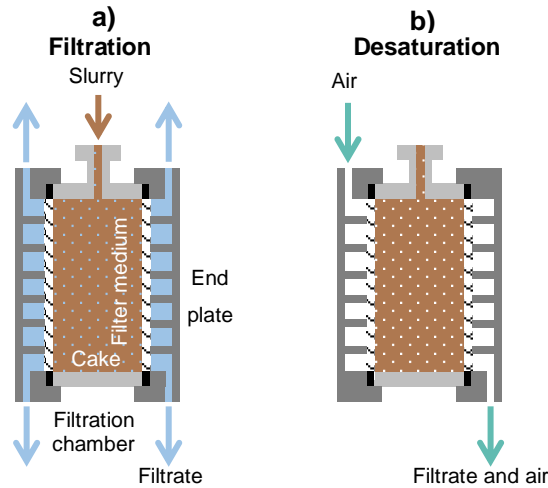


Figure 4-4: Schematic side view cross-section representation of lab filter press filtration (a) and desaturation procedure (b).

After filtration, it is possible to remove the cylinder together with cake and adhering filter media from the press. This allows subsequent positioning in a commercial tensile testing machine (velocity 10 mm min^{-1}) with minimal modification (Figure 4-5). First, the adhesion (shear) of the filter medium was measured by a crescent-shaped clamp, as proposed by Ginisty [60], by pulling of the fabric. Then, the cake was pushed halfway out of the cylinder using a disc spacer and afterwards the top half was sheared off with a lid to determine the cohesion (shear) of the cake analogues to a Jenike shear cell [146]. The maximum of the force-displacement curve related to the shear area represents the measured stress value. If the filtration is considered as preconsolidation and thus as preshearing of the network of solid particles, each shearing test value describes one point of the yield point, depending on the associated pair of values from normal stress and resulting shear stress. Different normal stresses can be realized by weight disks on the lid. In this way, a yield locus is obtained for each pressure and each cake post-treatment [140].

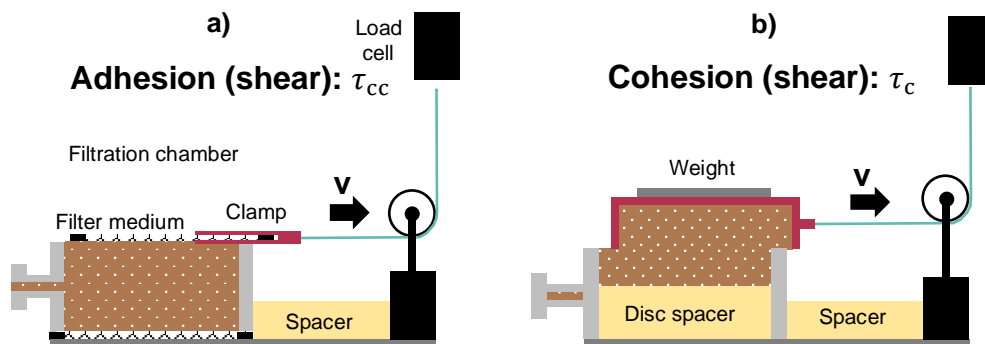
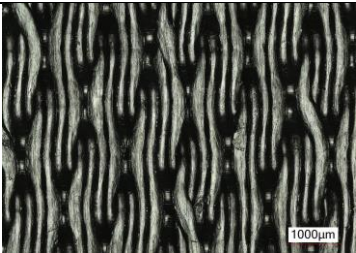
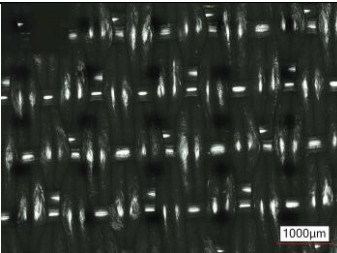
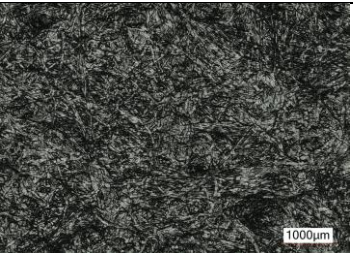


Figure 4-5: Schematic side view cross-section representations of the shear adhesion test (a) and the shear cohesion test (b).

4.1.3.3 Process parameters

Filtration tests were carried out with three filter media typical for tailings filtration application. Two cloths of polypropylene (PP) and nylon (NY) as well as a PP felt medium were compared. These were chosen to be able to compare two fiber materials and a cloth to a felt medium. Their properties are listed in Table 4-3. Filter medium resistance measurements were carried out in a pressurized filter cell according to VDI guideline 2762 [144].

Table 4-3: Properties of the three tailings filtration filter media.

	PP-cloth	NY-cloth	PP-felt
Image			
Weave-type	Twill	Plain	-
Fiber type	Mono/mono	Mono/mono	-
Fiber diameter (warp/weft)	$180 \pm 10/330 \pm 30 \mu\text{m}$	$280 \pm 20/310 \pm 20 \mu\text{m}$	-
Resistance	$2.6 \pm 0.6 \times 10^8 \text{ m}^{-1}$	$1.8 \pm 0.1 \times 10^8 \text{ m}^{-1}$	$7.4 \pm 0.9 \times 10^8 \text{ m}^{-1}$
Thickness	$1.1 \pm 0.1 \text{ mm}$	$1.0 \pm 0.1 \text{ mm}$	$2.2 \pm 0.2 \text{ mm}$

To investigate the influence of compaction, filtrations were performed at 250 kPa and 1250 kPa. For each pressure, there were tests with filtration only and tests with a desaturation cake post-treatment, as can be seen in Figure 4-6. This was a gas differential pressure desaturation at 250 kPa for filtrations at 250 kPa and at 550 kPa for filtrations at 1250 kPa. A pressure of 550 kPa is an industrially used value for gas differential pressure desaturation. However, gas differential pressure is limited by the filtration pressure (danger of cake back flow). So, 250 kPa was the maximum pressure usable for 250 kPa filtration pressure.

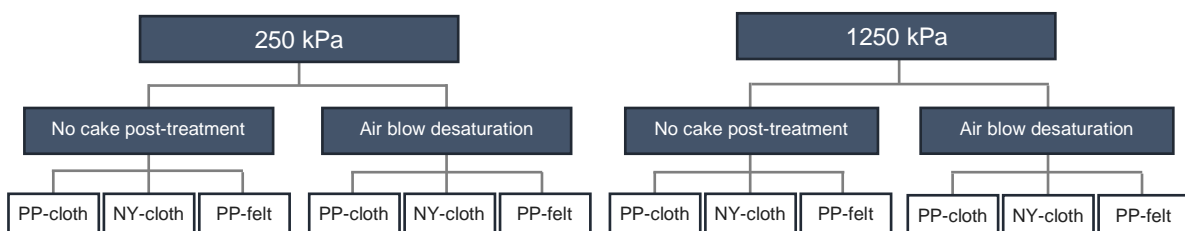


Figure 4-6: Overview of filtrations made for subsequent adhesion and cohesion tests.

Normally, a tailings filtration fabric is used for a thousand or more filtration cycles [43]. During this process, changes occur in the fabrics due to blinding and mechanical abrasion. This is not considered in this work. A new set of fabrics (two pieces) was used for each pressure level. In order to still be able to observe a steady state (e.g., turbidity impact constant), six filtrations were carried out previously with the filter media to soil them before a fivefold determination of each measuring point was made. No post-treatment and post-treatment measurements were carried out alternating.

4.1.3.4 Validation

To validate the theoretical description of the cake detachment behavior, various chambers for a laboratory recessed plate filter press (Simex Mini Mobil, Simex Filterpressen GmbH & Co. KG, (Calw, Germany)) were additively manufactured in order to be able to carry out tests with 5, 10, and 15 mm thick cakes. Three filter plates were printed in each case, i.e., two end plates and one intermediate plate with an edge length of 150 mm and a cake dimension of approx. 120 mm in width and height. For this investigation, the PP cloth was used. One set of cloth was used for each pressure level (250 kPa and 1250 kPa). At first, for each pressure level, six filtrations were made to ensure basic contamination of the cloth. At this number, the particle penetration occurring at the beginning of each filtration had decreased to an approximately constant amount. Then, five filtrations were made for each cake thickness.

4.1.4 Results

4.1.4.1 Adhesion Measurements to Determine Required Cake Thickness for Detachment

First, the shear adhesion values of the different fabrics for two filtration pressures and two cake post-treatments are presented. A plot of the shear stress to be applied for the individual fabrics is given in Figure 4-7, including the standard errors of the means. The black data series represents the measured values of saturated cakes and the white data series those of desaturated (undersaturated) cakes. The lowest adhesion is found for the lower filtration pressure (250 kPa) and a fully saturated cake ($S = 1$) for all fabrics. Desaturation after filtration at 250 kPa increases adhesion for all fabrics. The same applies to an increased filtration pressure (1250 kPa). For example, the adhesion of the PP cloth is approximately twice as high after a filtration at 1250 kPa without post-treatment than at 250 kPa without post-treatment, i.e., an almost twice as thick cake would be required to fulfill the detachment condition. Desaturation of the

cakes formed at higher filtration pressure further increases adhesion for the PP cloth at 250 kPa and 1250 kPa, the NY cloth at 250 kPa and 1250 kPa and the PP felt at 250 kPa, comparing measurements at the same filtration pressure level. These findings are consistent with theoretical considerations of fewer contact points and literature data on saturation influence. Only the felt filter medium for filtrations at 1250 kPa show an exception to this. Adhesion is slightly decreasing after desaturation. This results from the fact of a structure with lower permeability compared to the cloths reducing desaturation performance. Therefore, desaturation after 1250 kPa filtration has no further adhesion-increasing effect. For the iron ore tailings, 5 kN m⁻² corresponds approximately to 25 cm cake thickness by assuming a residual cake water content of 20 w%, ρ_s of 3050 kg m⁻³, ρ_l of 1000 kg m⁻³, a full saturated cake ($S = 1$) and no sealing edge.

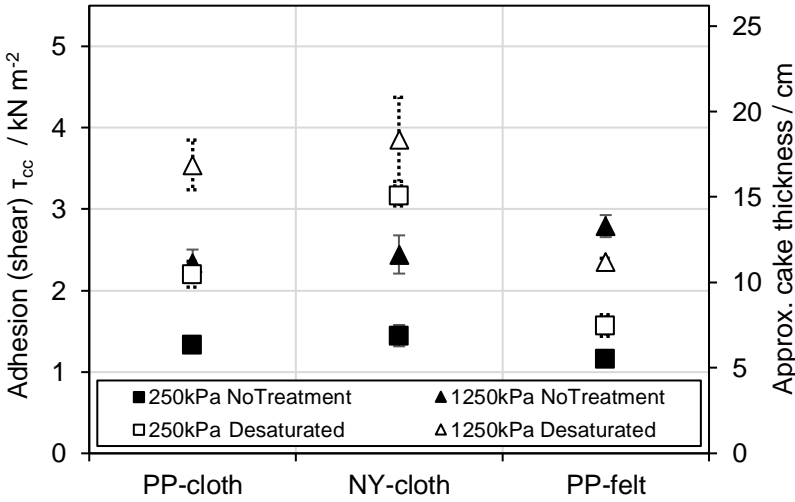


Figure 4-7: Adhesion (shear) τ_{cc} of the three filter fabrics for different process conditions.

In general, the residual water content of the filter cake is the key parameter in filter press operation. It allows direct conclusions to be drawn about the throughput and is partly used as a target parameter for successful discharge. If only the adhesion of the cake to the fabric is considered, it is obvious that the residual water content has a decisive influence on adhesion (Figure 4-8). Even a small change in residual water content changes adhesion significantly. Considering all data points of filtrations at different filtration pressure levels, with and without cake post-treatment by desaturation, the assumption of a quasi-linear increase in adhesion when decreasing residual water content is justified. Furthermore, standard error of the mean increases for decreasing water content, especially for the woven filter medium.

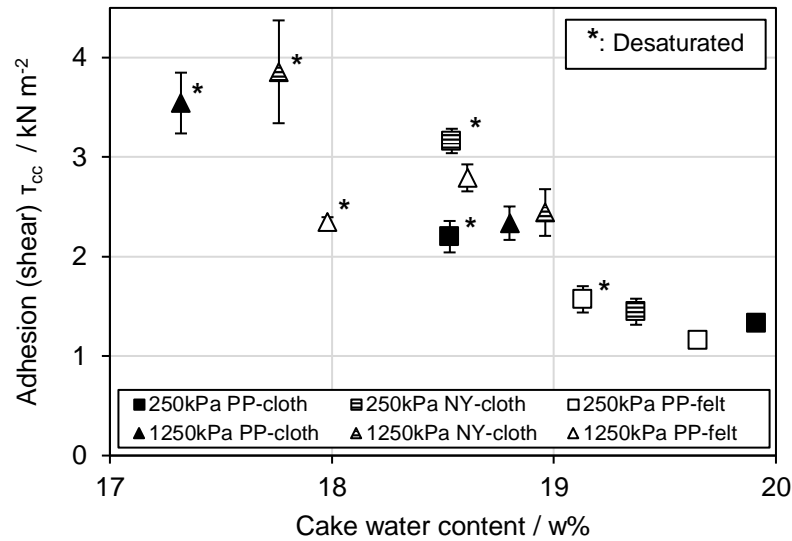


Figure 4-8: Adhesion (shear) τ_{cc} referred to corresponding residual cake water content of filtrations at different filtration pressure levels, with and without cake post-treatment by desaturation.

However, detachment behavior cannot be simply described by only using the adhesion of the cake to the fabric. This is obvious regarding the possible detachment cases mentioned above and the underlying interactions of the different stresses. Further differentiation is necessary, and the structure of the cake must be considered. First, the understanding of the adhesion increase with decreasing residual water content is useful. In fact, the residual cake water content is resulting out of two different processes. One is compacting, and the other is desaturation. Therefore, if only the residual water content is considered, information becomes lost. The effect of the different influences is visible, for example, in the representation of the adhesion referred to in the saturation of the network of solid particles (Figure 4-9). The networks are completely saturated ($S = 1$) for all filtrations without cake post-treatment of gas differential pressure desaturation. Depending on the available gas differential pressure (250 kPa or 550 kPa), further undersaturation and even higher adhesions can be achieved.

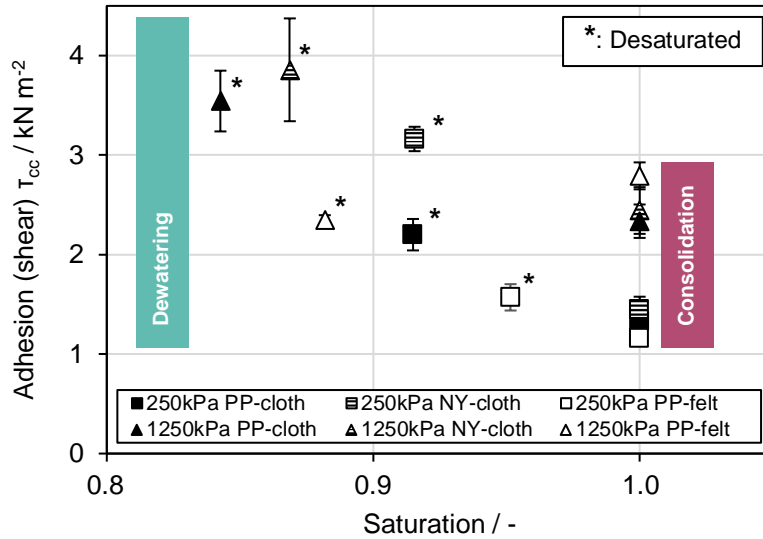


Figure 4-9: Adhesion (shear) τ_{cc} referred to corresponding saturation of the network of solid particles.

However, it should be noted that an increased filtration pressure acts as an antagonist. For compressible cakes and resulting compaction, the pores become smaller; thus, a higher capillary inlet pressure is required for desaturation.

4.1.4.2 Cohesion Measurements to Evaluate Shear Breaking Risk

The determination of the adhesion of the cake to the filter cloth helps to determine the required cake thickness for detachment (See Figure 4-2a (Falling cake: Gravity > Adhesion (shear): τ_{cc}) and Figure 4-2b (Sticking cake: Adhesion (shear): τ_{cc} > Gravity)). However, no statement can be made about the occurrence of the other possible scenarios (See Figure 4-2c (Shear breaking: Adhesion (tensile): σ_{cc} > Cohesion (shear): τ_c) and Figure 4-2d (Tensile breaking: Adhesion (tensile): σ_{cc} > Cohesion (tensile): σ_c)). For these, the other stress states on and in the filter cake as well as their relationship to each other play an important role, e.g., the ratio of τ_c/σ_c , which indicates the brittleness of the network of solid particles in simplified terms. A first step is to determine the shear cohesion, i.e., the shear strength of the filter cake, using the procedure shown in Figure 4-5. Figure 4-10 shows the results of these cohesion measurements for the PP felt medium over residual cake water content. Analogous to shear adhesion, an approximately linear relationship between shear cohesion and residual water content is evident, regardless of whether the lower residual cake water content results from increased compaction (due to a higher filtration pressure) or undersaturation (gas differential pressure desaturation)

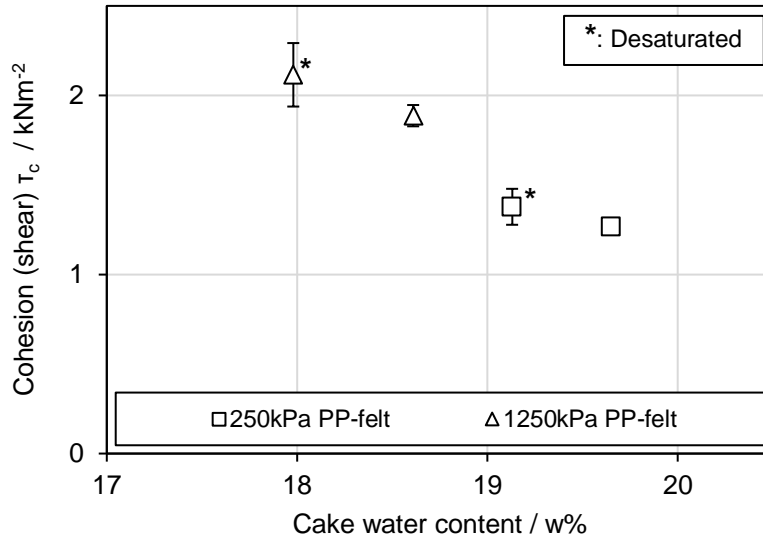


Figure 4-10: Cohesion (shear) τ_c referred to corresponding residual cake water content of filtrations at different filtration pressure levels for the PP felt medium, with and without cake post-treatment by desaturation.

Furthermore, the determination of the ratio of τ_c/σ_c can be carried out by determining the yield loci and expanding them into negative normal stresses. How these curves are to be expanded is discussed controversially [75]. Linear extrapolation of the yield locus slope at $\sigma = 0$ is a common simplified way to describe the relationship between τ_c and σ_c . However, this overestimates the tensile strength and underestimates τ_c/σ_c . Nevertheless, a statement about the detachment behavior can already be derived from the ratio of the slopes. This is discussed using the example of the yield loci for filtration at 250 kPa and 1250 kPa using the PP felt medium for no post-treatment of the cake and gas differential pressure desaturation (Figure 4-11). When looking at the linear fit, a higher slope, which is similar to the ratio of τ_c/σ_c at a higher filtration pressure, can be observed. Qualitatively, scenario c is thus less probable with filtration at 1250 kPa. A slight impact by cake post-treatment can be stated as well.

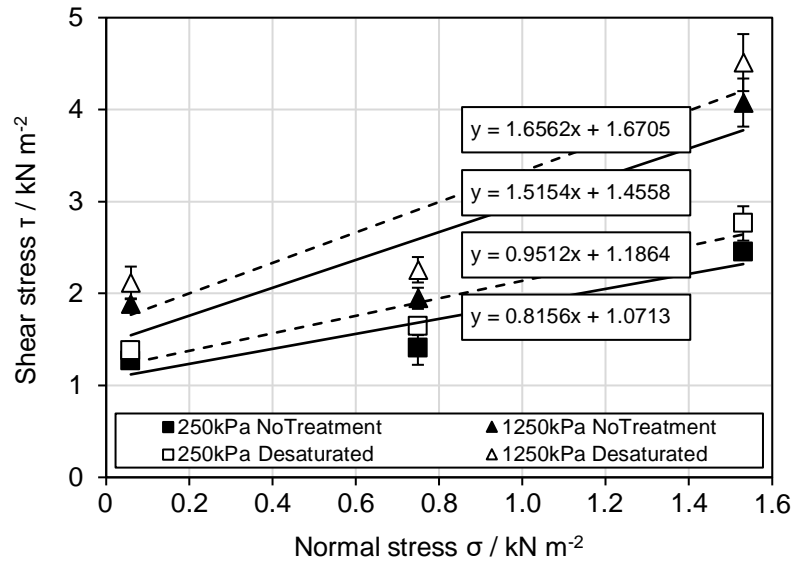


Figure 4-11: Yield locus excerpt of different filtration process parameters for PP felt medium.

4.1.4.3 Validation

The in the theory section in Figure 4-2 presented different scenarios a (Falling cake: Gravity $>$ Adhesion (shear): τ_{cc}), b (Sticking cake: Adhesion (shear): $\tau_{cc} >$ Gravity), c (Shear breaking: Adhesion (tensile): $\sigma_{cc} >$ Cohesion (shear): τ_c), and d (Tensile breaking: Adhesion (tensile): $\sigma_{cc} >$ Cohesion (tensile): σ_c) of cake detachments can be observed in laboratory tests. Figure 4-12 shows images of each scenario after filtration of the iron ore tailings using PP cloths in the laboratory recessed plate filter press. The first image shows scenario a, which is a complete detached cake after a filtration with 5 mm chambers at 250 kPa filtration pressure without cake post-treatment. In the next image, scenario b, a complete sticking cake can be seen after a filtration with 5 mm chambers at 250 kPa filtration pressure and without cake post-treatment. The third image shows a shear breaking (scenario c) after a filtration with a 5 mm cake at 250 kPa filtration pressure and without cake post-treatment. Scenario d is a breaking parallel to the cloth, which could often be observed after filtration with cake desaturation as shown in the image on the right side. This was also taken after a filtration at 250 kPa with 5 mm chambers and air blow.

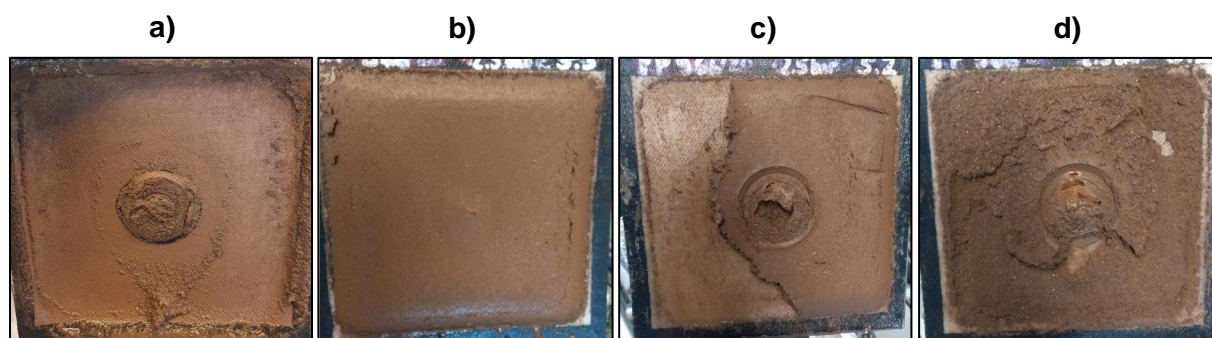


Figure 4-12: Different detachment behaviors seen in lab filtration: a) complete detachment (5 mm, 250 kPa, no cake post-treatment), b) complete sticking cake (5 mm, 250 kPa, no cake post-treatment), c) shear breaking (5 mm, 250 kPa, no cake treatment), and d) breaking parallel to cloth (5 mm, 250 kPa, air blow).

Figure 4-12 shows different scenarios observed for filtrations that do not differ in their chamber thickness. This is due to the fact that each detachment behavior has a certain probability for the process conditions. This stochastic distribution results, for example, from local inhomogeneities of the cake due to the broad particle size distribution. For example, shear breaking was observed for seven out of ten filter cakes having a thickness of 5 mm using PP cloths in the laboratory recessed plate filter press (see Table 4-4). This is the process parameter condition resulting in the highest residual cake water content. A five-fold determination of each combination using this two-chamber filter press gave ten detachments that can be observed. Shear breaking did not occur for thicker cakes at filtrations with 250 kPa and without post-treatment or at any other combination.

Table 4-4: Cake shear breaking probability of filtrations in the laboratory recessed plate filter press using the PP cloths.

Filtration pressure	Cake post-treatment	Shear breaking		
250 kPa	No treatment	5 mm: 7 of 10	10 mm: 0 of 10	15 mm: 0 of 10
250 kPa	Air blow desaturation	5 mm: 0 of 10	10 mm: 0 of 10	15 mm: 0 of 10
1250 kPa	No treatment	5 mm: 0 of 10	10 mm: 0 of 10	15 mm: 0 of 10
1250 kPa	Air blow desaturation	5 mm: 0 of 10	10 mm: 0 of 10	15 mm: 0 of 10

4.1.5 Discussion

In this study, several points are considered in a simplified way. Determination of filter media influences is limited since long-term behavior of the different filter media cannot be studied at the laboratory scale to an application-related extent. In addition, filter media having higher pressure losses reduces available gas differential pressure for desaturation and therefore hampers adhesion and cohesion comparisons. Generally,

extensive field data acquisition and comparison between field and laboratory data would be suggested.

In this study, only iron ore tailings are considered. It would be interesting for future work to compare tailings from different mines but also from the same mine at different exploration times. Changes in rock composition are a major challenge for the entire process chain but also explicitly for solid-liquid separation. Larger data sets would then also allow predictive control of this process.

4.1.6 Conclusion

First, a detailed view on cake detachment cases as well as underlying forces and tensions was depicted. Afterwards, measurement procedures combining filtration tests and cake-to-cloth shear adhesion as well as cake shear cohesion were presented, and their suitability for iron ore tailings was proven. The filtration process parameter influences on shear adhesion and shear cohesion could be shown. Increasing compaction of the cake by applying a higher filtration pressure leads to a higher shear adhesion, requiring a thicker cake to reach sufficient cake weight to fulfill the detachment condition as well as to a higher shear cohesion. Furthermore, decreasing cake saturation by cake post-treatment (gas differential pressure desaturation) also increases shear adhesion and shear cohesion. In summary, an approximately linear increase in shear adhesion as well as shear cohesion with decreasing residual cake water content can be observed, regardless of whether the decrease results from compaction (higher filtration pressure) or undersaturation (gas differential pressure desaturation). For the regarded amount of filtration cycles (relatively low compared to industrial use), no significant differences between cloth and felt media, as well as PP and NY, can be seen.

4.2 Copper Tailings Filtration: Influence of Filter Cake Desaturation⁵

Bernd Fränkle^a, Thien Sok^b, Marco Gleiß^a, Hermann Nirschl^a

^a Institute of Mechanical Process Engineering and Mechanics, Karlsruhe Institute of Technology, Karlsruhe, Germany

^b FLSmidth Inc., Salt Lake City Operations, Midvale, USA

4.2.1 Introduction

Increasing growth of population, technological progress and change in the energy and mobility sector cause a steady rise in demand for metallic and mineral commodities. Copper, lithium, cobalt, and nickel, which are essential for electric vehicles, are just four of many examples [29]. Ore mining, as the basis for the extraction of metals and minerals, is carried out in open-pit or underground operations. The mining cycle can be divided into exploration, evaluation, exploitation, mineral processing and reclamation [163]. The mineral processing step represents the concentration of the valuable metals or minerals in order to enable profitable transport and extraction [11]. This is done by crushing, separation, for example by froth flotation, and solid-liquid separation [3]. Since most of the processes in mineral engineering require a large amount of water, water management and recovery are important aspects [8, 10].

Only a small portion of the mined rock is valuable minerals [13]. A large amount of waste results from overburden, waste rock and ore residues. The latter are the milled but valueless part of the ore, also called tailings [164]. Furthermore, these tailings come out of the process as a suspension containing most of the process water [36]. Especially the traditional way to dispose this slurry in settling ponds causes a variety of problems such as enormous land footprint, water loss, dam failures and environmental contamination [5, 25, 27, 28]. The regularity of dam breaches [17, 18] and the increasing necessity to recover water led to the development of methods of disposing of tailings with less water, e.g. thickened or paste tailings, in the second half of 20th century [36]. However, these actions were insufficient. More recent dam breaches and increased media attention reinforced the development and regulations were tightened and new standards established [12, 34]. In addition to thickened or

⁵ The content of this chapter is in submission in *Minerals Engineering* and was adapted for the thesis.

paste disposal, tailings are now increasingly being filtered and then stacked [37, 39]. This enables safer storage, higher water recovery rates and further reduction of area footprint [35].

Due to the particle size distribution with a high proportion of fines [14] and the necessity to achieve sufficient dewatering and compacting, filter presses are used very often [36]. According to ISO specifications in geotechnical context a particle size of 63 μm is considered as fines [134]. Despite the optimization in terms of capacity and throughput, several filter presses must be operated in parallel in a mine [41]. For an application with 100,000 tons per day, big seven filter presses, e.g. FLSmidth AFP 2040 with a filtration area up to 2040 m^2 and 38.4 m^3 in one machine [165], are necessary [36]. A target water content of 20% can be assumed [32]. Thereby, tailings transportation on conveyor belts and dry stacking is possible, and, in general, a sufficient geotechnical stability and water recovery rate is reached. Especially achieving such water contents by undersaturated of the filter cake using pressurized air desaturation inhibit liquefaction of the stack due to a high shear cohesion, which is also referred to as shear strength [37].

However, operation of tailings filtration plants is a challenging task. Besides cloth lifetime related issues like abrasive wear or blinding by adhering particles [46, 47, 48, 42, 43], achievement of the required target water content as well as predicting cycle time including filtration and technical time correctly is crucial. Both requires a sufficient understanding of the filtration process in the filter press: For maximized throughput target water content has to be reached as fast as possible, e.g., by a short pressurized air cake post-treatment resulting in undersaturation. Moreover, a good cake detachment is required for keeping technical downtime low. Detachment behavior depends mainly on cake to fabric adhesion and cake stability which is also referred to as cohesion. In general, cakes having a low cake to fabric shear adhesion and behaving more brittle, i.e., having a high shear cohesion, detach easier [75].

Filter cake thickness, application time and air pressure are crucial parameters of the gas differential pressure desaturation post-treatment and influence the kinetics of the so-called air blow. An approach to describe the desaturation kinetics for incompressible filter cakes was given by Nicolaou, according to Equation 4-3 [144, 145]. $S(t)$ describes the time-dependent saturation of the voids in the filter cake, S_∞ is the saturation value at equilibrium for a certain desaturation pressure Δp . Also, the

capillary entry pressure p_{ce} , the thickness specific cake resistance α_h , the cake porosity ε , the dynamic viscosity of the liquid η_l , the cake thickness T and two fit parameters a and b are used.

$$\frac{S(t) - S_\infty}{1 - S_\infty} = \left(1 + a \cdot \frac{\Delta p - p_{ce}}{\alpha_h \cdot \varepsilon \cdot \eta_l \cdot T^2} \cdot t \right)^{-b} \quad \text{Equation 4-3}$$

The value of saturation at equilibrium for a certain gas differential pressure is a result of the capillary inlet pressure distribution and, thus, is given by the capillary pressure curve. Within the cake complete regions can have higher inlet pressures than the air blow pressure applied. This leads to isolated pores filled with water which limit the final water content that can be reached significantly [87]. Since compaction depends on filtration pressure and saturation at equilibrium depends on air blow pressure, an increase in cake thickness alters kinetics only [87]. Thicker cakes need more desaturation time to reach equilibrium [87]. After the post-treatment, the plate stack opens, the filter cakes detach and fall down.

The cake detachment process and the underlying mechanisms are very interdisciplinary. Previous publications and guidelines can be found in fields of filtration [44, 71, 77, 162], bulk material [141], geotechnical applications [166] and rheology [167] showing significant influences of compaction and desaturation on particulate network properties. These properties are mainly water content, saturation, cake to fabric adhesion and cohesion. Cohesion can be divided into tensile and shear cohesion both having a maximum of tensile and shear strength concerning level of saturation [76, 77, 78, 79, 135, 158].

Key findings of literature review and a previous study of tailings lab-scale filtration including adhesion and cohesion tests using iron ore tailings are [44, 75]:

- Tailings are supposed to generate slightly compressible filter cakes.
- The cake properties shear adhesion and shear cohesion are strongly dependent on process parameters, especially filtration pressure, desaturation time and desaturation pressure.
- Overcoming shear adhesion of filter cake to filter cloth by cake weight (mainly dependent on cake thickness) is crucial. The sealing edge influence increases the weight needed.
- Cake stability (cohesion) must be high enough for detachment.

The assumed main underlying mechanism for cake detachment in filter presses is that the gravitational force F_g of the cake overcomes the cake to fabric adhesion F_a . If cake stability is sufficient and influence of sealing edges and protruding parts is neglected, the force balance according to Equation 4-4 describes cake detachment [44, 75, 162]. T_c is the thickness, W_c the width, H_c the height, ε the porosity and S the void saturation of the cake. ρ_s is the density of the solids and ρ_l the density of the fluid.

$$T_c \cdot W_c \cdot H_c \cdot ((1 - \varepsilon) \cdot \rho_s + \varepsilon \cdot S \cdot \rho_l) \cdot g = F_g > F_a \quad \text{Equation 4-4}$$

Measurement of cake to fabric adhesion can be used to calculate the necessary cake thickness to overcome the shear adhesion to initiate detachment [75]. However, the resulting cake thickness is often above typical chamber dimension for recessed plate filter presses of 30-60 mm [44, 168], where, nevertheless, detachment is observed [44]. One reason is the simplification by the model. For example, Weigert stated that measured area-related adhesion values become smaller as test apparatus size increases [75]. This uncertainty must be considered with plate sizes of more than 2 m × 2 m in industrial application. In addition, the cake is subject to strong tensile stress before detachment when the plates are moved apart. A tensile adhesion between cake and fabric generates tensile and shear stresses within the cake before shear detachment. Also, it is possible that shear failure and shear breaking within the particulate network occurs [44]. A very stable cake, which is brittle, prevents this scenario.

In summary, the filtration with and the operation of recessed plate filter presses involves understanding of many factors like water content, saturation, adhesion and cohesion as well as their complex interaction. Some of these aspects are known from other fields, for example, behavior of undersaturated filter cakes having a maximum of tensile [79, 135, 158] and shear strength [76, 77, 78] or the description of the desaturation kinetics of a particulate networks depending on filtration parameters [100, 144]. Tailings are a complex particle system having a broad particle size distribution and consisting of different minerals [14] and are not often investigated yet. Furthermore, tailings filtration is a very specific application. For example, a rather short desaturation time is applied to maintain high throughputs resulting in a high residual saturation in mining. Especially, desaturation by pressurized air and its influence is investigated insufficiently for tailings.

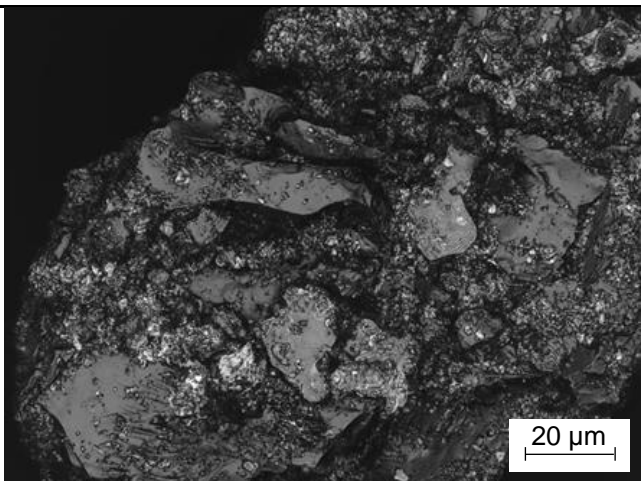
Therefore, there are two objectives of this article. The first one is the investigation of the influence of the filtration process parameters filtration pressure, cake thickness as well as gas differential pressure desaturation time and pressure on cake water content, saturation, cake to fabric adhesion and cake cohesion. The second one is the development of a mathematical description concerning water content, saturation, cake to fabric adhesion and cake cohesion. Thereby, an improved understanding of copper tailings behavior results which simplifies filtration plant operation.

4.2.2 Materials and Methods

4.2.2.1 Copper tailings

FLSmidth provided copper tailings as experimental material. A laser scanning microscopy (LSM) image shows the shape of the material with hundredfold magnification in Table 4-5. Furthermore, significant particle size distribution (PSD) data measured by laser diffraction (HELOS & QUIXEL, Sympatec, Clausthal-Zellerfeld, Germany) is listed. It is assumed that, as typical for tailing applications, a thickening process was applied, however, no information about flocculants is provided. As expected for tailings they have a broad distribution and a high fraction of fines. Density was determined using a gas pycnometer with helium (MultiVolume Pycnometer 1305, Micromeritics Instrument Co., Norcross, USA).

Table 4-5: LSM image, characteristic PSD data and density of the copper tailings.

Characteristics	Copper tailings
LSM image	
$x_{10,3} / \mu\text{m}$	2.5
$x_{50,3} / \mu\text{m}$	27.4
$x_{90,3} / \mu\text{m}$	144.0
Solid density / kg m^{-3}	2700

In addition, quantification of the main elements was carried out using wavelength-dispersive X-ray fluorescence (WDXRF) (S4 Explorer, Broker, Bruker Co, Billerica, USA). Results are shown in Table 4-6. The copper tailings consist mainly of silicon, aluminum, potassium, iron, and calcium.

Table 4-6: Main elements of the copper tailings measured by WDXRF.

Na	Mg	Al	Si	P	K	Ca	Ti	Mn	Fe	LOI
1%	2%	10%	65%	<1%	8%	4%	1%	<1%	5%	4%

A further distinction between quartz and other minerals containing silicon is useful since clay minerals have a significant influence on the filtration behavior [133]. For this reason, a mineralogical analysis was carried out. The results are listed in Table 4-7. Mineral composition was measured by X-ray diffraction (XRD) (Empyrean, Malvern Panalytical, Malvern, UK). Almost half of the tailings consist of quartz; however, silicon is also present in other silicate minerals like mica, illite, k-feldspar, plagioclase and pyroxene. Mica, illite are phyllosilicates, k-feldspar, plagioclase and quartz are tectosilicates and pyroxene is an inosilicate. Phyllosilicates are also called sheet silicates since they consist of parallel sheets of tetrahedra. Especially swelling clay minerals, for example montmorillonite, which are a certain group of phyllosilicates hamper filtration [132, 133].

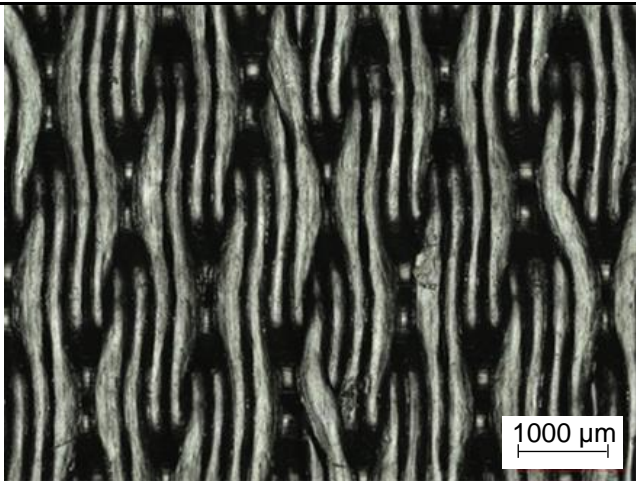
Table 4-7: XRD mineralogy analysis results of the copper tailings.

Mica	Gypsum	Illite	K-feldspar	Plagioclase	Pyroxene	Quartz
7.9	2.6	4.0	27.5	6.5	3.6	48.1

4.2.2.2 Filter cloth

A polypropylene cloth with a satin weave out of monofile fibers was used for filtration experiments. Table 4-8 shows the main characteristics. This cloth, which is suitable for tailings filtration concerning particle retention, was used in previous studies on abrasive wear and iron ore tailings lab filtration already. The plastic type reported by the manufacturer was confirmed using wide angle X-ray scattering (WAXS) [46].

Table 4-8: LSM image of the filter cloth and characteristics [44].

Characteristics	Copper tailings
LSM image	
Material	Polypropylene
Weave type	Satin
Fiber type	Monofile & monofile
Unused flow resistance / m ⁻¹	$2.6 \pm 0.6 \times 10^8$

4.2.2.3 Experimental Setup and Procedure

A stirred vessel was used for tailings slurry preparation. All filtrations were performed with a slurry solids volume concentration of 30% solids which replicates thickener underflow. By means of a riser tube compressed air fed the suspension pulsation-free into the same laboratory filter press used in previous publications [44, 162]. It has a cylindrical chamber (100 mm diameter, 40 mm cake height) which is fixed between two end plates. There is a filter medium on each side which was pre-used several times to guarantee constant filtration behavior. Each of the two end plates has a drainage structure and two filtrate outlet pipes, one on top and one on bottom, all equipped with valves. Figure 4-13a shows a schematic cross-cut during filtration. The filtrate pipes terminated on a scale that was connected to a process control system (Lab-View, National Instruments, Austin, USA), as were the compressed air supplies and valves.

The two pressure stages tested were 250 kPa and 1250 kPa filtration pressure. This covers a significant part of the tailings pressure filtration application range. After completion of filling, filter cake build-up and compaction by filtration, the valves of the lower filtrate outlet of one end plate and the upper outlet of the other end plate were closed if gas pressure desaturation was applied. Then pressurized air was introduced

using the open filtrate outlet on top, as can be seen in Figure 4-13b. By overcoming the capillary inlet pressure, the air desaturates the cake by pushing further filtrate out of the open bottom filtrate outlet on the opposite side. 250 kPa and 550 kPa gas differential pressure was used for desaturation. This covers the common range of industrial pressurized air equipment. The following three parameter combinations were investigated: 250 kPa filtration pressure (FP) with 250 kPa air blow (AB), 1250 kPa FP with 250 kPa AB and 1250 kPa FP with 550 kPa AB. For each filtration and air blow pressure combination 0 s, 15 s, 45 s, 90 s and 180 s desaturation time were applied. Thermal drying can be neglected for this desaturation times. In addition, a second chamber thickness of 55 mm was investigated for 250 kPa filtration pressure and 250 kPa air blow pressure for all desaturation times.

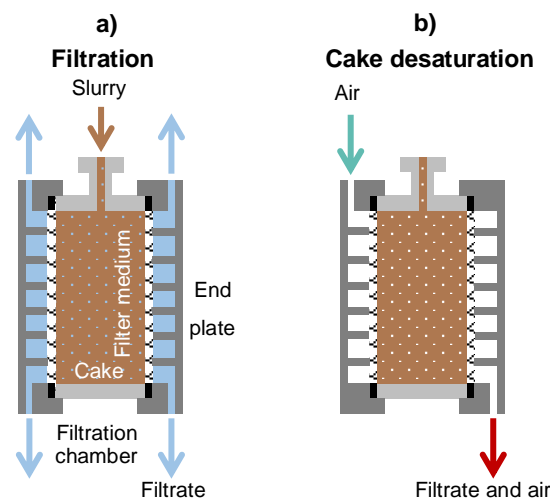


Figure 4-13: Schematic cross-cut of the lab filter press filtration and the cylindrical filtration chamber during filtration (a) and cake desaturation (b) [44].

The chamber including the filter cake inside and filter cloths still attached was taken out of the filter press after filtration or cake desaturation. Then, the chamber was placed horizontally on an add-on setup for a tensile testing machine. Using a crescent-shaped clamp, as proposed by Ginisty [60], the filter cloth of the air blow outlet side was pulled off with a velocity of 10 mm min^{-1} and the filter cake to filter fabric shear adhesion determined, as sketched in Figure 4-14a. Assuming a flat filtration area without sealing edge a simplified cake height necessary for detachment can be calculated according to Equation 4-4, taking solid and water density as well as cake solid and water content into account.

After the adhesion test, a spacer disc was placed below the filtration chamber, the cake was pushed halfway out of the cylinder and a lid was placed on the upper half of the

cake. The tensile testing machine pulled the lid with a velocity of 10 mm min^{-1} and sheared the cake analogues to a Jenike shear tester [146] (Figure 4-14b). The shear strength, also referred to as shear cohesion, was determined by relating the maximum force to the shear area.

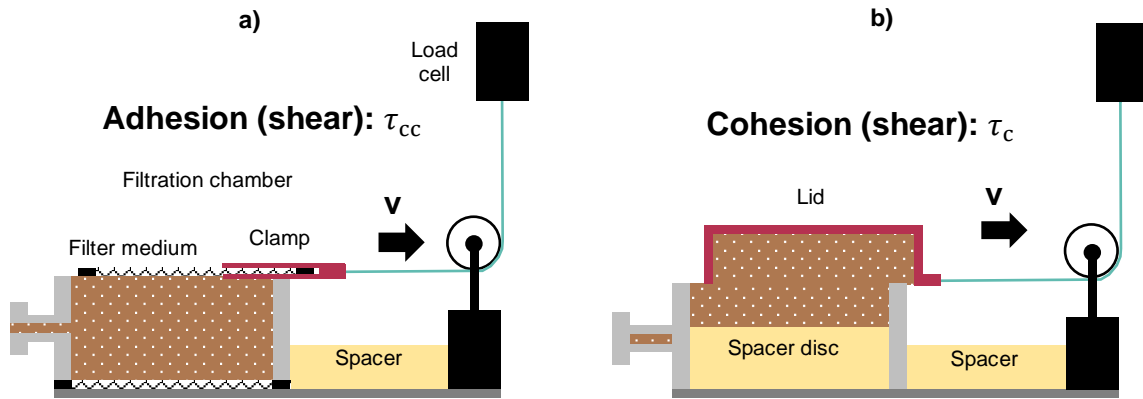


Figure 4-14: Schematic cross-cuts of filter cake to fabric shear adhesion (a) and cake shear cohesion (b) measurements [44].

Determination of residual filter cake water content was carried out by 24 hours thermal drying and weighing. The water content is defined based on the mass of water m_w and the mass of solids m_s according to Equation 4-5.

$$\text{Water content} = \frac{m_w}{m_w + m_s} \quad \text{Equation 4-5}$$

Saturation is calculated, also based on the weight of the filter cake. It is defined based on the volume of water-filled voids $V_{v,\text{water-filled}}$ and the total voids volume $V_{v,\text{total}}$, which are completely water-filled after filtration, according to Equation 4-6.

$$S = \frac{V_{v,\text{water-filled}}}{V_{v,\text{total}}} \quad \text{Equation 4-6}$$

The loss of liquid during desaturation was related to the average amount of liquid in a cake resulting from the same filtration pressure without desaturation.

4.2.2.4 Mathematical Model

In addition to measurement of the influence of gas differential pressure desaturation on water content, cake saturation, filter cake to filter fabric shear adhesion and filter cake shear cohesion, another objective of this work is the development of a simplified mathematical model. It is supposed to describe the mentioned quantities for different filtration pressures, gas differential pressures and desaturation times in sufficient

accuracy. In conjunction with the experimental setup described, it is intended to enable tailings behavior prediction with a small number of tests on site.

Some assumptions are made for this purpose and their justification is discussed in the results and discussion section. These facilitate the handling compared to existing approaches, e.g., for the description of saturation kinetics by Nicolaou (Equation 4-3) [144, 145]. In terms of filtration engineering his approach is useful since all parameters are measured during common tests in filtration engineering. However, this is randomly the case for tailings filtration. Therefore, a more holistic approach is proposed in this article to describe water content, cake saturation, filter cake to filter fabric shear adhesion and filter cake shear cohesion kinetics during air blow desaturation.

The first assumption is that the time-dependent kinetics of the above quantities is a constrained growth or decrease and can be described by an exponential function according to Equation 4-7. While this is justified for residual cake water content and saturation, the literature for adhesion and cohesion shows a different behavior when considering the complete saturation range from 0 to 1. However, since desaturation of tailings filter cake only occurs within a high range of saturation, the assumption is plausible. $x(t)_{i,j}$ is the quantity, $x_{i,j,\infty}$ the value at equilibrium, $x_{i,j,0}$ the initial value and $a_{i,j,h}$ the kinetics parameter. The indices of the time-dependent quantity i and j stand for the filtration pressure and air blow pressure, respectively. h states the cake height.

$$x(t)_{i,j} = x_{i,j,\infty} - (x_{i,j,\infty} - x_{i,j,0}) \cdot e^{-a_{i,j,h} \cdot t} \quad \text{Equation 4-7}$$

Furthermore, the initial value of the quantity is invariable, for example the cohesion of the saturated filter cake would be $cohesion_{i,j,0}$. The value of the fitted curve $x_{i,j,0}$ at that time is similar to the measured value $\hat{x}_{i,j,0}$ (see Equation 4-8). This is the second assumption.

$$x_{i,j,0} = \hat{x}_{i,j,0} \quad \text{Equation 4-8}$$

Assumption three is that $a_{i,j,h}$ is one of two fit parameters. It describes how fast the increase or decrease caused by desaturation proceeds. As shown in Equation 4-9, it is specific for every combination of filtration pressure, air blow pressure and cake thickness.

$$a_{1,1,1} \neq a_{2,1,1} \neq a_{2,2,1} \quad \text{Equation 4-9}$$

$x_{i,j,\infty}$ is the second fit parameter. It determines the limit of the constrained growth. However, it is specified that it depends only on the air blow pressure not on the filtration pressure for a certain cake thickness. This fourth assumption implicates Equation 4-10.

$$x_{1,j,\infty} = x_{2,j,\infty} \quad \text{Equation 4-10}$$

Concerning the tests in this study, in which 250 kPa air blow is performed for both filtration pressures, one average value at equilibrium is used for both.

Assumption five states, that 180 s is sufficient close to the saturation value at equilibrium for a specific air blow concerning a cake thickness of 40 mm and, thus, the ratio of a quantity resulting by two different air blow pressures is the same as for 180 s, according to Equation 4-11.

$$\frac{x_{i,2,\infty}}{x_{i,1,\infty}} = \frac{x_{i,2,180}}{x_{i,1,180}} = \frac{x_{1250,550,180}}{0.5 \cdot (x_{250,250,180} + x_{1250,250,180})} = \text{const.} \quad \text{Equation 4-11}$$

The two fit parameters for the present data are determined by minimizing the sum of square residuals for all three, according to Equation 4-12.

$$\min_{a_{i,j,h}; x_{i,j,\infty}} S = \sum_{k=1}^n (x_{1,1,k} - \hat{x}_{1,1,k})^2 + \sum_{k=1}^n (x_{2,1,k} - \hat{x}_{2,1,k})^2 + \sum_{k=1}^n (x_{2,2,k} - \hat{x}_{2,2,k})^2 \quad \text{Equation 4-12}$$

Another aspect of this article is to compare the behavior of the standard cake thickness of 40 mm and a thicker cake of 55 mm. According to Anlauf, the desaturation process differs only in its kinetics [87]. Therefore, the $x_{i,j,0}$ and $x_{i,j,\infty}$ values of the thinner cake are adopted for the mathematical modeling of the thicker cake.

4.2.3 Results and Discussion

The authors of this article assume t-distributed data. All charts give the estimated mean values and, in addition, the range of the 50% confidence level. Furthermore, the application of the modeling approach described above results in the fitted curves. The corresponding tables in the Appendix list the fit parameters. In general, the description of constrained growth or decrease meets the data with sufficient accuracy given the underlying assumptions. This justifies these simplifications.

4.2.3.1 Filtration Pressure and Air Blow Pressure Influence

Results of the water content for different filtration and air blow pressures over various desaturation times are shown in Figure 4-15. Since the two filtration pressures result in a different compression of the particulate network, the cake water content for fully

saturated filter cake, i.e., at a desaturation time of 0 s, is slightly lower for 1250 kPa filtration. Since these two filtration pressures approximately cover the range of technically applied filtration pressures in recessed plate filter presses, it is apparent that filtration without post-treatment limits the achievement of low residual water contents. By applying pressurized air desaturations, a significant further decrease in cake water content can be seen for all combinations of filtration and desaturation pressure. Especially for a high air blow pressure there is a strong decrease within a short time. However, the desaturation effect decreases with higher air blow application time. The water content is about to reach the value at equilibrium for the corresponding pressure at 90 s desaturation time for the investigated cake height of 40 mm. As assumed, it is a constrained decrease. A considerable amount of water remains within the cake due to isolated pores having higher capillary inlet pressures than the air blow pressure applied [87]. Overall, water content is reduced from approximately 20 w% to below 18 w% for 250 kPa and below 16 w% for 550 kPa air blow pressure by 180 s gas differential pressure desaturation. The intensity of the air blow is obviously the decisive variable for setting the residual water content. 550 kPa doubles the additional reduction in relation to filtration compared to 250 kPa.

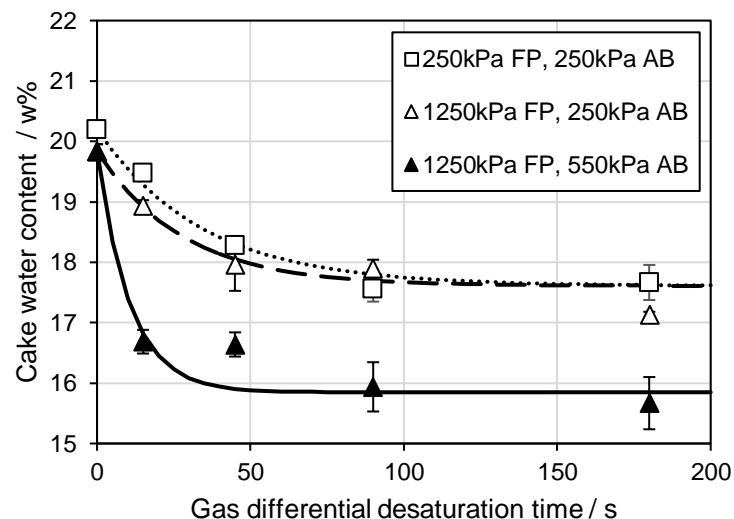


Figure 4-15: Filter cake water content of each filtration pressure and air blow pressure combination for variation of the desaturation time for a cake thickness of 40 mm.

Parameters of the water content fitted curves are listed in the Appendix. For the fits, the estimated value at equilibrium based on a ratio of 0.9004 is 17.61 w% for 250 kPa AB and 15.85 w% for 550 kPa AB. For a filter cake of 40 mm, mechanical desaturation and, therefore, filter cake desaturation mainly takes place in the first 90 s of air blow.

In general, saturation values behave analogous to the water content data for application of air blow. Data are given in Figure 4-16. In contrast to the water content, saturation curves for all three filtration and air blow pressure combination start at the full saturation of 100 v% since the corresponding unsaturated cake is the reference for each of them. Air blow decreases pore saturation for all combinations of filtration and desaturation pressure in a constrained decrease. A higher air blow pressure results in a stronger decrease and a lower final range for longer air blow times, whereas both data curves for 250 kPa air blow are nearly similar in trend. This supports the statement that the gas differential pressure is the decisive parameter for a slightly compressible filter cake. The mechanical desaturation limit due to isolated pores can be stated to be approx. 84 v% using 250 kPa and 75 v% applying 550 kPa desaturation pressure.

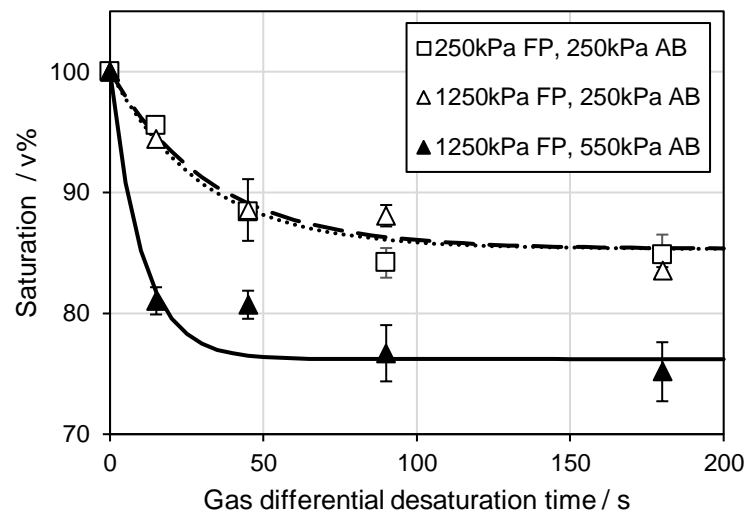


Figure 4-16: Filter cake saturation of each filtration pressure and air blow pressure combination for variation of the desaturation time for a cake thickness of 40 mm.

The Appendix section gives all parameters of the fitted saturation curves. Analogous to the cake water content, the value at equilibrium is reached within 60 to 90 s. This timeframe falls within the application times investigated, and the mathematical model is close to the measurements despite the simplifications. Fit values at equilibrium are 85.33 v% for 250 kPa AB and 76.20 v% for 550 kPa. The ratio is set at 0.8928.

Figure 4-17 shows the cake to filter cloth shear adhesion at different desaturation times for each combination of filtration and desaturation pressure. In contrast to water content and saturation, filter cake adhesion is a constrained growth in the investigated saturation range. Filtration without cake post-treatment results in the lowest filter cake adhesion at 0 s air blow time. A higher compaction of the cake, based on a higher filtration pressure, results in a higher initial adhesion. At short desaturation times

adhesion increases strongly. The effect is more distinct for the high air blow pressure. By trending towards the value at equilibrium a flattening of the curve can be seen with higher air blow times, analogous to the water content and saturation. The adhesion value at 180 s is only slightly higher for 550 kPa with 3.1 kN m^{-2} than for 250 kPa air blow with 2.9 kN m^{-2} (550 kPa AB) and 2.5 kN m^{-2} (250 kPa AB). In comparison to the corresponding fully saturated cake at 0 s air blow adhesion doubles approximately for a 1250 kPa filter cake desaturated 180 s at 550 kPa air blow and triples approximately for a 250 kPa filter cake desaturated 180 s at 250 kPa air blow. Consequently, the increase in adhesion raises the necessary cake thickness for gravity-based detachment significantly. Corresponding cake thicknesses, calculated according to Equation 4-4, are given by the second y-axis. This increase complicates the desired cake detachment, especially since the cake thicknesses are larger than usual chamber dimensions of 30-60 mm for mining applications [168]. However, adhesion measurements are strongly affected by the measurement system as well as dimensions and cake detachment might be observed for smaller thicknesses as mentioned in the introduction section [44, 71].

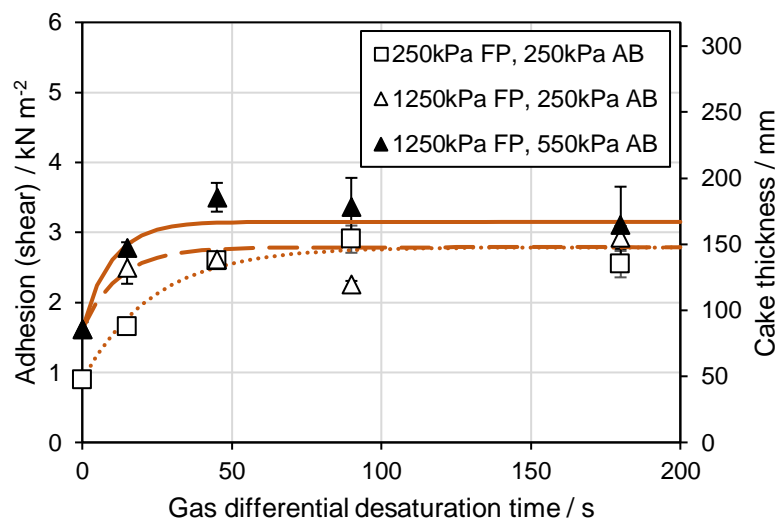


Figure 4-17: Filter cake shear adhesion and calculated corresponding cake height for gravity introduced detachment of each filtration pressure and air blow pressure combination for variation of the desaturation time for a cake thickness of 40 mm.

Adhesion fit parameters are listed in the Appendix. Based on a ratio of 1.1349 estimated value at equilibrium is 2.787 kN m^{-2} for 250 kPa AB and 3.150 kN m^{-2} for 550 kPa AB. Adhesion increase reaches the equilibrium for shorter desaturation time in comparison to water content and saturation.

Measurements of filter cake shear cohesion, which is similar to shear strength, are plotted in Figure 4-18. Analogous to the adhesion, the cohesion of the fully saturated filter cake starts at relatively low values and is a constrained growth in the investigated desaturation range. Evaluating the data points at 0 s air blow time leads to the finding that particulate structures which are stronger compressed due to higher filtration pressure have a slightly higher cohesion. Compared to the adhesion, cohesion of fully saturated filter cakes is in the same range between 1 and 2 kN m⁻². By pressurized air desaturation shear strength increases for each combination of filtration and air blow pressure investigated. Concerning the time which the desaturation is applied, there is an increase within the first two minutes. Afterwards the cohesion is approaching the value at equilibrium. Values at 180 s desaturation are 3.6 kN m⁻² (250 kPa FP, 250 kPa AB), 3.5 kN m⁻² (1250 kPa FP, 250 kPa AB) and 5.0 kN m⁻² (1250 kPa FP, 550 kPa AB). Compared to the fully saturated state shear cohesion more than triples for a 1250 kPa filter cake desaturated 180 s at 550 kPa air blow and nearly triples for a 250 kPa filter cake desaturated 180 s at 250 kPa air blow.

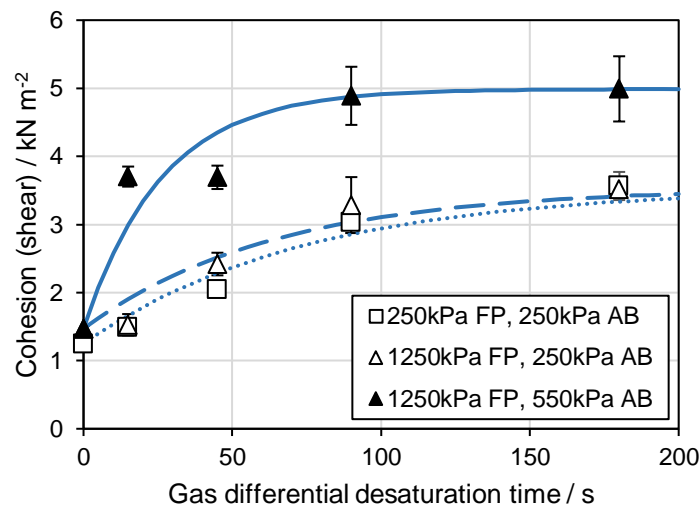


Figure 4-18: Filter cake shear cohesion of each filtration pressure and air blow pressure combination for variation of the desaturation time for a cake thickness of 40 mm.

Parameters of the fitted shear cohesion curves are given in the Appendix. The value at equilibrium is reached within the application times investigated, analogous to the shear adhesion, however, it takes longer. There is an acceptable deviation between fitted curves and measurements justifying the assumptions of the model. Values at equilibrium are 3.538 kN m⁻² for 250 kPa AB and 4.989 kN m⁻² for 550 kPa. The ratio is set at 1.4101.

In addition, the ratio of adhesion and cohesion is an important point for cake detachment. Adhesion should be as low as possible, while cohesion should be as high as possible [75]. Figure 4-19 shows the fits obtained from the methodology presented for both target quantities. Despite both are a constrained growth, it states out that independent of filtration and air blow pressure applied, adhesion kinetics are faster than cohesion kinetics. After 60 s each adhesion curve is close to the value at equilibrium, whereas cohesion curves need approximately 120 s for 40 mm cakes. Based on these findings a recommendation for plant operation be stated: There is supposed to be a trade-off between longer desaturation time associated with lower throughput and easier detachment linked to shorter technical downtimes caused by cake sticking and breakage.

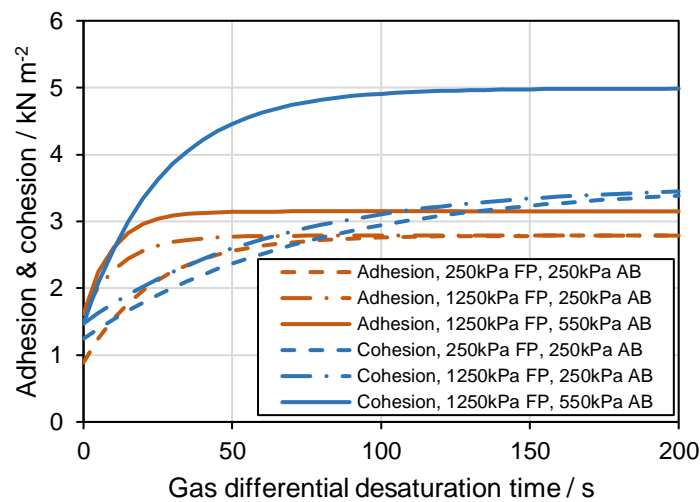


Figure 4-19: Filter cake to filter fabric adhesion and filter cake shear cohesion fits of each filtration pressure and air blow pressure combination for variation of the desaturation time for a cake thickness of 40 mm.

4.2.3.2 Filter Cake Thickness

Besides the detailed investigation for 40 mm filter cakes, tests with a second cake thickness of 55 mm were carried out for 250 kPa filtration pressure and 250 kPa air blow to evaluate changes in kinetics. Anlauf states that thicker cakes have the same values at equilibrium for identical filtration and air blow pressure stages [87]. Therefore, equilibrium and initial values are set identical to tests with 40 mm cake thickness. Only the kinetics parameter $a_{i,j,h}$ is allowed to change. Figure 4-20 shows water content of the 40 mm and 55 mm filter cakes for different air blow times. Furthermore, fitted curves according to the mathematical model presented and restrictions mentioned are given. As expected, the desaturation takes more time for the thicker cake. Overall, the effect is small for the variation investigated. The value at equilibrium is reached after

180 s instead of 90 s. Despite an increase in cake thickness of 37.5%, the in time needed for desaturation doubles. Based on the flattening of the curve the kinetics parameter decreases as can be seen in the Appendix.

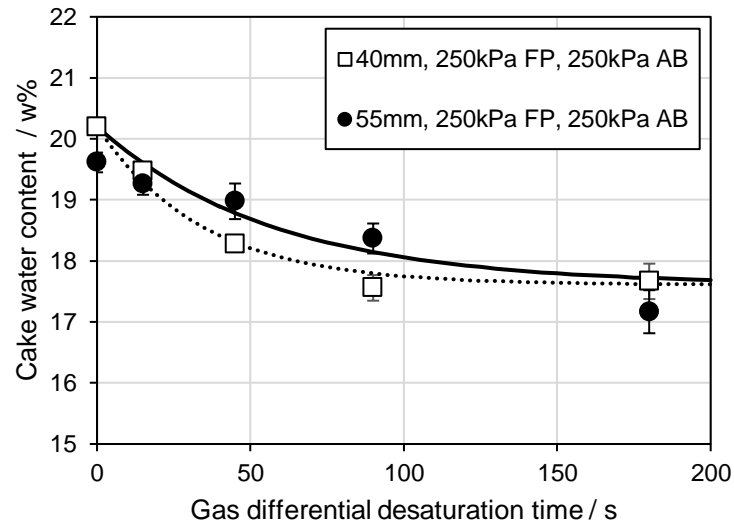


Figure 4-20: Filter cake water content of 250 kPa filtration pressure and 250 kPa air blow pressure combination for variation of the desaturation time for cake thicknesses of 40 and 55 mm.

Saturation, shear adhesion and shear cohesion of the 55 mm filter cakes including the corresponding 40 mm filter cake values are shown in the Appendix. In addition, the corresponding kinetics parameters of the fitted curves are listed. The desaturation of the 55 mm cakes behaves similarly to the water content. Desaturation takes longer compared to the 40 mm cake thickness and reaches the value at equilibrium after approximately 180 s. Also, shear adhesion increase is slower for thicker cakes, maximum values lie between 2 and 3 kN m^{-2} for the time range investigated. However, there is a delay in increase since the adhesion is measured on the opposite site of pressurized air application and 15 s are not sufficient to start desaturation within the whole cake thickness. Higher initial adhesion values are correlated to an ongoing blinding of the cloth. Shear cohesion values of the 55 mm cakes are close to the data of the 40 mm cakes since shear cohesion is measured in the middle of the cake, which is 27.5 mm and 20 mm. Therefore, it is quite similar.

4.2.3.3 Filter Cake Characteristics

It stands out that slight changes in compaction and, especially, application of desaturation result in decrease of water content in copper tailings filter cakes. In contrast, desaturation generates enormous increase in adhesion as well as cohesion and, therefore, appearance and behavior of the particulate network. This is illustrated

by exemplary pictures of filter cakes in Figure 4-21 which were taken after the shear cohesion tests. Additional stress applied by taking the cakes out of the test rig and placing them into dishes for drying results in dynamic liquefaction for the wetter cakes, e.g., 250 kPa filtration cakes without desaturation, as can be seen in Figure 4-21a. This behavior can be explained by the fact that, in terms of the Atterberg limits, these cakes are still able to flow. In soil mechanics and geotechnical engineering this is referred to as the so-called liquid limit established. This limit marks the transition from being able to flow to plastic behavior and is defined as a particulate network cohesion of about 2 kPa [36, 139]. The tailings filter cakes without post-treatment in this study have shear strengths of 1.2 kN m^{-2} (250 kPa filtration pressure) and 1.4 kN m^{-2} (1250 kPa filtration pressure). Desaturated filter cakes behave more brittle and maintain their shape. This characteristic is illustrated in Figure 4-21b, where a filter cake, produced under a filtration pressure of 1250 kPa and subjected to a 180 s air blow at 550 kPa, exhibits these properties, having an average shear cohesion of 5.0 kN m^{-2} .



Figure 4-21: Example of two 40 mm filter cakes: (a) 250 kPa filtration pressure, no air blow, average water content 20.2 w%, saturation 100 v%, average shear adhesion 0.9 kN m^{-2} , average shear cohesion 1.2 kN m^{-2} ; (b) 1250 kPa filtration pressure, 180 s air blow, 550 kPa air blow pressure, average water content 15.7 w%, average saturation 75 v%, average shear adhesion 3.1 kN m^{-2} , average shear cohesion 5.0 kN m^{-2} .

4.2.4 Conclusions

The first objective of this article was to investigate the influence of filtration pressure, air blow desaturation time, air blow pressure and cake thickness on copper tailings filter cake water content, saturation, filter cake to filter fabric adhesion and filter cake cohesion. Therefore, filtration, shear adhesion and shear cohesion tests were carried out using copper tailings, a laboratory filter press and a specially adapted shear test

rig in a modified tensile testing machine. The setup enables direct force measurements on the particulate network (filter cake) after filtration or air blow post-treatment. Thus, it generates a benefit in filtration lab test work regarding investigation of the adhesion and cohesion and their effect on the filtration process. This is of major importance considering maintenance of high throughputs in recessed plate filter presses, i.e., successful cake detachment, and geotechnical stability concerns for subsequent stacking.

In detail, a study of cake desaturation was carried out regarding desaturation pressure and desaturation time variation for two filtration pressures, two air blow pressures and two cake thicknesses. For the same cake thickness, a higher filtration pressure results in a slightly lower water content, higher cake to cloth adhesion and higher cohesion. However, slight compressibility of the copper tailings limits significant improvement of the dewatering by filtration pressure increase only. Thereof, adhesion and cohesion increase are also small without cake post-treatment. However, applying desaturation after filtration by pressurized air (air blow) leads to a significant decrease in water content and saturation and increase in adhesion and cohesion instantaneously. Since the kinetics behave as a constrained decrease or constrained growth, longer desaturation times enhance the effect up to a certain value at equilibrium. The range of the equilibrium is mainly dependent on the air blow pressure. In detail, a higher desaturation pressure generates a lower water content, a higher adhesion, and a higher cohesion for an identical filtration pressure. Furthermore, desaturation increases more sharply at the beginning for a higher air blow pressure. Thicker cakes need longer desaturation times. A mathematical model proposed describes the measurements sufficiently and its assumptions turned out to be justified.

It can be stated that desaturation is beneficial for cake detachment in two ways: Cohesion increases, i.e., the filter cakes are unable to flow, behave more brittle and maintain their shape. Furthermore, longer desaturation times increase cohesion more than adhesion. Therefore, it is more likely to detach the filter cake completely as a whole. Lower throughputs by longer desaturation times are supposed to reduce technical downtime, e.g., for filter fabric surface cleaning. In addition, a higher air blow pressure enhances the final ratio between shear cohesion and shear adhesion which can be reached by mechanical desaturation.

The presented measurement methodologies and the mathematical model support the design and operation of plants for tailings filtration. The behavior of the particulate network can be estimated with sufficient accuracy. This allows a specific selection of the process parameters to reach possible threshold values of target quantities.

Combining these conclusions with previous publications [44, 162], it is possible to provide an overview for troubleshooting common issues related to cake detachment (see Figure 4-22). If the cake adheres as a whole piece to one side of the chamber, the cohesion of the cake is assumed to be sufficiently high. Since detachment significantly depends on the cake's weight, it should be increased by having a larger cake thickness. Additionally, the selection of the filter medium offers improvement potential. It should exhibit low adhesion and ensure this throughout its lifespan. Therefore, it is essential to consider the blinding and regeneration behavior of the fabric. It should show minimal blinding tendencies and allow for sufficient regeneration. The latter should be applied regularly. If cake fragments remain in the chamber, it indicates insufficient cake strength. The cake residues can be removed through surface cleaning with water jets, aiming to prevent cake fragment entrapment at the sealing edges, for example. Proactively adjusting process parameters to increase the cohesion/adhesion ratio is advisable. If feasible, a higher cake thickness as a further option achieves a larger shear area and, therefore, improvement. Adhering base layers are another problematic aspect. An important consideration is also blinding. Particularly fine particles adhere to the fibers and block the pores, leading to increased adhesion, which results in strong cohesion of the cake at a layer of fine particles. Regular intra-fabric cleaning of blinding reduces this problem. Also, it makes sense to increase the cohesion-to-adhesion ratio through process parameter adjustment. Additionally, it is crucial to have a homogeneous cake to avoid porosity gradients and associated cohesion gradients perpendicular to the cloth. An example of this scenario would be prematurely terminated filtration with a remaining pocket, which is unconsolidated and has no shear strength, due to a non-coalesced cake.

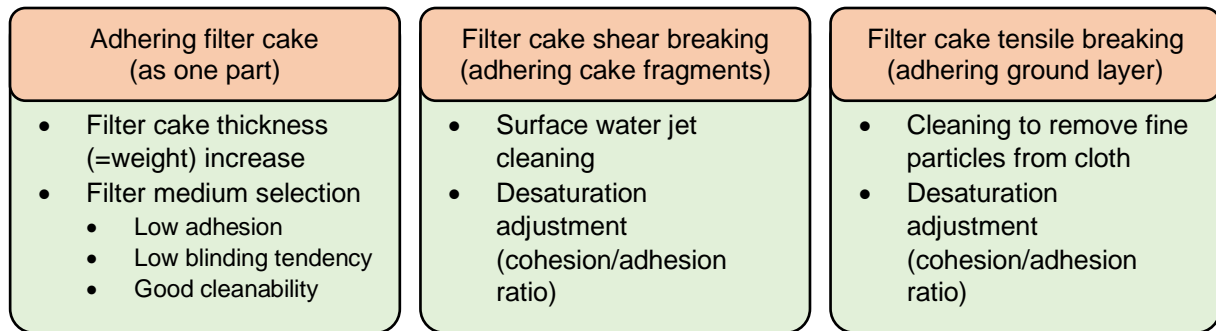


Figure 4-22: Overview for troubleshooting common issues related to cake detachment.

If individual cake fragments consistently occur in the same locations, a combination of causes should be considered, such as locally intensified blinding. In such cases, a combination of respective problem-solving approaches should be applied.

By summarizing and combining the lessons learned from this and previous experiments, the detachment behavior of cake in tailings filtration is better understood, and troubleshooting is outlined. Thereby, recessed plate filter presses performance can be improved.

5 Filter Media Abrasion

This chapter explains the advancement in testing filter media for tailings filtration in recessed plate filter presses concerning their ability to withstand abrasive wear. The results are published in a corresponding publication. A newly designed apparatus is utilized to replicate the interplay between the direction-orientated geometry of woven filter media and the direction-specific abrasive load by the detaching and falling cake. Additionally, a comparison is provided between different types of tailings filter media.

5.1 Tailings Filtration Using Recessed Plate Filter Presses: Improving Filter Media Selection by Replicating the Abrasive Wear of Filter Media Caused by Falling Filter Cake after Cake Detachment⁶

Bernd Fränkle^a, Patrick Morsch^a, Thien Sok^b, Marco Gleiß^a, Hermann Nirschl^a

^a Institute of Mechanical Process Engineering and Mechanics, Karlsruhe Institute of Technology, Karlsruhe, Germany

^b FLSmidth Inc., Salt Lake City Operations, Midvale, USA

5.1.1 Introduction

The increasing global demand for metals leads to a continuous growth in the extraction of related minerals from ores. Thereby, ore processing residues are a necessary mine waste stream. However, the storage of these tailings is already one of the major challenges in the mining industry. It has been regularly shown that the classical method of storing tailings in tailings ponds secured by dams is problematic due to water evaporation, space requirements and risk of dam failure. The Brumadinho dam breach, recorded on video, quickly gained media attention and led to new industry standards [34] and a demand to make information about such storage facilities available to the general public [169]. In the decade from 2015 to 2024, 18 catastrophic failures are expected [170], of which 13 have already occurred [171]. In terms of process technology, the method of dry stacked tailings has become more common [39]. In this process, the water content of the tailings slurry is first reduced by large thickeners and then dewatered using filter presses to a water content of usually less than 20 w% [32].

⁶ The content of this chapter was published in *Mining* 2022, 2, 425-437 and was adapted for the thesis.

Then, the resulting filter cake is transported by conveyor belts, stacked and compacted. In addition to a higher geotechnical stability of the deposit, this offers the advantage of an extensive process water recovery which is seen as one of the major potentials of this technology, especially in arid regions [59]. Usually, a large part of the water evaporates in the settling ponds. Effective water management is crucial for economical mineral processing since one ton of ore can require 0.8 m³ of water [172].

Normally, filtration of tailings in a mine takes place in several large recessed-plate filter presses operated in parallel. These were maximized by the suppliers in terms of size and minimized in terms of cycle time in order to realize the highest possible throughput and to reduce investment and operating costs [151].

Nevertheless, there are several problems in the operation of filter presses, mainly related to the selection of the filter medium and its regular replacement. The wear of the filter medium and filter plates represents the main wear problem of filter presses in tailings filtration, causing approximately 80% of the maintenance [43, 173]. Three of the main problems are abrasive wear, media blinding and cake sticking.

Abrasive wear is already known as a parameter to be considered in the selection of filter cloths [103], but it is of outstanding importance in applications with abrasive material as tailings filtration. The filter fabric is subjected to mechanical stress at several points in the filtration process [81, 100]:

- 1) Filling the filter, high flow velocities occur in the area around the chamber inlets. Over the years, patches have been sewn into these zones by suppliers to provide additional strength and counteract wear.
- 2) Increased velocities also occur near the filtrate outlets of the plates at the beginning of filtration before the first cake layer is formed. Particles passing the fabric cause abrasion on the filter medium.
- 3) Falling filter cake after detachment brushes the filter medium at the lower edge of the chamber frame and protruding parts of the chamber.
- 4) Remaining parts of the filter cake on the sealing surfaces get trapped between two opposing filter plates and filter media for the duration of the next filter cycle. Such repetitive pressing of solid particles causes stress to the fabrics and to the plates.

The permanent adhesion of fine-grained particles, which is referred to as blinding, leads to an increasing hydraulic resistance of the filter medium and, thus, has a negative effect on the filtration performance by prolonging filtration time [71].

The third important problem is an incomplete detachment of the filter cake after filtration. Often, it adheres to the filter fabric, in whole or in part, and reduce the available process chamber for the next filtration cycle. It is important to note that these problems are often interdependent. Progressive blinding will affect detachment by changing the filter medium surface, especially at a very high number of filtration cycles [43]. Furthermore, the limiting problem shifts if one of the points is optimized. If a more abrasion-resistant filter medium is used and the achievable number of cycles becomes extended, blinding will play a bigger role. The blinding or the chemical cleaning possibility of the filter cloths and also a detailed description of the detachment behavior and the necessary measurements have been discussed in previous publications [44, 48].

One purpose of this work is the development of a test method to characterize a filter medium in terms of abrasive wear by reproducing the load resulting from detaching filter cakes. A schematic visualization of the load occurring during cake falling and its locations is shown in Figure 5-1. Figure 5-1 illustrates an adhering cake before detachment. The five elevations in the middle of the plate are necessary from a certain plate size, as they stabilize the plates in the stack against bending. Likewise, the edges protrude, as they seal the plates.

In general, the whole plate is covered with filter medium. It is very important to mention, that the surface fibers of the filter cloths are orientated in vertical direction to improve cake detachment. The falling cake (Figure 5-1b) is sliding in the same direction which results in a recurrent direction-specific load.

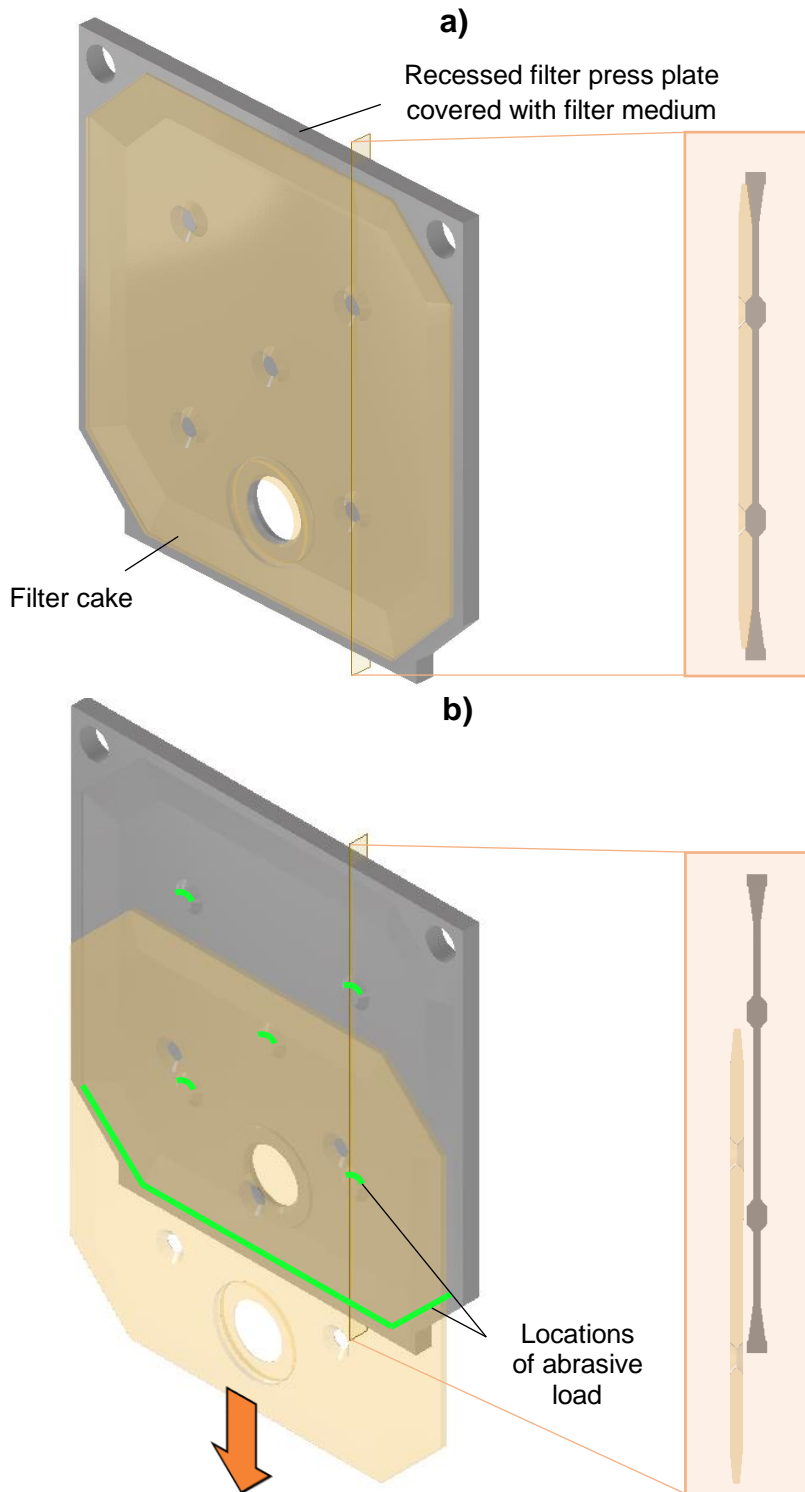


Figure 5-1: Schematic representation of the locations of abrasive load on the filter medium due to protruding parts of the filter plate. a) Filter cake adhering to filter cloth. b) Falling filter cake.

In general, suppliers give a rough wear classification of their filter media based on the materials used. Explicit information in relation to the application they are used for on individual fabrics is usually not provided.

Another aspect of developing an application-specific abrasion test methodology is the development and investigation of composite filter media, e.g., with microporous zeolite in the future [174, 175, 176, 177]. These are used in wastewater treatment, because of their ability to immobilize heavy metals [178]. Heavy metals are also an important issue in mineral and tailings processing. A modification of the filter media or the introduction of zeolite layers in tailings ponds offers the possibility to prevent heavy metals from entering the groundwater [179]. In addition, there are studies on the successful prevention of acid mine drainage [180]. An interesting fact is that zeolites themselves represent a reuse of, for example, bauxite and iron ore mine tailings [181] [182].

Standard wear tests also do not provide a recurrent direction-specific load, for example, use of a Taber Abraser. This test procedure is mentioned in various standards (ISO 9352 [183], ASTM D1044 [184], ISO 3537 [185], ISO 15082 [186]). Two friction rollers generate an abrasive load. These are pressed onto a rotating test sample with a specified force. Evaluation after the test is usually carried out by differential weighing, in which the abraded portion of the specimen is determined. Alternatively, measuring roughness or wear depth is conceivable [187]. The Taber Abraser is used to test a wide range of materials such as plastics, laminates, natural materials, and safety glazing [188]. Another common and standardized abrasion method is a pin-on-disk apparatus (ASTM G99 [189]) [83, 84, 190]. This test also results in an isotropic load. A uniaxial test used (e.g., for nonwovens) is the sliding block method using sandpaper according to ASTM D4886 standard [85, 191]. However, the abrasive stress is caused by a forward and backward movement and, therefore, represents a significant difference to the stress caused by a falling filter cake.

Summarizing, using one of the mentioned standards for replicating the problem under investigation would not be specific enough, since abrasion in filter press by cake detachment has a characteristic stress direction and cyclic behavior in one direction. Therefore, a brush apparatus causing such load has been developed.

5.1.2 Material and Methods

The abrasion apparatus is based on a chain brush system (Mink Kett-System[®], August Mink GmbH & Co., KG, Göppingen, Germany) alternately equipped with stainless steel brushes (120 mm width and 25 mm height) and spacers. The device is driven by an electric motor. Its height can be adjusted by four feet, and a pneumatic lifting device

allows the placing of a sample holder frame under the brushes. Figure 5-2 shows the structure of the lifted apparatus with a placed sample underneath.



Figure 5-2: a) Abrasion apparatus. b) Clamped filter medium sample.

Three stainless steel devices of different geometry were manufactured, over which filter media samples of 60 mm width can be clamped using a movable carriage and a threaded rod. These are of a square, a circular, and a hexagonal shape, whereby the highest point of each geometry is at an identical distance from the frame. The specimens are shown in Figure 5-3. Using a sensor counting the revolutions of the driving shaft and including the number of brushes, it is possible to evaluate the number of abrasions until rupture of a filter medium sample.

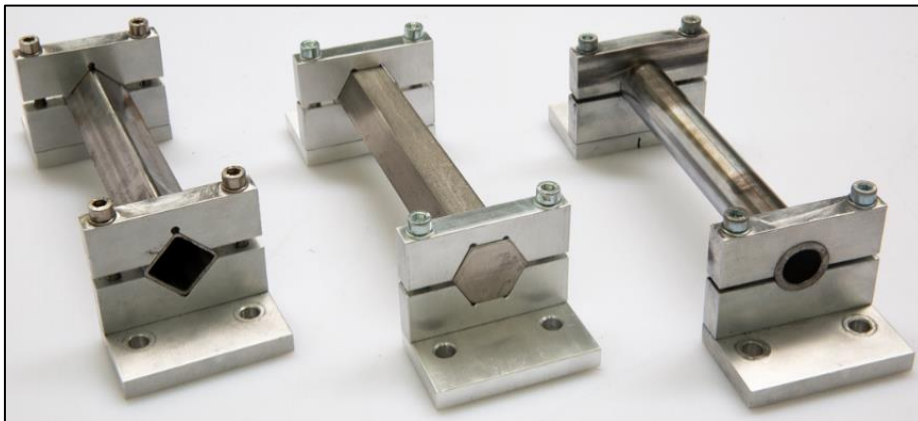


Figure 5-3: Square, hexagonal, and circular geometry variation for sample clamping.

The investigations are divided into two parts, illustrated in Figure 5-4. In the first series of tests, the investigation of the apparatus settings of clamping torque of the fabrics, overlap of the brushes and speed of the brushes were carried out with a thin nylon (NY) fabric. Three clamping torques (0.5, 0.75 and 1 Nm) were investigated, each in the elastic range of the sample. Furthermore, three overlaps (2, 4 and 6 mm) and three speeds resulting from three different rotational speeds of the motor (20 / 0.74, 40 / 1.47

and 60 rpm / 2.21 m s⁻¹) were evaluated. The limiting factor of the speed is the possibility of visual rupture observation by an operator (only possible when one of the spacers is directly over the sample). Furthermore, tests were carried out to characterize typical tailings filtration filter media provided by FLSmidth for all three edge geometries. All tests were performed six times.

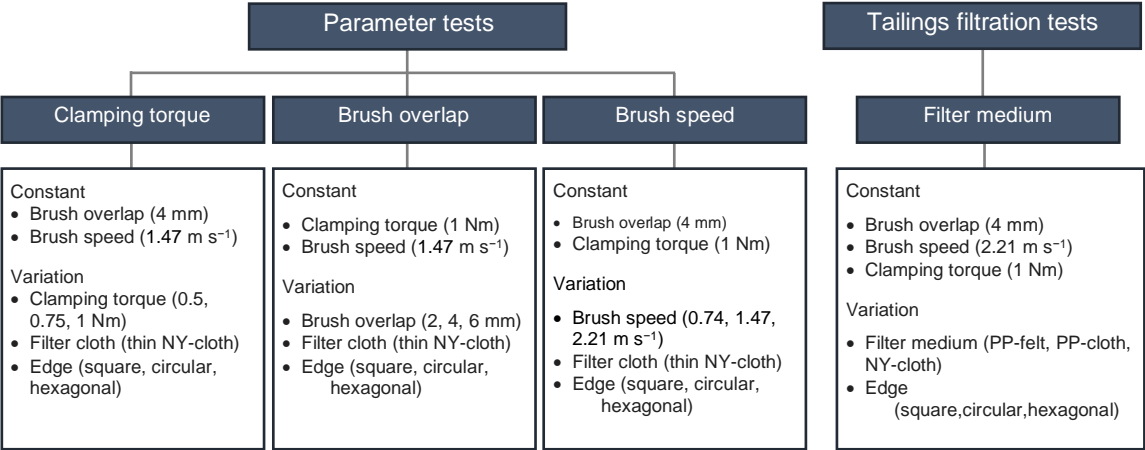


Figure 5-4: Overview of the abrasion tests for apparatus parameter evaluation and tailings filter media investigation.

A laser scanning microscopy (LSM) image and details of the filter medium used for apparatus parameter evaluation are listed in Table 5-1. Therefore, a thin plain-weave nylon cloth was used. A pressurized filter cell according to VDI Guideline 2762 was used to determine filter medium flow resistance using water [144].

Table 5-1: Properties of apparatus parameter tests filter cloth.

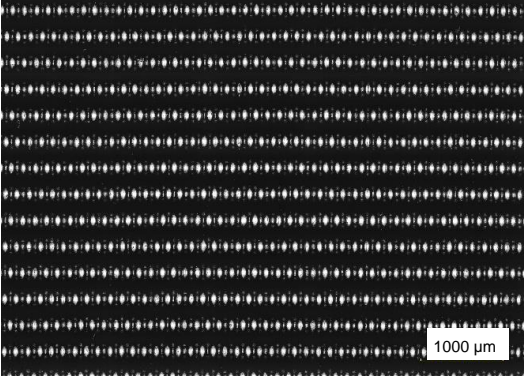
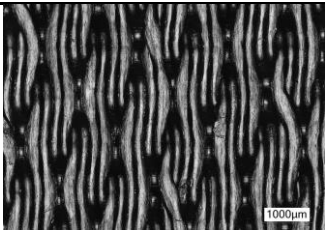
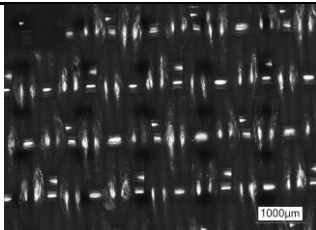
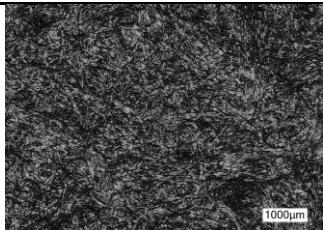
Thin NY-cloth	
LSM image	
Weave type	Plain
Fiber type	Mono/mono
Fiber diameter (warp/weft)	85 ± 4/95 ± 16 μm
Flow resistance	1.1 ± 0.1 × 10 ⁸ m ⁻¹
Thickness	0.16 ± 0.01 mm

Table 5-2 lists LSM images and data of the tailings filtration filter media (polypropylene (PP) cloth, nylon cloth and felt media out of PP). The two cloths differ in weave type, with filter medium flow resistances and thickness in the same range. The resistance of the felt medium is slightly higher and its thickness is about twice that of the cloths. These media were already part of investigations of filter cake adhesion after filtration [44].

Table 5-2: Properties of tailings filtration filter media [44].

	PP-cloth	NY-cloth	PP felt
LSM image			
Weave type	Twill	Plain	-
Fiber type	Mono/mono	Mono/mono	-
Fiber diameter (warp/weft)	180 ± 10/330 ± 30 µm	280 ± 20/310 ± 20 µm	-
Flow resistance	$2.6 \pm 0.6 \times 10^8 \text{ m}^{-1}$	$1.8 \pm 0.1 \times 10^8 \text{ m}^{-1}$	$7.4 \pm 0.9 \times 10^8 \text{ m}^{-1}$
Thickness	1.1 ± 0.1 mm	1.0 ± 0.1 mm	2.2 ± 0.2 mm

The manufacturer's specifications for the filter medium material were verified by wide-angle X-ray scattering (WAXS) measurements (Xeuss 2.0 Q-Xoom, Xenocs SA, Grenoble, France).

As soon as the operator detects a rupture of 50% ± 5 mm of the sample width (30 mm), he stops the apparatus and notes the turn counter of the motor. This, multiplied by the number of brushes (14), is noted as the number of abrasions until rupture. It has been observed that once a rupture has been started, it leads to a complete one within a few cycles. Figure 5-5 shows an example of a rupture for a test using the thin nylon fabric over a circular edge geometry.

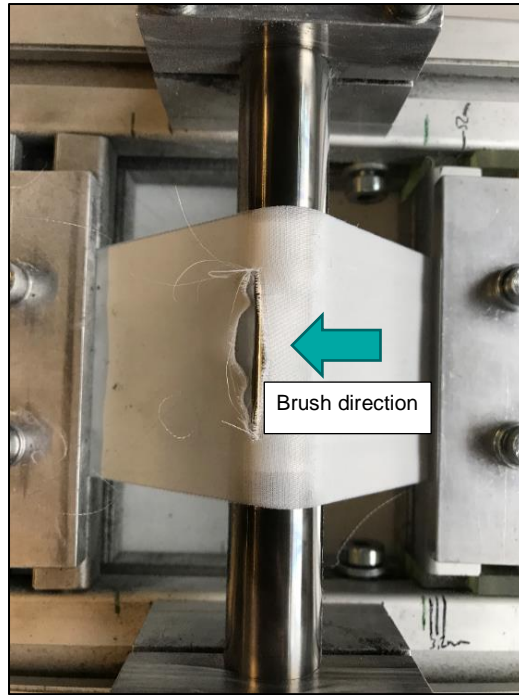


Figure 5-5: Point of rupture for the thin nylon cloth clamped over a circular edge geometry.

5.1.3 Results

The results section is divided in WAXS measurements of the filter media, tests concerning apparatus parameters, and investigations on tailings filtration filter media wear behavior.

5.1.3.1 Filter Media Material Characterization

The spectra of the thin polyamide fabric and the polyamide fabric used for tailings filtration are shown in Figure 5-6. They show two main peaks close to 20° and close to 23° and therefore agree with usual polyamide spectra [192, 193, 194, 195].

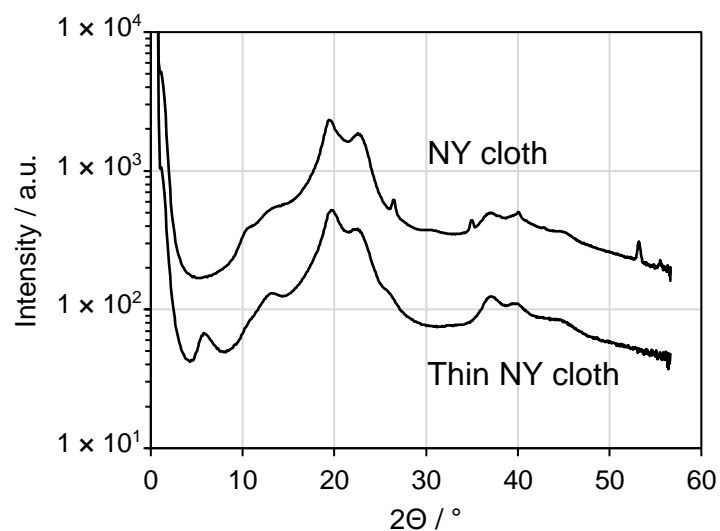


Figure 5-6: WAXS spectrum of the thin NY-cloth and the NY-cloth typical for tailings filtration.

Figure 5-7 shows the spectra of the PP-felt and the PP-cloth used in the abrasion tests. There are four main peaks close to 13° , 16° , 18° and 21° . This confirms that the material used is polypropylene [196].

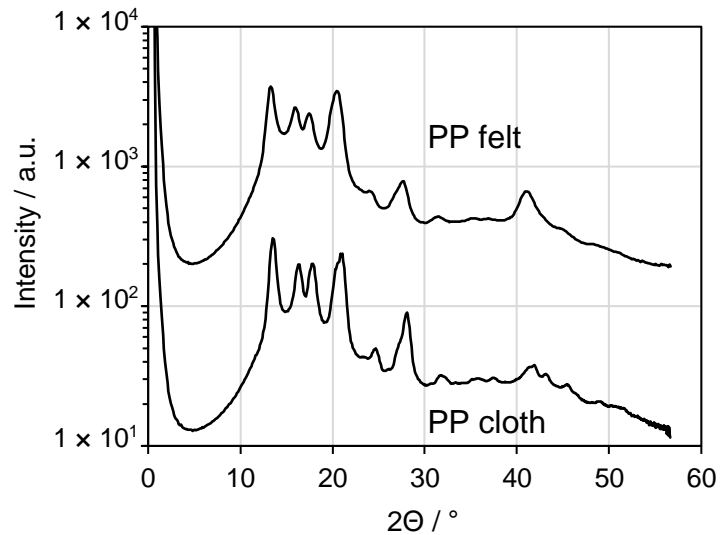


Figure 5-7: WAXS spectrum of the PP-felt and the PP-cloth typical for tailings filtration.

5.1.3.2 Brush Apparatus Parameter

The influences of the parameters that can be adjusted on the apparatus (clamping torque, brush to filter cloth overlap and speed of the brushes) are assessed using a thin nylon fabric. Figure 5-8 shows the number of abrasions until rupture for increasing clamping torque using the three different edge geometries including standard errors of the mean. For each geometry abrasions to rupture decrease with increasing clamping torque. Furthermore, it can be stated that a circular edge geometry results in the lowest number of abrasions, followed by the square geometry. The hexagonal edge has the highest abrasion values and highest uncertainties.

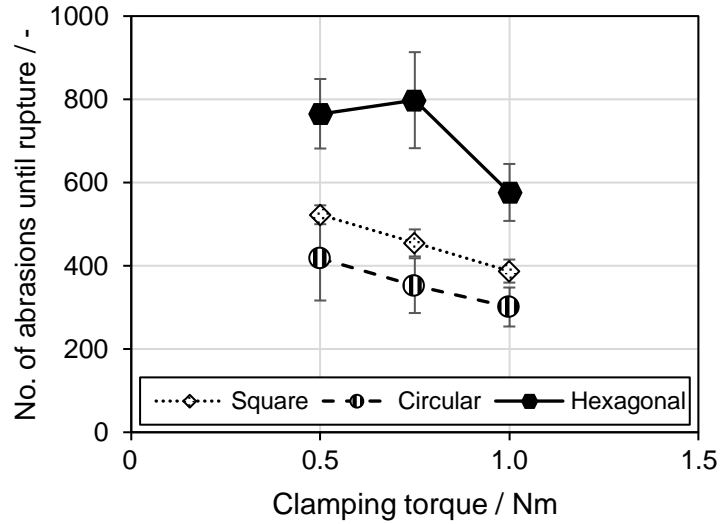


Figure 5-8: Number of abrasions until rupture of the thin nylon cloth for 0.5, 0.75, and 1.0 Nm for the square, the circular, and the hexagonal edge geometry.

Figure 5-9 shows the number of abrasions until rupture for the thin nylon cloth for the three different edge geometries and a variation of the brush overlap from 2 mm to 6 mm. Analogous to the clamping torque an increasing overlap results in decreasing abrasion values for each geometry. Again, the circular edge has the lowest and the hexagonal edge the highest number of abrasions to rupture. Furthermore, the uncertainties are higher if more abrasions are needed.

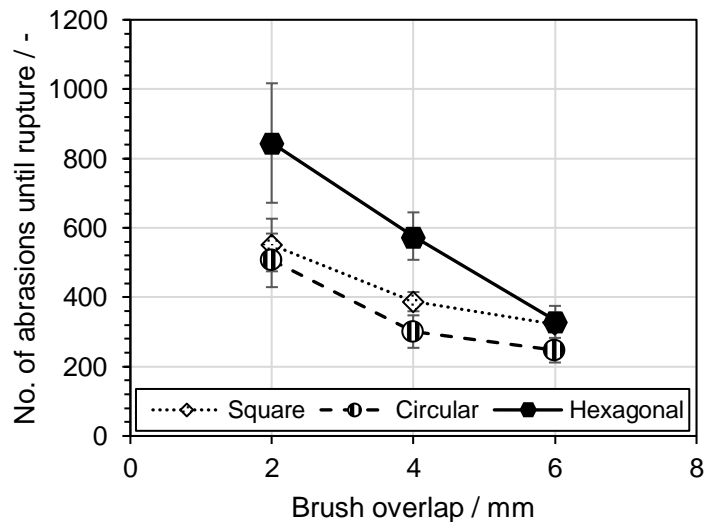


Figure 5-9: Number of abrasions until rupture of the thin nylon cloth for 2, 4 and 6 mm for the square, the circular, and the hexagonal edge geometry.

Figure 5-10 shows resulting abrasions values for a variation of brush speed (0.74, 1.47 and 2.21 m s⁻¹) resulting from a variation of motor speed (20, 40 and 60 rpm) for the thin nylon cloth for the three edge geometries. The ranking of the edge geometries is

consistent. The circular geometry results in the lowest abrasion resistance values and the hexagonal one in the highest. However, the tendency caused by the variation of brush speed is not analogous to clamping torque and brush overlap. A brush speed increase seems to slightly increase the number of abrasions until rupture. Concerning the uncertainties which are once again increased for higher abrasion values, an influence of the brush speed is negligibly small in the speed range considered.

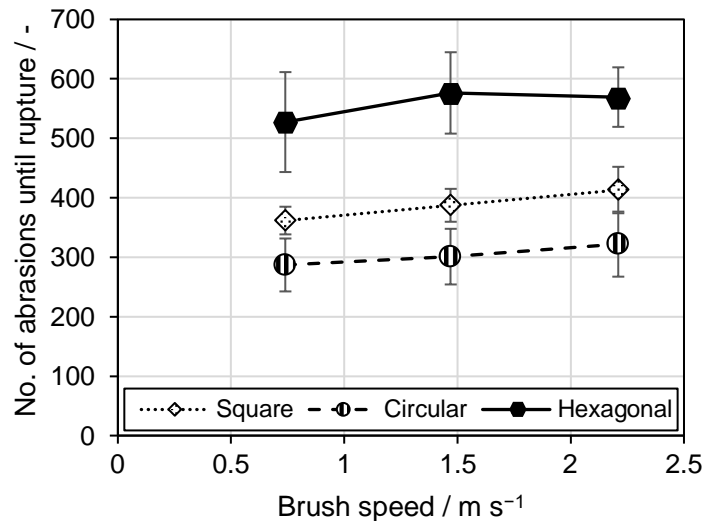


Figure 5-10: Number of abrasions until rupture of the thin nylon cloth for 0.74, 1.47 and 2.21 m s⁻¹ for the square, the circular, and the hexagonal edge geometry.

5.1.3.3 Tailings Filtration Filter Media

In addition to apparatus parameter tests, investigations were carried out on industrially used tailings filtration filter media. These pertain to the central aspect of this article: as the apparatus replicates the load, tailings filter media undergo in this specific operation, thereby offering a tool to enhance the selection of filter medium for tailings filtration.

Figure 5-11 shows the resulting number of abrasions until rupture for the PP-felt, the PP-cloth and the NY-cloth for the square, circular and hexagonal edge geometry. Due to the higher thickness of the filter media compared to the thin nylon cloth used in the apparatus parameter study, the abrasions to rupture are much higher. The PP-felt medium has the lowest abrasion resistance values. Number of abrasions to rupture is slightly higher for the PP-cloth in comparison to nonwoven fibers due to higher diameter of the single fibers. The highest abrasion resistance can be observed with NY-cloth, regardless of the edge geometry used. Concerning the edge geometry, it can be seen, analogous to the parameter tests, that the hexagonal edge has higher number

of abrasions until rupture for each filter media. Furthermore, the uncertainty increases with increasing number of abrasions.

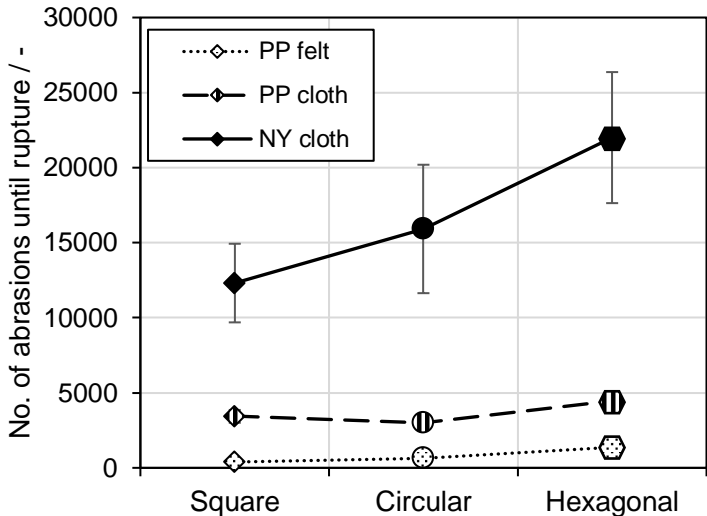


Figure 5-11: Number of abrasions until rupture of the PP-felt, the PP-cloth, and the NY-cloth for the square, the circular, and the hexagonal edge geometry.

Table 5-3 shows the differences in fabric resistances for uniaxial loading with repetition in one direction achieved with the brush apparatus. The increase of abrasions to rupture for each different edge geometry is listed in each combination. The largest increase results between the NY-cloth and the PP-felt for the round deflection with an increased service life of factor 31.8.

Table 5-3: Increase of abrasions to rupture of the filter media typical for tailings filtration in comparison with each other for the different edge geometries.

	Square	Circular	Hexagonal
NY-cloth to PP-cloth	3.6	5.3	4.9
NY-cloth to PP-felt	31.8	25.0	16.1
PP-cloth to PP-felt	8.9	4.7	3.3

5.1.4 Discussion

The presented brush apparatus, which induces a direction-specific load to simulate filter media abrasion in tailings filtration by detaching cakes, provides a reproducible means of comparing different filter media.

Important setting parameters of the apparatus were investigated using a thin nylon cloth and their influence on the number of abrasions until rupture was shown. It also allows comparison between media typical for tailings filtration. However, there is a simplification in defining the time of rupture with the time of a 50% rupture of the sample. This serves to improve detectability for the operator who determines the time of rupture. The influence of different operators must also be considered.

In general, it is important to know that a very large number of different filter medium types is available. This can be seen in the number of exhibitors of filter media manufacturers at filtration and separation trade shows, such as the Filtech or the World Filtration Congress. For this reason, it is important to compare three very different filter media in this article, all of which would be suitable for the same application.

By varying different clamping geometries, a potential area for optimization was demonstrated, which is of particular interest to filter plate manufacturers. However, it must be kept in mind that the process engineering tasks of the edge geometry, e.g., sealing of the process chamber, must be considered in a superordinate manner.

In conclusion, it can be stated that a coarse comparison of filter media for tailings filtration is already possible with currently standardized tests, but the presented methodology is closer to the specific loading case of detaching filter cakes in recessed plate filter presses.

5.1.5 Conclusions

One objective of this article is to introduce and validate a methodology aimed at enhancing the selection of filter fabrics for tailings filtration. This is achieved by simulating the specific abrasion process occurring at the protruding edges of the filter plates, offering a more accurate representation than standardized abrasion tests. Another objective is to compare the abrasion resistance of three different filter media that could be used for this filtration application.

The former objective results in the presentation of a brush apparatus that causes a repetitive uniaxial abrasion load in one direction. This apparatus allows the number of

abrasions up to a rupture of a fabric sample clamped over an interchangeable edge geometry to be determined. This load is closer to the abrasion caused by falling filter cakes than currently standardized wear test methods.

The proof of concept is carried out by means of a parameter study on important setting variables of the presented brush apparatus. These are sample clamping torque, brush to sample overlap, and brush speed. It turned out that an increased clamping torque reduces the number of abrasions, as does an increasing overlap of the brushes. The influence of brush speed in the range of a visual observable velocity by an operator is negligible.

Furthermore, the investigated square edge geometry results in the lowest number of abrasions until rupture, followed by the spherical one, whereas the hexagonal edge causes the highest abrasion resistance values for the same filter medium.

In addition, the investigations on possible filter media for filtration of tailings showed significant differences in abrasion resistance. The PP-felt medium is ruptured by the lowest number of abrasions, followed by the PP-cloth. A significant increase in the number of abrasions until rupture can be seen for the investigated NY-cloth.

Variations and tendencies by parameter adjustments (clamping torque, brush overlap, and brush speed) play a subordinate role in comparison to edge geometry, medium type, thickness, and material.

6 Filter Media Blinding

Besides abrasive wear, another important factor responsible for cloth exchange is filter media blinding by permanently adhering particles in the pores. This chapter eludes the progress made in cloth blinding regeneration which directly results from the research conducted in this dissertation. The investigation is based on three industrially blinded filter cloths provided by FLSmidth. The first publication embedded in this chapter focuses on jet water cleaning, the current industry standard. The results obtained for an iron ore tailings cloth, and the estimated cleaning costs are given. Additional information in the Appendix expands the investigations by a silver and a gold tailings cloth. The second publication explores the effectiveness of chemical and ultrasound cleaning for all three cloths. The corresponding cost estimation for chemical cleaning is provided in the Appendix.

6.1 Tailings Filtration: Water Jet Spray Cleaning of a Blinded Iron Ore Filter Cloth⁷

Bernd Fränkle^a, Maximilian Stockert^a, Thien Sok^b, Marco Gleiß^a, Hermann Nirschl^a

^a Institute of Mechanical Process Engineering and Mechanics, Karlsruhe Institute of Technology, Karlsruhe, Germany

^b FLSmidth Inc., Salt Lake City Operations, Midvale, USA

6.1.1 Introduction

For a modern way of life, the products that are needed originate in the mining of ores. For example, electric vehicles require a non-negligible amount of nickel and copper contained in their batteries [163]. As a result, the mining of minerals is constantly growing. Drawing the big picture, the mining cycle can be divided into exploration, evaluation, exploitation, mineral processing and reclamation [34]. The aim of mineral processing is the separation and concentration of valuable minerals from unusable rock. In terms of process technology, this is usually achieved by crushing associated with froth flotation or leaching [11]. In most cases, the valuable minerals represent only a low percentage of the mined rock, e.g., 30% for iron ore and 1% for copper ore [13].

⁷ The content of this chapter was published in *Minerals* 2023, 13, 416 and was adapted for the thesis.

Therefore, the enormously large mass flows of solids remain as residues referred to as tailings [3]. Furthermore, nearly all of the process water is included in the tailings slurry, increasing the mine waste volume even more. Normally, this suspension of fine-grained rock gets pumped into large settling ponds, which have to be secured by dams. Due to regular dam failures and a low recycling rate of the process water, methodologies for thickening this suspension were developed during the 20th century [36]. If the tailings disposal is conducted as a paste or even as a filter cake, safer storage, recovery of the majority of the process water and reduction in land footprint is possible [35].

The filtration and dumping of ore residues are referred to as dry stacked tailings. Often, recessed plate filter presses performing filtration by means of plastic filter media are used for this purpose. These ensure the dewatering of slurries containing particles that are too small for vacuum filtration or an increase in clay mineral content that is unfavorable for filtration caused, for example, by a change in the ore body [100]. In one mine only, several large recessed plate filter presses are operated in a parallel arrangement to handle the enormous mass flows (e.g., 7 for a 100.000 t per day tailings application [36]). Each filter medium has a lifetime of several thousand filtration cycles before it has to be changed due to abrasive wear or blinding [43]. Blinding is a ubiquitous and undesired side-effect during cake filtration using filter media describing the permanent adhering of particles inside a cloth or nonwoven fabric reducing its permeability and increasing its pressure drop, referred to as filter medium flow resistance [71, 197, 198]. This results in several negative effects concerning the filtration apparatus performance: if a defined filtrate volume is specified (for filter presses this corresponds to a specified residual cake water content of the filter cake), the filtration time will be extended; if the cycle time is fixed, the filtrate volume will be reduced and the filter cake will have a higher water content. In any case, a performance reduction and an increase in energy consumption will occur. The operator of the filtration plant is forced to define a tolerable limit value for the necessity of a filter medium replacement. Conversely, this means that extending the possible service life of the fabric increases energy and resource efficiency based on the reduction of wear material in terms of the filter medium and plant downtime. Especially in the mining industry with a continuous large mass flow, performance decrease of the filtration equipment and downtimes are very critical, as they quickly affect the overall processing in the concentrator plant and, thus, represent a bottleneck.

A successful filter medium cleaning faces the challenge of blinding, improves technical plant availability, and reduces spare part costs. Therefore, in addition to systems for a quick change of filter media, suppliers usually offer nozzle-cleaning systems for cloth washing [89, 98, 99]. The following advantages of spray washing are the main reasons for their implementation:

- The washing properties are very flexible and adjustable for each specific application. In detail, this means fluid velocity and pressure, distance between nozzle and surface as well as impinging angle [91].
- Easy implementation and reduced hazard potential compared to chemical cleaning, which is also present [199, 200]. Regarding the latter the chemical properties of the filter medium plastics are an additional limiting factor [119, 122, 201].

Due to these benefits and its prevalence in the industry, nozzle cleaning can be considered the standard for tailings filtration application. However, industrially used systems are currently based on the experience of operators and suppliers, and there is hardly any data published in the mining sector. The mining company Outotec gives a pressure of 1 to 3 MPa as a rough guide for cleaning particles trapped between fibers, and 5 to 10 MPa for cleaning precipitated or slimy solids [89].

Since intra-cloth contamination is a complex interaction of particle to fiber adhesion [127], particle to particle cohesion [71] and form closure (e.g., in multifile fibers) [67], these recommendations are insufficient. In addition, the complex geometry of the filter cloths and locally varying flow properties enhance the difficulty of cleaning [91]. Food and pharmaceutical engineering are areas where nozzle cleaning of filter media is scientifically studied, mainly for the reason that fabric contamination is a problematic point concerning the hygienic design of the process chain [202]. However, the cleaning behavior is stated as strongly dependent on the cleaning application [91]. Therefore, a direct transfer of specific solutions to the mining sector is not possible. The aim of this article is to improve the understanding of filter cloth water jet cleaning for iron ore tailings filtration by investigating the parameters flux, spray time and jet orientation, which are known as very important for the cleaning effectivity as well as water and energy consumption [91].

These parameters are of great industrial and scientific relevance:

- Permeability regeneration (flow resistance reduction);
- Water and energy consumption (ecological and economic benefit).

This article focuses on the regeneration of tailings filtration filter cloths from the processing of iron ore. In general, iron ore processing is well understood and broadly investigated, for example, in terms of iron mineral concentration by mechanical enrichment or flotation due to increasing demand and decreasing ore grades [203] [204]. Besides increasing the amount of residues, the necessity of processing low-grade ores drives innovative process design [205]. In addition, iron ore tailings gain more and more importance, as they are produced in large annual quantities all over the world [54]. Their relevance is also indicated by the large number of reuse applications that are being studied, such as usage in adsorbents, batteries, geopolymers, mortar and concrete, pigments and several more [54]. In addition, a previous study showed that the investigated filter fabric of iron ore tailings had low effectiveness in chemical cleaning and, therefore, another cleaning option is necessary.

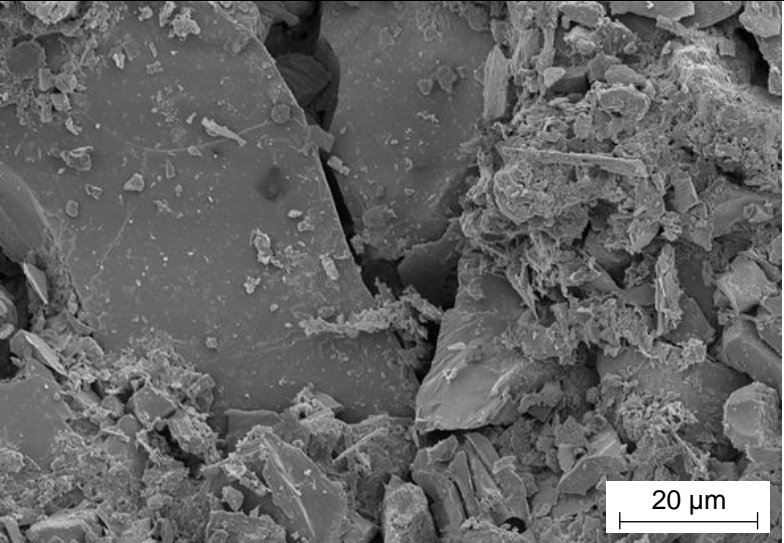
6.1.2 Materials and Methods

After a detailed description of the tailings from an iron ore mine used in the study, as well as the associated filter fabric, this section explains the experimental setup of the nozzle cleaning as well as the evaluation methodology of the fabric permeability in a pressure housing.

6.1.2.1 Iron Ore Tailings

Samples of tailings from an iron ore mine in Asia were provided by FLSmidth. These were first characterized by means of scanning electron microscope (SEM) images and a particle measurement by laser diffraction (HELOS & QUIXEL, Sympatec, Clausthal-Zellerfeld, Germany). Table 6-1 shows the SEM image of these tailings at a thousandfold magnification and gives characteristic values of the particle size distribution (PSD), which were measured in a previous publication [48]. The broadness of the distribution and the high fraction of small particles in the lower micrometer range is typical for tailings [14, 39, 110, 154].

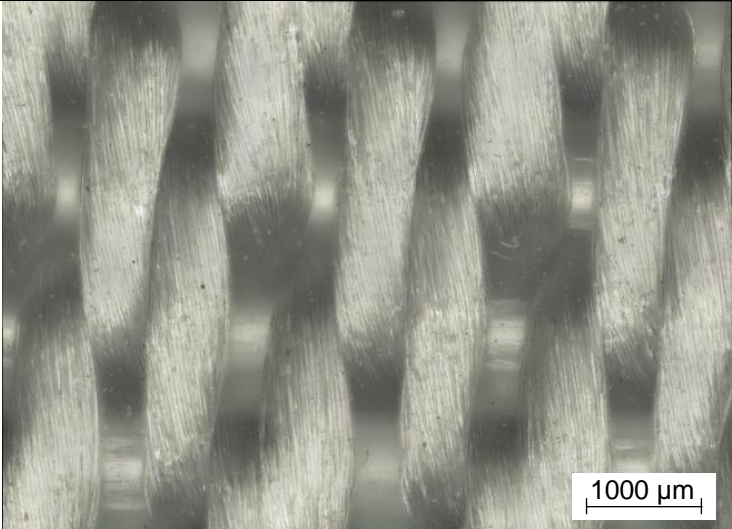
Table 6-1: SEM image (1000x) and characteristic PSD excerpts of the iron ore tailings.

Characteristics	Iron Ore Tailings
SEM image	
$x_{10,3} / \mu\text{m}$	7.2 [48]
$x_{50,3} / \mu\text{m}$	38.2 [48]
$x_{90,3} / \mu\text{m}$	120.8 [48]

6.1.2.2 Filter Cloth

In addition to the tailings, FLSmidth provided used filter cloths from the same mine and the corresponding unused version. The blinded cloth had run approximately 1000 filtration cycles. A color image taken with a laser scanning microscope (LSM) of the unused version at tenfold magnification is shown in Table 6-2 as well as further specifications. The structure of the polypropylene cloth is a twill weave made of monofile weft fibers and multifile warp fibers; the latter dominate on the surface. This cloth was part of a previous chemical cleaning investigation in which the flow resistance of the unused and the industrially used (blinded) version was measured [48].

Table 6-2: Color image (10x) of the unused cloth state taken with a LSM and characteristics.

Characteristics	Iron Ore Tailings
LSM image	
Material	Polypropylene
Weave type	Twill
Fiber type	Monofile and multifile
Unused flow resistance / m ⁻¹	$4.3 \pm 0.1 \times 10^8$ [48]
Used flow resistance / m ⁻¹	$2.4 \pm 1.9 \times 10^{11}$ [48]

6.1.2.3 Spray Nozzle Jet Cleaning of Iron Ore Tailings Filter Cloth Samples

The contamination of the industrially used fabric from tailings filtration of an iron ore mine after approximately 1000 filtration cycles is shown in Figure 6-1. It is visible that both the voids between the fibers and the interior of the multifilament fibers are completely blocked with particles. In order to regenerate the resulting additional flow resistance, these must be removed, overcoming the adhesion of particles to the fibers, particle-particle cohesion and form closure.

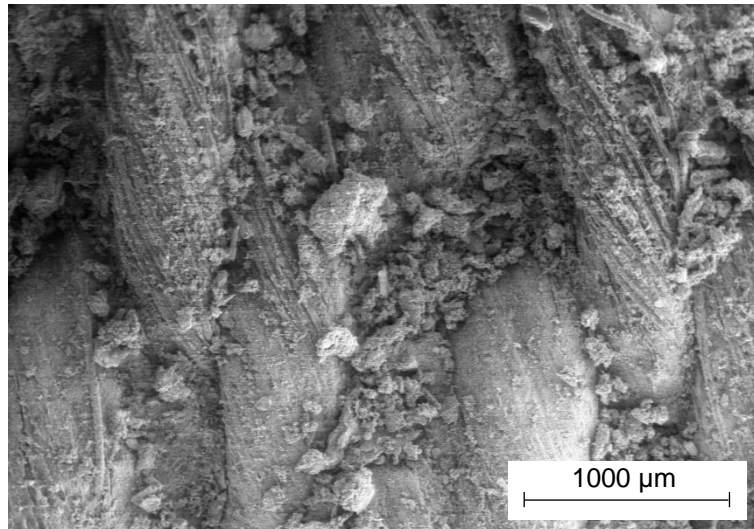


Figure 6-1: SEM image (85x) of the industrial used (blinded) iron ore tailings filter cloth surface showing the blocked particles between and within the fibers.

Table 6-3 shows the elemental composition measured by energy dispersive X-ray spectroscopy (EDX) of the particles adhering to the uncleaned cloth and the weight-based composition. This is in the range of the values in the literature for various mine sites [54].

Table 6-3: EDX analysis of adhering particles for the used filter cloth based on weight.

Element	Si	Al	Fe	K	Ca	Mn	Other
Adhering particle / $\mu\text{g cm}^{-2}$	769	100	1402	60	52	137	1117
Ratio / %	31	4	56	2	1	5	31

For the nozzle cleaning tests, circular filter media samples out of the industrially used cloths of the iron ore mine were prepared and sprayed, as shown in Figure 6-2, which can be used after cleaning for a permeability determination in a pressure housing. First, specimens with a diameter of 75 mm were cut from the 2 m \times 2 m tailings filter fabric. In the next step, these were sealed at the edge with liquid rubber, corresponding to the size encountered by the cleaning jet to adjust flux. This was followed by the assembly and the cleaning of the cloth using the nozzle test setup.



Figure 6-2: Methodology of permeability test samples preparation including jet cleaning.

The test setup consisted of a positive displacement pump (axial piston pump with three pistons of a high-pressure cleaner (Kärcher HD 6/15 C Plus, Alfons Kärcher, Winnenden, Germany) and a 60° full cone nozzle (4906041YCE000, Lechler, Metzingen, Germany). A full cone nozzle was selected since it provides a uniform distribution of the liquid and the impinging area. The impinging impact is well defined in comparison to a flat nozzle [147]. An impinging angle of 90° was selected since this ensures a uniform flux distribution at the entire impinging area for a full cone nozzle [147]. Furthermore, flatter impinging angles reduce the impact force according to Werner et al. [94].

Measurements determined a constant flow rate of tap water at a value of $7.5 \pm 0.1 \text{ L min}^{-1}$ ($1.25 \pm 0.02 \times 10^{-4} \text{ m}^3 \text{ s}^{-1}$) with a water temperature of $12.5 \pm 0.1 \text{ }^\circ\text{C}$ at a pressure of $1.6 \pm 0.1 \text{ MPa}$. The measured electrical power requirement for this setup is $1.19 \pm 0.02 \text{ kW}$. The full cone nozzle has a diameter of 2.05 mm at its narrowest point, which corresponds to an average velocity of $38 \pm 1 \text{ m s}^{-1}$ ($\text{Re} = 6.4 \pm 0.1 \times 10^4$) in this part of the nozzle. For the variation of the volumetric flux impinging on the filter sample, the impingement area of the cone was calculated based on the geometric data and the distance between the nozzle and media sample was adjusted. According to Werner et al., the cleaning distance should be within the core area of a jet or slightly above [91]. The core area apex is system-dependent but as a rule of thumb a distance-nozzle-diameter (DND) ratio of 5 can be assumed [206]. In addition, too small distances may inhibit cleaning due to a back flux. Therefore, as boundary values, a minimum impact diameter of 10 mm was chosen (DND ratio 4.2). As a maximum impinging diameter, 50 mm was set since this is the diameter of the pressure housing used for permeability determination. Within the range of the distance between the nozzle and cloth from 8.7 to 43.3 mm, the flux and, therefore, the jet impinging pressure changes drastically. Table 6-4 gives a schematic illustration of the

geometric relations using a cross-cut, positions of the test samples and resulting characteristics.

Table 6-4: Characteristics of the full cone nozzle, filter cloth sample positions and impinging areas.

Characteristics	Test setup			
Schematic illustration				
Impinging diameter / mm	10	14	22	50
Distance / mm	8.7	12.1	19.1	43.3
DND ratio	4.2	5.9	9.3	21.1
Impinging area / mm ²	79.2	153.3	382.0	1963.5
Flux / m ³ s ⁻¹ m ⁻²	1.59	0.81	0.33	0.06

It is not possible to predict from which side cleaning will be more effective [91]. For this reason, the variation of the flux and the spray time were carried out for a spraying from the front (cake side) as well as from the back. It should be noted that in industrial applications, only front-wash would be possible without disassembling the cloths and, thus, significantly lower downtime. However, spraying from the front possibly involves the risk of transporting particles deeper into the filter medium [111].

The setup shown in Figure 6-3 was used to position the specimen. The sample holder consisted of a support plate, backing cloth and a frame for clamping. The support plate, attached to a stand, has a cavity in the area behind the specimen, which is equipped with drainage channels for water passing through to the bottom and air inlet channels at the top. A coarse metal square mesh (mesh size 2 mm, wire diameter 1 mm) was used as a backing cloth. The clamping frame fixed the specimen and the backing cloth to the support plate and had an inner diameter of 60 mm and an angled transition to ensure the possibility of jet flow off to the side. This is essential for the displacement of dirt particles removed during spraying and absorbed in the cleaning fluid.

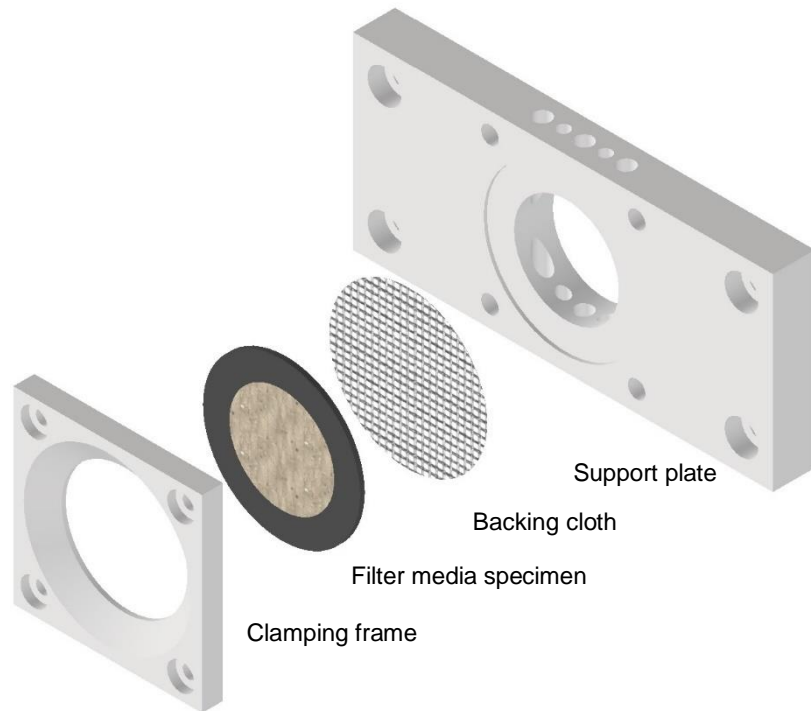


Figure 6-3: Design of the sample holder of the nozzle test station consisting of a support plate onto which the filter medium sample and a backing cloth are fixed with a clamping frame.

6.1.2.4 Evaluation of the Cleaning Performance

As a quantitative measurement to evaluate the cleaning performance, flow tests using a pressure housing according to VDI standard 2762 developed for lab filtration were performed. In the housing, the filter medium is fixed between a funnel at the bottom and a cylinder [109]. The cylinder can be closed and pressurized with compressed air. Clear water was filled in the cylinder above the medium and conveyed through the sample by applying a slight overpressure. By measuring the permeation of water gravimetrically at the fixed pressure, the filter medium clear water flow resistance $R_{\text{fm,clear water}}$ can be calculated using an adapted version of Darcy's law (Equation 6-1). $R_{\text{fm,clear water}}$ is dependent on the flow area A , the measured mass flow \dot{m} , the density of the liquid ρ_l , the applied pressure difference Δp and the dynamic viscosity of the liquid η_l . This resistance is the reciprocal value to the permeability of the fabric.

$$R_{\text{fm,clear water}} = \frac{A}{\dot{m}} \cdot \rho_l \cdot \frac{\Delta p}{\eta_l} \quad \text{Equation 6-1}$$

Furthermore, the ratio of the resulting mass flow through the cleaned sample to the mass flow of the used fabric according to Equation 6-2 is used to discuss the cleaning effect.

$$Flow\ ratio = \frac{\dot{m}_{fm,cleared}}{\dot{m}_{fm,used}} = \frac{R_{fm,used}}{R_{fm,cleared}} \quad \text{Equation 6-2}$$

The flow ratio allows a final labeling of the cleaning parameter combinations and is based on a threshold value for the improvement of the flow to a certain ratio. Based on this, the selection of an optimal parameter combination can then be evaluated to reduce the demand of spray water. For this purpose, the theoretical area-specific water demand $V_{w,area\ specific}$ is calculated by multiplying spray flux and spray time t_{cl} . In addition, there is a factor that considers the necessary overlapping of several nozzles during surface cleaning (Equation 6-3). The Lechler company specifies an overlap of the impinging surfaces of $1/4$ to $1/3$ [147]. Here, the conservative factor of $1/3$ is used.

$$V_{w,area\ specific} = \frac{3}{2} \cdot Flux_{cl} \cdot t_{cl} \quad \text{Equation 6-3}$$

Based on the measurement of the electrical power demand of the test setup including one nozzle $P_{e,single\ nozzle}$ in operation, the overlap factor for a multiple nozzle application, the cleaned area by one nozzle $A_{cl,single\ nozzle}$ and the spray time, the calculation of the required electrical energy for cleaning per square meter $E_{e,area\ specific}$ is carried out according to Equation 6-4.

$$E_{e,area\ specific} = P_{e,single\ nozzle} \cdot \frac{1}{\frac{2}{3} \cdot A_{cl,single\ nozzle}} \cdot t_{cl} \quad \text{Equation 6-4}$$

6.1.3 Results and Discussion

For nozzle cleaning from the front (cake side) as well as from the back, the filter medium flow resistances measured by means of flow-through tests are presented in this chapter and compared with the industrially used (blinded) and unused conditions. Originally, the apparatus used to perform the tests was developed for filtration tests instead of permeability tests. From these, important parameters are obtained for the design of a filter apparatus, primarily the filter cake resistance and the filter medium resistance. The latter is not the same as the pure flow resistance. The filter medium resistance is the resistance including the first particle layer of the filter cake, which forms the particle bridges that then act as a filter medium themselves. However, the measurement of the filter medium resistance based on filtration tests is not suitable for the specification of the state of blinding or its regeneration as the effect of bridging prevents quantification [48]. Therefore, permeability tests are necessary. In this article, a t-distribution of the parameter resistance is assumed and, in addition to the

estimation of the mean value, the range of the 50% confidence level is given. Moreover, a listing and evaluation of the area-specific requirement of water for cleaning, calculated from the resistance values is carried out. Furthermore, electric energy demand per square meter is determined as well as approximated cleaning costs. Eventually, an optical investigation of different cleaning states is carried out.

6.1.3.1 Front-wash Cleaning Performance and Water Demand

The filter medium flow resistance data achieved by front-washing for the different spray times are plotted over the flux in Figure 6-4. As a reference, the unused and used state of the cloth is given as a dot-dashed and a dashed line and the mean values are exemplarily connected to illustrate the cleaning performance tendency for the lowest spray time. Starting at the value of the industrially used blinded cloth at $2.43 \times 10^{11} \text{ m}^{-1}$, the flow resistance is drastically decreasing for each investigated spray time and the lowest flux ($0.06 \text{ m}^3 \text{ m}^{-2} \text{ s}^{-1}$) ranging between $1 \times 10^9 \text{ m}^{-1}$ and $1 \times 10^{10} \text{ m}^{-1}$. However, the value for the filter medium resistance for the unused state ($4.33 \times 10^8 \text{ m}^{-1}$) is not reached. At higher flux values, differences resulting from the various spray times are more pronounced. Concerning the shortest spray time of 5 s, there is only a slight improvement and values do not fall below $1 \times 10^9 \text{ m}^{-1}$ at a flux of $0.33 \text{ m}^3 \text{ m}^{-2} \text{ s}^{-1}$ and over. In contrast, higher spray times starting from 30 s reach resistances in the range of the unused cloth. This quantitatively shows that it is possible to clean the iron ore tailings blinding in the multifile fiber cloth using a water full cone nozzle jet from the front. Furthermore, it can be stated that the cleaning performance is more dependent on flux than on spray time.

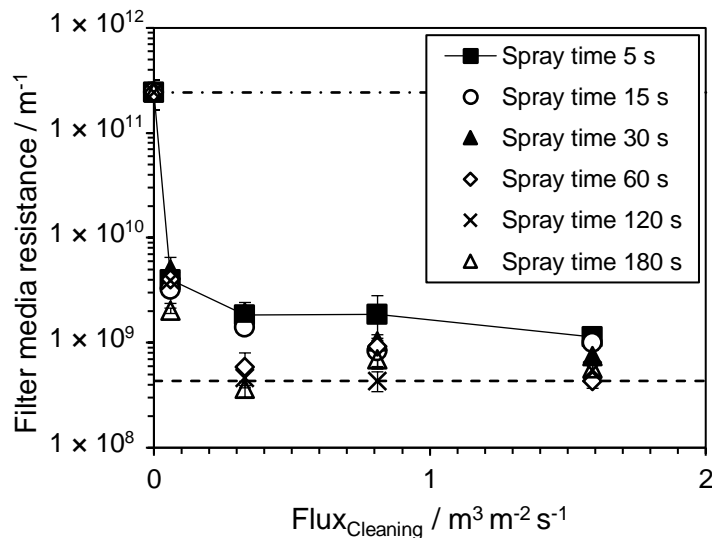


Figure 6-4: Filter medium flow resistance after front-wash cleaning for the different spray times over flux. Blinded (after 1000 filtration cycles) and unused state are depicted as a reference with a dot-dashed and a dashed line.

Of great interest to operators and suppliers of filter presses is ensuring adequate cleaning at the lowest possible cost. Therefore, a cleaning parameter combination has to be determined by combining a low enough filter medium flow resistance at low water consumption. To give a guideline, a resistance threshold of the resistances must be determined at first. This can be achieved by means of the flow ratio. Therefore, two aspects must be considered: First, complete cleaning of the blinded cloth and, thus, the production of the flow rate of the unused condition is very costly and not reasonable. A low number of adhering particles supports the formation of particle bridges at the beginning of filtration and, thus, reduces the turbidity impact at the beginning of cake filtration. Second, the flow ratio of the unused to the industrially used cloth state is 560. For this reason, further evaluation of the cleaning performance assumes that an improvement of the flow rate by a factor of 100 compared to the blinded condition is targetable. This refers to a filter medium flow resistance of $2.43 \times 10^9 \text{ m}^{-1}$. Table 6-5 shows all parameter combinations of the cleaning study with a colored background showing whether the cleaning resulted in a flow resistance above this threshold (red) or below (green). The listed value is the theoretical water demand per square meter calculated from flux and spray time. It can be observed that there is a region of low flux and low spray times where cleaning performance is insufficient. Furthermore, the successful cleaning parameter combination having the lowest water demand of 2.5 m^3 is highlighted, which results from a 5 s spray time using a flux of $0.33 \text{ m}^3 \text{ m}^{-2} \text{ s}^{-1}$ and including the overlap factor for a multiple nozzle setup. Reaching a good effect at short spray times is beneficial in an additional manner: it will

keep the down time as low as possible. The water requirement of 2.5 m^3 is not insignificant but the water might be recovered in the process.

Table 6-5: Water demand per square meter for all front-wash cleaning parameter combinations. The color background is based on the cleaning performance. A cleaning performance above the threshold of a one-hundred-fold increase in flow in relation to the blinded cloth is marked in green and insufficient regeneration in red. Highlighted in dark green is the successful combination with the lowest water demand.

		Spray time / s					
		5	15	30	60	120	180
Flux / $\text{m}^3 \text{ m}^{-2} \text{ s}^{-1}$	0.06	0.5 $\text{m}^3 \text{ m}^{-2}$	1.4 $\text{m}^3 \text{ m}^{-2}$	2.9 $\text{m}^3 \text{ m}^{-2}$	5.7 $\text{m}^3 \text{ m}^{-2}$	11.5 $\text{m}^3 \text{ m}^{-2}$	17.2 $\text{m}^3 \text{ m}^{-2}$
	0.33	2.5 $\text{m}^3 \text{ m}^{-2}$	7.4 $\text{m}^3 \text{ m}^{-2}$	14.8 $\text{m}^3 \text{ m}^{-2}$	29.6 $\text{m}^3 \text{ m}^{-2}$	59.2 $\text{m}^3 \text{ m}^{-2}$	88.8 $\text{m}^3 \text{ m}^{-2}$
	0.81	6.1 $\text{m}^3 \text{ m}^{-2}$	18.3 $\text{m}^3 \text{ m}^{-2}$	36.5 $\text{m}^3 \text{ m}^{-2}$	73.1 $\text{m}^3 \text{ m}^{-2}$	146.2 $\text{m}^3 \text{ m}^{-2}$	219.2 $\text{m}^3 \text{ m}^{-2}$
	1.59	11.9 $\text{m}^3 \text{ m}^{-2}$	35.8 $\text{m}^3 \text{ m}^{-2}$	71.6 $\text{m}^3 \text{ m}^{-2}$	143.2 $\text{m}^3 \text{ m}^{-2}$	286.5 $\text{m}^3 \text{ m}^{-2}$	429.7 $\text{m}^3 \text{ m}^{-2}$

6.1.3.2 Back-wash Cleaning Performance and Water Demand

Cleaning performance for back-wash is shown with the filter medium flow resistance data in Figure 6-5. Analogous to the front-wash results, values for the different spray times are plotted over the flux including a dot-dashed and a dashed line of the blinded and unused state of the investigated tailings filter cloth as a reference. Again, the mean values of the shortest spray time are exemplarily connected to illustrate cleaning performance tendency. While there is a reduction in resistances for all spray times at the lowest flux, it is not as effective in this cleaning orientation as in the front-wash scenario. Furthermore, these values are subject to greater uncertainties. The values of the lowest flux ($0.06 \text{ m}^3 \text{ m}^{-2} \text{ s}^{-1}$) are between $1 \times 10^9 \text{ m}^{-1}$ and $1 \times 10^{11} \text{ m}^{-1}$. Although a further decrease with a higher flux can be observed, only a few regeneration parameter combinations reach values below $1 \times 10^9 \text{ m}^{-1}$. In terms of tendency, the curves are flatter. Furthermore, the highest flux in combination with spray times of 60 s to 180 s achieves resistances in the range of the unused filter medium and, thus, a complete cleaning. These are fewer combinations than with the front-wash. In conclusion, cleaning from the back with the jet of the full cone nozzle is lower in efficiency than the front-wash for the blinded iron ore filter media investigated.

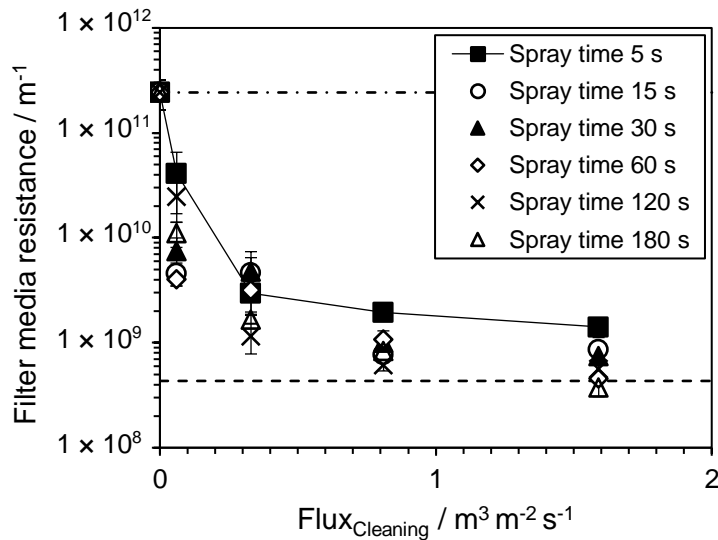


Figure 6-5: Filter medium flow resistance after back-wash cleaning for the different spray times over flux. Blinded (after 1000 filtration cycles) and unused state are depicted as a reference with a dot-dashed and a dashed line.

This difference to front-wash can also be seen by considering the water demand per square meter calculated using Equation 6-3 in Table 6-6. The region in which an increase in flow by at least a factor of 100 is achieved is smaller compared to front-wash. Therefore, it includes combinations of higher flux and longer spray time for back-wash. The lowest water demand for sufficient cleaning reaching the threshold of $2.43 \times 10^9 \text{ m}^{-1}$ is $6.1 \text{ m}^3 \text{ m}^{-2}$ including the overlap factor. This results from a flux of $0.33 \text{ m}^3 \text{ m}^{-2} \text{ s}^{-1}$ and a spray time of 5 s.

Table 6-6: Water demand per square meter for all back-wash cleaning parameter combinations. The color background is based on the cleaning performance. A cleaning above the threshold of a one-hundred-fold increase in flow in relation to the blinded cloth is marked in green and insufficient regeneration in red. Highlighted in dark green is the successful combination with the lowest water demand.

	Spray time / s					
	5	15	30	60	120	180
0.06	0.5 $\text{m}^3 \text{ m}^{-2}$	1.4 $\text{m}^3 \text{ m}^{-2}$	2.9 $\text{m}^3 \text{ m}^{-2}$	5.7 $\text{m}^3 \text{ m}^{-2}$	11.5 $\text{m}^3 \text{ m}^{-2}$	17.2 $\text{m}^3 \text{ m}^{-2}$
0.33	2.5 $\text{m}^3 \text{ m}^{-2}$	7.4 $\text{m}^3 \text{ m}^{-2}$	14.8 $\text{m}^3 \text{ m}^{-2}$	29.6 $\text{m}^3 \text{ m}^{-2}$	59.2 $\text{m}^3 \text{ m}^{-2}$	88.8 $\text{m}^3 \text{ m}^{-2}$
0.81	6.1 $\text{m}^3 \text{ m}^{-2}$	18.3 $\text{m}^3 \text{ m}^{-2}$	36.5 $\text{m}^3 \text{ m}^{-2}$	73.1 $\text{m}^3 \text{ m}^{-2}$	146.2 $\text{m}^3 \text{ m}^{-2}$	219.2 $\text{m}^3 \text{ m}^{-2}$
1.59	11.9 $\text{m}^3 \text{ m}^{-2}$	35.8 $\text{m}^3 \text{ m}^{-2}$	71.6 $\text{m}^3 \text{ m}^{-2}$	143.2 $\text{m}^3 \text{ m}^{-2}$	286.5 $\text{m}^3 \text{ m}^{-2}$	429.7 $\text{m}^3 \text{ m}^{-2}$

6.1.3.3 Electric Energy Demand

The electric energy demand per square meter was calculated for each combination of spray time and flux according to Equation 6-4 and is shown in Table 6-7. Concerning the threshold of sufficient cleaning for a flow rate improvement of 100, this results in a requirement of 6.5 kWh m⁻² for front-wash and 16.1 kWh m⁻² for back-wash. However, this is based on a parallel operation of full cone nozzles and one pump per nozzle. Therefore, a starting point of optimization would be an improved pump selection.

Table 6-7: Electric energy demand per square meter for all cleaning parameter combinations. Highlighted are the successful combination with the lowest water demand for front- and back-wash.

		Spray time / s					
		5	15	30	60	120	180
Flux / m ³ m ⁻² s ⁻¹	0.06	1.3 kWh m ⁻²	3.8 kWh m ⁻²	7.6 kWh m ⁻²	15.2 kWh m ⁻²	30.3 kWh m ⁻²	45.5 kWh m ⁻²
	0.33	6.5 kWh m⁻²	19.6 kWh m ⁻²	39.1 kWh m ⁻²	78.3 kWh m ⁻²	156.5 kWh m ⁻²	234.8 kWh m ⁻²
	0.81	16.1 kWh m⁻²	48.3 kWh m ⁻²	96.6 kWh m ⁻²	193.3 kWh m ⁻²	386.5 kWh m ⁻²	579.8 kWh m ⁻²
	1.59	31.6 kWh m ⁻²	94.7 kWh m ⁻²	189.4 kWh m ⁻²	378.8 kWh m ⁻²	757.6 kWh m ⁻²	1136.4 kWh m ⁻²

6.1.3.4 Calculation of Cleaning Costs

The calculation of the cleaning price refers to data from Kruyswijk, who estimated a water price of 2 € m⁻³ and an electric energy price of 0.1 € kWh⁻¹ for the comparison of processing tailings as a paste and dry stacking in 2021 [59]. Furthermore, a US\$ to € exchange rate of 1/1 is assumed. Combining water and electric energy prices, the cleaning of the blinded iron ore tailings filtration cloth by using a front-wash costs approximately 6 US\$ m⁻² for parallel operation of full cone nozzles and one pump per nozzle with the condition to increase the flow rate at least by a factor of 100. The cleaning costs presented refer to the operating costs (opex) without the procurement of the equipment (capex). However, a cost reduction would be possible by improving pump selection. Moreover, the consideration is strongly dependent on the specification of the required cleaning efficiency, i.e., increase in volume flow compared to the blinded state. The assumption of a factor of 100 as a threshold must be verified on a pilot plant. Furthermore, the prices for electricity, water and filter fabric have to be considered depending on the application and its location in order to be able to evaluate the economic efficiency. As a result, filter cloth spray washing is competitive to the replacement of the fabric at mid two-digit US\$ m⁻² range. In addition, reduction of

plastic waste by lifetime increase is a further benefit of spray cleaning instead of cloth change.

6.1.3.5 Optical Investigation

During the first seconds of the spray cleaning, absorption of adhering particles by the impinging water jet was observed. The water draining to the side had an increased turbidity corresponding to the same color as the tailings. For this reason, collected wash water should be processed before reuse.

Figure 6-6 shows SEM images with 80x magnification of the cloths regenerated using different cleaning combinations. In addition, selected pores at the crossing points of the fibers are pictured in detail (350x)

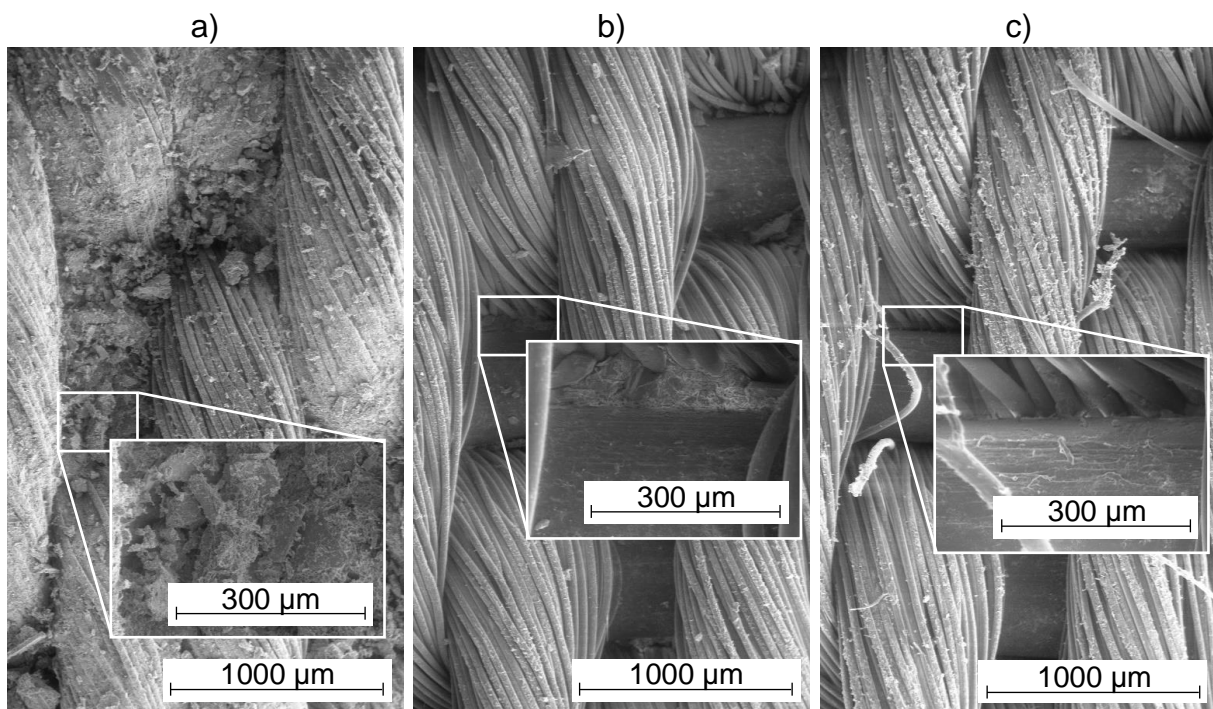


Figure 6-6: SEM images (80x) of different filter cloth states. a) Insufficient cleaning resulting in a resistance of $3.24 \times 10^{10} \text{ m}^{-1}$. b) Threshold cleaning (resistance $2.20 \times 10^9 \text{ m}^{-1}$). c) Excessive cleaning causing the fraying of multifile fibers (resistance $1.94 \times 10^8 \text{ m}^{-1}$).

Figure 6-6a shows an insufficient back-wash cleaning at the shortest spray time (5 s) and lowest flux ($0.06 \text{ m}^3 \text{ m}^{-2} \text{ s}^{-1}$) resulting in a resistance value of $3.24 \times 10^{10} \text{ m}^{-1}$. A large number of particles can be seen in the pores where the fibers cross and inside the multifile fibers. Therefore, the appearance is slightly browner compared to the other specimens. The sample in the middle (Figure 6-6b, front-wash, flux $0.06 \text{ m}^3 \text{ m}^{-2} \text{ s}^{-1}$, spray time 180 s) has a lower but still visible load of solids. Especially within the multifile fibers, there is a reduction. With a resistance of $2.20 \times 10^9 \text{ m}^{-1}$, this specimen

is just below the assumed threshold for successful cleaning of $2.43 \times 10^9 \text{ m}^{-1}$. Figure 6-6c shows an image of a sample with a very intensive cleaning (front-wash, flux $1.58 \text{ m}^3 \text{ m}^{-2} \text{ s}^{-1}$, spray time 180 s, resistance $1.94 \times 10^8 \text{ m}^{-1}$). While only a few adhering particles can be seen, short pieces of protruding filament from the multifilament fibers are noticeable. This indicates excessive mechanical stress by the jet and an incipient undesirable destruction by fraying of the multifilament fibers. It can be emphasized that intensive cleaning, therefore, has a negative effect on the fabric.

6.1.4 Conclusions

Due to the increasing mining of minerals, safe storage of the residues, for example by dry stacking, is necessary. The filter cloths of the filter presses used in this process become blinded and have to be replaced or regenerated in order to maintain economical operation. Therefore, a large number of filter press suppliers in the mining sector offer nozzle cleaning as an add-on device for their apparatuses. However, the regeneration of filter cloth blinding using nozzles is based on general experience and not yet quantified by structured experiments. Investigations of continuous full cone nozzle cleaning on an iron ore tailings cloth have shown that the flux of the impinging jet, the spray time, and the spray direction have decisive influences. A higher flux increases the cleaning effect significantly, whereas extended spray time results only in a slight improvement. Furthermore, a front-wash is more effective than a back-wash. Care must be taken in the design of the cleaning system to avoid damaging the fabrics by excessive force.

Front-wash cleaning with a flux of $0.33 \text{ m}^3 \text{ m}^{-2} \text{ s}^{-1}$ and a spray time of 5 s achieves a hundredfold filter medium flow rate compared to the blinded state. This is equivalent to a water demand of $2.5 \text{ m}^3 \text{ m}^{-2}$ and electric energy demand of 6.5 kWh m^{-2} . Theoretical considerations of water and energy requirements show that the costs of nozzle cleaning (6 US\$ m^{-2}) are in the same range as those of fabric replacement. Therefore, jet cleaning and reusing are beneficial since they save a large amount of plastic waste. Furthermore, the possibility of successful cleaning of the blinding has an impact on the fabric selection. In particular, abrasion resistance increases in importance.

6.2 Regeneration Assessments of Filter Fabrics of Filter Presses in the Mining Sector⁸

Bernd Fränkle^a, Patrick Morsch^{a,b}, Hermann Nirschl^a

^a Karlsruhe Institute of Technology (KIT), Straße am Forum 8, 76131 Karlsruhe Germany

^b FLSmidth A/S, Vigerslev Allé 77, 2500 Valby, Copenhagen, Denmark

6.2.1 Introduction

The Earth's mineral resources are mined in huge mines all over the planet. To ensure the greatest possible extraction of valuable materials, larger quantities of crushed ore that cannot be used have to be handled. Up to 98% of the ore processed do not contain minerals of value [3]. The separation of these so-called mine tailings takes place after all the material has been crushed and ground to release valuable minerals. That is why they are contained in a fine-grained suspension. Normally, large tailings ponds secured by dams are used to store this waste product, but there are two main reasons why it is aimed at reducing such kind of storage and filtered tailings solutions meet with increasing attention [50, 58]. One is the recirculation of a large amount of this water, which plays an important role in the entire process and, therefore, offers great potential. Gunson shows that the average water consumption of 0.76 m³ per t ore can be reduced by 59.2% (0.31 m³ per t ore) by filtration and by 74.0% (0.20 m³ per t ore) when combining filtration with other methods [10]. If, for example, the daily production capacity of 97,000 t ore per day of the Minera Esperanza Antofagasta in Chile as stated in the International Council of Mining and Metals report [113] and the prices for fresh water in such an arid region as stated by Concha (0.5 US\$ m⁻³) and of recovered process water (0.18 US\$ m⁻³) were taken as a basis [3], annual savings of about 6.4 M US\$ would result. The second reason to reduce the use of dams is that the danger of failures cannot be neglected [5]. Several recent failures led to deaths, destruction, and contamination of huge areas with heavy metals. However, the filtration of tailings is a complex task, as low residual cake water content levels must be

⁸ The content of this chapter was published in *Minerals Engineering* 2021, 168, 106922 and was adapted for the thesis.

achieved under challenging filtration conditions to ensure maximum cost reduction and safe storage of the tailings. In general, a target residual cake water content under 20 w% can be assumed [32]. From an engineering point of view, filter presses are appropriate means to achieve this water content level. Despite the non-continuous process, they allow for a high throughput at a high filtration pressure [87]. Unfortunately, the filter media used in filter presses have a limited service life. Besides mechanical damage, deposition of fine particles inside the filter cloth increases with increasing filtration cycles, which is referred to as blinding. As soon as the increased filter medium resistance is too high for economical operation, the fabric must be cleaned or replaced. Since the latter involves a high financial effort, effective cleaning methods are reasonable and a more detailed investigation of possible options is necessary.

6.2.2 Theory

The basis for the description of resistances of porous medium, such as filter cloths and filter cakes, is the Darcy equation [104] (Equation 6-5) [105]. It describes the flow rate \dot{m} of a liquid flowing through a porous structure as a function of the liquid density ρ_l , the surface area A , the permeability P , the applied pressure difference Δp , the cake thickness h_c , and the dynamic viscosity of the liquid η_l . This equation is valid for assumed laminar flow conditions and neglected friction.

$$\frac{\dot{m}}{\rho_l \cdot A} = P \cdot \frac{\Delta p}{h_c \cdot \eta_l} \quad \text{Equation 6-5}$$

The properties of the object passed by flow can be found in the permeability. For the flow through a particulate network, it corresponds reciprocally to the height-specific resistance α_h . A commonly used approximation is the equation of Kozeny and Carman [207] (Equation 6-6). Based on the hydraulic diameter of a system of spherical particles, this results in the following relationship involving the Sauter diameter d_S and porosity ε . [105].

$$\alpha_h \approx 180 \cdot \frac{(1 - \varepsilon)^2}{\varepsilon^3 \cdot d_S^2} \quad \text{Equation 6-6}$$

It can be seen that a reduction of the diameter has a strong negative effect on the permeability. Furthermore, the filtration literature classifies the $\alpha_h \cdot \eta_l$ product in the range between well to very well filterable (10^{11} mPas m⁻²) and almost unfilterable (10^{16} mPas m⁻²) systems [105].

These model ideas form the basis for dealing with more complex filtration tasks in reality, where particle size distributions and particles that are spherical to a certain extent only have to be separated. Tailings, for example, usually have relatively broad particle size distributions with a high proportion of fines [14, 39, 57, 110, 152]. This is important in the filtration process in several respects. Increasingly compressible behavior of smaller particles due to interactions of the particles with the fluid and with each other leads to higher residual cake water contents [101]. In order to ensure compaction and the resulting structure of small pores with high flow resistance, apparatuses with a higher pressure difference as a driving force have to be used [208] [209]. For this reason, filter presses are commonly used for tailings filtration [32]. With these, the residual water content levels of approximately 20 w% and lower required for dry stacking can be achieved [32, 39, 151, 153, 154].

Furthermore, many problems affecting the cloth, such as a strong turbidity surge at the beginning of filtration and the accumulation of permanently adhering particles (blinding), are caused by the presence of fines [101]. Figure 6-7 shows this behavior schematically for a cloth cross-section. The initial smallest free pore diameter d_p between two adjacent fibers is reduced to the diameter $d_{p,blinding}$ by particles adhering to the fibers or already deposited particles.

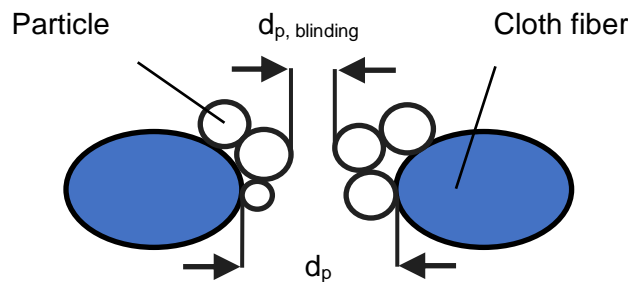


Figure 6-7: The initial smallest free pore diameter d_p between two adjacent fibers is reduced to the diameter $d_{p,blinding}$ by particles adhering to the fibers or already deposited particles.

Decreasing pore diameters not only affect the efficiency of the filtration process by increasing the filter medium resistance, but also make it more difficult to regenerate the filter press between the individual cycles as cake discharge is aggravated [71, 86].

Figure 6-8 shows filtrate volume flows over the time of several consecutive, constant pressure filtration cycles for a theoretically optimal regeneration of the filter medium. It also presents the filtrate volume flows considering blinding of the filter medium. The requirement is the achievement of a certain residual cake water content. Assuming a

constant filtration volume and feed slurry concentration, the same amount of water must be discharged in each cycle, requiring the same area under each filtrate volume flow versus time curve. In the first filtration process, it can be seen that the filtrate flow decreases degressively from a certain initial filtrate flow until a specific time T_s at which the cake is sufficiently dewatered, and the press is regenerated. If a theoretically optimal regeneration of the fabric is included, the same initial resistance would always be achieved for the following filtration and T_s would remain constant. However, the described blinding leads to a deviating behavior in real operation. The original initial filtrate flow cannot be achieved and increasingly deteriorates in the following cycles. To ensure identical dewatering, filtration must be increasingly longer and with lower filtrate flow. If the tailings accumulation remains constant, this leads to the need for timely fabric replacement.

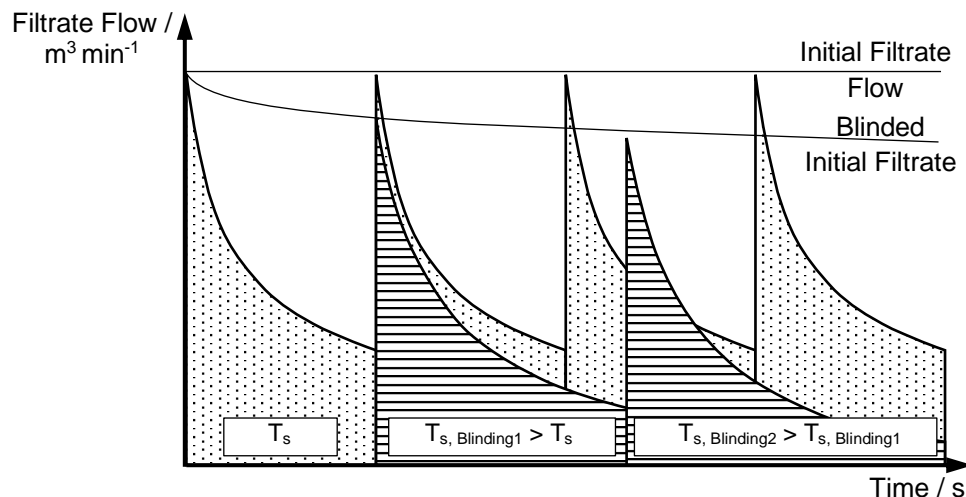


Figure 6-8: Schematic representation of consecutive filtration cycles for tailings filtration under theoretically optimal regeneration conditions and under consideration of blinding.

As can be seen in literature, the major focus in the filtration of tailings is on filtration itself. Publications deal with a pretreatment with lime and flocculation [32, 210, 211, 212]. Moreover, the influence of shear and conditioning of the process water are subject of current research [213, 214]. Another aspect that is crucial to increasing economic efficiency is to change [215] or split the particle size distribution (PSD) [216, 217]. The selection of suitable fabrics for filtration of tailings is often know-how of the companies distributing the filtration equipment and of their suppliers. Publications show that in addition to the use of woven fabrics [110], membranes can be used [218]. However, filter medium resistance is subject to a constant increase with the high

number of filtration cycles, which is why a deeper understanding of the cleaning behavior is necessary.

First of all, the cleaning options for filter media of filter presses should be discussed in general terms. A distinction should be made between surface contamination and contamination in the fabric. The former is the result of incomplete cake dropping where the adhesion of the cake to the cloth outweighs the cohesion of the cake [75]. In addition to time-consuming manual cleaning of the filter cloth, there are various technical approaches to removing the adhering cake residues. Besides tilting the plates [219], use of vibration [220], an impact load [221], a grid inlay [222] or installation of a scraper [223], jet cleaning [92, 93] is one of the most common methods. While jet cleaning has been found to reduce surface contaminants, it is associated with the risks of transporting contaminants deeper into the cloth [111].

The removal of adherent particles can be divided into several mechanisms. Physical cleaning is based on the fact that the adhesion between particles and fabric is overcome by a sufficient peeling force [127]. This can be achieved by flow, often induced by backwash in the case of filtration [65, 224], or by ultrasound [225, 226, 227, 228]. During operation of an ultrasonic bath, standing sound waves are generated. In an elastic medium, sound occurs in the form of mechanical vibrations. The basic cleaning process is the removal and transport of dirt particles according to the cavitation principle. The vibrations introduced into the liquid cause local negative and positive pressure phases, in which the negative pressure is below the vapor pressure of the liquid. Existing germs thus expand into vapor bubbles, which then implode at excess pressure. In the vicinity of the wall, this does not happen in a spherically symmetric way, but rather results in the formation of a so-called microjet. In the vicinity of a surface, this results in a considerable application of force by the accelerated liquid, which can lead to component destruction. If the excitation frequency is higher, the germs must be smaller. This results in smaller cavitation bubbles, which is why the cavitation is less violent and the cleaning gentler [229]. It should be mentioned that cleaning operations with ultrasound represent an enormous challenge in design and process control due to local differences in the oscillating field, especially in large baths [229, 230]. Although the use of an ultrasonic bath is suitable for cleaning particles smaller than 30 μm [229], the effectiveness of application for cleaning inter-weave filter fabrics contamination is questioned, because literature refers to the difficulty of cleaning blind holes [230]. Since the particles responsible for the reduction of filtrate

accumulation in the course of blinding are located in the small pores, effective cleaning is doubted. Also, the risk of cloth damage must be investigated. Chemical cleaning of adhering particles can be achieved by either their partial or complete dissolution [88] [231] or by wetting effects. By wetting the surface of the particle and the cloth, a liquid film is formed in between, which reduces the adhesion forces. Dispersion and diffusion of the particles into the liquid are facilitated. Furthermore, surfactants can be used to reduce reattaching of removed particles [232].

The cleaning of filter cloths in minerals processing, especially in the area of tailings, has been investigated to a limited extent. However, conclusions can be drawn from the current solutions of manufacturers and suppliers as well as other areas. Major suppliers of filtered tailings solutions offer jet cleaning for their filter presses [43, 89, 90]. Acid cleaning is recommended by several companies [89, 199, 200]. It is also known for its use in ceramic filter media for ore concentrates [88] and in wastewater sludge dewatering [231].

6.2.3 Experimental Studies

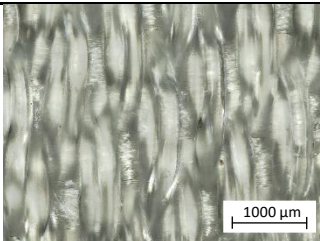
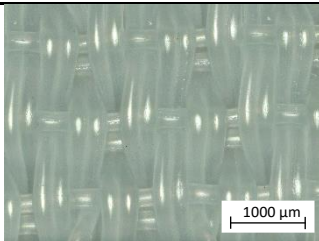
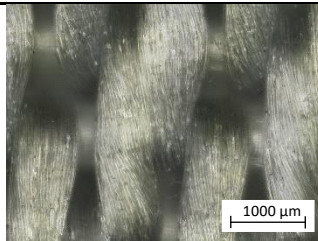
An investigation of cloth regeneration is of interest, because mineral processing requires handling of large process flows containing a significant fraction of particles in the lower micrometer range. The aim of this work therefore is to evaluate different cleaning procedures using four acids (hydrochloric, acetic, sulfamic, and formic acid), two bases (sodium and potassium hydroxide), and two types of ultrasonic baths (47 kHz/35 W and 130 kHz/100 W) for three industrial filter cloths used at a silver, gold and iron mine. Furthermore, acid and ultrasonic treatment at the same time, different application times, and varying concentrations are examined. The evaluations are based on permeability measurements, porometry tests, and elemental analysis. Mechanical properties are investigated to determine whether cleaning the synthetic filter cloths using the methods mentioned resulted in any degradation.

6.2.3.1 Sample Characterization

As process streams in the range of 5000 tph [217] are not uncommon, tailings filtration takes place in multiple filter presses connected in parallel. Each filter is as large as possible [40]. The industrial cloths investigated in this work therefore have a size of four square meters. We examine a polyamide medium from a silver mine after around 5000 filtration cycles, another nylon cloth with around 6500 cycles from a gold mine, and a polypropylene cloth from an iron mine after around 1000 cycles. These numbers

of filtration cycles are in the normal range for cloth exchange [43]. The samples were sent from North America and Asia to Germany in dried condition. Cloth washes were carried out on these fabrics when necessary during operation. Their specific properties in the unused state are listed below in Table 6-8. The laser scanning microscope (LSM) images (10x) show that they differ in weave pattern and fiber types. The silver mine medium has satin weave made of mono- and multifil fibers, the gold mine cloth is a mono/mono plain weave, and the iron medium has a kind of twill weave with mono- and multifil fibers. The flow resistances of the cloths in the unused condition are measured with a pressurized filter housing and calculated based on the Darcy equation (Equation 6-5). In addition, the diameters of the mean flow pore (MFP) are listed for each cloth in its unused state. They are calculated from porometry tests (Equation 6-8). The test and calculation methods are explained in detail in chapter 6.2.3.2. As is to be expected due to the multifilament fibers used, the iron ore cloth has the lowest MFP, followed by the silver and the gold cloth. This is compensated by the permeability of this type of fiber, which means that the filter medium resistances are in a comparable range.

Table 6-8: Listing of the filter cloth properties in the unused state including material, weave type (incl. DIN 9354 nomination [118], fiber type, filter medium resistance, and mean flow pore diameter.

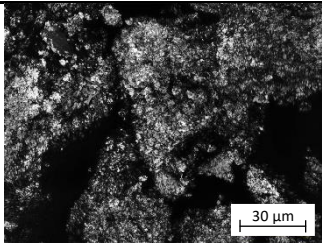
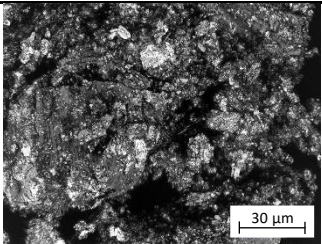
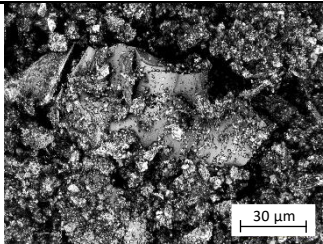
	Silver mine filter medium	Gold mine filter medium	Iron mine filter medium
Image			
Material	PA	PA	PP
Weave	Satin (30-04 01-02-02)	Plain (10-01 01-02 00)	Twill (21-01 03-01-01 02 03)
Fiber type	Mono/multi	Mono/mono	Mono/multi
Resistance	$5.2 \pm 2.9 \times 10^8 \text{ m}^{-1}$	$6.6 \pm 5.5 \times 10^7 \text{ m}^{-1}$	$4.3 \pm 0.1 \times 10^8 \text{ m}^{-1}$
MFP	$35.8 \pm 2.2 \text{ }\mu\text{m}$	$54.4 \pm 1.4 \text{ }\mu\text{m}$	$10.5 \pm 0.6 \text{ }\mu\text{m}$

Thickened tailings are dewatered at all three sites. Their filtration is challenging due to their particle size distribution. In case of a monodisperse spherical distribution in the order of the $x_{50,3}$ values given in Table 6-9, the system would be in an unproblematic range of cake resistance for filtration based on the equation of Kozeny and Carman

[105]. However, particle size distributions of tailings are usually very broad, i.e., they have a large fraction of fines below their $x_{50,3}$ value [14]. This has a decisive influence on the filterability. Small particles build up compressible cakes due the increasing impact of interparticle forces, particularly, if their size is $<10 \mu\text{m}$ [101]. Furthermore, the small particles bleed through the cloth at the beginning of filtration and also lead to the blinding of the filter medium. There are two major blinding mechanisms – particles getting between the fibers and particles migrating into multifilament yarns.

Table 6-9 lists an excerpt of the sum distributions of the three tailings measured by laser diffraction. The high fraction of fine particles and the broad distribution are obvious for all tailings. More than ten percent of the solid mass exists in the form of particles with an equivalent diameter of $<10 \mu\text{m}$. Furthermore, $x_{50,3}$ values below $40 \mu\text{m}$ are measured, while the $x_{90,3}$ values are between 79.0 and $120.8 \mu\text{m}$. This broad PSD and the resulting effect are also obvious from the laser microscope images, magnified by a factor of 100, of the tailings particles. They show that the smallest fraction adheres to the larger particles due to interparticle forces.

Table 6-9: Laser images (100x) of the tailings particles and an excerpt of the sum distributions of the three mine tailings.

	Silver mine tailings	Gold mine tailings	Iron mine tailings
Image			
$x_{10,3}$	$1.3 \mu\text{m}$	$2.4 \mu\text{m}$	$7.2 \mu\text{m}$
$x_{50,3}$	$8.9 \mu\text{m}$	$11.5 \mu\text{m}$	$38.2 \mu\text{m}$
$x_{90,3}$	$79.0 \mu\text{m}$	$82.1 \mu\text{m}$	$120.8 \mu\text{m}$

Angle dispersive X-ray fluorescence (XRF) analyses were performed to determine whether there is an influence of elemental composition of filter cloth surface particles on cleaning efficiency. The results of these tests are listed in Table 6-10 and show that all three particle systems consist mainly of silica and also comparable fractions of aluminum, potassium, and calcium. While the silver tailings have the highest silica amount, the gold tailings contain highest aluminum and calcium concentrations, whereas the iron tailings stand out in manganese and iron.

Table 6-10: Results of angle dispersive XRF. Combined values of the elements independent of the present oxidation numbers.

	Na	Mg	Si	Al	P	K	Ti	Mn	Fe	Ca	LOI
Silver tailings	1%	1%	60%	8%	<1%	5%	1%	<1%	4%	4%	17%
Gold tailings	2%	3%	41%	11%	<1%	5%	<1%	<1%	6%	17%	16%
Iron tailings	1%	3%	39%	7%	<1%	3%	<1%	5%	30%	5%	6%

6.2.3.2 Testing

The experimental studies presented in this work are basically structured as follows: First, samples of the industrially used media from different tailings filtrations are cleaned, with the parameters of cleaning agent, ultrasound, time, and concentration being varied, which is explained in detail below. The effectiveness of the different cleaning procedures is evaluated based on the process engineering parameters of permeability and pore size determined by flow measurements and permeability tests. Subsequently, an additional elementary analytical examination of selected sample states is carried out to determine whether the composition of the tailings particles on the surface of the filter cloth influences regeneration capacity. Possible negative effects on the mechanical properties of the cloths, both by the high number of filtration cycles and by the cleaning process, are analyzed by means of tensile tests.

The cleaning procedures consist of the use of 100 ml cleaning agent or demineralized water in PP plastic containers, into which a round permeability sample (44.2 cm² surface area) and a round porometer sample (3.8 cm² surface area) are placed. An overview of the different procedures is given in Figure 6-9. 30 min of cleaning with four different 1-molar acids (hydrochloric, acetic, sulfamic, and formic acid) and with two 1-molar bases (sodium and potassium hydroxide) is performed for each of the three filter media, which corresponds to an area-related cleaning-agent load of 20.83 mol m⁻². The selection of these cleaning media is based on their good and comparatively cheap availability. Each filter medium is also treated for thirty minutes in an ultrasonic bath with 47 kHz and 35 W and with 130 kHz and 100 W in demineralized water. These tests are carried out with typical laboratory ultrasound equipment (Bransonic 1210E-MT (47 kHz, Branson Ultrasonics Corp.), Transonic TI-H-5 (130 kHz, Elma Schmidbauer GmbH)). Although sound between a frequency of 20 kHz (just above the audible range) and 1 GHz is considered to be ultrasound by definition,

frequencies of 20 kHz to 100 kHz are normally used for ultrasound-assisted immersion cleaning [233]. This usual range is covered by the baths used. Ultrasonic cleaning with simultaneous treatment with 0.1-molar hydrochloric acid was evaluated to determine the potential for enhanced regeneration. Based on the above-mentioned tests, the time of application of the cleaning agent is reduced to 15, 5 and 2 min for the samples from the silver and gold mines in 1-molar hydrochloric or acetic acid. Samples from these tailings are also subjected to thirty-minute cleanings with reduced concentrations of 0.1 and 0.01-molar hydrochloric and acetic acid.

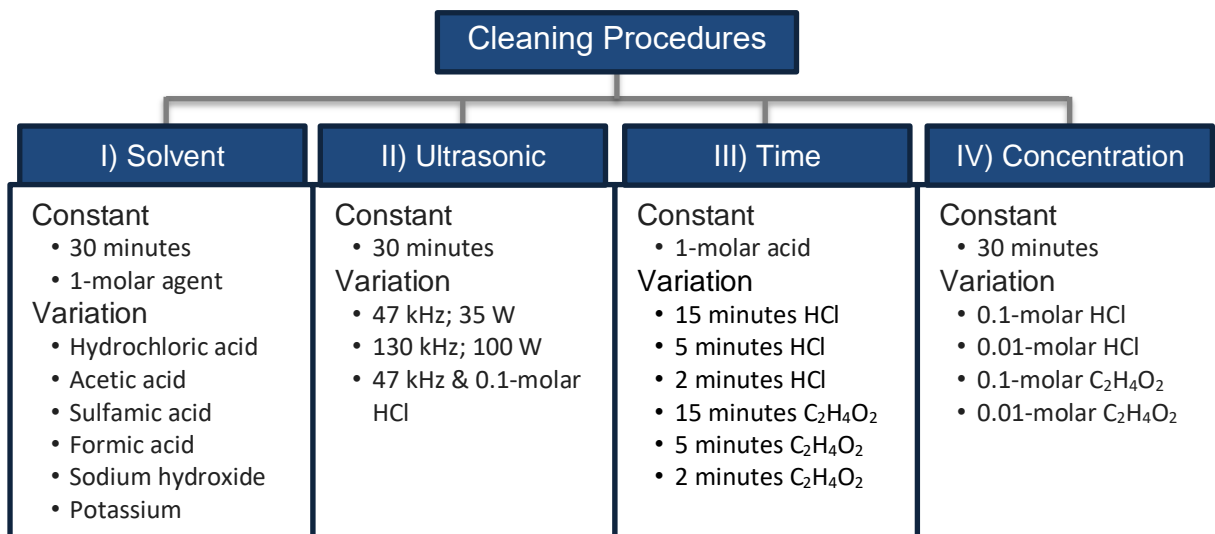


Figure 6-9: Overview of the used cleaning methods.

A pressurized filter cell according to VDI guideline 2762 [107] is used for permeability tests. For virgin fabric characterization, it is usual to give a specific permeability per area and time at a certain pressure. However, to obtain a pressure-independent pure filter medium resistance $R_{\text{fm,clear water}}$, an adapted form of the Darcy equation (Equation 6-7) can be used [106]. This is done by gravimetrically measuring the permeate accumulation \dot{m} of a laminar flow of demineralized water through the fabrics and by neglecting friction.

$$R_{\text{fm,clear water}} [\text{m}^{-1}] = \frac{A}{\dot{m}} \cdot \rho_1 \cdot \frac{\Delta p}{\eta_1} \quad \text{Equation 6-7}$$

The effects of progressive blinding, which in terms of process engineering are reflected by a decreasing permeability and an increasing filter medium resistance, are due to a permanent, non-regenerable reduction of the pore necks in the fabric by embedded particles (Fig. 4). Porometry tests are suitable for measuring this directly. Basically, the pore distribution is measured by means of gas flow. In the case of a sample wetted

with silicone oil in advance, the flow pressure is first increased continuously, and the corresponding volume flow is recorded to plot the wet curve. Based on the Young-Laplace equation for cylindrical pores (Equation 6-8), the pore diameters d_p are emptied with increasing pressure difference Δp depending on the surface tension of the oil γ and the wetting angle θ between oil and sample. Despite the highly non-cylindrical pore shape, porometer tests are the method of choice for various analogous applications, such as porous structures [148].

$$d_p = \frac{4 \cdot \gamma \cdot \cos \theta}{\Delta p} \quad \text{Equation 6-8}$$

At a certain pressure, the emptying of the first and thus largest pore of the sample is detected. This represents the so-called bubble point pore diameter. With increasing pressure, smaller pores can be emptied, and in parallel the flow rate through already opened pores increases. If the flow rate is only increased by increasing the pressure and not by further emptying, the dry curve is recorded by continuously decreasing the pressure. The pore size at which half of the volume flow rate is reached, the so-called mean flow pore diameter, can be determined mathematically from both curves.

The tests are carried out using a capillary flow porometer CFP 1500 AFX (Porous Materials Inc.) and linear, non-reactive polydimethylsiloxane AK 10 (Wacker Chemie AG) as wetting agent. According to the manufacturer's data, this agent has an approximate surface tension of 20 mN m^{-1} [234] and, therefore, leads to complete wetting of the low-energy solid samples of PP (critical surface tension: 29 mN m^{-1}) and PA (46 mN m^{-1}) [235]. The critical surface tension of the mineral tailings is assumed to be higher and, hence, the tailings are also wettable. The choice of AK 10 as wetting agent is based on extensive comparative tests in literature of commercially available wetting agents [236]. For example, one advantage of using a silicone oil is the low volatility. This means that the test results can be regarded as independent of the time taken to carry out the measurement. Measurements were made up to a differential pressure of 300 kPa, which can empty a capillary of approximately down to $0.27 \mu\text{m}$ for the given wetting agent and complete wetting.

To evaluate whether the elemental composition of the tailings influences the regenerability of the filter medium, investigations with energy dispersive XRF are made. These tests are carried out for the used condition of the silver and gold mine

cloths as a reference as well as after thirty minutes of cleaning in 1-molar hydrochloric acid and after thirty minutes of ultrasonic cleaning at 130 kHz and 100 W.

Potential change in the mechanical properties of the fabrics due to the number of filtration cycles passed and additional cleanings using solvents and/or ultrasonic treatments is studied by means of tests on a tensile testing machine. The sample shape is based on ASTM standards for textile testing [237, 238, 239]. Fabric cut-outs from 3 cm to 7 cm with bilateral tapering in the middle of the long side are used in warp and weft direction. Besides reference measurements of the unused fabric, the used fabric, and the fabric after 30 min cleaning in 100 ml 1-molar hydrochloric acid and ultrasound treatment at 47 kHz and 35 W is investigated. For permeability and porometry testing, the samples are treated either for 30 min with a 1-molar HCl solution (based on their surface area, this corresponds to a loading of 20.83 mol m^{-2}), with ultrasound (47 kHz), or simultaneously with 0.1-molar HCl solution and ultrasound exposure (47 kHz). The tensile tests were carried out to detect potential damage to the fabrics by a higher loading of detergent (47.62 mol m^{-2}) due to the smaller sample size with simultaneous exposure to the more abrasive ultrasound (larger cavitation bubbles [229]). This is to outline what could happen if the chemical or ultrasonic cleanings were applied multiple times to the same fabric. The PA fabric from the gold mine was selected for this purpose. Polypropylene is very well-resistant over a large pH range. Polyamide is only partly resistant in the acidic environment. In addition to a wealth of standardized tests for the determination of polymer properties [240], direct statements on chemical resistance in fiber form are published [122]. In this paper, the mechanical property to be compared is the tensile strength of the fabric and its conditions in warp and weft direction.

6.2.4 Results & Discussion

The results of the permeability measurements are the primary evaluation metrics. They allow the most direct conclusions to be drawn with respect to the behavior in operation. For this purpose, Figure 6-10 shows logarithmically on the ordinate axis the cloth resistances of the samples in the unused and used states as well as for the cleanings with the different agents (hydrochloric / acetic / sulfamic / formic acid & sodium / potassium hydroxide). In all measurements the values were determined in triplicate due to the limited availability of industrial sample material. The highest and lowest measured values are represented by the limits of the deviation bars. It is obvious that the industrially loaded media (silver 5000 / gold 6500 / iron 1000 filtration cycles) with

values in the range of 10^{11} to 10^{12} have a significantly higher resistance than the corresponding unused states with resistances in the range of 10^7 to 10^8 . These enormous differences justify the determination of filter medium resistances by means of permeability tests instead of the usual extraction from filtration data, since the resistance increases by a factor of 2-5 due to interaction of the fabric with the first particle layer according to Purchas and Sutherland [86]. As expected, the resistances of the cleaned states lie between those of the unused and used states. The acid cleanings are more effective than the base variants except for acetic acid. Basically, the cleaning characteristics of the different filter fabrics and, thus, the effectiveness of the different chemicals are comparable for all three fabrics. However, it is clearly shown that for the silver mine and iron mine the level of the unused medium is not reached, but all resistances are by a factor of 10 at least higher. The lowest resistance values can be reached with hydrochloric and sulfamic acid, but all regenerations are far away from the unused state. The results of the permeability measurements for the cloth of the gold mine contrast with this. An almost complete regeneration for the treatment with acids, especially with hydrochloric, sulfamic, and formic acid, followed by acetic acid, can be seen. Analogous to the silver and iron tailings, the base regenerations reduce the resistances insufficiently and are therefore not to be considered effective. Treatments of unused cloths with the cleaning types do not lead to a significant change compared to the untreated virgin filter medium. Therefore, only the resistances in unused state are shown as reference.

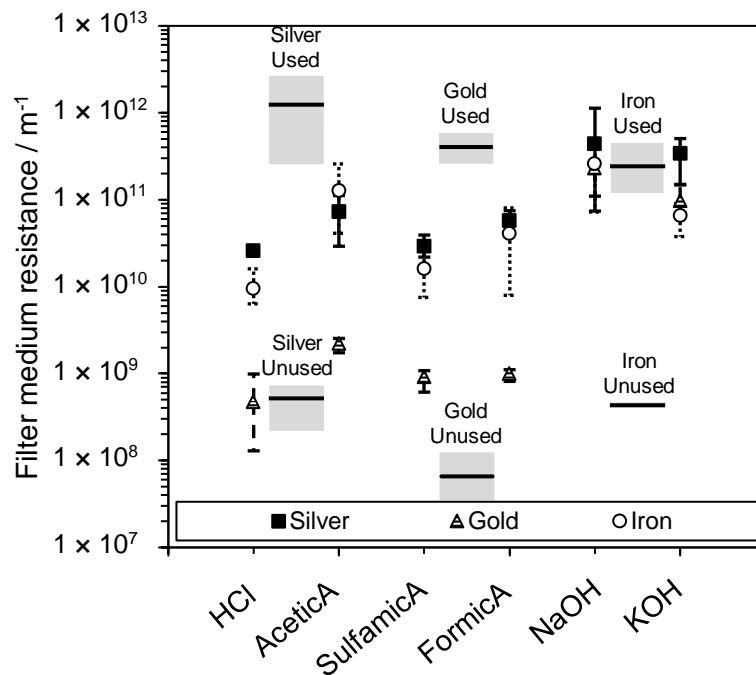


Figure 6-10: Representation of the filter medium resistances measured by permeability tests in the unused and used states and after 30 min of cleaning with different 1-molar solvents (hydrochloric acid, acetic acid, sulfamic acid, formic acid, sodium hydroxide or potassium hydroxide solution) for the silver, gold, and iron mine cloths.

A visual examination illustrates these results. When looking at fabric sections of the gold mine in the unused (Figure 6-11a), the used (Figure 6-11b), and after thirty minutes of cleaning with 1-molar hydrochloric acid cleaned state (Figure 6-11c) at tenfold magnification, the causes of the different permeabilities can be identified.

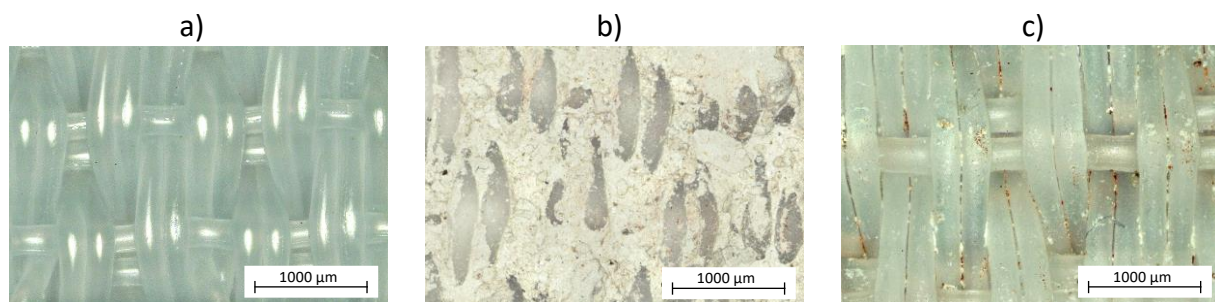


Figure 6-11: Microscopies of the gold mine cloth (cake side) in the unused (a) and used states (b) and after 30 min of cleaning with 1-molar HCl (c).

Many particles are permanently deposited in all spaces on the cake side of the used fabric, including the pores. Those particles are almost completely removed after cleaning. Only a few remaining particles can be detected. The danger of a resulting change in mechanical properties makes it necessary to check these properties by means of tensile tests.

Due to their frequent use in industrial cleaning applications, the investigation of ultrasonic treatments is another part of this work. Figure 6-12 shows the filter medium resistances of the three fabrics for the unused and used state and after treatments in two different ultrasonic baths (47 kHz and 35 W; 130 kHz and 100 W) as well as after thirty minutes of cleaning in 0.1-molar hydrochloric acid. In addition, the values for a combination of the low-frequency ultrasonic bath and the above-mentioned acid cleaning are shown. All regeneration procedures result in a resistance between the unused and used condition. The effects of the two different ultrasound treatments as well as of cleaning with 0.1-molar HCl can be considered similar in terms of measurement accuracy. For the silver and gold cloths, the resistances are improved by a factor of about ten, whereas for the iron cloth the improvement is less significant (less than a factor of ten). The reason is the presence of multifilament fibers on the surface of the iron fabric. These have a finer pore structure and, thus, exhibit increased intra-fiber impurities, which are more difficult to clean with both ultrasound and chemicals. Cavitation bubble or microjet forming and chemical reactions due to low convection are not pronounced there. Moreover, the diagram shows that a superposition of ultrasound and acid does not have any additional positive effect. This can be observed for all tailings.

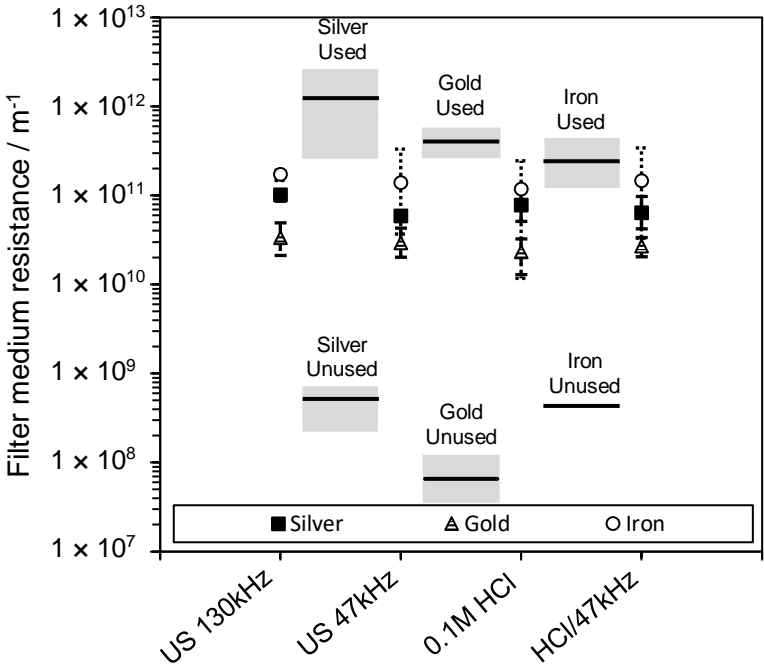


Figure 6-12: Representation of the resistances measured by permeability tests for the silver, gold and iron cloths in the unused and used states and after varied ultrasonic treatments (30 min ultrasonic treatment with 130 kHz and 47 kHz, 30 min 0.1-molar hydrochloric acid and ultrasonic-acid superposition).

Ultrasound treatments as well as cleaning with 0.1-molar acid is noticeably less effective than the addition of 1-molar hydrochloric acid. This is evident from Figure 6-13, which shows the logarithmic variation of the acid concentrations for hydrochloric and acetic acid from 1 to 0.01-molar for the cloth of the gold tailings. An increase in the medium resistance with decreasing acid concentration is found. The concentration dependence is very pronounced. Starting from the unused state, almost the complete range to the used reference state is crossed. At a higher concentration of acid, more hydronium ions are available for cleaning. For the silver fabric, which can only be cleaned incompletely, this dependence must be confirmed for hydrochloric acid cleaning, but to a smaller extent. The dependence cannot be noticed for acetic acid. Since this weak acid only partly dissociates in aqueous solution, ineffective cleaning is observed even at the highest concentration used.

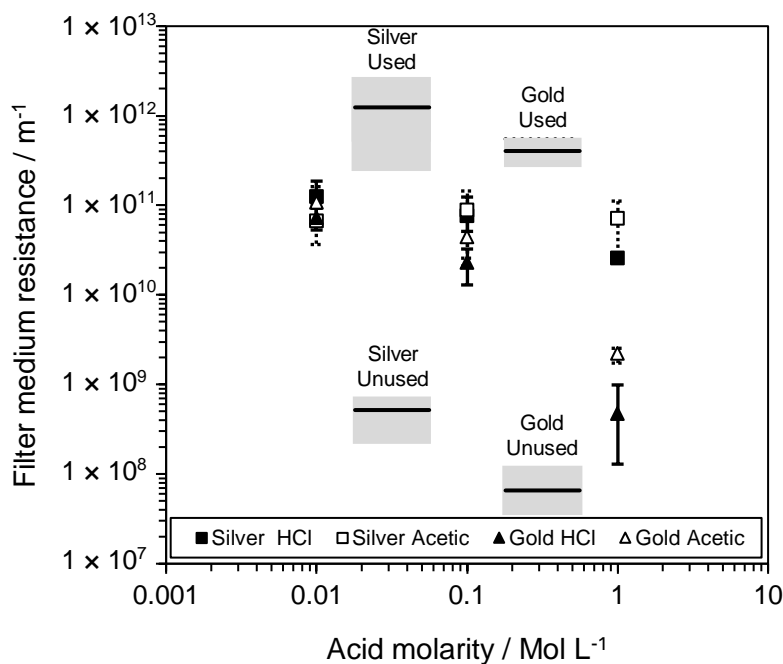


Figure 6-13: Representation of the resistances measured by permeability tests for the silver and the gold cloths in unused, used, and cleaned states at variable concentrations (1, 0.1 and 0.01-molar hydrochloric or acetic acid).

The variation in time is different. Figure 6-14 shows the gold and silver tailings filter medium resistances treated with 1-molar hydrochloric and acetic acid baths for 2, 5, 15, and 30 min. For the silver fabric, chemical cleaning is not noticeable due to the multifilament fibers. The values measured for the gold fabric show that cleaning is time dependent and approaches a constant value. Furthermore, it is shown again that cleaning with HCl is more effective than with acetic acid in the time interval considered.

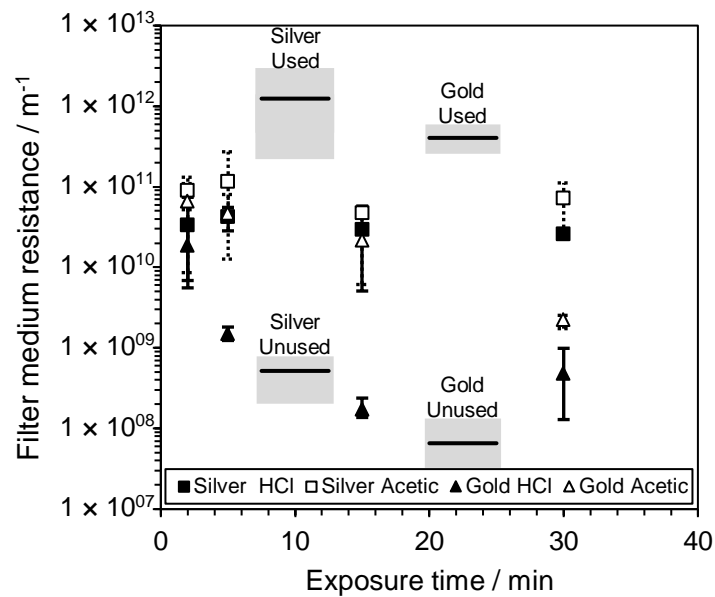


Figure 6-14: Representation of the resistances measured by permeability tests for the silver and the gold cloths in the unused, used, and cleaned states for variable treatment times (2, 5, 15, and 30 min 1-molar hydrochloric or acetic acid).

As explained, the reduction in permeability results from the size of the pores that decreases with increasing blinding. Therefore, exemplary pore size testing was performed for verification of the flow through tests after treatment with various cleaning agents. Since damages and defects in the medium influence bubble point measurements, the change in MFP diameter was determined. Figure 6-15 shows the MFPs for the four acid and the two base procedures of all three fabric types as well as the values of the corresponding used state in relation to the values of the unused medium. The unused fabrics have very large pores (silver 35.8 μm / gold 54.4 μm / iron 10.5 μm), with the MFP of the gold medium being highest due to the exclusive use of monofilaments. In contrast to this, the pores of the used state are far smaller (silver 9.4% / gold 3.2% / iron 10.2%), indicating how much the pore size is reduced as a result of blinding. Cleaning of the silver and the iron medium did not result in increasing the MFP diameter significantly. The pore diameters for the gold cloth increase significantly, especially for hydrochloric, sulfamic, and formic acid. For sulfamic acid, the diameter even is in the range of the unused medium. The conclusion that acetic acid is the least effective acid cleaning agent is confirmed by the permeability measurements. For all samples, the base purifications turn out to be insufficient. Beyond confirming the permeability tendencies, the MFP results allow the conclusion to be drawn that the cleaning of the particle inclusions in the multifilament fibers is not significant, while monofilament fabrics are well regenerable. In order to investigate the influence of the measurements based on a flow with increasing pressure on the results

proper, another three measurements of the same samples were carried out. No changes outside of measurement inaccuracies were measured.

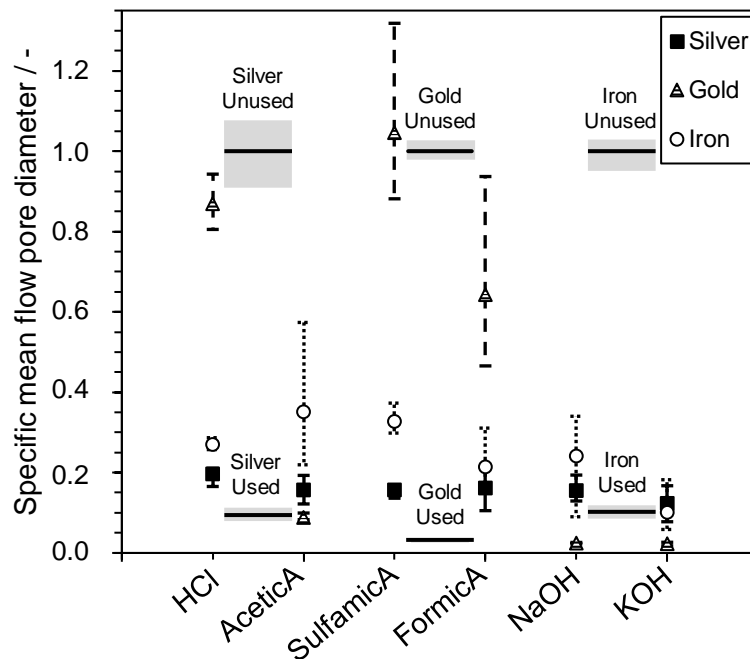


Figure 6-15: Representation of the mean flow pore results in the used state and after 30 min of cleaning with different 1-molar solvents (hydrochloric acid, acetic acid, sulfamic acid, formic acid, sodium hydroxide or potassium hydroxide solution) related to the unused value for the silver, gold, and iron mine cloths.

Apart from the fiber type, differences in the elemental composition of the tailings are to be considered a potential reason for deviating cleaning efficiencies, especially if the cleaning agents are varied. For this reason, elemental analysis of the particles by angle dispersive XRF is complemented by investigations of the main elements of the particles in the cloth by energy dispersive XRF for different cloth states. First, it has to be clarified whether all elements present are cleanable and whether an influence of the fiber types used can be detected. For this reason, the silver fabric was measured as a representative of fabrics with mono- and multifilament fibers and the gold fabric was measured as a representative of purely monofilament filter media. Table 6-11 lists the loadings of the used condition as well as those of the condition treated for thirty minutes in 1-molar hydrochloric acid and thirty minutes in a higher-frequency ultrasonic bath (130 kHz). The main elements (Si / Al / Fe / K / Ca / Mn) are given in $\mu\text{g cm}^{-2}$ without differentiating their oxidation states. Despite the increased error liability caused by the measuring method, statements can be derived from the measurements of the light elements, since these represent by far most of the particles and show clear tendencies independent of the influence of other elements. The ultrasonic cleaning of both fabrics

results in a slight reduction of all main elements only, an increase of the Ca- value is an indication of the measurement inaccuracy. Notwithstanding this, the hydrochloric acid bath reduces all main elements to a quantitatively larger extent. In addition to these two findings that all elements are cleanable and that the acid cleaning is more effective than the ultrasonic treatment, it is notable that the total load can be reduced much more for the purely monofilament fabric compared to the cloth containing multifilament fibers. Considering that all main elements are cleanable, it may be concluded that the use of multifilament fibers limits the cleaning success rather than the elementary composition, because particles contained in the fibers cannot be removed effectively either mechanically or by chemicals.

Table 6-11: Results of energy dispersive XRF. Combined value of the elements independent of the present oxidation numbers.

Cloth	State	Si / μg cm ⁻²	Al / μg cm ⁻²	Fe / μg cm ⁻²	K / μg cm ⁻²	Ca / μg cm ⁻²	Mn / μg cm ⁻²	Sum / μg cm ⁻²
Silver	Used	625.2	104.5	196.6	62.0	35.0	13.2	1036.5
	Ultrasonic	446.9	86.6	169.8	46.7	37.8	11.0	798.8
	HCl	345.6	77.1	97.9	37.4	5.4	3.2	566.6
Gold	Used	1794.6	246.6	207.7	118.4	187.2	3.6	2558.1
	Ultrasonic	678.3	109.4	129.2	69.4	260.7	2.2	1249.3
	HCl	113.4	13.6	41.7	10.2	17.7	0.7	197.3

In addition to the positive effects of fabric cleaning on the service life and, thus, on the operating costs of a filtration plant, tensile tests are carried out to assess potential risks associated with cleaning. As apart from progressive blinding, mechanical defects limit the application duration of the filter medium, three sets of tests are carried out. The PA fabric was investigated, because these fibers have a limited chemical resistance compared to PP fibers, especially in an acidic environment [122]. As a baseline, the mechanical strength of the unused fabric in warp and weft direction is determined. Subsequently, a measurement of the material in the used state is carried out for both directions to check whether the high number of filtration cycles causes a change in the maximum transmissible tension. The third set are tests after a thirty-minute cleaning in a 1-molar hydrochloric acid bath with simultaneous exposure to the lower-frequency, more abrasive ultrasound (47 kHz). This corresponds to more than two cycles of chemical cleaning carried out for the permeability samples in the chemical load. The measured tensile stresses for destruction are shown in Figure 6-16. In the warp direction, the used and cleaned values are below those of the unused state. The

reduction in tensile strength is associated with wear resulting from operation, but the used and cleaned conditions are very similar on the average. While a slight negative tendency of the mechanical properties is found to result from industrial use, the cleaning used for this test does not increase this tendency. In the weft direction, the maximum transmissible stresses of all conditions are significantly lower. This can be explained primarily by the lower number of weft threads per area as a result of the production process. In contrast to the warp direction, however, even higher tensions can be transferred in the used and the cleaned states than in the unused condition. This shows that even for the chemically more volatile material, a simulated stress of more than two cleanings does not have any negative effect on the mechanical properties. However, this publication is not intended to examine the long-term behavior of the fibers for chemical resistance in any way, but to show that chemical cleaning may be an option even for conditionally stable materials. The influence on cleaning is just derived by exposing the material to limited cleaning measures in this paper. For application in industry, a long-term use would be relevant. Many influences affect the properties of plastics, so they should be tested directly in their specific area of application. Field tests would also be necessary to find out how often a chemical cleaning should be applied before the fabric must be replaced according to a risk evaluation as described by Wisdom [43], for example.

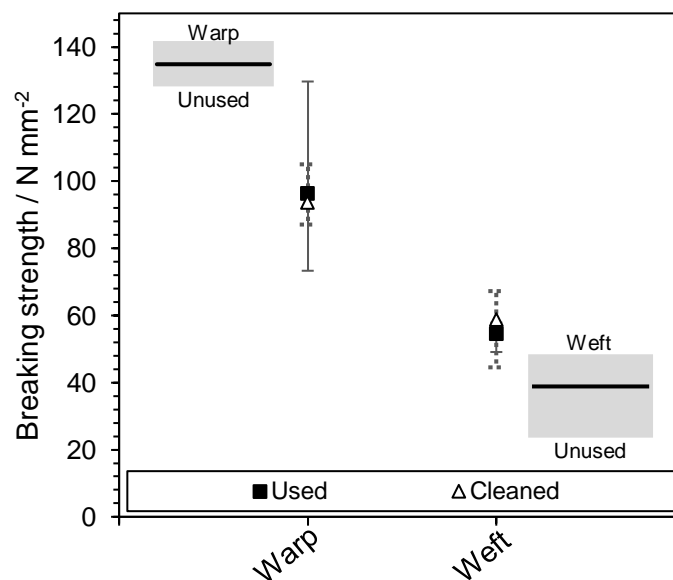


Figure 6-16: Representation of the gold mine cloth breaking strength values in the unused and used states and after 30 min of cleaning with 1-molar hydrochloric acid and simultaneous ultrasonic treatment in warp and weft direction.

6.2.5 Conclusions and Outlook

The applicability of cleaning procedures for filter cloths in tailings filtration was evaluated by tests using solvents and ultrasound. On a laboratory scale, an enlargement of the pore diameters and, as a consequence, of the permeabilities could be demonstrated, independent of the tailings. Regeneration up to the unused state was achieved by using acids. Ultrasonic baths and base cleaning procedures were less effective. Simultaneous application of ultrasound and acid did not result in any further positive effect. In general, it can be stated that not the elementary composition, but the fiber types present in the fabric play a decisive role for cleaning. Incomplete cleaning was evident for multifilament fibers, complete cleaning was observed when only monofilament fibers were used. Additional, admittedly limited investigations on negative effects of the cleanings used on mechanical properties of the fabrics by means of tensile tests did not reveal any significant deterioration. Long-term tests in the real process and integration into the process chain will be needed next in order to be able to select the optimal times for the chemical cleaning and to investigate the stress induced in the cloth by the necessary cleaning steps.

7 Conclusion

The explained aim of this thesis is to characterize the main challenges of the tailings filtration process, namely cake detachment, abrasive wear and blinding of the filter cloth, and additionally to provide guidelines for process optimization. In general, it can be concluded that the filtration process in recessed plate filter presses is highly complex, and its optimization depends on the interplay of multiple elements. These process elements can be likened to the links of a chain. Although each can be optimized individually, the overall performance of the process is primarily determined by the weakest link. While awareness of this interdependency is crucial for process optimization, it is advisable to analyze and evaluate each sub-element separately. For this reason, the present dissertation focuses on individual investigations of cake detachment, abrasive wear of the filter medium caused by the falling cake and blinding of the filter cloth by permanently adhering particles before placing them in a holistic context.

The detachment of the cake is a crucial step in the filtration process which directly impacts subsequent elements. Specifically, it influences filter medium abrasion and blinding. Thus, in the sequence of the sub-element optimization, cake detachment should be considered first. To enable this, a methodology is introduced which is based on filtration tests and shear tests analogous to a Jenike shear tester. This approach is associated with higher uncertainties compared to newer methods such as ring shear tester or triaxial testing but simplifies on-site application since it is performed using the filtration chamber with adhering filter cake and cloths directly after the filtration process. Thus, the main advantage of the selected methodology is the possibility to determine the impact of process parameters such as filter medium, filtration pressure, air blow desaturation pressure and air blow time on cake characteristics. In particular, the presented procedure allows to assess compaction, saturation, adhesion, and cohesion. Both, compaction and saturation impact adhesion and cohesion. In terms of filter process optimization, detaching the cake in one whole piece is crucial. Thus, process parameters should be adjusted to decrease adhesion between cake and filter cloth and increase cohesion and, therefore, the stability of the cake.

The evaluation of the different filter media yielded no significant differences in the considered detachment parameters. This is attributable to the preselection of suitable filter media in terms of particle retention and energy consumption for the specific

separation task. Additionally, the observation in the laboratory is limited by the number of cycles which is far below the four-digit range in the real process. Furthermore, deviating long-term behavior occurs in industrial recessed plate filter presses for different regions of the filter medium, for example due to a different distance to the inlet or filtrate outlet. While the comparably low number of cycles influences the impact of the filter cloth, it is not relevant for the other process parameters. Thus, an evaluation regarding the impact of the filtration pressure on cake detachment is possible. The measurements for different filtration pressures indicate a positive correlation with both, adhesion and cohesion. Furthermore, since the relative change in adhesion exceeds that of cohesion, an increase in filtration pressure leads to a worsening of cake detachment. In contrast, if the filtration pressure is too low, no filter cake forms due to insufficient cohesion. As a consequence, the possibilities to improve cake detachment by filtration pressure optimization are limited. Therefore, it is advisable to perform a gas differential pressure desaturation. This process is shown to strongly influence adhesion and cohesion characteristics. Of interest, the two observed process parameters, namely air blow pressure and air blow time, differ in their effect on detachment. Therefore, simultaneous adjustment of the two parameters allows for substantial cohesion elevation with only minor increase in adhesion. In more detail, to reduce the impact of adhesion, higher air blow times are crucial since both, cohesion and adhesion eventually reach a stable plateau but adhesion increases instantaneously at short air blow times. However, a trade-off regarding the throughput of the tailings filtration application needs to be considered and settled upon. In a second step an increase of the air blow pressure allows to elevate cohesion while maintaining a comparably low adhesion. Due to the interdependency of the two air blow parameters, optimization is complex and a mathematical model to describe the desaturation from a holistic point of view is necessary. The common and presumably most precise mathematical approach by Nicolaou requires the experimental determination of multiple parameters and is, therefore, not suitable for mining applications. For this reason, a new and simplified mathematical approach is introduced in this thesis, which is tailored to tailings filtration and, thus, is limited to the range of desaturation prior to the strength peak. The application of the new mathematical model allows to reduce the number of required experiments for the determination of the optimal air blow parameters which are fundamental for cake detachment optimization.

Successful adjustment of the process parameters and the resulting effective detachment and falling of the filter cake in one piece results in a strong abrasive load on the filter medium at protruding elements of the filter plate, such as the stay bosses and the lower sealing edge. Thus, after the optimization of cake detachment the abrasive wear of the filter cloth by the falling cake is the next sub-element of the filtration process which is analyzed in this thesis. Usual abrasion tests are not considering the direction-specific load in combination with the surface structure of the filter fabric. To overcome this limitation, an apparatus is developed in the framework of this dissertation which enables for the first time the replication of the application-specific load on the filter medium. This scientific advance allows to consider the direction-dependent surface structure and demonstrates conformity with the real process through visual comparison of the abrasion pattern.

The subsequent experiments evaluated the impact of filter medium type and edge geometry on the number of abrasions until rupture. The comparison of different filter media suitable for tailings filtration demonstrates significant influence of materials and filter medium type. Specifically, to improve filter cloth lifetime polyamide cloths are to be preferred over polypropylene or needle felt. Additionally, optimization of the edge geometry of the filter chambers represents a second but less impactful opportunity to reduce abrasive wear. However, in terms of edge geometry optimization it is important to consider other functions, e.g., sealing and stability of the plate stack. At this point the evaluation in the laboratory apparatus is limited. A comparison of the laboratory measurements with real operation beyond the level of visual examination is also crucial to further validate this promising yet experimental approach. In more detail, this includes checking the absolute values and the ratio of number of abrasions until rupture between the different filter media. Furthermore, the load case is simulated with a focus on the direction and repetition of the load. However, the behavior of the metal brushes used differs in part from that of a falling filter cake, for example due to bending.

Once the selection of the filter medium is sufficiently optimized regarding abrasive wear, the main reason for replacement of the filter medium shifts towards blinding. This is due to the fact that at some point, the increasing pressure loss due to more and more permanently adhering particles slows down the filtration process to an unacceptable extent. To reverse this process and to reduce the resulting plastic waste by cloth exchange and, if possible, to reduce costs, fabric cleaning is to be preferred.

Therefore, as a third aspect of this thesis the possibilities of cloth regeneration are investigated on industrially used blinded tailings cloths.

The performed measurements demonstrate that the cleaning technique which enables the best results largely depends on the filter fabric. For fabrics with multifilament fibers water jet cleaning is most sufficient. For this method, the regeneration depends on the flux and the spray time. However, excessive spraying leads to fraying of the fibers and should be avoided. In conclusion, with appropriate flux and spray times, water jet cleaning is advisable for multifilament fabrics. A simplified cost calculation, based on water and energy requirements, shows it to be competitive with cloth replacement. These results do not translate to the investigated monofilament gold mine cloth, for which water jet cleaning insufficiently improves the flow resistance. This is attributed to the rigid structure and a matrix of precipitated CaCO_3 . Therefore, alternative regeneration techniques are considered in a second study, namely cleaning in acid, base and ultrasonic baths as well as combination of acid and ultrasound application. For the gold mine cloth most effective regeneration was achieved by a hydrochloric acid bath. This technique is dependent on both concentration and time. Compared to water jet cleaning, this approach is more expensive and, therefore, not competitive to filter medium exchange. However, the treatments in this study are proven to cause no damage to the filter cloth, thus in terms of waste reduction a regeneration by hydrochloric acid might still be worth considering. In summary, both cleaning studies are simplified and do not include peripheral or safety aspects. Therefore, more precise economic, scale-up and case-by-case considerations are necessary. On the one hand, there is a reduction in plastic waste, but on the other hand, the recirculation of additional process water and the use of chemicals must be considered. Furthermore, the current prices of electricity, water, raw materials, and equipment are important. If successful and cost-effective cleaning of the blinding is possible, the main reason for filter cloth exchange shifts again towards abrasion. As a result, the selection of an abrasion resistant fabric gains importance.

The quintessence of the conclusions of the different sub-elements is their interdependency and the relevance to consider tailings filtration in a holistic point of view. The chronological sequence of the individual elements is relevant and, furthermore, an improvement in one aspect increases the importance of the others. The scientific advance provided by the present thesis generates benefit for operators and suppliers in the field of tailings filtration not only by the progress achieved in the

individual aspects but by bringing them together and demonstrating their linkage. Besides, it provides starting points for further research.

8 Outlook

Based on this work, it is possible to expand the research of tailings filtration in recessed plate filter presses in several directions. Further assets for mining companies and equipment suppliers would be the comparison of site and lab data as well as a scale-up of the characterization methods introduced. Concerning the cake detachment studies, the usage of a small-scale recessed plate filter press instead of a lab scale chamber filter press would give the opportunity to scale-up and include membrane squeeze technology. However, the transfer of adhesion and cohesion measurements directly after filtration is more complex. Concerning filter media abrasion resistance more tailings filter media should be tested since a nearly unlimited extent of different filter media is available on the market. In addition, the number of abrasions until rupture in real-world application should be compared to the lab data shown in this thesis. This includes the number of loads for a specific fabric as well as the ratio between the different types tested. In addition, further improvement of the apparatus is recommended. In this regard, one possibility is to equip the abrasion elements with mine specific tailings particles. Building upon this, suppliers could use the apparatus to improve plate edge geometry. Furthermore, operators have the possibility to compare plate geometries of different suppliers by cut-outs of filter plates instead of simplified geometries. Regarding the cleaning of filter media, the effectiveness of the different regeneration methods in lab scale must be compared to mine site application. In addition, the extension of the cost calculation by the peripheral equipment in real-world application would provide more insights. Long-term tests in mineral processing plants will show if undesirable side effects, for example fabric damage, occur. In addition, safety aspects for the usage of chemicals and high-pressure nozzles must also be integrated in site design. The recirculation of cleaning water or disposal of chemicals must also be coordinated with the overall concept of the filtration plant.

Beyond the aspects discussed in this work, the inclusion of digital technologies into the design and operation of tailings filtration plants is an interesting field for operators, suppliers, and researchers. One aspect is the usage of sensor technology. Online process monitoring integrated into the plates to determine cake water content enables quality control and throughput optimization. Coupled with further research into the filtration behavior of tailings and its mathematical description, a model-predictive control system could be implemented. Furthermore, location- and time-resolved

simulations will enable operation and design improvement of the filter presses if the corresponding computing power is available. Due to the closed plate stack, the filling process has not yet been adequately described. The velocity of the slurry feed and the stack geometry could be optimized by simulating the splitting of the feed into the individual chambers. In addition, a simulation of the cake structure build-up would be useful for determining the filtration time. Both require a detailed characterization of the corresponding tailings suspension and their particulate network. Of outstanding importance are the rheological and sedimentation behavior of the slurry as well as the compression properties of the network. All three are significantly influenced by the volume concentration of the solids.

Within this work the number of tailings and filter media is limited to a few mine sites. Since every mineral processing plant is different, investigation of further tailings particle systems and corresponding filter media is recommended. A specific focus should be laid on the swelling clay minerals because their presence alters the filtration behavior and, therefore, filtration plant throughput significantly. Especially, the effect of clay content variation for a specific mine site due to deeper mining in the pit is a challenge faced by plant operators. By adding swelling clay minerals to tailings in laboratory studies, it would be possible to develop mathematical models for the dependence of the relevant filtration parameters. Furthermore, mining is forced to process finer ore bodies due to increasing demand in mineral commodities paired with reduced ore grade. This requires finer grinding for mineral separation which represents a major challenge in filtration due to elevation of the specific cake resistance and, therefore, filtration time. Although the effects are known from other applications, specific studies and mathematical modeling using real tailings systems would represent an interesting field of research.

In this regard further potential can be found in the enormous quantities of tailings themselves. Since the processes for the separation of minerals improve and the price of the individual components elevates compared to the time of mining, they can be used as a secondary source of commodities such as rare earth elements. As they are already comminuted, processing is easier compared to rock. Further approaches are the alternative use as a building material, sand substitute or CO₂ storage. In the latter, atmospheric CO₂ is bound in the form of carbonates.

Overall, this thesis has provided valuable insights and recommendations for optimizing tailings filtration processes and simultaneously paved the way for future investigations. In this regard the newly developed mathematical model for desaturation optimization and the apparatus for direction-specific abrasive wear simulation are particularly noteworthy. By continuing to explore and apply these methods, we can strive towards more efficient and environmentally friendly solutions for tailings management.

Symbols

Latin Symbols

A	Area
$A_{cl, \text{single nozzle}}$	Cleaned area by one single nozzle
a	Fit parameter
$a_{i,j,h}$	Filtration pressure-, air blow pressure- and height-dependent kinetics fit parameter
b	Fit Parameter
C_t	Experimentally determined constant
d_S	Sauter diameter
d_p	Pore diameter, initial smallest free pore diameter
$d_{p, \text{blinding}}$	Reduced diameter by particles adhering to the fibers or already deposited particles
$E_{e, \text{area specific}}$	Required electrical energy for cleaning per square meter
F_a	Adhesion force
F_c	Capillary force
F_g	Gravitational force
F_l	Line force
g	Gravitational constant
H_c	Cake height
$H_c(t)$	Time-dependent cake height
i	Variable for air blow pressure
j	Variable for filtration pressure
K	Experimentally determined constant
L	Length

m	Mass
m_w	Mass of water
m_s	Mass of solids
\dot{m}	Mass flow
$\dot{m}_{\text{fm,cleaned}}$	Mass flow of the cleaned filter medium
$\dot{m}_{\text{fm,used}}$	Mass flow of the used filter medium
n	Experimentally determined constant
P	Permeability
$P_{\text{e,single nozzle}}$	Electrical power demand of the test setup including one nozzle
p_c	Capillary pressure
p_{ce}	Capillary inlet pressure
R	Flow resistance
$R(t)$	Time dependent
R_1	Inner radius of a liquid bridge
R_2	Curvature radius of a liquid bridge
R_c	Flow resistance of the filter cake
R_{fm}	Flow resistance of the filter medium
$R_{\text{fm,unused}}$	Flow resistance of the unused filter medium
R_{in}	Interference flow resistance
$R_{\text{fm,cleaned}}$	Flow resistance of the cleaned filter medium
$R_{\text{fm,clear water}}$	Filter medium clear water flow resistance
$R_{\text{fm,used}}$	Flow resistance of the used filter medium
S	Saturation
$S(t)$	Time-dependent saturation
S_∞	Saturation value at equilibrium

T	Cake thickness
T_c	Cake thickness
T_s	Specific time for cake dehumidification before press regeneration
t	time
t_{cl}	Spray cleaning time
$V_{v,water-filled}$	Volume of water-filled voids
$V_{v,total}$	Total volume of voids
V_s	Volume of solids
V_v	Volume of voids
$V_{w,area\ specific}$	Area-specific water demand
v	Velocity
v_v	Velocity in the voids
v_s	Stokes' sedimentation velocity
v_{total}	Total velocity
W_c	Cake width
x	Particle diameter
$x(t)_{i,j}$	Time-, filtration pressure- and air blow pressure-dependent quantity
$x_{i,j,\infty}$	Filtration pressure- and air blow pressure-dependent value at equilibrium of a quantity
$x_{i,j,0}$	Filtration pressure- and air blow pressure-dependent initial value of a quantity
$\hat{x}_{i,j,0}$	Measured filtration pressure- and air blow pressure-dependent initial value of a quantity
$x_{10,3}$	Volume-related equivalent diameter at 10% of the sum function

$x_{50,3}$	Volume-related equivalent diameter at 50% of the sum function
$x_{90,3}$	Volume-related equivalent diameter at 90% of the sum function

Greek symbols

α	Angle
α -value	Cake resistance
α_h	Height-specific cake resistance
γ	Surface tension
β -value	Filter medium Resistance
$\dot{\gamma}$	Shear rate
Δp	Pressure difference
ε	Porosity
η	Dynamic viscosity
η_l	Dynamic viscosity of the liquid
θ	Wetting Angle
ρ_l	Fluid density
ρ_s	Solid density
σ	Tensile stress, tensile strength
σ_1	Main tensile stress
σ_2	Main tensile stress
σ_c	Filter cake tensile cohesion
σ_{cc}	Filter cake to filter cloth tensile adhesion
σ_n	Normal stress
σ_t	Tensile strength
σ_{xx}	x-x-tensile stress

σ_{yy}	y-y-tensile stress
τ	Shear stress, shear strength
τ_c	Filter cake shear cohesion
τ_{cc}	Filter cake to filter cloth shear adhesion
τ_{max}	Maximum tensile strength
τ_s	Shear strength
τ_{xy}	x-y-shear stress
τ_{yx}	y-x-shear stress
τ_{ys}	Yield shear stress
φ	Angle

Abbreviations

AB	Air blow (=Gas differential pressure dewatering)
AMD	Acid mine drainage
CAPEX	Capital expenditure
DND	Distance-nozzle-diameter
EDX	Energy-dispersive X-ray spectroscopy
FP	Filtration pressure
LSM	Laser scanning microscope, laser scanning microscopy
MFP	Mean flow pore
NY	Nylon
OPEX	Operating expense
PA	Polyamide
PP	Polypropylene
PSD	Particle size distribution
SEM	Scanning electron microscope
TSF	Tailings storage facilities
WAXS	Wide-angle X-ray scattering (WAXS)
WDXRF	Wavelength-dispersive X-ray fluorescence
XRD	X-ray diffraction
XRF	X-ray fluorescence

List of Figures

Figure 1-1: Simplified illustration of copper ore processing in a big scale mine including exemplary water and mass flows. Icons are extracted from [29, 30, 31]. Data and split ratios are based on [5, 6, 8, 9, 10, 32]. 3

Figure 1-2: Overview of the investigated problems of tailings filtration in recessed plate filter presses. The illustration shows a sliding filter cake (brown) in front of the filter plate (white). The plate equipped with a filter medium (beige), is discolored by adhering particles in the filtration area (lighter brown). Filter cloth abrasion image: ©FLSmidth. 6

Figure 2-1: Simplified illustration of filtration steps in a recessed plate filter press using a cross-sectional view of two plates and one chamber in the middle of the plate stack: (a) During filling slurry level rises; (b) Differential pressure between cake and filtrate drainage system generates a liquid flow through the filter medium and a cake build-up by retained particles; (c) For further water content reduction pressurized air is introduced into the filtrate pipes of every second plate. By overcoming capillary inlet pressure desaturation of the cake is carried out. 13

Figure 2-2: SEM-image of a needle felt (left) and woven (right) tailings filtration filter medium..... 18

Figure 2-3: Schematic representation of main weave structures a) and their characteristic repeating unit (green): a) plain weave, b) twill weave and c) satin weave. 20

Figure 2-4: General distinctions among contamination mechanisms, their corresponding effects, and regeneration opportunities for filter fabrics. 23

Figure 2-5: Schematic cross-sectional view of a filter medium affected by blinding [48]. 24

Figure 2-6: Schematic representation of different rheological behaviors, adapted from [36]..... 28

Figure 2-7: Shear yield stress data of different tailings from various commodities [36, 138]..... 29

Figure 2-8: Schematic representation of the two-dimensional stress state..... 30

Figure 2-9: Schematic representation of Mohr's circle..... 31

Figure 2-10: Schematic representation of the Mohr-Coulomb failure criterion with Mohr's circles using shear tests and Hill's method, along with a schematic representation of the yield locus.	32
Figure 2-11: Schubert's capillary pressure and tensile stress data of limestone filter cakes ($\varepsilon = 0.415$; diameter $x = 71 \mu\text{m}$), adapted from [79].	34
Figure 3-1: Laboratory filter press in open condition including filter cloths inserted into the end plate.	36
Figure 3-2: Schematic cross-sectional view of the lab filter press filtration (a) and desaturation procedure (b) [44, 45].	37
Figure 3-3: Schematic cross-sectional view of the shear adhesion test (a) and the shear cohesion test (b) [44, 45].	38
Figure 3-4: a) Specimen positioning below the brush apparatus. b) Specimen with the load defined as the threshold value of a rupture of half the sample width. c) Industrial filter cloth abrasion appearance (©FLSmidth).	40
Figure 3-5: Schematic representation of the cleaning test workflow based on the industrially blinded $2 \times 2 \text{ m}$ filter cloths. Specimens the size of pressure filter according to VDI 2762 were cut out and then subjected to a cleaning method.	41
Figure 4-1: Schematic representation of important stresses for the description of cake detachment. (a) Shear adhesion: τ_{cc} (b) Tensile adhesion σ_{cc} (c) Shear cohesion: τ_c (d) Tensile cohesion σ_c . Blue: volume on which the force acts. Orange: stress area.	46
Figure 4-2: Schematic representation of different detachment behaviors regarding underlying mechanisms. (a) The weight of the cake is sufficient. The cake falls off in one piece. (b) The weight force is too low; the cake adheres. (c) The tensile stresses transmitted during plate moving rupture the cake. If there are several fractures, partial falling may occur. (d) A higher adhesion (tensile) than cohesion (tensile) splits the cake. If there are several fractures, partial falling may occur. Green: stress area without detachment. Red: stress area with detachment.	47
Figure 4-3: Schematic representation of yield locus, τ_c and σ_c	49
Figure 4-4: Schematic side view cross-section representation of lab filter press filtration (a) and desaturation procedure (b).	52

Figure 4-5: Schematic side view cross-section representations of the shear adhesion test (a) and the shear cohesion test (b).	52
Figure 4-6: Overview of filtrations made for subsequent adhesion and cohesion tests.	53
Figure 4-7: Adhesion (shear) τ_{CC} of the three filter fabrics for different process conditions.	55
Figure 4-8: Adhesion (shear) τ_{CC} referred to corresponding residual cake water content of filtrations at different filtration pressure levels, with and without cake post-treatment by desaturation.	56
Figure 4-9: Adhesion (shear) τ_{CC} referred to corresponding saturation of the network of solid particles.	57
Figure 4-10: Cohesion (shear) τ_C referred to corresponding residual cake water content of filtrations at different filtration pressure levels for the PP felt medium, with and without cake post-treatment by desaturation.	58
Figure 4-11: Yield locus excerpt of different filtration process parameters for PP felt medium.	59
Figure 4-12: Different detachment behaviors seen in lab filtration: a) complete detachment (5 mm, 250 kPa, no cake post-treatment), b) complete sticking cake (5 mm, 250 kPa, no cake post-treatment), c) shear breaking (5 mm, 250 kPa, no cake treatment), and d) breaking parallel to cloth (5 mm, 250 kPa, air blow).	60
Figure 4-13: Schematic cross-cut of the lab filter press filtration and the cylindrical filtration chamber during filtration (a) and cake desaturation (b) [44].	69
Figure 4-14: Schematic cross-cuts of filter cake to fabric shear adhesion (a) and cake shear cohesion (b) measurements [44].	70
Figure 4-15: Filter cake water content of each filtration pressure and air blow pressure combination for variation of the desaturation time for a cake thickness of 40 mm....	73
Figure 4-16: Filter cake saturation of each filtration pressure and air blow pressure combination for variation of the desaturation time for a cake thickness of 40 mm....	74
Figure 4-17: Filter cake shear adhesion and calculated corresponding cake height for gravity introduced detachment of each filtration pressure and air blow pressure combination for variation of the desaturation time for a cake thickness of 40 mm....	75

Figure 4-18: Filter cake shear cohesion of each filtration pressure and air blow pressure combination for variation of the desaturation time for a cake thickness of 40 mm....	76
Figure 4-19: Filter cake to filter fabric adhesion and filter cake shear cohesion fits of each filtration pressure and air blow pressure combination for variation of the desaturation time for a cake thickness of 40 mm.....	77
Figure 4-20: Filter cake water content of 250 kPa filtration pressure and 250 kPa air blow pressure combination for variation of the desaturation time for cake thicknesses of 40 and 55 mm.....	78
Figure 4-21: Example of two 40 mm filter cakes: (a) 250 kPa filtration pressure, no air blow, average water content 20.2 w%, saturation 100 v%, average shear adhesion 0.9 kN m^{-2} , average shear cohesion 1.2 kN m^{-2} ; (b) 1250 kPa filtration pressure, 180 s air blow, 550 kPa air blow pressure, average water content 15.7 w%, average saturation 75 v%, average shear adhesion 3.1 kN m^{-2} , average shear cohesion 5.0 kN m^{-2}	79
Figure 4-22: Overview for troubleshooting common issues related to cake detachment.	82
Figure 5-1: Schematic representation of the locations of abrasive load on the filter medium due to protruding parts of the filter plate. a) Filter cake adhering to filter cloth. b) Falling filter cake.....	86
Figure 5-2: a) Abrasion apparatus. b) Clamped filter medium sample.....	88
Figure 5-3: Square, hexagonal, and circular geometry variation for sample clamping.	88
Figure 5-4: Overview of the abrasion tests for apparatus parameter evaluation and tailings filter media investigation.	89
Figure 5-5: Point of rupture for the thin nylon cloth clamped over a circular edge geometry.....	91
Figure 5-6: WAXS spectrum of the thin NY-cloth and the NY-cloth typical for tailings filtration.	91
Figure 5-7: WAXS spectrum of the PP-felt and the PP-cloth typical for tailings filtration.	92

Figure 5-8: Number of abrasions until rupture of the thin nylon cloth for 0.5, 0.75, and 1.0 Nm for the square, the circular, and the hexagonal edge geometry.	93
Figure 5-9: Number of abrasions until rupture of the thin nylon cloth for 2, 4 and 6 mm for the square, the circular, and the hexagonal edge geometry.	93
Figure 5-10: Number of abrasions until rupture of the thin nylon cloth for 0.74, 1.47 and 2.21 m s ⁻¹ for the square, the circular, and the hexagonal edge geometry.	94
Figure 5-11: Number of abrasions until rupture of the PP-felt, the PP-cloth, and the NY-cloth for the square, the circular, and the hexagonal edge geometry.	95
Figure 6-1: SEM image (85x) of the industrial used (blinded) iron ore tailings filter cloth surface showing the blocked particles between and within the fibers.	105
Figure 6-2: Methodology of permeability test samples preparation including jet cleaning.	106
Figure 6-3: Design of the sample holder of the nozzle test station consisting of a support plate onto which the filter medium sample and a backing cloth are fixed with a clamping frame.	108
Figure 6-4: Filter medium flow resistance after front-wash cleaning for the different spray times over flux. Blinded (after 1000 filtration cycles) and unused state are depicted as a reference with a dot-dashed and a dashed line.	111
Figure 6-5: Filter medium flow resistance after back-wash cleaning for the different spray times over flux. Blinded (after 1000 filtration cycles) and unused state are depicted as a reference with a dot-dashed and a dashed line.	113
Figure 6-6: SEM images (80x) of different filter cloth states. a) Insufficient cleaning resulting in a resistance of $3.24 \times 10^{10} \text{ m}^{-1}$. b) Threshold cleaning (resistance $2.20 \times 10^9 \text{ m}^{-1}$). c) Excessive cleaning causing the fraying of multifile fibers (resistance $1.94 \times 10^8 \text{ m}^{-1}$).	115
Figure 6-7: The initial smallest free pore diameter d_p between two adjacent fibers is reduced to the diameter $d_{p,Blinding}$ by particles adhering to the fibers or already deposited particles.	119
Figure 6-8: Schematic representation of consecutive filtration cycles for tailings filtration under theoretically optimal regeneration conditions and under consideration of blinding.	120

Figure 6-9: Overview of the used cleaning methods.....	126
Figure 6-10: Representation of the filter medium resistances measured by permeability tests in the unused and used states and after 30 min of cleaning with different 1-molar solvents (hydrochloric acid, acetic acid, sulfamic acid, formic acid, sodium hydroxide or potassium hydroxide solution) for the silver, gold, and iron mine cloths.	130
Figure 6-11: Microscopies of the gold mine cloth (cake side) in the unused (a) and used states (b) and after 30 min of cleaning with 1-molar HCl (c).	130
Figure 6-12: Representation of the resistances measured by permeability tests for the silver, gold and iron cloths in the unused and used states and after varied ultrasonic treatments (30 min ultrasonic treatment with 130 kHz and 47 kHz, 30 min 0.1-molar hydrochloric acid and ultrasonic-acid superposition).	131
Figure 6-13: Representation of the resistances measured by permeability tests for the silver and the gold cloths in unused, used, and cleaned states at variable concentrations (1, 0.1 and 0.01-molar hydrochloric or acetic acid).....	132
Figure 6-14: Representation of the resistances measured by permeability tests for the silver and the gold cloths in the unused, used, and cleaned states for variable treatment times (2, 5, 15, and 30 min 1-molar hydrochloric or acetic acid).....	133
Figure 6-15: Representation of the mean flow pore results in the used state and after 30 min of cleaning with different 1-molar solvents (hydrochloric acid, acetic acid, sulfamic acid, formic acid, sodium hydroxide or potassium hydroxide solution) related to the unused value for the silver, gold, and iron mine cloths.	134
Figure 6-16: Representation of the gold mine cloth breaking strength values in the unused and used states and after 30 min of cleaning with 1-molar hydrochloric acid and simultaneous ultrasonic treatment in warp and weft direction.....	136

List of Tables

Table 2-1: Ranking of the different types of fibers and fabrics according to their performance in various aspects of filtration technology [86] based on [121].....	20
Table 2-2: Chemical properties of polypropylene and polyamide graded as poor, fair, good, or excellent [86, 122].	21
Table 2-3: Selected mechanical and thermal properties of polypropylene and polyamide graded as poor, fair, good, or excellent [86, 122, 125].	21
Table 2-4: Relative cost of polypropylene and polyamide filter media [86].	22
Table 4-1: Exemplary calculation of critical τ_c/σ_c ratio whose undercutting causes shear breaking.....	50
Table 4-2: Properties of the iron ore tailings.	51
Table 4-3: Properties of the three tailings filtration filter media.	53
Table 4-4: Cake shear breaking probability of filtrations in the laboratory recessed plate filter press using the PP cloths.	60
Table 4-5: LSM image, characteristic PSD data and density of the copper tailings..	66
Table 4-6: Main elements of the copper tailings measured by WDXRF.....	67
Table 4-7: XRD mineralogy analysis results of the copper tailings.	67
Table 4-8: LSM image of the filter cloth and characteristics [44].	68
Table 5-1: Properties of apparatus parameter tests filter cloth.	89
Table 5-2: Properties of tailings filtration filter media [44].	90
Table 5-3: Increase of abrasions to rupture of the filter media typical for tailings filtration in comparison with each other for the different edge geometries.	95
Table 6-1: SEM image (1000x) and characteristic PSD excerpts of the iron ore tailings.	103
Table 6-2: Color image (10x) of the unused cloth state taken with a LSM and characteristics.....	104
Table 6-3: EDX analysis of adhering particles for the used filter cloth based on weight.	105

Table 6-4: Characteristics of the full cone nozzle, filter cloth sample positions and impinging areas.107

Table 6-5: Water demand per square meter for all front-wash cleaning parameter combinations. The color background is based on the cleaning performance. A cleaning performance above the threshold of a one-hundred-fold increase in flow in relation to the blinded cloth is marked in green and insufficient regeneration in red. Highlighted in dark green is the successful combination with the lowest water demand.112

Table 6-6: Water demand per square meter for all back-wash cleaning parameter combinations. The color background is based on the cleaning performance. A cleaning above the threshold of a one-hundred-fold increase in flow in relation to the blinded cloth is marked in green and insufficient regeneration in red. Highlighted in dark green is the successful combination with the lowest water demand.113

Table 6-7: Electric energy demand per square meter for all cleaning parameter combinations. Highlighted are the successful combination with the lowest water demand for front- and back-wash.114

Table 6-8: Listing of the filter cloth properties in the unused state including material, weave type (incl. DIN 9354 nomination [118], fiber type, filter medium resistance, and mean flow pore diameter.123

Table 6-9: Laser images (100x) of the tailings particles and an excerpt of the sum distributions of the three mine tailings.....124

Table 6-10: Results of angle dispersive XRF. Combined values of the elements independent of the present oxidation numbers.125

Table 6-11: Results of energy dispersive XRF. Combined value of the elements independent of the present oxidation numbers.135

Appendix

A Additional Information to Chapter 4.2

Table A-1: Fit parameter of water content modeling for a cake thickness of 40 mm.

Combination	Parameter	Value
250 kPa FP, 250 kPa AB, 40 mm	$Water\ content_{250,250,0}$	20.20
	$Water\ content_{250,250,\infty}$	17.61
	$a_{250,250,40}$	0.02917
1250 kPa FP, 250 kPa AB, 40 mm	$Water\ content_{1250,250,0}$	19.84
	$Water\ content_{1250,250,\infty}$	17.61
	$a_{1250,250,40}$	0.03603
1250 kPa FP, 550 kPa AB, 40 mm	$Water\ content_{1250,550,0}$	19.84
	$Water\ content_{1250,550,\infty}$	15.85
	$a_{1250,550,40}$	0.09449
$x_{i,j,\infty}$ ratio	$\frac{Water\ content_{1250,550,180s}}{0.5 \cdot (Water\ content_{250,250,180s} + Water\ content_{1250,250,180s})}$	0.9004

Table A-2: Fit parameter of saturation modeling for a cake thickness of 40 mm.

Combination	Parameter	Value
250 kPa FP, 250 kPa AB, 40 mm	$Saturation_{250,250,0}$	100
	$Saturation_{250,250,\infty}$	85.33
	$a_{250,250,40}$	0.03308
1250 kPa FP, 250 kPa AB, 40 mm	$Saturation_{1250,250,0}$	100
	$Saturation_{1250,250,\infty}$	85.33
	$a_{1250,250,40}$	0.03008
1250 kPa FP, 550 kPa AB, 40 mm	$Saturation_{1250,550,0}$	100
	$Saturation_{1250,550,\infty}$	76.20
	$a_{1250,550,40}$	0.09752
$x_{i,j,\infty}$ ratio	$\frac{Saturation_{1250,550,180s}}{0.5 \cdot (Saturation_{250,250,180s} + Saturation_{1250,250,180s})}$	0.8928

Table A-3: Fit parameter of shear adhesion modeling for a cake thickness of 40 mm.

Combination	Parameter	Value
250 kPa FP, 250 kPa AB, 40 mm	$Adhesion_{250,250,0}$	0.890
	$Adhesion_{250,250,\infty}$	2.787
	$a_{250,250,40}$	0.04196
1250 kPa FP, 250 kPa AB, 40 mm	$Adhesion_{1250,250,0}$	1.617
	$Adhesion_{1250,250,\infty}$	2.787
	$a_{1250,250,40}$	0.08254
1250 kPa FP, 550 kPa AB, 40 mm	$Adhesion_{1250,550,0}$	1.617
	$Adhesion_{1250,550,\infty}$	3.150
	$a_{1250,550,40}$	0.10426
$x_{i,j,\infty}$ ratio	$\frac{Adhesion_{1250,550,180s}}{0.5 \cdot (Adhesion_{250,250,180s} + Adhesion_{1250,250,180s})}$	1.1349

Table A-4. Fit parameter of shear cohesion modeling for a cake thickness of 40 mm.

Combination	Parameter	Value
250 kPa FP, 250 kPa AB, 40 mm	$Cohesion_{250,250,0}$	1.245
	$Cohesion_{250,250,\infty}$	3.538
	$a_{250,250,40}$	0.01346
1250 kPa FP, 250 kPa AB, 40 mm	$Cohesion_{1250,250,0}$	1.471
	$Cohesion_{1250,250,\infty}$	3.538
	$a_{1250,250,40}$	0.01565
1250 kPa FP, 550 kPa AB, 40 mm	$Cohesion_{1250,550,0}$	1.471
	$Cohesion_{1250,550,\infty}$	4.989
	$a_{1250,550,40}$	0.03995
$x_{i,j,\infty}$ ratio	$\frac{Cohesion_{1250,550,180s}}{0.5 \cdot (Cohesion_{250,250,180s} + Cohesion_{1250,250,180s})}$	1.4101

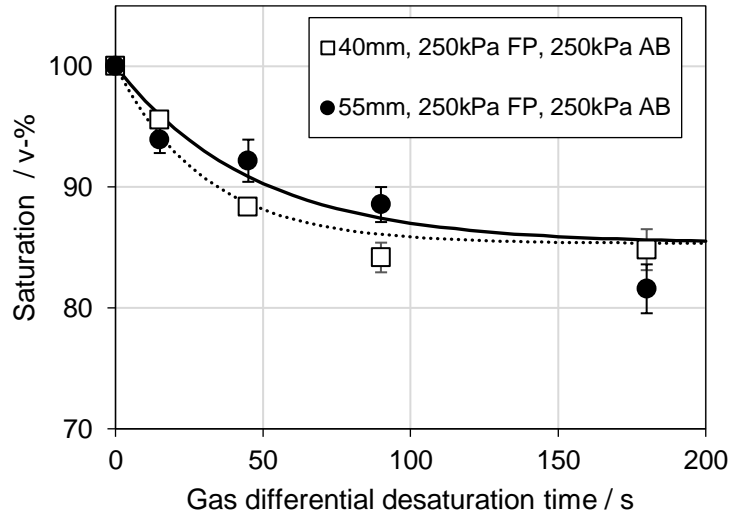


Figure A-1: Filter cake saturation of 250 kPa filtration pressure and 250 kPa air blow pressure combination for variation of the desaturation time for cake thicknesses of 40 and 55 mm.

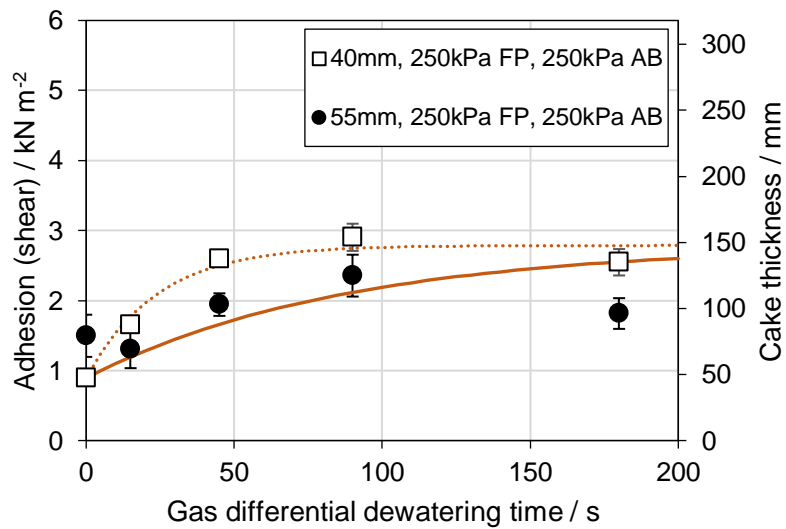


Figure A-2: Filter cake to filter fabric shear adhesion of 250 kPa filtration pressure and 250 kPa air blow pressure combination for variation of the desaturation time for cake thicknesses of 40 and 55 mm.

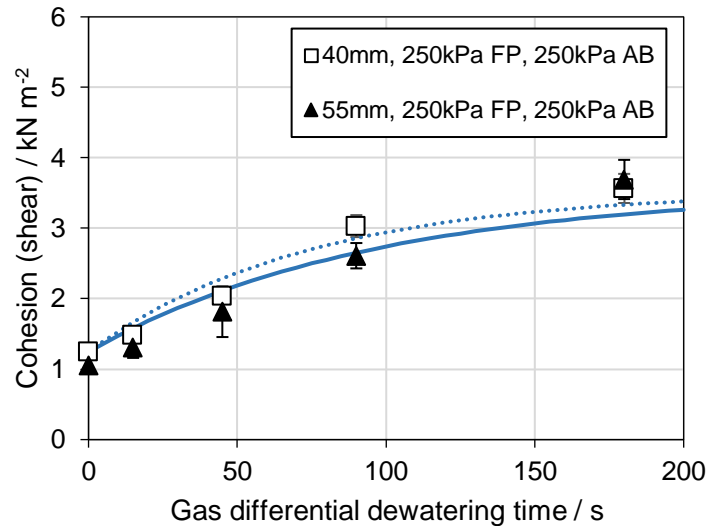


Figure A-3: Filter cake shear cohesion of 250 kPa filtration pressure and 250 kPa air blow pressure combination for variation of the desaturation time for cake thicknesses of 40 and 55 mm.

Table A-5: Fit parameter of water content modeling for a cake thickness of 55 mm.

Combination	Parameter	Value
250 kPa FP, 250 kPa AB, 55 mm	$Water\ content_{250,250,0}$	20.20
	$Water\ content_{250,250,\infty}$	17.61
	$a_{250,250,55}$	0.01752

Table A-6: Fit parameter of saturation modeling for a cake thickness of 55 mm.

Combination	Parameter	Value
250 kPa FP, 250 kPa AB, 55 mm	$Saturation_{250,250,0}$	100
	$Saturation_{250,250,\infty}$	85.33
	$a_{250,250,55}$	0.01375

Table A-7: Fit parameter of filter fabric to filter cake shear adhesion modeling for a cake thickness of 55 mm.

Combination	Parameter	Value
250 kPa FP, 250 kPa AB, 55 mm	$Adhesion_{250,250,0}$	0.890
	$Adhesion_{250,250,\infty}$	2.787
	$a_{250,250,55}$	0.01156

Table A-8: Fit parameter of shear cohesion modeling for a cake thickness of 55 mm.

Combination	Parameter	Value
250 kPa FP, 250 kPa AB, 55 mm	$Cohesion_{250,250,0}$	1.245
	$Cohesion_{250,250,\infty}$	3.538
	$a_{250,250,55}$	0.01057

B Additional Information to Chapter 6.1

The publication in Chapter 6.1 deals with water jet cleaning of an industrially blinded iron ore filter cloth. The first part of this Appendix section extends the investigation by further measurements of the silver and the gold mine cloth also provided by FLSmidth. These two additional fabrics are part of the chemical and ultrasound cleaning study in Chapter 6.2 and, therefore, the supplementary data enable comparison. Furthermore, an estimation of cleaning costs for the chemical filter cloth regeneration (Chapter 6.2) is provided in the second part of this Appendix section.

B1 Silver Mine Filter Cloth Water Jet Cleaning

Figure B1-1 shows the flow resistances resulting from front-wash water jet cleaning of the silver mine polyamide filter medium having monofile and multifile fibers for different water flux and spray time. The industrial blinded cloth has around 5000 filtrations cycles and, therefore, a very significant difference in flow resistance between the used state ($1.24 \times 10^{12} \text{ m}^{-1}$), shown by the dot-dashed line, and the unused state ($5.19 \times 10^8 \text{ m}^{-1}$), shown as dashed line. Analogous to the iron ore cloth, water jet cleaning reduces the flow resistance drastically even for low flux and spray time. However, the effect is declining for higher flux. The cleaning effect is mainly dependent on the water jet flux and is only slightly affected by the spray time. The assumed required cleaning threshold based on a hundredfold improvement in flow resistance compared to blinded state amounts to $1.24 \times 10^{10} \text{ m}^{-1}$. The threshold is reached for all combinations of flux and spray time excluding 5 and 15 s spray time at the lowest flux of $0.06 \text{ m}^3 \text{ m}^{-2} \text{ s}^{-1}$. Therefore, water jet cleaning can be stated effective for this filter medium. However, there is no further improvement of flow resistance above a flux of $0.81 \text{ m}^3 \text{ m}^{-2} \text{ s}^{-1}$ and it is not possible to achieve an unused state of the filter medium resistance by spray cleaning. Since a small number of adhering particles supports bringing and cake build-up at the beginning of the filtration, this is no disadvantage.

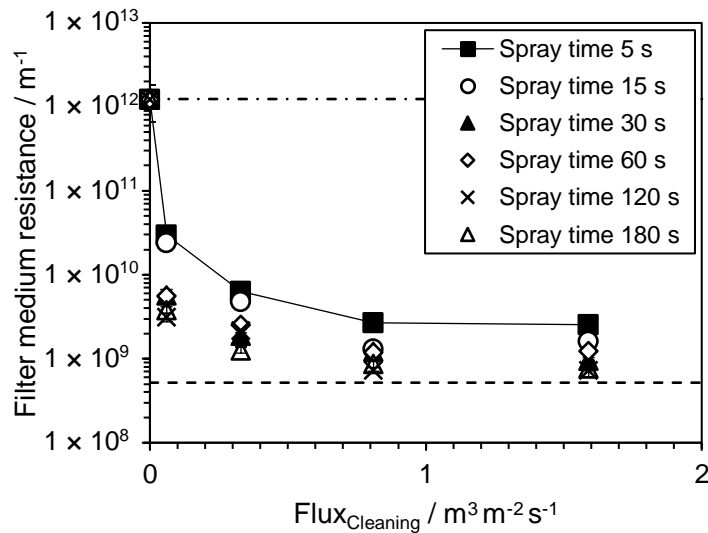


Figure B1-1: Silver mine filter medium flow resistance after front-wash cleaning for the different spray times over flux. Blinded (after 5000 filtration cycles) and unused state are depicted as a reference with a dot-dashed and a dashed line.

The silver mine filter cloth flow resistances resulting from back-wash water jet cleaning for different flux and spray time are shown in Figure B1-2. Analogous to the front-wash cleaning, a strong decrease of the flow resistance even for a low flux can be seen. Higher flux and spray time results in an increased cleaning effect, whereby, the flux is the significant influence. Furthermore, the resistance decrease is declining and spraying with higher flux than $0.81 \text{ m}^3 \text{ m}^{-2} \text{ s}^{-1}$ shows no further regeneration effect. Therefore, unused filter medium state is not achieved. In contrast to the front-wash less combinations of flux and spray time reach the threshold resistance of $1.24 \times 10^{10} \text{ m}^{-1}$ and the cleaning curves are flatter. Nevertheless, it can be stated that back-wash water jet cleaning is also effective for this cloth.

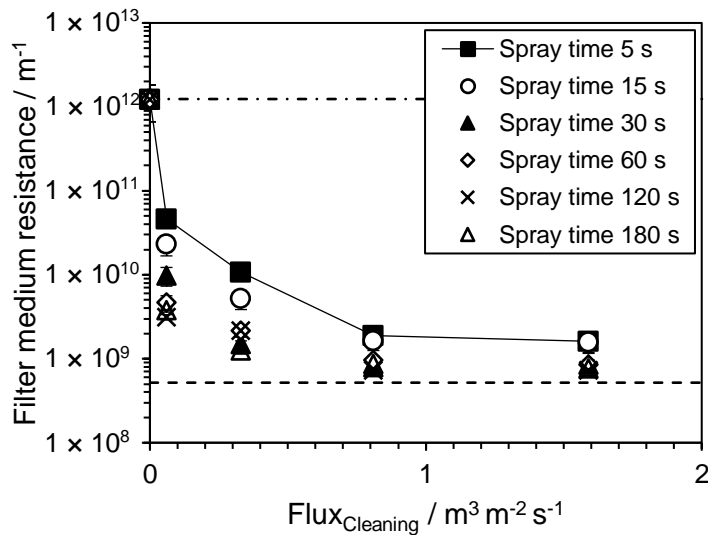


Figure B1-2: Silver mine filter medium flow resistance after back-wash cleaning for the different spray times over flux. Blinded (after 5000 filtration cycles) and unused state are depicted as a reference with a dot-dashed and a dashed line.

Overall, it can be concluded that water jet spray cleaning of the silver mine filter cloth is possible but front-wash is easier to apply for tailings filtration applications. Furthermore, front-wash cleaning is slightly more effective for this fabric than back-wash spraying. This is similar to the behavior of the iron cloth investigated in Chapter 6.1.

B2 Gold Mine Filter Cloth Water Jet Cleaning

Figure B2-1 shows resulting flow resistance by front-wash water jet cleaning with different flux and spray time for the gold mine cloth consisting of monofile polypropylene fibers. The unused flow resistance of $6.57 \times 10^7 \text{ m}^{-1}$ and the used state of $4.04 \times 10^{11} \text{ m}^{-1}$ is shown as dashed and dot-dashed line, respectively. There is a decrease in resistance by water spraying even for low flux, however, the effect is poor. Furthermore, the cleaning effect is not enhanced for higher flux and, again, the spray time has no significant effect. By taken a hundredfold improvement of the flow resistance as a reference, which amounts to $4.04 \times 10^9 \text{ m}^{-1}$, none of the combinations of flux and spray time results in a sufficient cleaning.

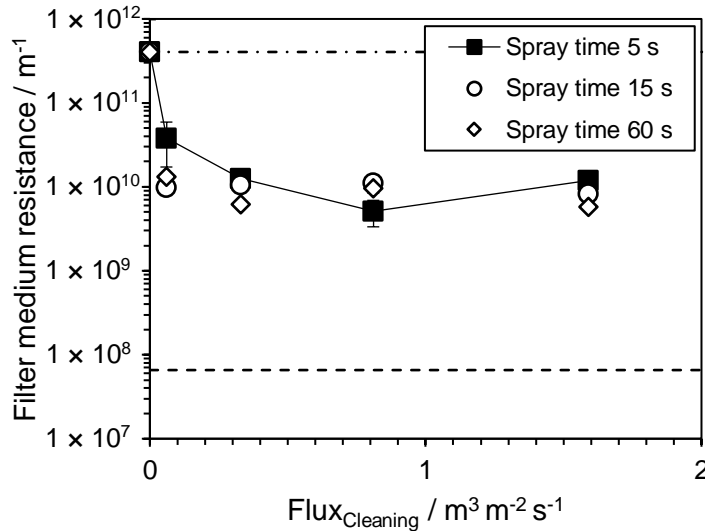


Figure B2-1: Gold mine filter medium flow resistance after front-wash cleaning for the different spray times over flux. Blinded (after 6500 filtration cycles) and unused state are depicted as a reference with a dot-dashed and a dashed line.

Back-wash water jet cleaning results for the gold mine cloth for different flux and spray time are shown in Figure B2-2. Analogous to front-wash, there is only a small decrease in flow resistance for all combinations of flux and spray time. Both the set threshold resistance of $4.04 \times 10^9 \text{ m}^{-1}$ and the unused condition of the cloth is not reached. Therefore, back-wash water jet cleaning is also not effective for the gold mine cloth.

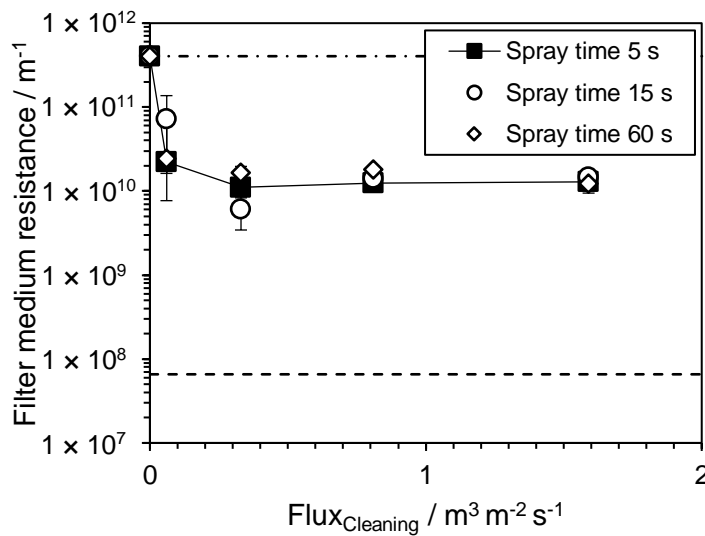


Figure B2-2: Gold mine filter medium flow resistance after front-wash cleaning for the different spray times over flux. Blinded (after 6500 filtration cycles) and unused state are depicted as a reference with a dot-dashed and a dashed line.

In conclusion, it can be stated that water jet cleaning of the monofile gold mine cloth is not successful. This is caused by a precipitated CaCO_3 matrix embedding the particles consisting of the other minerals and the rigid behavior of the monofile fibers and the plain weave.

C Additional Information to Chapter 6.2

The results in Chapter 6.1 show that water jet cleaning is an effective cleaning method for two of the three industrially blinded filter cloths provided by FLSmidth. Furthermore, it is cost effective in first estimation. The fabric from the gold mine which could not be cleaned by jet cleaning could be sufficiently regenerated by chemical cleaning, as can be seen Chapter 6.2.

In addition to the investigations in the corresponding publication of the chemical cleaning, a simplified cost estimation for all chemicals was made. Simplified, small quantities in technical quality at the current price from Carl Roth were taken and correlated to the used concentration of 20.83 mol m⁻². The results are listed in Table C-1. The prices per mole do not show significant differences. For the applied cleaning method, this results in costs per m² in the range between 35 and 61 €. Since hydrochloric acid cleaning performed best this price is most relevant. It is estimated to cost 44 € m⁻². Therefore, it is significantly more expensive than water jet cleaning and is assumed not to be competitive with filter fabric replacement in terms of cost and effort. However, the advantage of plastic waste reduction would be given.

Table C-1: Cost estimation of chemical cleaning of filter fabrics for the reagents used in Chapter 6.2.

Chemical	Price / € mol ⁻¹	Price / € m ⁻²
Hydrochloric acid	2.1 [241]	44
Acetic acid	2.8 [242]	59
Sulfamic acid	2.9 [243]	61
Formic acid	1.8 [244]	37
Sodium hydroxide	1.7 [245]	35
Potassium hydroxide	2.8 [246]	58

D Copyright Information of Industrial Filter Media Abrasion Image

Image Copyright Permission

Permission is hereby granted to Mr. Bernd Fränkle to use and thereby publish the following image in his doctoral dissertation, with credit to copyright by FLSmidth (©FLSmidth).



Thien Sok

Sok, Thien

List of Publications, Presentations and Posters

Journal Publications

- Fränkle, B., Morsch, P., Nirschl, H., 2021. Regeneration Assessments of Filter Fabrics of Filter Presses in the Mining Sector. *Minerals Engineering*, 168, 106922.
- Fränkle, B., Morsch, P., Kessler, C., Sok, T., Gleiß, M., Nirschl, H., 2022. Iron Ore Tailings Dewatering: Measurement of Adhesion and Cohesion for Filter Press Operation. *Sustainability*, 14, 3424.
- Fränkle, B., Morsch, P., Sok, T., Gleiß, M., Nirschl, H., 2022. Tailings Filtration Using Recessed Plate Filter Presses: Improving Filter Media Selection by Replicating the Abrasive Wear of Filter Media Caused by Falling Filter Cake after Cake Detachment. *Mining*, 2, 425-437.
- Bächle, V., Morsch, P., Fränkle, B., Gleiß, M., Nirschl, H., 2021. Interaction of Particles and Filter Fabric in Ultrafine Filtration. *Eng*, 2, 126-140.
- Xie, D., Fränkle, B., Klahn, C., Dittmeyer, R., 2022. Fabrication of Sectionally Permeable Components with Curved Surface by Laser-Beam Powder-Bed Fusion, *Chemie Ingenieur Technik*, 94(7), 983–992.
- Fränkle, B.; Stockert, M.; Sok, T.; Gleiß, M.; Nirschl, H., 2023. Tailings Filtration: Water Jet Spray Cleaning of a Blinded Iron Ore Filter Cloth. *Minerals*, 13, 416.
- Fischer, A., Martirosian, P., Machann, J., Fränkle, B., Schick, F., 2024. Frequency Shifts of Free Water Signals from Compact Bone – Simulations and Measurements Using a UTE-FID Sequence. *Magnetic Resonance in Medicine*, 1-12.
- Fränkle, B.; Sok, T.; Gleiß, M.; Nirschl, H., In Submission. Copper Tailings Filtration: Influence of Filter Cake Desaturation. *Minerals Engineering*.

Conference Publications

- Fränkle, B., Morsch, P., Nirschl, H., 2021. Towards Prediction of Cake Detachment in Tailings Filtration. In *Proceedings of the 24th International Conference on Paste, Thickened and Filtered Tailings: Paste 2021*. Perth/Online, Australian Centre for Geomechanics.

Presentations

- Fränkle, B., Morsch, P., Nirschl, H., 2021. Regeneration von Filtergeweben im Bergbau. Jahrestreffen der ProcessNet-Fachgruppen Mechanische Flüssigkeitsabtrennung, Zerkleinern und Klassieren sowie Agglomerations- und Schüttguttechnik, 15.-16.03.2021, Online, Dechema.
- Fränkle, B., Morsch, P., Nirschl, H., 2021. Towards Prediction of Cake Detachment in Tailings Filtration. 24th International Conference on Paste, Thickened and Filtered Tailings: Paste 2021. 21.-23.09.2021, Perth/Online, Australian Centre for Geomechanics.
- Fränkle, B., Morsch, P., Nirschl, H., 2021. Regeneration of Filter Press Fabrics in the Mining Sector. 25th International Conference on Tailings and Mine Waste: Tailings and Mine Waste '21., 07.-10.11.2021, Banff/Online, University of Alberta Geotechnical Center.
- Fränkle, B., Nirschl, H., 2022. Düsen-Regeneration von Filtergeweben im Bergbau. Jahrestreffen der ProcessNet-Fachgruppen Mehrphasenströmungen, Mechanische Flüssigkeitsabtrennung sowie Zerkleinern und Klassieren, 21.-22.02.2022, Online, Dechema.
- Fränkle, B., 2022. Regeneration of Filter Press Fabrics in the Mining Sector. FILTECH, 08. 10.03.2022, Cologne, Filtech Exhibitions.
- Fränkle, B., Morsch, P., Sok, T., Gleiß, M., Nirschl, H., 2022. Investigations on Abrasive Wear of Filter Media in Tailings Filtration. 13th World Filtration Congress, 05.-09.10.2023, San Diego, American Filtration and Separations Society.
- Baust, H., Fränkle, B., Gleiß, M., Nirschl, H., 2023. Solid-liquid Separation in Filter Presses: A Sustainable Design and Optimization of Multi-scale Processes Through Digitalization. Sustainable Minerals '23, 07.-08.06.2023, Falmouth, MEI Conferences.
- Fränkle, B., Nirschl, H., 2023. Aspects in Ore Residue Filtration. PARTEC 2023 International Congress on Particle Technology, 26.-28.09.2023, Nuremberg, VDI.

Posters

- Fränkle, B., 2022. Filter Media Research in Tailings Filtration. 139th BASF International Summer Course, 14.-20.08.2022, Ludwigshafen, BASF.
- Fränkle, B., Chaponnel, J., Nirschl, H., 2023. Ore Residue Filtration - Cake Post-dewatering by Pressurized Air. FILTECH, 14.-16.02.2023, Cologne, Filtech Exhibitions.
- Fränkle, B., Gleiß, M., Nirschl, H., 2023. Filtration von Erzaufbereitungsrückständen: Untersuchungen zur Gasdifferenzdruckentfeuchtung. Jahrestreffen der DECHEMA-Fachgruppen Grenzflächenbestimmte Systeme, Kristallisation sowie Prozesse und Mechanische Flüssigkeitsabtrennung, 09.-10.03.2023, Frankfurt am Main, Dechema.
- Baust, H., Fränkle, B., Gleiß, M., Nirschl, H., 2023. Ortsaufgelöste Simulation der Filtration in einer Kammerfilterpresse. Jahrestreffen der DECHEMA-Fachgruppen Grenzflächenbestimmte Systeme, Kristallisation sowie Prozesse und Mechanische Flüssigkeitsabtrennung, 09.-10.03.2023, Frankfurt am Main, Dechema.

References

- [1] FLSmidth, "FLSmidth Discover Mining - Battery Minerals on the Charge," 2019.
- [2] D. Flanagan, "Minerals Yearbook Copper 2018 (Advanced Release): U.S. Geological Survey Report," U.S. Geological Survey, Reston, 2022.
- [3] F. Concha A., *Fluid Mechanics and Its Applications - Solid-Liquid Separation in the Mining Industry*, Cham: Springer International Publishing Switzerland, 2014.
- [4] K. Johnson, J. Hammarstrom, M. Zientek and C. Dicken, "Estimate of undiscovered copper resources of the world, 2013: U.S. Geological Survey Fact Sheet," U.S. Geological Survey, Reston, 2014.
- [5] C. Roche, K. Thygesen and E. Baker, "Mine Tailings Storage: Safety Is no Accident," United Nations Environment Programme and GRID-Arendal, Nairobi and Arendal, 2017.
- [6] G. Mudd, C. Roche, K. Thygesen and E. Baker, "An Average Day in a Large-sized Copper Mine in Mine Tailings Storage: Safety Is No Accident," United Nations Environment Programme and GRID-Arendal, Nairobi and Arendal, 2015.
- [7] C. Dieter, M. Maupin, R. Caldwell, M. Harris, T. Ivahnenko, J. Lovelace, N. Barber and K. Linsey, "Water Availability and Use Science Program - Estimated Use of Water in the United States in 2015," U.S. Department of the Interior - U.S. Geological Survey, 2018.
- [8] D. Bleiwas, "Estimated Water Requirements For the Conventional Flotation of Copper Ores: U.S. Geological Survey Open-File Report," U.S. Geological Survey, Ranson, 2012.
- [9] M. Singh, "Water Consumption at Copper Mines in Arizona," Arizona Geological Survey, Phoenix, 2010.
- [10] A. Gunson, B. Klein, M. Veiga and S. Dunbar, "Reducing Mine Water Requirements," *Journal of Cleaner Production*, vol. 21, no. 1, pp. 71-82, January 2012.
- [11] B. Wills and J. Finch, *Wills' Mineral Processing Technology - An Introduction to the Practical Aspects of Ore Treatment and Mineral Recovery*, 8. ed., Oxford: Elsevier Ltd. (Butterworth-Heinemann), 2015.
- [12] E. Baker, M. Davies, A. Fourie, G. Mudd and K. Thygesen, "Mine Tailings Facilities: Overview and Industry Trends in Towards Zero Harm - A Compendium of Papers Prepared for the Global Tailings Review," *Global Tailings Review* (Oberle, B.; Brereton, D.; Mihaylova, A.), London, 2020.
- [13] C. Mortimer and U. Müller, *Chemie*, 9. ed., Stuttgart: Georg Thieme Verlag, 2007.
- [14] C. Wang, D. Harbottle, Q. Liu and Z. Xu, "Current State of Fine Mineral Tailings Treatment: A Critical Review on Theory and Practice," *Minerals Engineering*, no. 58, pp. 113-131, April 2014.
- [15] M. Kalin-Seidenfaden and W. Wheeler, *Mine Waste and Water, Ecological Engineering and Metals Extraction - Sustainability and Circular Economy*, Cham: Springer Nature Switzerland, 2022.
- [16] C. Wels, A. Robertson and P. Madariaga, "Water Recovery Study for Pampa Pabellon Tailings Impoundment, Collahuasi, Chile," *Proceedings of the Eleventh Tailings and Mine Waste Conference*, 2004.
- [17] K. Islam and S. Murakami, "Global-scale Impact Analysis of Mine Tailings Dam Failures: 1915–2020," *Global Environmental Change*, vol. 70, no. 102361, 2021.
- [18] L. Piciullo, E. Storrøsten, Z. Liu, F. Nadim and S. Lacasse, "A New Look at the Statistics of Tailings Dam Failures," *Engineering Geology*, vol. 303, no. 106657, 2022.

References

- [19] WISE, "World Information Service on Energy and Uranium Project," 2023. [Online]. Available: <https://www.wise-uranium.org/index.html>. [Accessed 17 July 2023].
- [20] D. Turi, J. Pusztai and I. Nyari, "Causes and Circumstances of Red Mud Reservoir Dam Failure In 2010 at MAL Zrt Factory Site in Ajka, Hungary," in *Seventh International Conference on Case Histories in Geotechnical Engineering*, St. Louis, 2013.
- [21] E. Petticrew, S. Albers, S. Baldwin, E. Carmack, S. Déry, N. Gantner, K. Graves, B. Laval, J. Morrison, P. Owens, D. Selbie and S. Vagle, "The Impact of a Catastrophic Mine Tailings Impoundment Spill Into one of North America's Largest Fjord Lakes: Quesnel Lake, British Columbia, Canada," *Geophysical Research Letters*, no. 42, p. 3347–3355, 2015.
- [22] E. Zabolotnii, N. Morgenstern and G. Wilson, "Mechanism of failure of the Mount Polley Tailings Storage Facility," *Canadian Geotechnical Journal*, no. 59, p. 1503–1518, 2022.
- [23] D. J. Williams, "Mine Tailings Facilities: Overview and Industry Trends in Towards Zero Harm - A Compendium of Papers Prepared for the Global Tailings Review," *Global Tailings Review* (Oberle, B.; Brereton, D.; Mihaylova, A.), London, 2020.
- [24] M. Karim, M. Rahman, K. Rajibul, A. Fourie and D. Reid, "Characteristics of Copper Tailings in Direct Simple Shearing: A Critical State Approach," *Journal of Geotechnical and Geoenvironmental Engineering*, vol. 149, no. 5, 2023.
- [25] D. Kossoff, W. Dubbin, M. Alfredsson, S. Edwards, M. Macklin and K. Hudson-Edwards, "Mine Tailings Dams: Characteristics, Failure, Environmental Impacts, and Remediation," *Applied Geochemistry*, no. 51, pp. 229-245, 2014.
- [26] F. Pacheco, R. do Valle Junior, M. de Melo Silva, T. Tarlé Pissarra, G. de Souza Rolim, M. de Melo, C. Valera, J. Moura and L. Fernandes, "Geochemistry and Contamination of Sediments and Water in Rivers Affected by the Rupture of Tailings Dams (Brumadinho, Brazil)," *Applied Geochemistry*, vol. 152, no. 105644, 2023.
- [27] B. Lottermoser, *Mine Wastes - Characterization, Treatment and Environmental Impacts*, 3. ed., Springer-Verlag Berlin Heidelberg, 2010.
- [28] B. Lottermoser, *Predictive Environmental Indicators in Metal Mining*, Cham: Springer International Publishing Switzerland, 2017.
- [29] FLSmidth Minerals Technology Center, "Tailings Management - Sustainable and Complete Dewatering Solutions," 2019. [Online]. Available: <https://www.flsmidth.com/-/media/brochures/brochures-solutions/2019/fls-tailings-management-brochure-web-20190503.pdf>. [Accessed 23 June 2023].
- [30] FLSmidth, "The Mine of Today," 2023. [Online]. Available: <https://missionzeromine.com/#tdy>. [Accessed 23 June 2023].
- [31] FLSmidth, "Mission Zero Mine," 2023. [Online]. Available: <https://missionzeromine.com/#mzm>. [Accessed 23 June 2023].
- [32] R. Gomes, G. De Tomi and P. Assis, "Iron Ore Tailings Dry Stacking in Pau Branco Mine, Brazil," *Journal of Materials Research and Technology*, vol. 5, no. 4, pp. 339-344, 2016.
- [33] Global Tailings Review, *Towards Zero Harm: A Compendium of Papers Prepared for the Global Tailings Review*, B. B. D. M. A. Oberle, Ed., London: Global Tailings Review, 2020.
- [34] International Council on Mining and Metals (ICMM), United Nations Environment Programme (UNEP) and Principles of Responsible Investment (PRI), *Global Standard on Tailings Management*, London: Global Tailings Review (Oberle, B.; Brereton, D.; Mihaylova, A.), 2020.
- [35] J. Morrill, D. Chambers, S. Emerman, R. Harkinson, J. Kneen, U. Lapointe, A. Maest, B. Milanez, P. Personius, P. Sampat and R. Turgeon, *Safety First: Guidelines for Responsible Mine Tailings Management v2.0*, Earthworks, MiningWatch Canada, London Mining Network, 2022.
- [36] R. J. Jewell and A. B. Fourie, *Paste and Thickened Tailings – A Guide*, 3 ed., Australian Centre for Geomechanics, 2015.

-
- [37] M. Davies and S. Rice, "An Alternative to Conventional Tailing Management - Dry Stack," in *Proceedings of the Tailings and MineWaste Conference*, Vancouver, 2001.
- [38] C. Cacciuttolo and E. Atencio, "An Alternative Technology to Obtain Dewatered Mine Tailings: Safe and Control Environmental Management of Filtered and Thickened Copper Mine Tailings in Chile," *Minerals*, vol. 12, no. 1334, 2022.
- [39] M. Davies, "Filtered Dry Stacked Tailings – The Fundamentals," in *Proceedings Tailings and Mine Waste*, Vancouver, 2011.
- [40] J. Chaponnel and T. Wisdom, "FLSmith Colossal Filter – Demonstration Plant," in *Proceedings of the 21st International Seminar on Paste and Thickened Tailings*, Perth, 2018.
- [41] K. Rahal and T. Wisdom, "The Impact of Thickening on Fast Filtration of Tailings," in *Proceeding of the Tailings and Mine Waste Conferene*, Virtual, 2020.
- [42] N. Blanchet, "Use of Statistical Approach in Tailings Filtration: Learnings from Cloth Failures," in *Proceeding of Alumina Conference*, Gladstone, 2018.
- [43] T. Wisdom, "Maintaining High Availability and Low Operational Costs for Filtered Tailings Facilities," in *Paste 2019: 22nd International Conference on Paste, Thickened and Filtered Tailings*, Cape Town, 2019.
- [44] B. Fränkle, P. Morsch, C. Kessler, T. Sok, M. Gleiß and H. Nirschl, "Iron Ore Tailings Dewatering: Measurement of Adhesion and Cohesion for Filter Press Operation," *Sustainability*, vol. 14, no. 6, 3424, 2022.
- [45] B. Fränkle, T. Sok, M. Gleiß and H. Nirschl, "Copper Tailings Filtration: Influence of Filter Cake Desaturation," In Submission.
- [46] B. Fränkle, P. Morsch, T. Sok, M. Gleiß and H. Nirschl, "Tailings Filtration Using Recessed Plate Filter Presses: Improving Filter Media Selection by Replicating the Abrasive Wear of Filter Media Caused by Falling Filter Cake after Cake Detachment," *Mining*, vol. 2, no. 2, pp. 425-437, 2022.
- [47] B. Fränkle, M. Stockert, T. Sok, M. Gleiß and H. Nirschl, "Tailings Filtration: Water Jet Spray Cleaning of a Blinded Iron Ore Filter Cloth," *Minerals*, vol. 13, no. 3, 416, 2023.
- [48] B. Fränkle, P. Morsch and H. Nirschl, "Regeneration Assessments of Filter Fabrics of Filter Presses in the Mining Sector," *Minerals Engineering*, vol. 168, no. 106922, 2021.
- [49] International Council on Mining and Metals (ICMM), *Tailings Reduction Roadmap*, London, 2022.
- [50] N. Amoah, W. Dressel and A. Fourie, "Characterisation of Unsaturated Geotechnical Properties of Filtered Tailings in Dry Stack Facility," in *Proceedings of the 22st International Seminar on Paste, Thickened and Filtered Tailings*, Perth, 2018.
- [51] D. Machin, C. Espinoza Asencios and C. Leon Aguilar, "Evaluation of Commingled Tailings and Waste Rock as an Integrated Approach to Mine Waste Management: Outcomes of a Pre-pilot Trial," *Paste 2023: 25th International Conference on Paste, Thickened and Filtered Tailings*, Edmonton, 2023.
- [52] J. Morgan, A. Boudreau, M. Verdugo, F. Meloni and D. Colombo, "New Satellite Sensors for Monitoring Mining Areas: A Look at the Future," *Slope Stability 2020: Proceedings of the 2020 International Symposium on Slope Stability in Open Pit Mining and Civil Engineering*, 2020.
- [53] M. Laker, "Environmental Impacts of Gold Mining—With Special Reference to South Africa," *Mining*, no. 3, pp. 205-220, 2023.
- [54] O. Carmignano, S. Vieira, A. Teixeira, F. Lameiras, P. Brandão and R. Lago, "Iron Ore Tailings: Characterization and Applications," *Journal of the Brazilian Chemical Society*, vol. 32, no. 10, 2021.

References

- [55] R. Nkuna, G. Ijoma, T. Matambo and N. Chimwani, "Accessing Metals from Low-Grade Ores and the Environmental Impact Considerations: A Review of the Perspectives of Conventional versus Bioleaching Strategies," *Minerals*, vol. 12, no. 506, 2022.
- [56] L. Bullock, R. James, J. Matter, P. Renforth and D. Teagle, "Global Carbon Dioxide Removal Potential of Waste Materials From Metal and Diamond Mining," *Frontiers in Climate*, vol. 3, no. 694175, 2021.
- [57] T. Wennberg, A. Stalnacke and A. Sellgren, "Commissioning and Operational Experience of a Thickened Tailing Facility with Two Thickeners.," in *Proceedings of the 23rd International Seminar on Paste, Thickened and Filtered Tailings*, Santiago, 2020.
- [58] N. Amoah, "Large-scale Tailings Filtration and Dry Stacking at Karara Magnetite Iron Ore Operation," in *Proceedings of Tailings and Mine Waste*, Vancouver, 2019.
- [59] J. Kruyswijk, "The Balance between Energy and Water Preservation in the Deposition of Dry Tailings in Wet Climates," in *In Proceedings of the 24th International Conference on Paste, Thickened and Filtered Tailings—Paste 2021*, Perth, 2021.
- [60] P. Ginisty, B. Legoff, J. Olivier, J. Vaxelaire, T. Hervé and J. Paixao, "Measurement of Adhesion Strengths and Energy between Calcium Carbonate Cake and Filter Cloth," *Particle Separation 2016: Advances in Particle Science and Separation: Meeting Tomorrow's Challenges*, Oslo, 2016.
- [61] K. Morris, R. Allen and R. Clift, "Adhesion of Cakes to Filter Media," *Filtration & Separation*, 1987.
- [62] P. Morsch, P. Ginisty, H. Anlauf and H. Nirschl, "Factors Influencing Backwashing Operation in the Liquid Phase after Cake Filtration," *Chemical Engineering Science*, vol. 213, no. 115372, 2020.
- [63] P. Morsch, H. Anlauf and H. Nirschl, "The Influence of Filter Cloth on Cake Discharge Performances during Backwashing into Liquid Phase," *Separation and Purification Technology*, vol. 254, no. 117549, 2021.
- [64] P. Morsch, M. Bauer, C. Kessler, H. Anlauf and H. Nirschl, "Description of the Filter Cloth Deformation During Backwashing Filtration," *Separation and Purification Technology*, vol. 253, no. 117504, 2020.
- [65] P. Morsch, P. Ginisty, H. Anlauf and H. Nirschl, "Influence of Regeneration Variables during Backwashing Treatment into Gas-phase after Liquid Filtration," *Separation and Purification Technology*, vol. 249, no. 117073, 2020.
- [66] P. Morsch, *Detachment of Fine-grained Thin Particle Layers from Filter Media - Dissertation*, Karlsruhe: Fakultät für Chemieingenieurwesen und Verfahrenstechnik des Karlsruher Instituts für Technologie (KIT), 2021.
- [67] R.-S. Möller and H. Nirschl, "Adhesion and Cleanability of Surfaces in the Baker's Trade," *Journal of Food Engineering*, no. 194, pp. 99-108, 20 September 2016.
- [68] H. Müller, R. Kern and W. Stahl, "Adhesive Forces between Filter Cloth and Cake," *Filtration & Separation*, 1987.
- [69] A. Ward, "Cake Filtration - The Adhesion of The Cake to the Filter Cloth," *Filtration & Separation*, 1971.
- [70] T. Weigert and S. Ripperger, "Versuchsstand zur Untersuchung von Filtermitteln für die Kuchenfiltration," *Chemie Ingenieur Technik*, vol. 68, pp. 1143-1146, 1996.
- [71] T. Weigert and S. Ripperger, "Effect of Filter Fabric Blinding on Cake Filtration," *Filtration & Separation*, pp. 507-510, 1997.
- [72] T. Weigert and S. Ripperger, "Haftung von Filterkuchen an Polymeren Filtermedien," *Chemie Ingenieur Technik*, vol. 71, p. 992, 1999.
- [73] T. Weigert and S. Ripperger, "Filterkuchenhaftung an Textilfiltermedien - Teil 1: Experimentelle Untersuchungen und Ihre Auswertung," *Filtrieren & Separieren*, vol. 15, no. 5, pp. 221-228, 2001.

-
- [74] T. Weigert and S. Ripperger, "Filterkuchenhaftung an Textilfiltermedien - Teil 2: Physikalische Beschreibung und Modellierung," *Filtrieren & Separieren*, vol. 16, no. 1, pp. 7-12, 2002.
- [75] T. Weigert, *Haftung von Filterkuchen bei der Fest/Flüssig-Filtration - Dissertation (VDI-Fortschrittsbericht)*, Düsseldorf: VDI-Verlag, 2001.
- [76] O. Ozcan, B. Gonul, A. Bulutcu and H. Manav, "Correlations between the Shear Strength of Mineral Filter Cakes and Particle Size and Surface Tension," *Colloids and Surfaces*, no. 187-188, pp. 405-413, 2001.
- [77] O. Ozcan, M. Ruhland and W. Stahl, "Shear Strength of Mineral Filter Cakes," *Studies in Surface Science and Catalysis*, no. 128, pp. 573-585, 2000.
- [78] O. Ozcan, M. Ruhland and W. Stahl, "The Effect of Pressure, Particle Size and Particle Shape on the Shear Strength of Very Fine Mineral Filter Cakes," *International Journal of Mineral Processing*, vol. 59, no. 2, p. 185-193, 2000.
- [79] H. Schubert, *Untersuchungen zur Ermittlung von Kapillardruck und Zugfestigkeit von feuchten Haufwerken aus körnigen Stoffen - Dissertation*, Karlsruhe: Universität Karlsruhe, 1972.
- [80] A. Erk, *Rheologische Eigenschaften feindisperser Suspensionen während ihrer Fest-Flüssig-Trennung in Filtern und Zentrifugen - Dissertation*, Aachen: Shaker Verlag, 2006.
- [81] Micronics, "Micronics' HPR Feed Neck Design Improves Filter Press Cloth Performance," 2022. [Online]. Available: <https://www.micronicsinc.com/filtration-news/hpr-feed-neck-design/>. [Accessed 10 January 2022].
- [82] FLSmidth Salt Lake City Operations, *Personal Communication*, 2021.
- [83] C. Chairman, M. Ravichandran, V. Mohanavel, T. Sathish, A. Rashedi, I. Alarifi, I. Badruddin, A. Anqi and A. Afzal, "Mechanical and Abrasive Wear Performance of Titanium Di-Oxide Filled Woven Glass Fibre Reinforced Polymer Composites by Using Taguchi and EDAS Approach," *Materials*, vol. 14, no. 5257, 2021.
- [84] B. Sharath, C. Venkatesh, A. Afzal, N. Asfattahi, A. Aabid, M. Baig and B. Saleh, "Multi Ceramic Particles Inclusion in the Aluminium Matrix and Wear Characterization through Experimental and Response Surface-Artificial Neural Networks," *Materials*, vol. 14, no. 2895, 2021.
- [85] J. Lin, C. Lou, C. Lei and C. Lin, "Processing Conditions of Abrasion and Heat Resistance for Hybrid Needle-punched Nonwoven Bag Filters," *Composites Part A: Applied Science and Manufacturing*, vol. 37, no. 1, pp. 31-37, 2006.
- [86] D. Purchas and K. Sutherland, *Handbook of Filter Media*, 2. ed., Oxford: Elsevier, 2002.
- [87] H. Anlauf, *Wet Cake Filtration - Fundamentals, Equipment, and Strategies*, Weinheim: Wiley-VCH Verlag, 2019.
- [88] J. Smith, C. Sheridan, L. van Dyk, S. Naik, N. Plint and H. Turrer, "Optimal Ceramic Filtration Operating Conditions for an Iron-ore Concentrate," *Minerals Engineering*, vol. 115, pp. 1-3, 2018.
- [89] Outotec and J. Palmer, *Practical solutions for Mine tailings - Part 2, 05/14/2020*, Webinar: Outotec, 2020.
- [90] Aqseptance Group / Diemme Filtration, "Filter Press GHT-F," 2020. [Online]. Available: <https://www.aqseptance.com/app/en/products/diemme-filtration-fast-cycling-filter-press-ght-f/>. [Accessed 1 May 2020].
- [91] R. Werner, D. Geier and T. Becker, "The Challenge of Cleaning Woven Filter Cloth in the Beverage Industry - Wash Jets as an Appropriate Solution," *Food Engineering Reviews*, vol. 12, p. 520-545, 2020.
- [92] P. Morsch, A. Arnold, H. Schulze, R. Werner, H. Anlauf, D. U. Geier, T. Becker and H. Nirschl, "In-situ Cleaning Process of Chamber Filter Presses with Sensor-controlled and Demand-oriented Automation," *Separation and Purification Technology*, vol. 256, no. 117793, 2021.

References

- [93] P. Morsch, J. Kühn, R. Werner, H. Anlauf, D. U. Geier, T. Becker and H. Nirschl, "Influence of the Filter Cloth and Nozzles Type on the In-situ Cleaning Procedure of Filter Presses," *Chemical Engineering Science*, vol. 226, no. 115889, 2020.
- [94] R. Werner, L. Schappals, D. Geier and T. Becker, "Pulsed Forward Flushes as a Novel Method for Cleaning Spent Grains-loaded Filter Cloth," *Food Science + Technology*, no. 57, pp. 4575-4585, 2022.
- [95] C. Weidemann, *Reinigungsfähigkeit von Filtermedien mithilfe von kontinuierlicher und puslierender Strömung - Dissertation*, Karlsruhe: KIT Scientific Publishing, 2015.
- [96] Z. Lam, *Untersuchungen zur Dünnschichtfiltration mit Polymermembranen - Dissertation*, Karlsruhe: Karlsruher Institut für Technologie, 2022.
- [97] S. Ripperger, W. Gösele, C. Alt and T. Loewe, "Filtration, 2. Equipment," in *Ullmann's Encyclopedia of Industrial Chemistry*, Weinheim, Wiley-VCH Verlag, 2013.
- [98] FLSmidth, "AFP2525 Automatic Filter Press Flyer," 2021. [Online]. [Accessed 2 January 2023].
- [99] Aqseptence, "Diemme Filtration - GHT5000F Domino," 2023. [Online]. Available: <https://www.diemmefiltration.com/filterpress-for-sludge/filter-press-ght-5000f-domino/>. [Accessed 2 January 2023].
- [100] Micronics, "Micronics' New Mine-XLL™ Filter Cloth Delivers over 10,000 Cycles in Select Mineral Processing Applications," 2020. [Online]. Available: <https://www.micronicsinc.com/de/filtration-news/new-mine-xll-mining-filter-cloth/>. [Accessed 23 June 2023].
- [101] R. Wakeman, "The Influence of Particle Properties on Filtration," *Separation and Purification Technology*, no. 58, pp. 234-241, 2007.
- [102] E. Vorobiev, "Nonlinear Consolidation Model for the Prediction of Constant Pressure Expression of Semi-solid Materials," *Chemical Engineering Science*, vol. 235, no. 116458, 2021.
- [103] R. Wakeman, "Filter media: Testing for Liquid Filtration," *Filtration & Separation*, vol. 44, no. 3, pp. 32-34, 2007.
- [104] H. Darcy, *Les Fontaines Publiques de la Ville de Dijon*, Paris, 1856.
- [105] S. Ripperger, W. Gösele, C. Alt and T. Loewe, "Filtration, 1. Fundamentals," in *Ullmann's Encyclopedia of Industrial Chemistry*, Weinheim, Wiley-VCH Verlag, 2013.
- [106] J. Tichy, *Zum Einfluss des Filtermittels und der auftretenden Interferenzen zwischen Filterkuchen und Filtermittel bei der Kuchenfiltration - Dissertation*, Düsseldorf: VDI-Verlag, 2007.
- [107] VDI, *Mechanical Solid-liquid-separation by Cake Filtration: Part 1*, Düsseldorf: Verein Deutscher Ingenieure e.V., 2010.
- [108] D. Purchas, "Art, Science and Filter Media," *Filtration & Separation*, 1980.
- [109] VDI, *Mechanical Solid-liquid Separation by Cake Filtration: Determination of Filter Cake Resistance*, Düsseldorf: Verein Deutscher Ingenieure e.V., 2010.
- [110] H. Mamghaderi, M. Gharabaghi and M. Noaparast, "Optimization of Role of Physical Parameters in the Filtration Processing with Focus on the Fluid Flow From Pore," *Minerals Engineering*, vol. 122, no. 220-226, 2018.
- [111] A. Rushton, A. Ward and R. Holdich, *Solid-Liquid Filtration and Separation Technology*, 2. ed., Weinheim: Wiley-VCH, 2000.
- [112] S. Tarleton and R. Wakeman, *Solid/Liquid Separation: Equipment Selection and Process Design*, Elsevier, 2006.
- [113] International Council on Mining and Metals (ICMM), "Water Management in Mining: A Selection of Case Studies," London, 2012.

-
- [114] Outotec, „Outotec - Larox FFP Filters,“ 2022. [Online]. Available: <https://www.mogroup.com/portfolio/larox-ffp-membrane-filter-press/>. [Zugriff am 7 Dezember 2022].
- [115] Micronics, "1500mm Zinc Purification Filter Press Upgrades," 2023. [Online]. Available: <https://www.micronicsinc.com/filtration-news/zinc-purification-upgrades/>. [Accessed 18 September 2023].
- [116] Markert Filtration GmbH, *Personal Communication*, 2022.
- [117] T. Sparks, "Alumina: Filtration in the Alumina Production Process," *Filtration & Separation*, vol. 47, no. 3, pp. 20-23, 2010.
- [118] ISO, *ISO 9354:1989/Cor 1:2000 Textiles – Weaves - Coding system and examples. Technical Corrigendum 1*, Geneva: International Organization of Standardization, 2000.
- [119] H. Anlauf, "Filtermedien zur Kuchenfiltration – Schnittstelle zwischen Suspension und Apparat," *Chemie Ingenieur Technik*, vol. 79, no. 11, pp. 1821-1831, 2007.
- [120] L. Svarovsky, *Solid-Liquid Separation*, 4 ed., Oxford: Butterworth-Heinemann, 2000.
- [121] S. Ehlers, "The Selection of Filter Fabrics Re-examined," *Industrial and Engineering Chemistry*, vol. 53, no. 7, p. 552–556, 1961.
- [122] H. Bremus, "Einsatzkriterien für textile Filtermedien," *Chemie Ingenieur Technik*, vol. 53, p. 433–438, 1981.
- [123] Sefar AG, *Chemical Resistances of Polymer Materials (3105-0001-002-00 | EN | 22.03.2018)*, 2018.
- [124] H. Domininghaus, *DOMININGHAUS - Kunststoffe*, 8 ed., Berlin Heidelberg: Springer-Verlag, 2012.
- [125] J. Sentmanat, "Chemical Engineering - An Overview of Synthetic Filter Media," 2023. [Online]. Available: <https://www.chemengonline.com/an-overview-of-synthetic-filter-media/>. [Accessed 19 September 2023].
- [126] E. Hardman, "Some Aspects of the Design of Filter Fabrics for Use in," *Filtration & Separation*, vol. 31, no. 60, pp. 813-818, 1994.
- [127] S. Wu, R. Cai and L. Zhang, "Research Progress on the Cleaning and Regeneration of PM2.5 Filter Media," *Particuology*, vol. 57, pp. 28-44, 2021.
- [128] M. Gomo, "Conceptual Hydrogeochemical Characteristics of a Calcite and Dolomite Acid Mine Drainage Neutralised Circumneutral Groundwater System," *Water Science*, vol. 32, no. 2, pp. 355-361, 2018.
- [129] A. Akcil and S. Koldas, "Acid Mine Drainage (AMD): Causes, Treatment and Case Studies," *Journal of Cleaner Production*, no. 12-13, pp. 1139-1145, 2006.
- [130] N. Gow and G. Paolo Lozej, "Bauxite," *Geoscience Canada*, vol. 20, no. 1, pp. 9-16, 1993.
- [131] S. Ruyters, J. Mertens, E. Vassilieva, B. Dehandschutter, A. Poffijn and E. Smolders, "The Red Mud Accident in Ajka (Hungary): Plant Toxicity and Trace Metal Bioavailability in Red Mud Contaminated Soil," *Environmental Science & Technology*, vol. 45, no. 4, pp. 1616-1622, 2011.
- [132] X. Ma, Y. Fan, X. Dong, R. Chen, H. Li, D. Sun and S. Yao, "Impact of Clay Minerals on the Dewatering of Coal Slurry: An Experimental and Molecular-Simulation Study," *Minerals*, vol. 8, no. 400, 2018.
- [133] A. Grosso, F. Kaswalder and A. Hawkey, "Clay-bearing Mine Tailings Analysis and Implications in Large Filter Press Design," in *Proceedings of the 24th International Conference on Paste, Thickened and Filtered Tailings*, Perth, 2021.
- [134] ISO, *ISO 14688-1:2017 - Geotechnical investigation and testing — Identification and classification of soil — Part 1: Identification and description*, Geneva: International Organization for Standardization, 2017.
- [135] H. Rumpf, "Die Wissenschaft des Agglomerierens," *Chemie Ingenieur Technik*, vol. 46, no. 1, pp. 1-11, 1974.

References

- [136] L. Martinson, R. Martinson and R. Cooke, "Pipe Loop Tests at Codelco Pilot Plant," in *Paste 2013: Proceedings of the 16th International Seminar on Paste and Thickened Tailings*, Perth, 2013.
- [137] A. D. Stickland, *Solid-Liquid Separation in the Water and Wastewater Industries - Ph.D. Thesis*, Melbourne: Faculty of Engineering, Chemical and Biomolecular Engineering, The University of Melbourne, 2005.
- [138] F. Sofra, "Rheological Properties of Fresh Cemented Paste Tailings," in *Paste Tailings Management*, E. Yilmaz and M. Fall, Eds., Cham, Springer International Publishing Switzerland, 2017, pp. 33-57.
- [139] ASTM, *ASTM D4318-17e1; Standard Test Method for Liquid Limit, Plastic Limit, and Plasticity Index of Soils*, West Conshohocken: ASTM International, 2018.
- [140] D. Schulze, "Flow Properties of Powders and Bulk Solids," 2011. [Online]. Available: <https://www.dietmar-schulze.de/grdle1.pdf>. [Accessed 9 April 2021].
- [141] S. Hammerich, A. Stickland, B. Radel, M. Gleiss and H. Nirschl, "Modified Shear Cell for Characterization of the Rheological Behavior of Particulate Networks under Compression," *Particuology*, vol. 51, pp. 1-9, 2020.
- [142] D. Kolymbas, *Geotechnik - Bodenmechanik, Grundbau und Tunnelbau*, 4. ed., Berlin: Springer Vieweg, 2016.
- [143] J. Tomas and B. Reichmann, "In-situ-Messung der Kompressibilität, Permeabilität und des Fließverhaltens von hochdispersen Filterkuchen mit einer Press-Scherzelle," *Chemie Ingenieur Technik*, vol. 74, p. 76–81, 2002.
- [144] VDI, *Mechanical Solid-liquid Separation by Cake Filtration: Mechanical Deliquoring of Incompressible Filter Cakes by Undersaturation Using a Gas Pressure Difference*, Düsseldorf: Verein Deutscher Ingenieure e.V., 2017.
- [145] I. Nicolaou, *Fortschritte in Theorie und Praxis der Filterkuchenbildung und -entfeuchtung durch Gasdruckdifferenz - Dissertation*, Düsseldorf: VDI-Verlag, 1999.
- [146] ASTM, *ASTM D6128–16; Standard Test Method for Shear Testing of Bulk Solids Using the Jenike Shear Tester*, West Conshohocken: ASTM International, 2016.
- [147] Lechler, "Lechler GmbH - Spray Nozzles and Accessories," January 2020. [Online]. Available: https://www.lechlerusa.com/fileadmin/media-usa/Literature/Catalog/CATALOG_501.pdf. [Accessed 25 Januar 2023].
- [148] ASTM, *ASTM E128-99; Standard Test Method for Maximum Pore Diameter and Permeability of Rigid Porous Filters for Laboratory Use*, West Conshohocken: ASTM International, 2019.
- [149] FLSmidth, "Sustainability Report 2020," 2021. [Online]. Available: https://ungc-production.s3.us-west-2.amazonaws.com/attachments/cop_2021/495014/original/flsmidthsustainabilityreport2020.pdf?1616590187. [Accessed 9 April 2021].
- [150] T. Fitton and A. Roshdieh, "The Impact on Slurry Rheology on Tailings and Disposal Options," in *Proceedings of the Four Case Studies Paper Presented at IIR Slurry Pipelines Conference*, Perth, 2012.
- [151] T. Wisdom, R. Neumann and J. Chaponnel, "Development and Testing of the World's Largest Capacity Tailings Filter Press," in *Proceedings of the 23rd International Conference on Paste, Thickened and Filtered Tailings—PASTE 2020*, Santiago, 2020.
- [152] F. Kaswalder, D. Cavalli, A. Hawkey and A. Paglianti, "Tailings Dewatering by Pressure Filtration: Process Optimisation and Design Criteria," in *Proceedings of the 21st International Conference on Paste, Thickened and Filtered Tailings—Paste 2018*, Perth, 2018.
- [153] L. Bowker and D. Chambers, "The Risk, Public Liability, & Economics of Tailings Storage Facility Failures," 2015. [Online]. Available: <https://files.dnr.state.mn.us/input/environmentalreview/polymet/request/exhibit3.pdf>. [Accessed 12 April 2021].

-
- [154] F. Kaswalder, I. Fritzke, D. Cavalli and A. Bassi, "High Capacity Dewatering Plants," in *Proceedings of the 23rd International Conference on Paste, Thickened and Filtered Tailings—Paste 2020*, Santiago, 2020.
- [155] T. Puff and W. Stahl, "Presentwässerung mit nachgeschalteter Gasdifferenzdruckentwässerung," *Chemie Ingenieur Technik*, vol. 64, no. 3, p. 298–299, 1992.
- [156] W. Batel, "Einige Eigenschaften feuchter Haufwerke," *Chemie Ingenieur Technik*, vol. 28, no. 3, pp. 195–200, 1956.
- [157] H. Rumpf and E. Turba, "Über die Zugfestigkeit von Agglomeraten bei verschiedenen Bindemechanismen," *Berichte der Deutschen Keramischen Gesellschaft*, vol. 41, pp. 78–83, 1964.
- [158] H. Schubert, *Kapillarität in Porösen Feststoffsystemen*, Berlin: Springer, 1982.
- [159] A. Douglas, "Tensile Strength of Granular Materials," *Nature*, vol. 215, p. 952–953, 1967.
- [160] J. Schwedes, *Fließverhalten von Schüttgütern in Bunkern*, Weinheim: Verlag Chemie, 1968.
- [161] R. Tittel, K. O. Borchers and F. Nacken, "Erfahrungen mit der Entwässerung feinstkörniger Rückstände aus einer Bodenwaschanlage," *Aufarbeitungs-Technik*, vol. 36, p. 366–371, 1995.
- [162] B. Fränkle, P. Morsch and H. Nirschl, "Towards Prediction of Cake Detachment in Tailings Filtration," in *Paste 2021: 24th International Conference on Paste, Thickened and Filtered Tailings*, Perth/Online, 2021.
- [163] M. Bustillo Revuelta, *Mineral Resources - From Exploration to Sustainability Assessment*, Cham: Springer International Publishing AG, 2017.
- [164] B. Higman, A. Mattox, D. Coil and E. Lester, *Mine Tailings*, G. T. Trekking, Ed., 2019.
- [165] FLSmidth Minerals Technology Center, "EIMCO® Colossal™ Automatic Filter Press (AFP)," 2012. [Online]. Available: https://www.flsmidth.com/-/media/brochures/brochures-products/filtration/pressure-filters/colossalfilterpress_brochure_email.pdf. [Accessed 24 July 2023].
- [166] Z. Xiu, F. Meng, F. Wang, S. Wang, Y. Ji and Q. Hou, "Shear Behavior and Damage Evolution of the Interface between Rough Rock and Cemented Tailings Backfill," *Theoretical and Applied Fracture Mechanics*, vol. 125, no. 103887, 2023.
- [167] T. Das, S. Usher, D. Batstone, M. Othman, C. Rees, A. Stickland and N. Eshtiaghi, "Impact of Volatile Solids Destruction on the Shear and Solid-liquid Separation Behaviour of Anaerobic Digested Sludge," *Science of The Total Environment*, no. 164546, 2023.
- [168] Metso Outotec, "Metso:Outotec Pressure Filtration - Larox® FFP & VPA Filters," 2022. [Online]. Available: <https://www.metso.com/globalassets/portfolio/larox-ffp-vpa-filters-brochure.pdf?r=3>. [Accessed 26 July 2023].
- [169] GRID Arendal, "Global Tailings Portal," 2022. [Online]. Available: <https://tailing.grida.no/#header>. [Accessed 5 January 2022].
- [170] World Mine Tailings Failures, "State of World Mine Tailings Portfolio," 2022. [Online]. Available: <https://worldminetailingsfailures.org/>. [Accessed 11 January 2022].
- [171] Mining.com, "Tailings Pond Collapse Affects World's Highest Human Settlement," 2022. [Online]. Available: <https://www.mining.com/tailings-pond-collapse-affects-worlds-highest-human-settlement/>. [Accessed 11 January 2022].
- [172] F. Concha A., "Challenges in Solid-liquid Separation—Thickening Theory and Applications," in *Proceedings of the International Mineral Processing Congress*, Santiago, 2014.
- [173] E. Furnell, K. Bilaniuk, M. Goldbaum, M. Shoaib, O. Wani, X. Tian, Z. Chen, D. Boucher and E. R. Bobicki, "Dewatered and Stacked Mine Tailings: A Review," *ACS ES&T Engineering*, vol. 2, no. 5, p. 728–745, 2022.

- [174] S. Top, H. Vapur and A. Ekicibil, "Characterization of Zeolites Synthesized from Porous Wastes Using Hydrothermal Agitational Leaching Assisted by Magnetic Separation," *Journal of Molecular Structure*, vol. 1163, p. 4–9, 2018.
- [175] T. Bao, T. Chen, M. Wille, N. Ahmadi, S. Rathnayake, D. Chen and R. Frost, "Synthesis, Application and Evaluation of Non-sintered Zeolite Porous Filter (ZPF) as Novel Filter Media in Biological Aerated Filters (BAFs)," *Journal of Environmental Chemical Engineering*, vol. 4, no. 3, pp. 3374-3384, 2016.
- [176] A. Lahnafi, A. Elgamouz, N. Tijani, L. Jaber and A. Kawde, "Hydrothermal Synthesis and Electrochemical Characterization of Novel Zeolite Membranes Supported on Flat Porous Clay-based Microfiltration System and Its Application of Heavy Metals Removal of Synthetic Wastewaters," *Microporous and Mesoporous Materials*, vol. 334, no. 111778, 2022.
- [177] K. Sun, J. Noh, Y. Choi, S. Jeong and Y. Kim, "Zeolite and Short-cut Fiber-based Wet-laid Filter Media for Particles and Heavy Metal Ion Removal of Wastewater," *Journal of Industrial Textiles*, vol. 50, p. 1475–1492, 2021.
- [178] U. Sükrü, S. Musa, T. Soner and T. İrfan, "Removal of Heavy Metals from Wastewater Solution Using a Mechanically Activated Novel Zeolitic Material," *Journal of Mining Science*, vol. 56, p. 1010–1023, 2020.
- [179] T. Hwang and C. Neculita, "In Situ Immobilization of Heavy Metals in Severely Weathered Tailings Amended with Food waste-based Compost and Zeolite," *Water, Air, & Soil Pollution*, vol. 224, no. 1388, 2013.
- [180] V. Rey, C. Ríos, L. Vargas and T. Valente, "Use of Natural Zeolite-rich Tuff and Siliceous Sand for Mine Water Treatment from Abandoned Gold Mine Tailings," *Journal of Geochemical Exploration*, vol. 220, no. 106660, 2021.
- [181] X. Shen, G. Qiu, C. Yue, M. Guo and M. Zhang, "Multiple Copper Adsorption and Regeneration by Zeolite 4A Synthesized from Bauxite Tailings," *Environmental Science and Pollution Research*, vol. 24, p. 21829–21835, 2017.
- [182] J. Izidoro, M. Kim, V. Bellelli, M. Pane, A. Botelho Junior, D. Espinosa and J. Tenório, "Synthesis of Zeolite A Using the Waste of Iron Mine Tailings Dam and its Application for Industrial Effluent Treatment," *Journal of Sustainable Mining*, vol. 18, no. 4, p. 277–286, 2019.
- [183] ISO, *ISO 9352:2012 - Plastics—Determination of Resistance toWear by Abrasive Wheels.*, Geneva: International Organization for Standardization, 2012.
- [184] ASTM, *ASTM D1044-19 - Standard Test Method for Resistance of Transparent Plastics to Surface Abrasion by the Taber Abraser*, West Conshohocken: ASTM International, 2019.
- [185] ISO, *ISO 3537:2015 - Road Vehicles—Safety Glazing Materials—Mechanical Tests*, Geneva: International Organization for Standardization, 2015.
- [186] ISO, *ISO 15082:2016 - Road Vehicles—Tests for Rigid Plastic Safety Glazing Materials*, Geneva: International Organization for Standardization, 2016.
- [187] Fraunhofer-Institut für Schicht- und Oberflächentechnik, "Abriebfestigkeit prüfen mit dem Taber-Abraser-Test," 2023. [Online]. Available: <https://www.ist.fraunhofer.de/de/kompetenzen/analytik-prueftechnik/taber-abraser.html>. [Accessed 20 September 2023].
- [188] K. Sommer, R. Heinz and J. Schöfer, *Verschleiß Metallischer Werkstoffe*, Wiesbaden: Springer Vieweg, 2018.
- [189] ASTM, *ASTM G99-17; Standard Test Method for Wear Testing with a Pin-on-Disk Apparatus*, West Conshohocken: ASTM International, 2017.
- [190] M. Akhtar, T. Sathish, V. Mohanavel, A. Afzal, K. Arul, M. Ravichandran, I. Rahim, S. Alhady, E. Bakar and B. Saleh, "Optimization of Process Parameters in CNC Turning of Aluminum 7075 Alloy Using L27 Array-Based Taguchi Method," *Materials*, vol. 14, no. 4470, 2021.
- [191] ASTM, *ASTM D4886-18; Standard Test Method for Abrasion Resistance of Geotextiles (Sandpaper/Sliding Block Method)*, West Conshohocken: ASTM International, 2018.

-
- [192] L. Castelan-Velazco, J. Mendez-Nonell, S. Sanchez and L. Ramos, "Morphology and Osteogenetic Characteristics of Polyamide/NanoHydroxyapatite Biocomposites," *Polymer Bulletin*, vol. 62, p. 99–110, 2009.
- [193] A. Boric, A. Kalendová, M. Urbanek and T. Pepelnjak, "Characterisation of Polyamide (PA)12 Nanocomposites with Montmorillonite (MMT) Filler Clay Used for the Incremental Forming of Sheets," *Polymers*, vol. 11, no. 1248, 2019.
- [194] R. Lima, T. Pereira and E. Silva Filho, "Polyamide 11 Porous Films by NIPS: The Influence of Miscibility and Polymer Crystalline Formation in Pores Structure and Morphology," *Química Nova*, vol. 44, p. 675–682, 2021.
- [195] H. Shanak, K. Ehses, W. Götz, P. Leibenguth and R. Pelsteret, "X-ray Diffraction Investigations of Alpha-polyamide 6 Films: Orientation and Structural Changes upon Uni- and Biaxial Drawing," *Journal of Materials Science*, vol. 44, p. 655–663, 2009.
- [196] K. Chrissopoulou and S. Anastasiadis, "Polyolefin/layered Silicate Nanocomposites with Functional Compatibilizers," *European Polymer Journal*, vol. 47, p. 600–613, 2011.
- [197] A. Rushton, "Effect of Filter Cloth Structure on Flow Resistance, Bleeding, Blinding and Plant Performance," *Chemical Engineering*, no. 273, pp. 88-94, 1970.
- [198] T. Buchwald and U. Peuker, "Evaluation of Filter Media That Can Be Used in Automatic Filters," in *Filtration and Separation Technologies International Edition*, Essen, Vulkan-Verlag GmbH, 2022.
- [199] Micronics, "Is Chemical Cleaning Effective for Cleaning My Filter Cloth?," 2020. [Online]. Available: <https://www.micronicsinc.com/filtration-news/chemical-cleaning-filter-cloth>. [Accessed 5 May 2020].
- [200] Universal Filtration & Pumping Solutions, "Acid Cleaning," 2020. [Online]. Available: <http://automaticfilterpress.com/acid-cleaning/>. [Accessed 5 May 2020].
- [201] A. Horrocks and S. Anand, *Handbook of Technical Textiles*, Cambridge: Woodhead Publishing Ltd, 2000.
- [202] S. Stahl, S. Siggelkow and H. Nirschl, "A Microbiological Test Method to Determine the Cleanability of Filter Media in Solid-Liquid-Separation Applications," *Engineering in Life Science*, vol. 7, no. 2, pp. 136-142, 30 März 2007.
- [203] M. Srivastava, S. Pan, N. Prasad and B. Mishra, "Characterization and Processing of Iron Ore Fines of Kiriburu Deposit of India," *International Journal of Mineral Processing*, no. 61, pp. 93-107, 2001.
- [204] K. Fabrice Kapiamba and M. Kimpiab, "The Effects of Partially Replacing Amine Collectors by a Commercial Frother in a Reverse Cationic Hematite Flotation," *Heliyon*, vol. 7, no. 3, 2021.
- [205] U. Srivastava and S. Komar Kawatra, "Strategies for Processing Low-grade Iron Ore Minerals," *International Journal of Mineral Processing*, vol. 30, no. 4, pp. 361-371, 2009.
- [206] A. Guha, R. Barron and R. Balachandar, "An Experimental and Numerical Study of Water Jet Cleaning Process," *Journal of Materials Processing Technology*, vol. 211, no. 4, pp. 610-618, 1 April 2011.
- [207] J. Kozeny, "Über kapillare Leitung des Wassers im Boden," *Sitzungsberichte der Akademie der Wissenschaften in Wien - mathematisch-naturwissenschaftliche Classe*, vol. 136, no. 2a, p. 271–306, 1927.
- [208] F. Johns, "High Pressure Filtration of Fine Particle Slurries," in *Filtech*, Karlsruhe, 1991.
- [209] C. Kujawa, J. Winterton, R. Jansen and R. Cooke, "Innovative Process Engineering to Create Better Tailings Facilities," in *Proceedings of 6th International Seminar on Tailings Management*, 2019.
- [210] B. Mosher, N. Romaniuk, J. Fox, N. Hariharan, J. Leikam and M. Tate, "High Performance Fine Tailings Dewatering with Hydrated Lime Slurry," in *Proceedings of Tailings and Mine Waste*, Vancouver, 2019.

- [211] A. Beveridge, P. Mutz and D. Reid, "Tailings Co-disposal Case Study – Art or Science?," in *Proceedings of the 18st International Seminar on Paste and Thickened Tailings*, Perth, 2015.
- [212] N. Alam, O. Ozdemir, M. Hampton and A. Nguyen, "Dewatering of Coal Plant Tailings: Flocculation Followed by Filtration," *Fuel*, vol. 90, no. 1, pp. 26-35, 2011.
- [213] C. Torres López, M. Catling, J. Bellwood and L. Boxill, "The Effect of Preconditioning of Tailings Prior to Inline Flocculation and Deposition," in *Proceedings of the 22st International Seminar on Paste, Thickened and Filtered Tailings*, Perth, 2019.
- [214] A. Vietti, S. Rabie and K. Ntshabele, "Process Water Conditioning to Improve Slurry Dewatering," in *Proceedings of the 22st International Seminar on Paste, Thickened and Filtered Tailings*, Perth, 2019.
- [215] T. Kinnarinen, R. Tuunila and A. Häkkinen, "Reduction of the Width of Particle Size Distribution to Improve Pressure Filtration," *Minerals Engineering*, vol. 102, pp. 68-74, 2017.
- [216] C. Kujawa, J. Winterton, R. Jansen and R. Cooke, "Creating Better Tailings Facilities Using Innovative Process Engineering," in *Proceedings of Tailings and Mine Waste*, Vancouver, 2019.
- [217] K. Rahal and T. Wisdom, "Evaluation of a Split Stream Dewatering Flowsheet for Tailings," in *Proceedings of Tailings and Mine Waste*, Vancouver, 2019.
- [218] D. Liu, M. Edraki, A. Malekizadeh, P. Schenk and L. Berry, "Introducing the Hydrate Gel Membrane Technology for Filtration of Mine Tailings," *Minerals Engineering*, vol. 135, pp. 1-8, 2019.
- [219] J. Goltermann and H. Hedlund, "Method for Emptying the Press Chambers of a Press Filter and an Apparatus Therefor". USA Patent 5728307, 1998.
- [220] A. Iwatani, "Apparatus for Cake Removal in a Filter Press". USA Patent 4900436, 1990.
- [221] M. Carlsson and T. Jönson, "Verfahren zum Ablösen von Filterkuchen und Filterpresse zur Durchführung des Verfahrens". GER Patent 3891215 C2, 1992.
- [222] H. Takeshi, "Method and Device for Removing Cake of Filter Press". JAP Patent 03242207 A, 1991.
- [223] M. Oelbermann, "Filterpresse". GER Patent 3933740 A1, 1991.
- [224] J. Cai, W. Hao, C. Zhang, J. Yu and T. Wang, "On the Forming Mechanism of the Cleaning Airflow of Pulse-jet Fabric Filters," *Journal of the Air & Waste Management Association*, vol. 67, no. 12, pp. 1273-1287, 2017.
- [225] P. Steenstrup, "A Method of Filter-cleaning and an Apparatus for Carrying Out the Method". WO Patent 1989009646 A1, 1988.
- [226] B. Ekberg and N. Goran, "Method of Cleaning Filter Discs in a Suction Dryer Using Ultrasonic Vibration". USA Patent 4946602 A, 1988.
- [227] T. Busch-Sorensen, "Filter for Filtration of Fluids". USA Patent 5085772 A, 1990.
- [228] T. Tuori, H. Sekki, J. Ihalainen, P. Pirkonen and H. Mursunen, "Combined Ultrasonic Cleaning and Washing of Filter Disks". USA Patent 6217782, 2001.
- [229] M. Kristen, Experimentelle Untersuchungen zur ultraschallunterstützten Tauchreinigung - Dissertation, Düsseldorf: VDI-Verlag, 2005.
- [230] A. Kern, Numerische Simulation von ultraschallunterstützten Reinigungsprozessen - Dissertation, Düsseldorf: VDI-Verlag, 2005.
- [231] DIN, *DIN 19569-9, Wastewater Treatment Plants – Principles for the Design of Structures and Technical Equipment – Part 9: Mechanical Drainage of Sewage Sludge*, Berlin: Deutsches Institut für Normung e. V., 2017.

-
- [232] M. Rosen, *Surfactants and Interfacial Phenomena*, 3 ed., New Jersey: John Wiley & Sons, 2004.
- [233] R. Lerch, G. Sessler and D. Wolf, *Technische Akustik: Grundlagen und Anwendungen*, Berlin Heidelberg: Springer-Verlag, 2009.
- [234] Wacker Chemie AG, "AK 10 Data Sheet," 2020. [Online]. [Accessed 1 May 2020].
- [235] S. Ebnesajjad, *Surface Treatment of Materials for Adhesive Bonding*, 2 ed., Oxford: Elsevier, 2014.
- [236] H. Kolb, R. Schmitt, A. Dittler and G. Kasper, "On the Accuracy of Capillary Flow Porometry for Fibrous Filter Media," *Separation and Purification Technology*, vol. 199, pp. 198-205, 2018.
- [237] ASTM, *ASTM D6614-07; Standard Test Method for Stretch Properties of Textile Fabrics — CRE Method*, West Conshohocken: ASTM International, 2015.
- [238] ASTM, *ASTM D2261-13; Standard Test Method for Tearing Strength of Fabrics by the Tongue (Single Rip) Procedure (Constant-Rate-of-Extension Tensile Testing Machine)*, West Conshohocken: ASTM International, 2017.
- [239] ASTM, *ASTM D3822/D3822M-14; Standard Test Method for Tensile Properties of Single Textile Fibers*, West Conshohocken: ASTM International, 2020.
- [240] E. Campo, *Selection of Polymeric Materials*, Norwich: William Andrew Inc, 2008.
- [241] Carl Roth, "Hydrochloric Acid, 1 l, 32 %, Extra Pure," 2023. [Online]. Available: <https://www.carlroth.com/de/en/a-to-z/hydrochloric-acid/p/x896.1>. [Accessed 31 October 2023].
- [242] Carl Roth, "Acetic acid, 1 l, 40 %, pure," 2023. [Online]. Available: <https://www.carlroth.com/de/en/a-to-z/acetic-acid/p/1ee0.1>. [Accessed 31 October 2023].
- [243] Carl Roth, "Sulphamic acid, 1kg, ≥99 %, cryst.," 2023. [Online]. Available: <https://www.carlroth.com/de/en/a-to-z/sulphamic-acid/p/4714.1>. [Accessed 31 October 2023].
- [244] Carl Roth, "Formic acid, 1 l, glass, 45 %, pure," 2023. [Online]. Available: <https://www.carlroth.com/de/en/a-to-z/formic-acid/p/6739.1>. [Accessed 31 October 2023].
- [245] Carl Roth, "Sodium hydroxide solution, 1 l, 50 %, extra pure," 2023. [Online]. Available: <https://www.carlroth.com/de/en/a-to-z/sodium-hydroxide-solution/p/8655.1>. [Accessed 31 October 2023].
- [246] Carl Roth, "Potassium hydroxide solution, 1 l, 50 %, extra pure," 2023. [Online]. Available: <https://www.carlroth.com/de/en/a-to-z/potassium-hydroxide-solution/p/7949.1>. [Accessed 31 October 2023].
- [247] B. Dolinar and S. Škrabl, "Atterberg limits in relation to other properties of fine-grained soil," *Acta Geotechnica Slovenica*, no. 2, pp. 5-13, 2013.